Modelling colorectal cancer in *Drosophila*

Establiment d'un model de càncer colorectal a *Drosophila*

Òscar Martinell Aleman

,

MODELLING COLORECTAL CANCER IN *DROSOPHILA*

Establiment d'un model de càncer colorectal a Drosophila

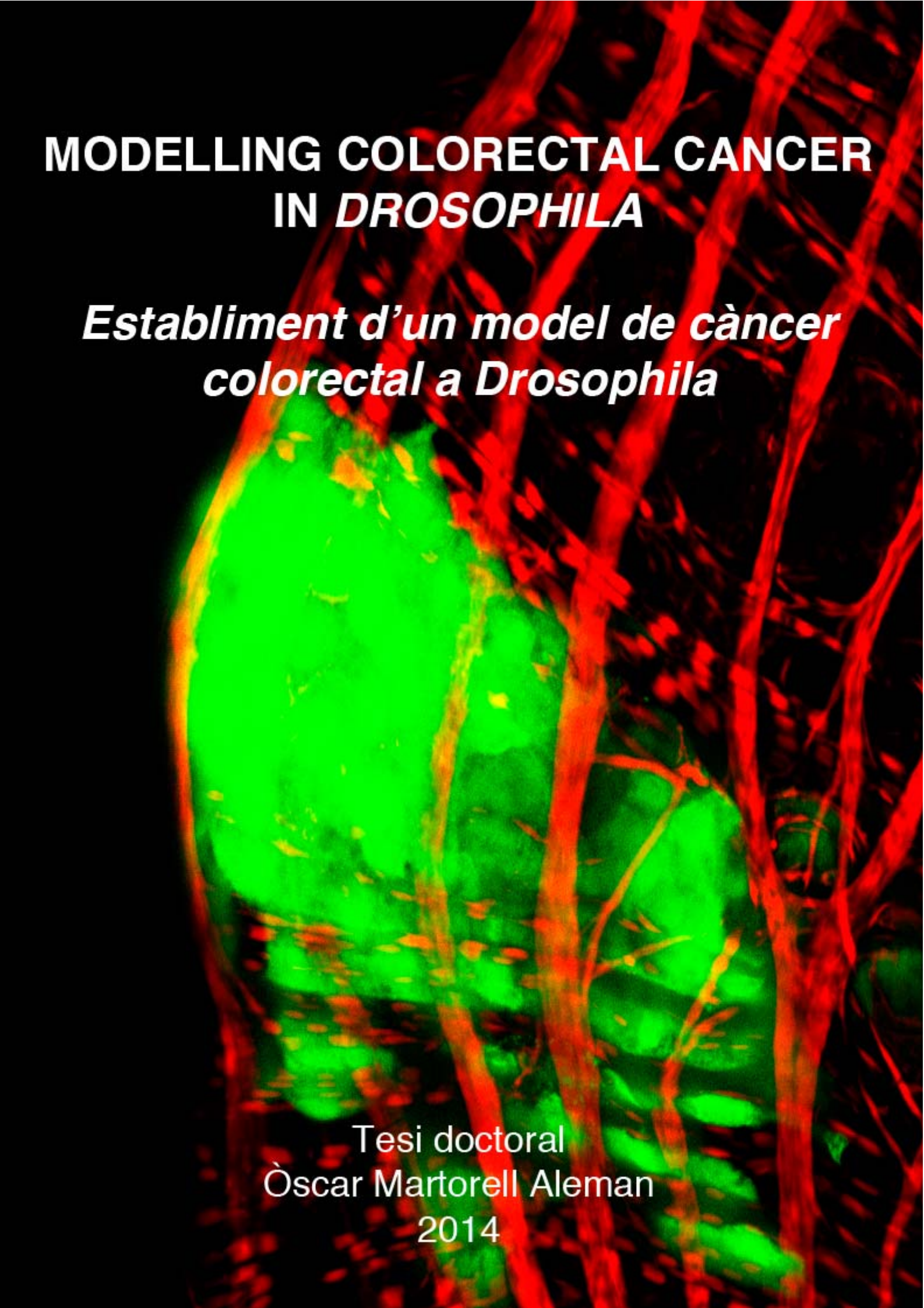

Tesi doctoral

Òscar Martorell Aleman

2014

Departament de Genètica
Facultat de Biologia
Universitat de Barcelona

TESI DOCTORAL:

MODELLING COLORECTAL CANCER IN *DROSOPHILA*

"Establiment d'un model de càncer colorectal a Drosophila"

Òscar Martorell Aleman
Barcelona, 2014

Departament de Genètica
Facultat de Biologia
Universitat de Barcelona

MODELLING COLORECTAL CANCER IN *DROSOPHILA*

"Establiment d'un model de càncer colorectal a Drosophila"

Memòria presentada per
ÒSCAR MARTORELL ALEMAN
per aspirar al grau de DOCTOR
per la Universitat de Barcelona

Aquest treball ha estat realitzat sota la direcció del Dr. Andreu Casali Taberner a l'Institut de Recerca Biomèdica de Barcelona (IRB Barcelona) i a l'Institut de Biologia Molecular de Barcelona (IBMB-CSIC).

Vist i plau del Director	El Tutor/a	L'Autor
Dr.Andreu Casali Taberner	Dr.Emili Saló Boix	Òscar Martorell Aleman

Per a la meva família,

"La felicitat és un camí, no una meta"

Agraïments

Ja està, hem arribat a la part final d'aquesta tesi... els agraïments... també coneguts com a discussió sentimental de la tesi. Han passat ja 6 anys de que em vaig incorporar al laboratori. Era novembre de 2007 i un jovenet Òscar que no havia acabat la carrera entrava per fer una col·laboració de pràctiques i mira on som ara, més de 6 anys després! Es diu fàcilment que han passat 6 anys. Vaig entrar que era un nen i mira'm ara...un nen més vell! Durant aquests 6 anys he aprés moltíssimes coses tan a nivell acadèmic com personal i ha estat en bona mesura gràcies a tota la gent que m'ha envoltat. Del laboratori en surt un noi més o menys format que una persona ha estat modelant tots aquests anys amb força traça. Aquests agraïments no tindrien sentit si no anessin especialment dirigits al meu director de tesi, l'Andreu.

Andreu, hem arribat al final del camí i t'ho haig de agrair immensament. Has estat un director magnífic. Sempre he considerat que les teves aptituds científiques i de dedicació són d'admiració! Sempre tens una resposta adequada per aquella pregunta sense resposta i una idea magnífica que et fa sortir del despatx buscant un despistat doctorant que et diu amb cara de circumstància: Ah sí, sí m'ho apunto!... Ai Andreu, agrair-te haver suportat tots els meus errors i defectes que en són uns quants. Has sabut fer-me adonar dels meus defectes i intentar corregir-los amb paciència. I vet aquí que has aconseguit que sigui més crític amb el que m'envolta i amb la meva feina (que és molt important!!). Gràcies sincerament, per què si tant he aprés en el laboratori ha estat en gran mesura gràcies a tu.

Per altre banda, ja se sap que al laboratori no tot són flors i violes i que alguns moments voldries escanyar el teu director de tesi o algú altre i necessites desfogar-te. Per això estan els amics.

En primer lugar y sin lugar a dudas quiero agradecer muy muy sinceramente y de todo corazón a ti Pilar por todo el cariño y ayuda que me has dado estos años. Hemos llorado juntos pero sobretodo hemos reído! Estos años a tu lado han estado magníficos. Aunque te hayas ido aún salgo de mi laboratorio hacia el tuyo pensando: esto se lo digo a Pilar! Gracias por tus consejos y también por tus reprimendas en los momentos adecuados, no por todas las que te gusta dar Mama Pilar ;-). Estoy seguro que en el futuro nos iremos reencontrando y nos reiremos como hemos hecho durante años en la sala de moscas. Gracias por todo!

Also I want to acknowledge Arzu for all her kindness and for her limitless heart. You have been always taking care of all of us and I appreciate so much your efforts. Gaylorcitoooo, gracias por compartir espacio vital durante todos años y por tu ayuda en les experimentos!! Seguro que todo te irá genial! Neus! Merci per tots els moments de riure i frikisme junts!!!! Yolandaaaaaaa!! Primero agradecerte tu trabajo como técnica y lab manager. Siempre has estado ahí para echar un cable cuando lo hemos necesitado!!! Y sobretodo por tu corazón, tus consejos y todas tu riiiiisas!!!! Gracias por todas las risas a la pareja más alocada del lab: Pablo y Delia. Ahhhh y gracias a el trio calavera: Pablo, Guille y Guillem por el video estrella que están haciendo! Ivet et desitjo el millor durant aquests anys, em tindràs dos pisos més a dalt pel que necessitis! Marco, gracias por todo el conocimiento y ayuda que brindaste a todo el laboratorio. Elisenda, gràcies per endinsar-me en el món de la comunicació científica!! Mahi, good luck with the guts and obviously with the baby!! 2014 will be a tough year!
Gràcies Jordi per deixar-me entrar al lab, per les discussions científicques i per les tafaneries polítiques juntament amb el grup de tafaneria política: Marc i Nico!
Gràcies a tots els altres membres del lab: Ale, Friedi, Nico, Kira, Sara, Marc, Marta, Sofia, Bárbara, Anni, Xavi, Cristina i espero no deixar-me ningú >_<
Majoooooo!!!!!! Gràcies per el teu carinyo i per fer-me veure moltes coses que ningú m'havia fet veure! Ets una persona molt especial i he gaudit i après molt al teu costat! Ens veurem aviat! A la Núria per la seva dedicació pels altres i per la seva ajuda als tallers! Nacheteeeee! Muchas gracias por estar siempre ahí, por todos los cotilleos y por cuidar de mi!!! Gràcies al laboratori de Azorín per la seva ajuda i en especial a en Salva, la Marta Lloret (Orxeta) i la Sónia: Ànims que ja queda poc!!!!! And thanks Sarah for helping me to contruct my future!

Finalment, gràcies a la meva familia, als meus amics i a en Pere per ser al meu costat.

GRÀCIES A TOTS!

0. Index

Introduction

1. Introduction

1.1 The biology of cancer

During decades many researchers have been trying to elucidate which are the causes of the origin and development of tumorigenic processes. In 1954 Leslie Foulds was the first to introduce the term tumour progression and to propose a set of rules that would drive this progression in a continuous process of malignancy (Foulds, 1954). Since Foulds' rules many observations have confirmed that cancer is a multi-step process caused by the accumulation of several genetic alterations, provoking a progressive transformation of normal cells into tumoral cells. Although each tumour develops in a different manner, Douglas Hanahan and Robert A. Weinberg proposed in 2001 that a common group of capabilities would be essential for any oncogenic progression (Hanahan, 2000). These capabilities, revised in 2011 and largely supported by the scientific community, are known as the hallmarks of cancer and are: Self-sufficiency in growth signals, insensitivity to growth-arrest signals, evasion of programmed cell death, limitless replicative potential, sustained angiogenesis, tissue invasion and metastasis, cellular metabolism deregulation, protection against immune system, genome instability and the use of the inflammatory processes as a promoting growth signal (Hanahan, 2000; Hanahan, 2011) (Figure 1). These capabilities help the transformed cell to surpass different levels of anti-tumour defences coming from the host.

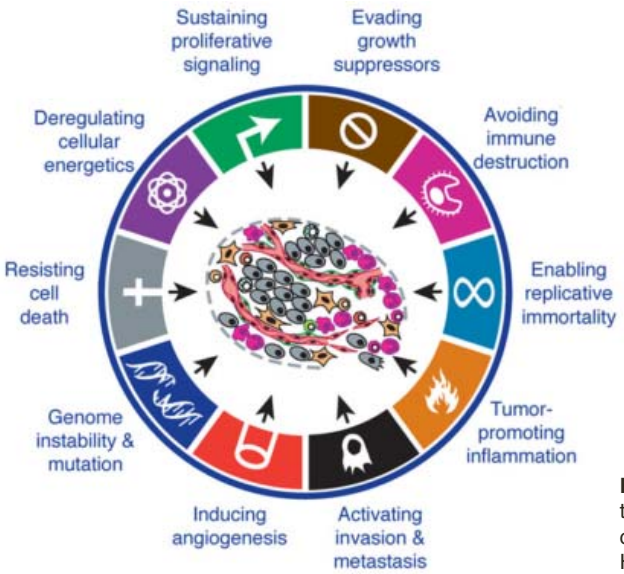

Figure 1. Hallmarks of cancer. Each one of these capabilities is an essential step of many or even all types of cancers. Modified from Hanahan D. 2011

Each cancer acquires these capabilities in a different order and by different ways. Before and now, the aim of cancer researchers has been to understand the genetic and molecular mechanisms that drive normal cells progress into malignancy in each cancer type. Unfortunately, these mechanisms, far from being simple threats, are becoming a large group of tightly interconnected nets. These nets include still unclear processes such as DNA modifications and epigenetics or microRNA expression. Once discovered and described, these molecular mechanisms could be used as therapeutic targets to block the tumorigenic growth and eventually kill any tumour.

1.2 The colorectal cancer

Colorectal cancer (CRC) is one of the most common cancers in the developed countries. The term CRC includes all those malignant lesions that affect the large intestine, the rectum and the appendix. The major risk factors are: age, male gender, high fat diet and alcohol intake. Most of the CRC cases are not due to genetic inheritance, being those inherited cases around a 15% of all CRC cases. The other 85% are sporadic and usually arise from adenomas or adenomatous polyps that are small benign lesions that can turn into a malign lesion if they are not treated (Fearon, 2011). Adenomatous polyps grow inside the mucosa layer. In further stages if the tumour progress, the tumour starts to invade the underlying tissues such as the intestinal serosa. The invasion of the external layers of the colon correlates with an advance stage of CRC and poor prognosis diagnostic. When the tumour invades the outer layers, it can reach the blood vessels or the lymphatic ganglions, being then able to migrate to distant places and generate metastasis (Figure 2). Not-treated CRC are highly metastatic and usually develop into hepatic metastasis (Fearon, 2011).

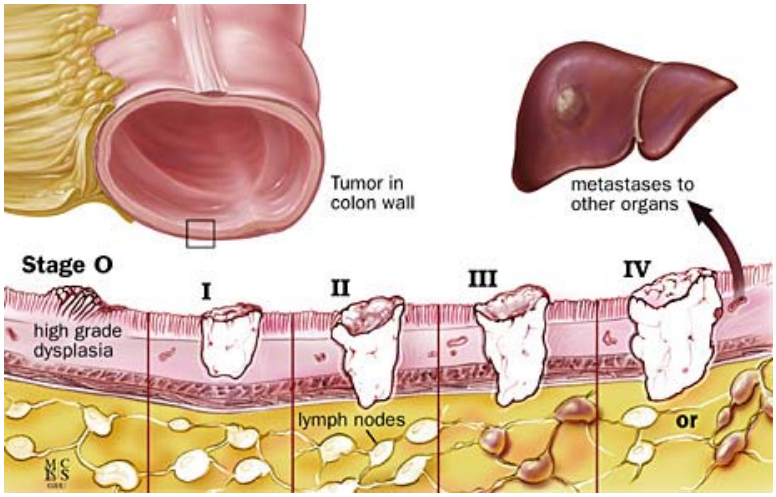

Figure 2. Clinical stages of CRC. The stages are established by the degree of invasion of the tumour. Taken from John Hopkins Colon Cancer Center.

1.3 Genetics and molecular mechanisms in colorectal cancer (CRC) progression

1.3.1 Overview of CRC genetic regulation.

In 1990, Fearon and Vogelstein presented a genetic model to explain how CRC arises from pre-malign lesions that, by the accumulation of a set of mutations, increase progressively the malignancy of the tumour cells (Fearon, 1990). After more than 20 years, the model, still valid, has been refined and nowadays more than a dozen mutations have been placed in the transition of different stages of the disease (Figure 3). This malignant progression is known as the adenoma-carcinoma sequence.

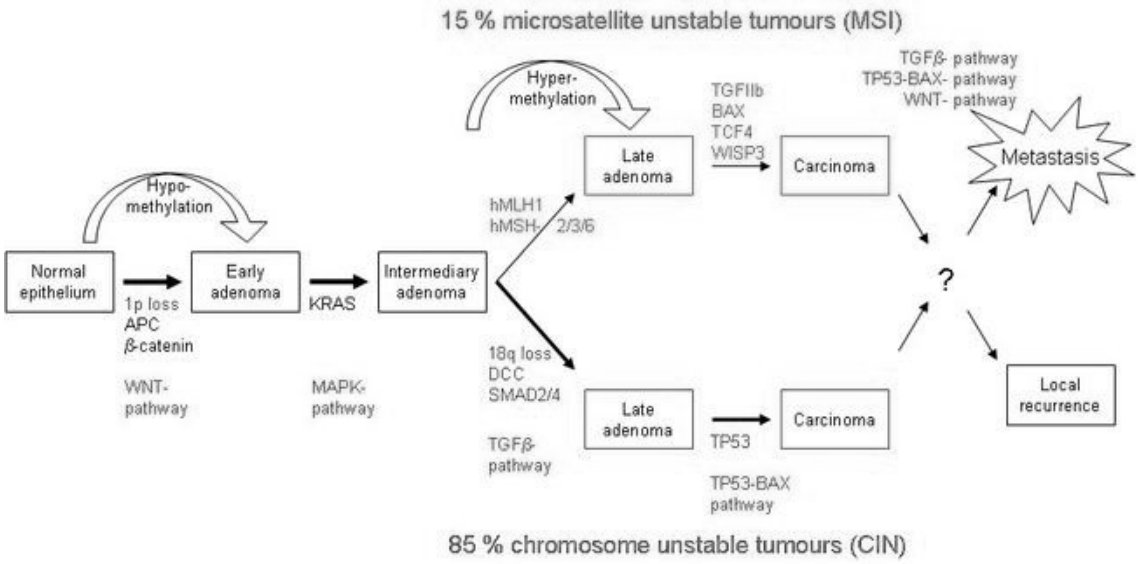

Figure 3. Adenoma to carcinoma sequence. The progression from a normal epithelium to a fully developed carcinoma requires the accumulation of several mutations. The presence of defects in the DNA mismatch repair genes affects CRC progression by the induction of several mutations in microsatellite regions.

Although the term CRC is treated as a unique disease there are, in fact, several subtypes. Around 15-30% of CRC cases have an hereditary component (Fearon, 2011), mainly related to two main syndromes: Familiar Adenomatous Polyposis (FAP) and Hereditary Nonpolyposis Colorectal Cancer (HNPCC) or Lynch syndrome. In FAP patients, the inheritance of mutations in the gene APC produces the apparition of multiple adenomatous polyps early in life. In contrast, the inherited mutations in DNA mismatch repair genes (MMR) in HNPCC patients produce a rapid development of the disease due to the lack of DNA mismatch reparation mechanisms and, consequently, the high accumulation of mutations in the DNA.

Conversely, most of CRC cases are sporadic and occur by the accumulation of somatic mutations during the life of the patient. There are two major types of sporadic cancers: those with alterations in DNA mismatch repair genes and as a consequence, microsatellite instability and hyper-mutation state; and those with stable microsatellites but chromosomally unstable that contribute to develop aneuploidies (Network, 2012). However, both types finally converge in the alteration of four main signalling pathways that control cell proliferation and cell differentiation in the adult colon. Those signalling pathways are the Wnt pathway, the EGFR pathway, the TGF-β pathway and the PI3K pathway. The alteration of these four pathways and in the protein TP53 in colonic cells is enough to produce malignant lesions in the adult colon (Figure 4). Recently, a scientific consortium has performed a deep study of the molecular basis of CRC to identify the genetic alterations of more than 200 cases of CRC (Figure 4) (Network, 2012).

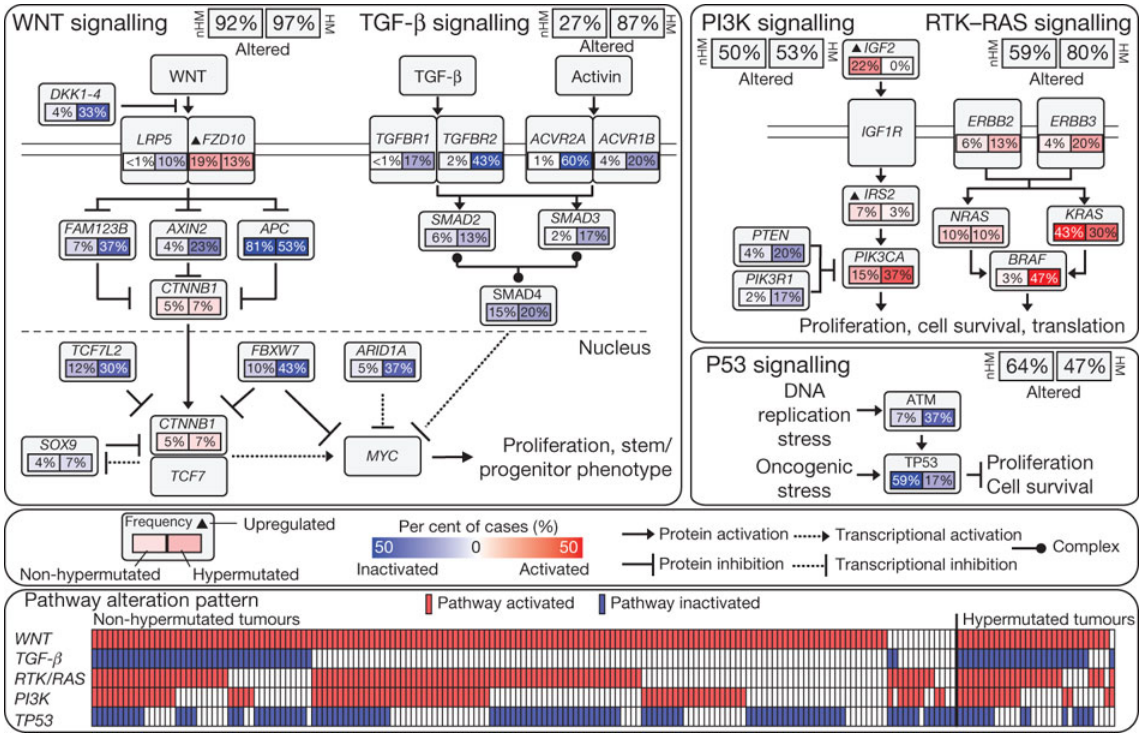

Figure 4. Percentage of genetic alterations in the main signalling pathways and in its components. At the top: the main pathways implicated in CRC progression and the percentage of genetic alterations on their components. At the bottom: the number of CRC that have alterations on each pathway (Network, 2012).

More than 90% of CRC cases have activating mutations in components of the Wnt pathway, and its activation is considered one of the first events in CRC progression. The second more altered signalling pathway is the RTK-RAS pathway, with activating mutations in around 60% of the cases with no hypermutation phenotype.

These two pathways are considered the main effectors of the early progression of the CRC (Figure 3). Mutations in TP53 (64%), PI3K (50%) or TGF-β (27%) pathways are also considered main events for CRC progression (Network, 2012).

1.3.2 The role of the Wnt pathway in CRC progression.

The Wnt pathway is one of the central signalling pathways along the animal kingdom and controls critical functions such as proliferation, migration or cell differentiation. In humans, the Wnt pathway is activated by different Wnt ligands that bind to the receptors Frizzled and Lipoprotein receptor-related protein (LRP). The activation of the receptor complex induces the degradation of an inhibitor complex that sequesters the Wnt transducer β-catenin in the cytoplasm. Consequently, the activation of the Wnt pathway allows the entrance of β-catenin into the nucleus where β-catenin binds to the activating complex TCF and activates the transcription of several target genes (Bienz, 2000).

Activating mutations of the Wnt pathway are found in more than 90% of sporadic CRC cases. Specifically, in one of the members of the β-catenin inhibitor complex, *Adenomatous polyposis coli (APC),* that is mutated in around 80% of CRC patients (Network, 2012). Usually, APC mutations cause the loss of the binding sites to β-catenin (Rowan et al., 2000), rendering a mutant form unable to sequester β-catenin. At its turn, β-catenin is then free to enter into the nucleus, bind to the cofactor TCF and activate the Wnt target genes. Therefore, mutations on APC lead to a constitutive activation of the Wnt pathway. In addition, APC germ-line mutations cause a hereditary type of CRC, the Familiar adenomatous polyposis (FAP). FAP patients develop hundreds of small adenomatous polyps that progress into malignant CRC early during patient life, with a 100% to develop CRC at the age of 40 years.

The activation of the Wnt pathway imposes a progenitor fate, expanding the stem cell compartment and creating an overproliferative epithelium (van de Wetering, 2002). The role of the Wnt pathway in cancer is consistent with its in normal homeostasis, as Wnt activation is essential for normal proliferation of the intestinal progenitor cells in the adult intestine (Sancho, 2004).

Finally, it is commonly accepted that mutations in the APC gene are a very early event in CRC progression (Figure 3), as the rate of APC mutations does not change between very early adenomas and late carcinomas. Moreover, mutations in APC have been described in very small lesions in the colonic epithelium, indicating that APC

mutations appear in the first stages of the disease and are critical for the initiation of the tumour (Fearon, 2011).

1.3.3 The K-RAS/B-RAF Pathway

The activation of the RAS signalling pathway has been extensively linked to cancer progression and cell proliferation (Malumbre, 2003). The K-RAS/B-RAF cassette is a common intracellular signalling cascade that acts downstream of a vast list of RTK (receptor tyrosine kinase) and GPCR (G protein coupled receptors) receptors. Activation of the K-RAS/B-RAF cassette induces a wide variety of cellular functions essential for tumour development, such as activation of cell proliferation or inhibition of cell apoptosis (Malumbres, 2003) (Figure 5).

The K-RAS/B-RAF pathway plays a role in CRC, as recent data shows that around 69% of the sporadic CRC patients carry activating mutations in it, rate that increases to 80% in hypermutated microsatellite-unstable (MSI-H) tumours (Figure 4). The more frequently mutated genes in the pathway are those occurring on the K-RAS or B-RAF genes. Interestingly, the incidence of the mutations on each depends on the microsatellite (MS) state (Rajagopalan, 2002). Those tumours with stable MS have mutations in K-RAS whereas MS unstable tumours concentrate mutations in B-RAF. Mutations in the K-RAS/B-RAF pathway are produced during mid-stages of the tumour progression rather than in the initial stages, as are usually found in large adenomas and carcinomas, but not in early adenomas (Fearon, 1990). Consistently, the apparition of induced K-RAS adenomas in mouse models is infrequent in comparison to Wnt-activated adenomas (Janssen, 2003; Zeineldin, 2013). This data taken together with observations of *in vitro* cultures that reveal the extrusion of K-RAS activated cells when surrounded of normal cells (Hogan, 2009) can explain the necessity of previous mutations to K-RAS to promote tumour survival.

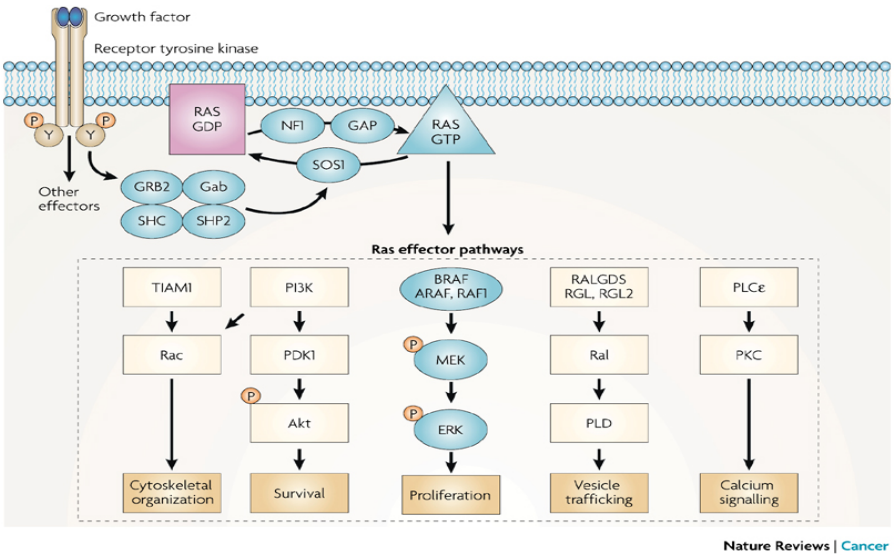

Figure 5. Ras controls many downstream signalling cascades. Ras is a signalling hub where multiple upstream signals converge and multiple downstream signals become activated depending on many factors, intensity of the signal, duration, etc. (Schubbert, 2007)

1.3.4 TGF-β signalling pathway: one pathway with multiple roles in CRC

The TGF-β (transforming growth factor β) pathway is one of the pathways with more roles in human development and disease (Massagué, 2008). There is a plethora of ligands, comprising TGF-β cytokines, bone morphogenetic proteins (BMPs) and Activins, that bind to an heterodimeric receptor complex formed by a type I and Type II receptors. The activation of the receptor is transduced inside the cell by a phosphorylation cascade. Inside the cell, the vast SMAD family proteins transduce the signal depending on the ligand bound to the receptors. The large number of pathway components can explain in part the large number of roles of TGF-β signalling pathway during development and cancer (Figure 6). The most known functions of TGF-β in tumour progression are those related with the anti-tumorigenic roles during the firsts stages of tumour development, including cytostasis, induction of cell differentiation, senescence and apoptosis (Massagué, 2008). Loss-of-function mutations in the TGF-β pathway, required to skip those anti-tumorigenic functions, are found in 30% of non-hypermutated CRC (Microsatellite Stable or MS-stable samples) cases and in 80% of the hypermutated CRC tumours. Most of the mutations occur in SMAD 4 in MS-stable cancers and in the TGF-β receptor II (TGF-βRII) in MS-unstable samples (Figure 4) (Network, 2012). Mutations in TGF-βRII are MS-unstable-specific due to the existence of a polyadenine sequence inside the coding region susceptible to accumulate errors during DNA replication that cannot be repaired if the DNA mismatch repair machinery

is affected in the tumour cell. Finally, it is important to remark that some CRC become resistant to TGF-β without identificable alterations in any component of the TGF-β pathway, suggesting the possible existence of other regulatory mechanisms able to block the response to this signal (Levy, 2006; Grady, 1999).

Paradoxically, TGF-β has also been related with some pro-tumorigenic functions in breast and pancreas cancer (Massagué, 2008). Evasion of the immune system, induction of the epithelial-mesenchymal transition, promotion of metastasis and second site colonization are examples of this tumorigenic potential of the TGF-β signalling pathway (Massagué, 2008). In CRC, high levels of circulating TGF-β cytokines can be found in some patients, correlating with a poor prognosis diagnostic (Elliott, 2005). A recent report demonstrates, however, that TGF-β promotes CRC tumorigenesis and metastasis through its effect on the tumour stroma (Calon, 2012).

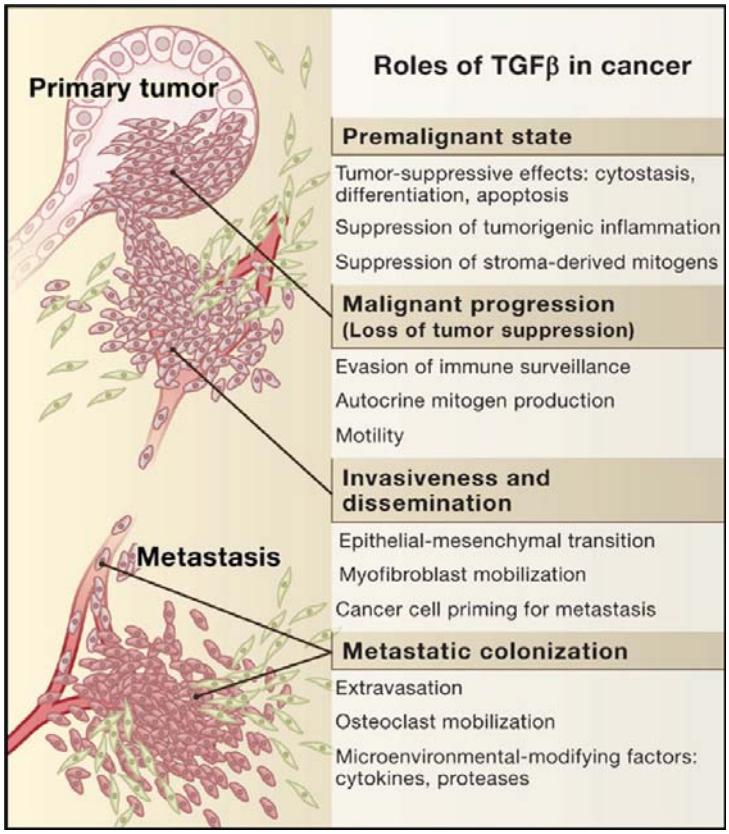

Figure 6. Multiple roles of TGF-β during cancer progression. The complete role of TGF-β during cancer is far from being understood. It has been proved that TGF-β has a dual role anti- and pro-tumorigenic both in the primary tumour and in the second metastatic site (Massagué, 2008).

1.3.5 Other signalling pathways implicated in CRC: PI3K and TP53 pathways.

There are other two signalling pathways that are frequently mutated during CRC progression, the phosphatidylinositol (PIP3) pathway and the protein TP53. Phosphatidylinositol-3,4,5 (PIP3) is a second intracellular messenger that controls cell

growth, proliferation and survival. PIP3 is produced by PI3 Kinases (PI3K), usually activated by RTK-RAS signalling, and transformed in PIP2 by PIP3 Phosphatases. Activating mutations of the PI3K Pathway occur in around 50% of CRC cases (Figure 4). Mutations mainly affect the gene PI3KCA, one of the PI3Ks, and the negative regulator of the pathway and PIP3 phosphatase, PTEN (Network, 2012). Published studies suggest that although the PI3K pathway acts downstream of the RAS pathway, mutations in PI3K pathway occur frequently in tumours previously mutated in K-RAS (Baldus, 2010). Apparently the oncogenic form K-RAS does not activate efficiently PI3K, and mutations in the PI3K pathway are necessary for proper tumour progression (Li, 2004).

Around 70% of CRCs show a missense mutation in TP53 combined with a 17p chromosome deletion, the chromosomal position of TP53 (Baker, 1990). This combination leads to a complete loss of TP53, severely affecting cell cycle regulation. TP53 acts as a negative transcriptional regulator of cell cycle proteins and as a promoter of apoptosis. With the loss of TP53, the regulation of the mitosis checkpoints becomes critically affected and the external anti-tumorigenic signals lack the main intracellular protein to induce cell cycle arrest and/or apoptosis (Fearon, 2011).

1.3.6 Causes of genetic alterations in CRC: Chromosome Instability, Microsatellite Instability and CpG Island Metilator Phenotype.

There are two main causes of genetic alterations in CRC development: Chromosome instability (CIN) and Microsatellite Instability (MSI). The first one includes all those defects that affect gene copy number such as partial or complete loss or gain of chromosomes (aneuploidy). The loss or gain of chromosomes affects the copy number of genes and usually the regions deleted or added include known tumour suppressor genes or oncogenes. The two most common lesions in CRC are the loss of the 17p arm (56% of CRCs) and the loss of the entire chromosome 18 (66% of CRCs). Those regions respectively include Smad4 and TP53, two tumour suppressor genes implicated in CRC progression (Network, 2012).

On the other hand, microsatellite instability is the result of DNA mismatch repair (MMR) system defects. The alterations in DNA mismatch repair genes produces a hypermutated condition where multiple sensitive sequences, the microsatellites, appear frequently mutated due to the lack of repair mechanisms after DNA replication. Microsatellites are repeated sequences of 1-6 bases units that are sensible to

introduce errors during DNA replication. CRCs are usually classified into MSI-high (often called hypermutated tumours) and MSI-low (Jass, 2007). 15% of CRC are MSI-H, a small fraction from those correspond to those patients with HNPCC where germ-line mutations in MMR genes provoking the apparition of multiple mutations in microsatellite containing genes. The rest of MSI-H tumours usually present a hypermetylation of the MMR gene promoters that causes the inactivation of the MMR genes. MSI-H tumours contain large numbers of mutations and although the same pathways that are affected in MSI-L and MSI-H tumours, frequently the affected genes are different. For example, B-RAF and Activin receptor 2A (ACVR2A) mutations are almost exclusive from MSI-H tumours although the effects that provoke are similar to the ones that occur in MSI-L tumours with mutations in K-RAS or Smad 4. Interestingly, MSI and CIN are two situations that are almost mutually exclusive. The 15% of CRC are MSI-H but are chromosomally stable. In contrast, the other 85% are MSI-L but chromosomally unstable (E. R. Fearon, 2011).

Epigenetic changes are also observed in CRC and the most important is the CpG island methylation state. CpG are localized regions of high content in CpG dinucleotides. In mammals these regions are located in the 50% of all the genes and the hypermethylation of these regions is associated with the silencing of the downstream genes. Most CRCs present hypomethylation of these regions in comparison with normal intestinal mucosa although the reason for this state is still unclear (Fearon, 2011). In contrast, a small fraction of CRC cases present hypermethylation of CpG islands and they are called CpG Island methylator phenotype positive ($CIMP^+$) tumours. In general, $CIMP^+$ tumours present hypermethylation of MMR gene promoters, silencing in this way the MMR repair genes and correlate with oncogenic mutations in B-RAF (Jass, 2007).

1.4 *Drosophila* as a model in cancer research

For a long time, *Drosophila* has been used as a model organism to elucidate many of the genetic and molecular mechanisms that drive the development and the basic cellular processes of an animal organism. But it has not been so long that *Drosophila* has started to be used as a model organism to solve basic questions of human diseases. Nowadays, a large community of scientists study basic tumorigenic processes using *Drosophila* as a model organism and it has emerged as a powerful tool to understand the basic processes that rule tumour progression. As other model organisms, *Drosophila* has advantages and disadvantages. As advantages, genetic studies in *Drosophila* are boosted by the large amount of descendants, the *Drosophila* short life cycle and the large amount of genetic tools that *Drosophila* scientists have developed during all the years of study with *Drosophila*. Moreover, those tumorigenic processes that rely on cellular and molecular mechanisms are almost always reproducible in *Drosophila*. Focusing in this work, *Drosophila* present many advantages to create a CRC model in the adult midgut. The *Drosophila* adult midgut shares many similarities with the human colon. The *Drosophila* midgut contains similar cell types and cellular organization to the human colon. Moreover, during the last years several reports have described that most of the pathways that control ISC balance and homeostasis in the human colon also control *Drosophila* midgut homeostasis (Casali, 2009; Jiang, 2011).

As disadvantages, the tumorigenic processes that depend on systemic responses such as immunological or inflammatory responses are more difficult to reproduce in a lower-organism model such *Drosophila.* Also the lack of a closed circulatory system in *Drosophila* is a disadvantage. The study of the circulatory system is crucial for the comprehension of the biology of cancer. This is because the creation of new vessels, in a process called angiogenesis, provides the tumour the oxygen requirements and an optimal substrate for the migration of tumour cells towards distant organs by metastasis. Despite of the lack of a closed circulatory system, the role of the circulatory system in *Drosophila* is carried out by the respiratory system that responds to low levels of oxygen creating new branches. Interestingly, the mechanisms that controls both processes are common and both organs respond to similar signals and allow the study of angiogenesis in *Drosophila* (Mortimer, 2009).

Despite its disadvantages, it has been demonstrated that *Drosophila* can develop tumours by natural ways (Salomon, 2008), supporting the use of *Drosophila* to

study tumorigenic processes as something natural and not as an artificial situation. Moreover, metastatic events also have been demonstrated in *Drosophila* (Gonzalez, 2013). Nowadays, cancer-related researches that are in progress in *Drosophila*, could be used in the future scientists to unravel part of the unsolved questions of the disease and the use of *Drosophila* as a massive drug tester will boost the anti-cancer chemical research to find new components to fight against the disease.

1.5 The *Drosophila* adult midgut as a model for stem cell and cancer research

1.5.1 Drosophila Gastrointestinal (GI) tract structure

The *Drosophila* GI tract is the organ that absorbs the nutrients, ions and water from the food. The *Drosophila* GI tract is subdivided in 3 parts and each part has different functions (Royet, 2011). The first segment, the foregut, is a thin tube that transports the food from the oral cavity to the proventriculus. The foregut has two accessory organs, the salivary glands and the crop, a temporary food container cavity. The medial part of the GI tract is the midgut. The midgut is the longest part of the GI tract and is where nutrient absorption mainly takes place. It starts with a pear-shaped structure, the proventriculus, which initiates the mechanical breakdown of the food and secretes the peritrophic membrane, a membrane that will surround the food. The peritrophic membrane is a chitin-based membrane analogous to the mammalian intestinal mucus and plays a dual role: facilitates the nutrient absorption and protects the intestinal epithelial from bacteria and mechanical injury. After the proventriculus, the midgut is subdivided into 3 major regions by differences on the pH and different overall cell morphology (Figure 8). The anterior midgut has a slightly alkaline pH and histologically can be subdivided into 2 subregions (Figure 7). A short and thick zone with a very acidic pH follows the anterior midgut, the iron-cooper region or gastric region, with stomach-like functions. In this region, the big and goblet-shaped iron-copper cells secrete H^+ and other acidic ions similarly to the parietal cells in the mammalian stomach, although the mechanism is still unclear (Shanbhag, 2009). After the iron-cooper region, the alkaline posterior region continues until the zone where the excretory structures, the malpighian tubules, arise and the hindgut starts. A recent paper deeps into the midgut compartmentalization suggesting the existence of 14 specific subregions supported by morphological and genetic evidences, such as the presence of physical constrictions and the specific expression of transcription factors (Figure 7) (Buchon, 2013). The last part of the GI tract is the hindgut, where water and ions are absorbed. It ends in the rectum from where the food leftovers are expulsed. The foregut and the hindgut are ectodermal tissues whereas the midgut develops from the endodermic embryonic layer. During metamorphosis, the larval tissues are removed and the adult gut is generated from the adult midgut progenitor (AMP) cells (Jiang, 2011; Micchelli, 2012).

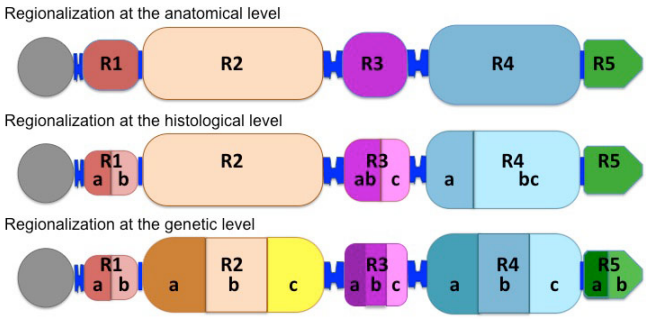

Figure 7. Midgut compartmentalization by 3 different approaches. Taken from Buchon et al 2013

Surrounding the GI tract, there are multiple neurons, two rows of muscles and a large number of trachea, necessary to control food intake and movement and preserve homeostatic balance among other functions (Figure 8).

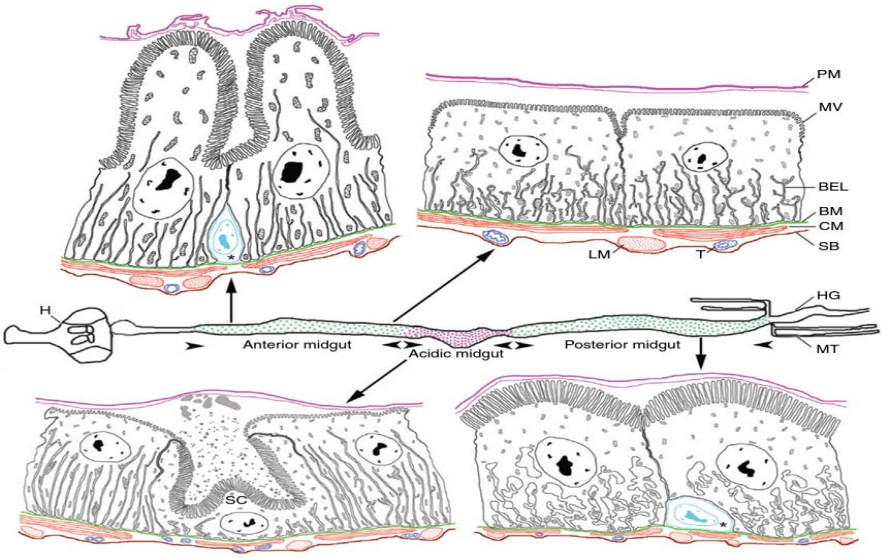

Figure 8. Ultrastructure of the adult *Drosophila* midgut. The midgut subdivides into 3 parts: the anterior and posterior slightly alkaline and the central midgut, acid. The different parts of the midgut have specific overall cellular structures due to determinate absorptive functions. PM: peritrophic membrane, MV: microvilli, BEL: basal extracellular labyrinth, BM: basement membrane, CM: circular musculature, LM: longitudinal musculature, T: Tracheae, SB: serosal barrier, H: head, HG: hindgut, MT: Malpighian Tubule, SC: secretory cell or iron-copper cell. Asterisks mark the ISC. Adapted from Shanbhag, 2009.

1.5.2 Cellular organization of the adult midgut

The *Drosophila* adult midgut epithelium is a pseudo-stratified monolayer of cells. All the cells lie on top of a basement membrane surrounded by 2 layers of muscles, the circular and the longitudinal muscles, and many tracheas. Although all the cells are attached basally to the basement membrane not all reach the epithelial surface facing the GI lumen and this provokes that two rows of nuclei can be visualized. The most basal nuclei are small and correspond to 3 different populations:

the Intestinal stem cells (ISC), the Enteroblasts (EB) and the Enteroendocrine cells (EE), while the most apical nuclei are big, polyploid, and correspond to the Enterocyte cells (EC) (Figure 9). The ISC are the only proliferative cells in the adult midgut and give rise to all the other cell types (Micchelli, 2006; Ohlstein, 2006). The EB is a transient cell type that differentiates to an EC or EE without undergoing mitosis. The last 2 populations are the differentiated cell types and the ones with digestive functions: the EC absorbs the nutrients and water and the EE secretes several hormones to facilitate the digestive process (Veenstra, 2008) (Figure 9). Several markers have been described for each cellular type: High levels of Dl for ISC (Ohlstein, 2007), Su(H) lacZ for the EB, Pros for the EE and finally, Pdm1, MyoIA and MyoIB for the EC (Apidianakis, 2011; Hegan, 2007).

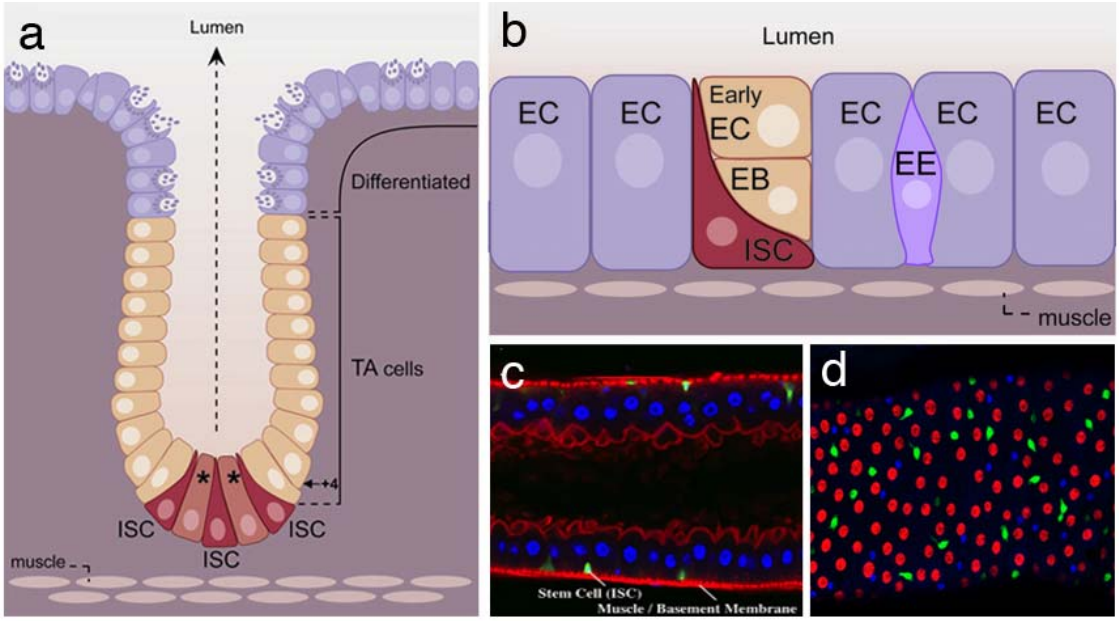

Figure 9. Cell types in the adult midgut. a. Diagram showing the structure of the human colon ISC: Intestinal stem cells TA: Transit amplifying cell b**.** Diagram showing the structure of the adult midgut EC: Enterocyte EE: Enteroendocrine cell M: Muscle. (From Casali 2009) **c**: longitudinal cut of the adult midgut, in red actin, in blue DAPI (from Micchelli, 2006) **d**: midgut epithelia. In green: EsgG4>GFP marks ISC and EB, in blue, Prospero a marker for EE, in red TkvlacZ a reporter for EC

This cellular organization is very similar to the one that exist in humans (Figure 9). In the human colon there are few stem cells that reside at the bottom of the intestinal crypts. This cells eventually divide giving rise to a new stem cell and a transit amplifying cell. The transit amplifying cell is a undifferentiated cell with a high proliferation ratio than the stem cell and produces many daughter cells that differentiate progressively while they migrate towards the surface of the gut. The differentiated cells of the colon are the enterocytes; the enteroendocrine cells and goblet cells, that secrete mucus (Sancho et al., 2004).

1.5.3 ISC and midgut epithelium renewal

The GI tract of all organisms is subject to an important mechanical stress due to a constant transit of food that damages the digestive epithelium. Because of that, the GI tract has a high renewal turnover in order to constantly replenish the gut with new and healthy cells and deplete the old or injured ones. In the adult *Drosophila* midgut, is the ISC population who plays this replacement role. ISCs are small cells that reside at the bottom of the midgut epithelia (Figure 9), a safer place from external bacteria or mechanical stress. The ISCs have the ability to refill the midgut epithelium, giving rise to different cell types (multipotency) including themselves (self-renewal). To pursue this role, ISCs divide asymmetrically, in response to multiple signals, into two new cells types: a new ISC and an EB. The EB will then differentiate into a fully differentiated cell, either an EE or EC (Micchelli, 2006; Ohlstein, 2006) (Figure 10).

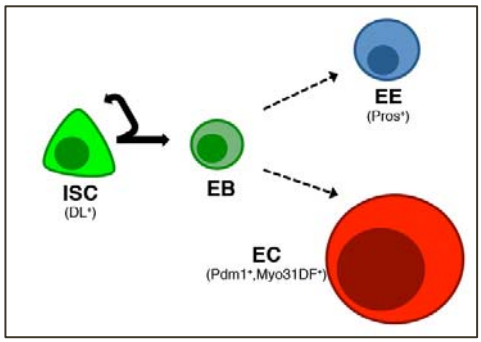

Figure 10. The model of division and differentiation in the adult midgut In Parentheses the most common cell markers for ach cell type.

Despite the simplicity of the model, the system is tightly regulated by several signals such as Wg, EGFR or Notch in order to maintain the correct number of cell divisions that are necessary and sufficient to balance the intestinal homeostasis (Jiang, 2011). The deregulation of any of these signals can lead to the alteration of the intestinal homeostasis and create overgrowths as in the initial steps of CRC (Jiang, 2011). The source and the nature of these signals of surveillance is an intensive and active field of study, both in *Drosophila* and mammals, and several sources have been postulated. One of the principal sources of controlling signals in *Drosophila* is the dying EC. Dying ECs seem to be one of the main regulators of the ISC division processes producing several mitotic signalling molecules, such as cytokines or growth factors, linking the death of old cells with the creation of new ones regulating in this way the intestinal homeostatic balance (Jiang, 2009). Other sources have been demonstrated such as the muscular fibres (Guo, 2013).

1.5.4 The Wingless pathway is a key regulator of ISC division during midgut homeostasis and regeneration.

Due to the central role of the Wnt pathway in the mammalian ISC renewal and its implications in CRC, the role of the Wnt/Wingless pathway has been intensively studied in the *Drosophila* adult midgut. Wingless (Wg) is a secreted molecule that binds to its receptor, Frizzled (Fz). The binding of the ligand to the receptor leads to the phosphorylation of the cytosolic protein Dishevelled (Dsh). Phosphorylated dishevelled blocks the formation of an inhibitory complex formed by the proteins Axin, Shaggy/GSK-3 and Apc. In absence of Wg, this inhibitory complex sequesters and induces the degradation of the Wingless transcription factor Armadillo/β-catenin (Arm). In presence of Wg, the inhibitory complex is not formed and therefore Arm, free in the cytoplasm, can translocate into the nucleus and bind to its co-factor Pangolin/TCF. This complex binds to several target genes activating its transcription (Figure 11) (Seto, 2004).

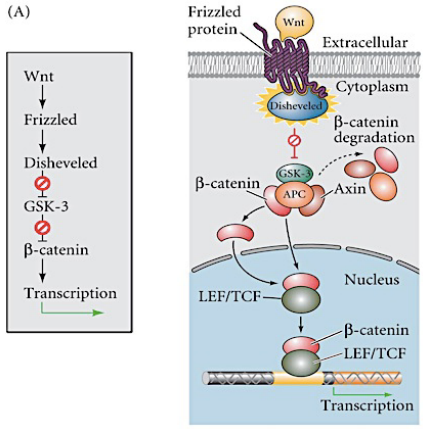

Figure 11. Diagram showing the signalling cascade of the Wingless/Wnt Pathway. From Gilbert S, *Developmental biology,* 9th edition.

In the adult midgut, Wg signalling is necessary for ISC division and self-renewal (Lin, 2008). In homeostatic conditions Wg is expressed and secreted by the visceral muscular layer, proposed to be the ISC niche (Lin, 2008). The constitutive activation of the pathway in ISCs leads to the increase in its mitotic ratio, generating a hyperproliferation, similarly to what happens in mammals. Interestingly, Wg-activated clones show an increase in the number of ISCs, but normal levels of mature cells, suggesting a role in ISC self-renewal but not in differentiation (Lin, 2008). Conversely, ISCs mutant for Fz, Dsh or Arm block almost completely ISC division, although differentiated cells and ISC were found in the clones, suggesting that Wg is necessary for ISC division but not for differentiation neither ISC self-renewal (Lin, 2008). In 2009,

Lee & Micchelli, 2009 refined the role of Wg pathway in midgut homeostasis by looking the function of the tumour suppressor protein, Apc. Lee *et al* demonstrated that Wg signalling controls only the process of division and not the self-renewal of the ISC, while supported the Wg-independent regulation of the differentiation process. Despite of the results, the central role of Wg pathway in ISC division has been discussed due the mild effects of pathway disruption in comparison to other proliferative signals such Jak/Stat and EGFR (Lee, 2009). Recently, 2 different reports from Cordero & Stefanatos showed an important role of Wg pathway during midgut regeneration as well as a crosstalk of Wg with other pathways to perform its role (Cordero, 2012; Cordero, 2012). In the first publication, they suggest an independent regulation of ISC homeostasis and tissue regeneration by Wg. Wg would act in both processes but by two different ways. Wg protein becomes upregulated in the mucosal epithelia after injury, specifically in the Enteroblast, the undifferentiated daughter of the ISC, providing a new source of the Wg pathway ligand. They also demonstrated that is only this source, the EB, and not the muscular Wg, the responsible for Wg activation in the ISC after injury. As a consequence of this role, the blockage of the Wg pathway supress completely the activation of the regeneration program in the ISC. Finally, they demonstrated that Wg acts in the ISC mainly through the activation of the oncogene protein Myc. In the second publication, Cordero *et al* demonstrates that $Apc^{-/-}$ driven hyperproliferation situation is mediated by the downstream activation of Myc and a crosstalk with the Enterocytes. In a hypothetical model, they suggested that the activation of Myc would be sensed by the EC through the release of the EGFR ligand Spitz and the consequent activation of the EGF Pathway in the EC. Then, the EC would secrete the Jak/Stat ligand Ump3 activating in this way the Jak/Stat Pathway in the ISC. Although this paracrine crosstalk and the role of the EC are still unclear, they nicely demonstrate that the paracrine activation of the Jak/Stat is a strict requirement for the hyperproliferation of the ISC in an $Apc^{-/-}$ context. Given these results, it is possible to suggest that the Wg plays a more central role in the division of the ISC in damaged or oncogenic scenarios rather than during homeostasis and normal ISC division. Further studies are necessary to elucidate clearly the role of Wg pathway in the *Drosophila* adult midgut.

1.5.5 EGFR pathway is a powerful mitogenic signal in the Adult Drosophila midgut.

It is generally known the role of the EGFR pathway as a powerful tumorigenic signal, mainly through GOF mutations in two of its components, the oncogenes K-RAS and B-RAF. In CRC, around a 60% of the cases have mutations in this pathway (Network, 2012). The EGFR Pathway is one of the members of the Receptor Tyrosine Kinase family (RTK) and acts mainly through the MAPK intracellular pathway. In *Drosophila*, the EGFR Pathway has 5 secreted ligands: Gurken, Spitz, Vein, Keren and Argos, being the last one an inhibitory signal of the pathway. Except Vein, all the other ligands need to be processed by a serine protease, Rhomboid or Stet depending the substrate, in order to be functional (Shilo, 2003). After this processing, the ligand bounds to the EGF receptor, DER in *Drosophila,* and as a consequence the oncogene protein Ras becomes activated (by the DER-Drk-Sos complex) inducing in this way the activation of the MAPK pathway. The MAPK signalling pathway is a cascade of kinases that phosphorylates other downstream kinases. In *Drosophila,* phosphorylated Ras85D (K-Ras) phosphorylates Pole hole (B-RAF) and this phosphorylates Dsor1 (MEK). Dsor1 then, phosphorylates Rolled (MAPK) and phospho-Rolled activates different transcription factors by phosphorylation such Myc, Fos and Pointed among others sending in this way the signal to the nucleus (Figure 12).

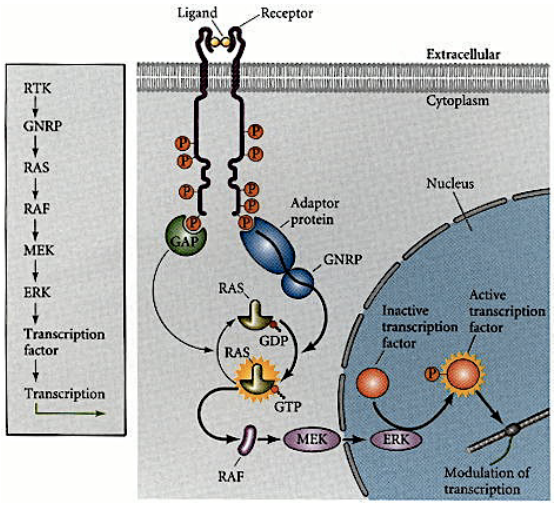

Figure 12. The EGFR and MAPK signalling pathways. From Gilbert S, *Developmental biology*, 9th edition.

In the *Drosophila* adult midgut, the EGFR Pathway acts as a strong mitogenic signal that controls the division of ISC both during normal homeostasis and regeneration. EGFR pathway is activated in normal conditions solely in the progenitor cells as reported by the staining against di-phospho-ERK, the activated form of the

MAPK Rolled. Three ligands are present in the adult midgut: Vein secreted from the visceral muscle and Keren and Spitz expressed and processed in the Enteroblast. The lack or blockage of the EGFR pathway in the ISC blocks completely ISC division in both regeneration and normal conditions and also impinges ISC maintenance. In contrast, the ectopic activation of the pathway leads the midgut epithelium to a hyperproliferative phenotype due to an increase of the mitotic rate of the ISC (Biteau, 2011; Buchon, 2010; Jiang, 2011; Xu, 2011). Additionally, neither activation nor blockage of the EGFR pathway affects the differentiation of the ISC lineage. Other roles have been proposed for EGFR pathway in the Adult Midgut. EGFR pathway is activated in damaged EC after bacterial infection and this activation leads to the delamination of the injured cells. This process is not coupled to the apoptotic program as the blockage of the EGFR pathway after infection stops EC delamination but not EC cell death. Consistently, the activation of the EGFR pathway in healthy EC leads the delamination of those cells without any apoptosis marker staining visible, suggesting that healthy cells are being extruded. In a similar way, EGFR pathway seems to be controlling EC morphogenesis and shape during EB differentiation (Buchon, 2010). Finally, some reports suggest a close relationship of EGFR and Jak/Stat pathways although none of them show a consistent hierarchical relation (Buchon, 2010; Cordero, 2012; Xu, 2011)

1.5.6 The Jak/Stat pathway acts as a paracrine mitogenic signal during homeostasis and regeneration in the Adult Drosophila midgut.

In *Drosophila,* the Jak/Stat pathway is activated by three secreted ligands called unpaireds: Outstretched (Upd), Upd2 and Upd3. Two molecules of the receptor Domeless (Dome) and two molecules of the Janus kinase, Hopscotch (Hop) form the receptor complex. The activation of the receptor results in the phosphorylation of the receptor and the Janus kinase, Hop. This phosphorylated residues act as docking sites for the Stat92E, the signal transducer. Binding to the phosphorylated residues of the receptor, Stat92E becomes phosphorylated by the Janus Kinase and dimerizes being able to translocate to the nucleus where it will bind to the DNA, activating the transcription of several target genes (Figure 13) (Arbouzova, 2006). It is well known the role of the Jak/Stat pathway in several roles related with cell division and germ stem cell maintenance (Arbouzova, 2006). For that reason, Jak/Stat role has been intensively studied in the *Drosophila* adult midgut and has been postuled as one of the

main signalling pathways controlling midgut homeostasis and ISC cell division and self-renewal.

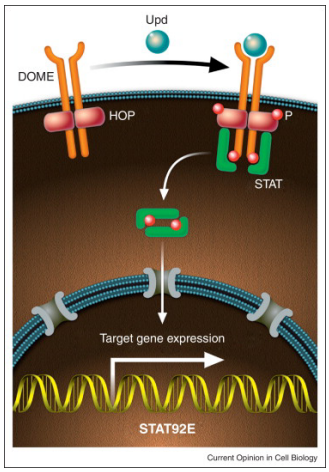

Figure 13. Diagram of the Jak/Stat pathway in *Drosophila*. Adapted from Resende, 2012.

Jak/Stat pathway plays a central role during midgut regeneration. Upd3 is expressed and secreted from the EC. This secretion is restricted to very few EC in normal conditions but largely enhanced in all the midgut EC after bacterial infection. Secreted Upd3 is received by the ISC that starts the cellular division. This crosstalk between the EC and the ISC has been postulated as a homeostatic loop where the damaged cells induce the ISC to create new and healthy cells to take their place. Interestingly, the blockade of the Jak/Stat pathway after injury stops the capability of regeneration of the midgut and the flies die after some hours from infection (Buchon, 2009; Cordero, 2012; Jiang, 2009; Guonan, 2010). On the other hand, in normal conditions, the role of Jak/Stat seems to be more related with the ability of the EB to differentiate as the total blockade of the pathway in the ISC does not block ISC division or survival but turns the EB unable to differentiate (Beebe, 2010). This role of Jak/Stat controlling differentiation has been postulated to be downstream or in parallel to the Notch pathway, which controls primarily the EB differentiation process. Conversely, the overactivation of Jak-Stat in the adult midgut creates a hyperproliferative scenario stronger than the situation created by Wg or EGFR Pathway activation (Beebe, 2010; Liu, 2010).

The results seem to demonstrate that the Jak/Stat pathway would be activated at low levels during midgut homeostasis promoting normal levels of differentiation, whereas a second role activating cell division would imply higher levels of Jak/Stat activation during regeneration after injury or infection.

1.5.7 The Notch pathway controls EB differentiation and restricts ISC division

Stem cell fate maintenance and differentiation are two processed extensively studied and both of them have been related several times with the activity of the Notch signalling pathway, both in *Drosophila* and mammals. The Notch pathway is one of the major signalling pathways and probably the most important juxtacrine signal. Its ligands, in *Drosophila* the proteins Delta and Serrate, are not-secreted proteins that reside in the plasma membranal as transmembranal proteins. For that reason, the activation of the Notch signalling needs cell-cell contact interactions. When the ligand contacts the receptor Notch, an enzymatic complex named γ-secretase cleaves Notch. This cleavage provokes the internalization of the extracellular domain of Notch bounded to the ligand inside the “donor" cell and simultaneously, the internalization of the intracellular domain of Notch, the NICD (Notch IntraCellular Domain) in the “receiving” cell. The NCID goes to the nucleus coupling to the transcription factor Suppressor of Hairless and the coactivator Mastermind activating the transcription of several target genes (Figure 14) (Bray, 2006).

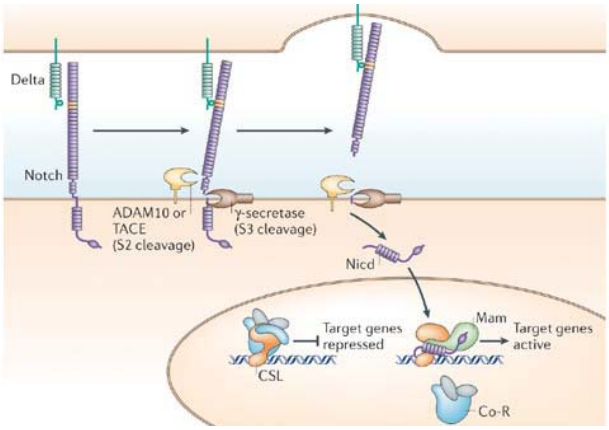

Figure 14. Diagram showing the signalling cascade of the Notch pathway. From Bray S., 2006

In the adult midgut, it has been demonstrated that the Notch signalling pathway is the main regulator of cell differentiation. The expression of the receptor is restricted to the progenitor compartment, both the ISC and EB, while the ligand Delta is expressed at high levels just in the ISC. When the asymmetric division occurs, the expression of Dl keeps restricted in one of the two daughters, the one that will be the new ISC. The molecules of Delta in the new ISC bind to Notch in the other cell, the EB, activating the expression of the Notch target genes forcing the EB to differentiate. Although the mechanism by how the ISC can maintain their stemness is mainly unknown, its has been postulated that the repressor activity of Hairless blocking the

expression of the *Enhancer of Split* complex genes in combination with the expression of the Daughterless transcription factor would be essential to maintain ISC fate by blocking Notch activity in the ISC (Bardin, 2010). Conversely, the induction of the Notch pathway in the EB activates the process of differentiation by the expression of *Enhancer of Split* complex and the inactivation of Daughterless (Bardin, 2010). Furthermore, it has been demonstrated that different levels of Notch expression in the EB lead to a different final cell fate (Ohlstein, 2007). High levels of Notch turn the EB into an EC but low or null levels of Notch pathway transform the cell into a small EE. Interestingly, the total absence of Notch in a clone produces the creation of hyperproliferative clones with a high rate of EE and ISC. In contrast, clones activating Notch block ISC division and bias cell differentiation towards and EC fate creating small EC containing clones. This data suggest a dual role of the Notch pathway promoting EC differentiation and blocking ISC division as well as demonstrates that Notch signal is not essential for EB differentiation towards EE.

1.5.8 Dpp pathway acts as a cytostatic signal in the adult Drosophila midgut and is an essential factor for proper gastric region formation.

Dpp signalling controls several processes during *Drosophila* development such as wing patterning, leg formation or early embryo development. The main ligand is Decapentaplegic (Dpp), which is a secreted molecule that creates a gradient from the source. It binds to a heterodimeric complex formed by the type I and II receptors: Punt and Thickveins (Put and Tkv), respectively. These two proteins are serine-threonine kinases that phosphorylate themselves respectively and phosphorylate the nuclear transducer Mother against Dpp (Mad). The phosphorylation of Mad allows the co-transducer Medea (Med) to bind to Mad and to form a complex that enters to the nucleus and activates several target genes (Figure 15). Many negative regulators of the pathway have been described such as Daughters of Dpp (Dad), a target gene of the pathway, co-repressors such as Brinker or Shnurri or diffusible negative ligands such as Short gastrulation (Sog).

Many of the aforementioned signalling pathways play a role in the induction of ISC division with the exception of Notch pathway. Recently, few papers tried to elucidate the role of the Dpp signalling pathway in the adult *Drosophila* midgut. Two different roles have been proposed for Dpp signalling pathway in the *Drosophila* midgut. First, Dpp has been described as an essential signal for proper copper cell

specification in the gastric region of the midgut. Loss of Dpp signal produces the disappearance of the copper cell region in the adult *Drosophila* midgut (Guo, 2013; Li, 2013). Dpp signal is essential for proper copper cell region specification and although it has been suggested that the overexpression of Dpp signal can lead to an expansion of the copper cell region towards the anterior midgut it has not been corroborated by other publications (Guo et al., 2013; H. Li et al., 2013). Hence, a more careful analysis should be performed to elucidate this issue. Additionally, Dpp has been described as a negative regulator signal for ISC division in normal conditions and during regeneration (Guo, 2013; Li, 2013). The specific deletion of Dpp signalling in ISC increases the number of dividing ISC along the midgut whereas an overexpression of it provokes a blockade in ISC division rate. Although the existence of alterations in ISC division rate, Mad or Tkv null clones show differentiated cells, suggesting that Dpp is essential to restrict ISC division rate but is dispensable for ISC daughter cell fate (Guo, 2013). A previous report suggested that Dpp will act non-autonomously in EC to control ISC division rate (Li, 2013) but further publications are contradictory with this data. In addition, some experiments suggest that Dpp can be induced by Jak-Stat pathway during regeneration and also suggest a requirement of EGFR pathway in the Dpp-depletion phenotype (Guo, 2013).

Further analysis are required to understand and characterize the role of Dpp in the normal homeostasis in the *Drosophila* adult midgut. The analysis should specially focus in which are the emitting and responding cells because the data about the normal expression patterns of the different components is still confusing and controversial.

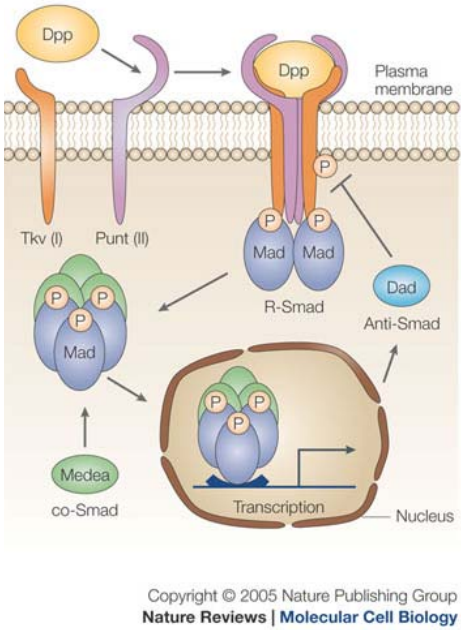

Figure 15. Diagram of the ocmponents of the Dpp signalling pathway. (Häcker, 2005)

1.5.9 Other Pathways involved in the Drosophila adult midgut homeostasis and ISC maintenance.

Many pathways have been involved in the adult midgut homeostasis and in the control of the ISC proliferation. In addition of the aforementioned ones, several papers have proposed other different pathways as regulators of some aspects of the adult midgut homeostasis.

The activation of the JNK (*Drosophila* Jun N-terminal Kinase) pathway is a general response to stress or injury signals and there are several evidences that the pathway is activated in the adult midgut after injury or bacterial infection rather that in homeostatic conditions (Biteau, 2008). The pathway seems to be an activating signal of the Jak/Stat and EGFR pathways in the ISC by promoting the secretion of the respective ligands in the damaged EC. Also it is activated in the ISC after bacterial infection, mediating by both ways ISC division in response to damage. The role of JNK pathway under homeostatic conditions is still controversial, but it has been suggested that its activation is related with the aging and acts as a protective signal. The lacking of the pathway in homeostatic clones seems to not affect ISC survival, probably because it is not active in young flies, while the overactivation leads to a hyperproliferation of ISC, activating the stress program in the ISC (Biteau, 2008).

Many publications have explored the role of the Hippo pathway in the *Drosophila* intestine. Hippo signalling pathway, known by its anti-proliferative effects, has an important role in the adult midgut regeneration although its role in gut homeostasis seems not relevant. The suppression of the pathway in the ISC slightly increases ISC proliferation, whereas yki RNAi has no effect, suggesting that Hippo pathway is not necessary under homeostatic conditions. Strikingly, the blockade of the Hippo pathway in the mature EC leads to a fully hyperproliferative scenario, principally by the secretion of Upd and EGFR ligands, being a mitogenic boost such as the JNK activation. Additionally, Hippo pathway is overactivated in EC after bacterial infection inducing ISC division. This paracrine effect suggests, as in JNK activation scenario, an important role of Hippo pathway during regeneration more that a direct contribution in the ISC homeostasis (Karpowicz, 2010; Ren, 2010; Shaw, 2010; Staley, 2010).

Recently, two different receptor tyrosine kinases pathways, the insulin receptor (InR) and the PDGF- and VEGF-receptor related (Pvr) pathways, have been involved in the control of ISC division. The activation of InR affects negatively ISC division and positively EB differentiation towards EC. Conversely, the lack of InR pathway impairs

EB differentiation into EC as well as ISC normal division rate (Choi, 2011). Pvr is normally expressed in ISC and its overexpression leads to a hyperproliferative condition. In contrast, the lack of the pathway blocks ISC division as well as EB differentiation (Bond, 2012).

Some other molecular mechanisms have been identified to have a role in ISC proliferation and maintenance such as the redox in the gut (Hochmuth, 2011), the role of integrins in the asymmetric division process (Goulas, 2012) or the presence of matrix metalloproteinases (Lee, 2012).

Signalling pathway	Gain of function	Loss of function
Wingless	Hyperproliferation, increase of ISC, normal differentiation	No cell division, normal differentiation, presence of ISC
EGFR	Hyperproliferation, normal differentiation	No cell division, ISC depletion
Jak/Stat	Hyperproliferation, normal differentiation	EB differentiation failure
Notch	No cell division, EC-fate differentiation	Hyperproliferation, EC lacking clones.
Dpp	Reduction in cell division	Uncontrolled hyperproliferation after damage
JNK	Hyperproliferation, misdifferentiation, *Hyperproliferation*	No effect, *reduction of ISC division after damage*
Hippo	No effect, *reduction of ISC division after damage*	Slight increase in cell division, normal differentiation, *Hyperproliferation*

Table 1. Effects of the activation or depletion of the main signalling pathways in the midgut. Normal letters refers to an autocrine effect in the ISC and their progeny. *Italic letters refers to non-autonomous effect in the ISC lead by expression on mature EC.*

1.5.10 Other Intestinal Stem Cells in Drosophila

Other ISCs have been described as independent pools of stem cells in the *Drosophila* gut. There are few evidences of their existence, so a stronger effort to elucidate their role its necessary in the next years. Gastric Stem Cells (GaSC) are a specific and a small pool of dividing cells in the proventriculus of the midgut (Singh, 2011). They are able to divide and differentiate and the authors suggest a migratory behaviour of its descendants. Also, they suggest a role for Jak/Stat, Wg and Hedgehog pathways in division, self-renewal and differentiation of the GaSC, respectively. Further studies are required to corroborate this data as any other paper has confirmed their existence.

Other putative Gastric Stem Cells have been discovered in other part of the midgut, reflecting the lack of consensus about anatomic homologies when comparing *Drosophila* and Mammalian structures. This new so-called Gastric Stem cells, GSSC, are mainly quiescent and they reside in the Fe/Co region in the middle of the midgut. These cells divide very infrequently and give rise to the very specialized acid secretory cells. In addition, Wg signalling has been involved in GSSC self-renewal and maintenance (Strand, 2011).

Finally, although putative hindgut stem cells were described in the midgut/hindgut border (Takashima, 2008), proper lineage tracing experiments demonstrated that that cells were not proper stem cells but dividing cells in response to damage. (Fox, 2009)

Objectives

2. Objectives

The progression from normal epithelia to malignant tumour during CRC progression is still a not fully understood process. The role of many signalling pathways and transcription factors is mainly unknown. For this reason, the creation of new cancer animal models is a very useful tool to reach the fully comprehension of the CRC. In this context, the main aim of this thesis was to establish and characterize a *Drosophila* model for CRC to further understand the tumoral processes and identify new genes involved in CRC progression. In consequence, the specific objectives are:

- Due to the relevance of inactivating mutations on the gene APC and activating mutations of the gene K-RAS in CRC progression, the main aim of this work was to establish and characterize clones bearing and inactivating allele of Apc and a activating allele of Ras genes in the *Drosophila* adult midgut as a model for CRC.

- Perform a transcriptional profile of Apc Ras cells to identify new putative genes and functions involved in tumour progression.

- Due to the critical role of TGF-β as a growth barrier during CRC progression we decided to investigate the role of the Dpp pathway during Apc Ras clone progression.

Materials and methods

3. Materials and methods

MARCM technique

The *Mosaic analysis with a repressible cell marker* or MARCM technique is a genetic technique used in *Drosophila* to create labelled clones of homozygous mutant cells in a heterozygous background. As a clone, all the cells come from a single progenitor. In addition to become mutant, the clones can express one or more transgenes by the use of the Gal4 system.

The technique relies in the existence of the FLP/FRT system in the cells of the organism. The FLP/FRT is a site-specific recombination system where a recombinase enzyme called Flipase (FLP) binds to FRT sequences and induces the recombination between sister chromatids. In MARCM the expression of the FLP normally is under a heat shock promoter that permits to activate the gene when is necessary. Hence, when heat is applied to the flies a stochastic recombination takes place in the FRT sequences specifically in those cells that are dividing in the moment of heat induction. For that reason, a division in the first cell is necessary to allow the creation of the MARCM clones.

In the MARCM clone additionally the GAL4/UAS system is used to drive the expression of one or more transgenes. One of this transgenes is typically a fluorescent protein that permits to label the cells. Although the existence of the GAL4 protein in the cells, the expression of the UAS transgenes is restricted to the labelled mutant cells. This is because all the cells contain one copy of GAL80 protein, the repressor for the GAL4 protein, blocking in this way UAS transgene expression. With the heat shock, some cells recombine the FRT sites and become homozygous for the mutant allele. In addition, the recombination produces the loss of the GAL80 transgene and consequently the expression of the UAS transgenes starts. In this way, only the cells that are homozygous for the mutant allele are visualized by the expression of a coloured reporter.

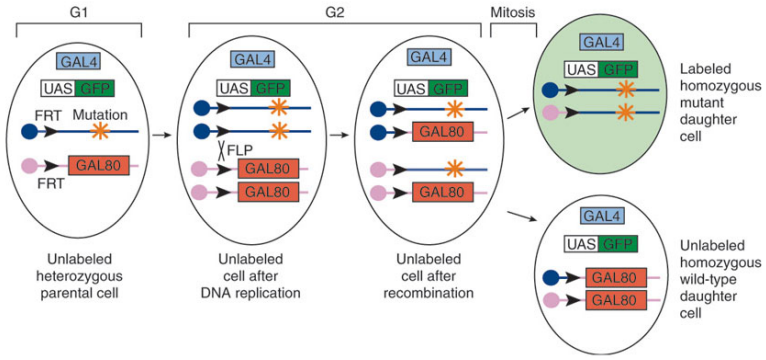

Figure 16. Scheme of MARMC clone formation. (Adapted from Wu & Luo, 2006)

Generation of MARMC clones

MARCM clones were generated by a 1hr heat shock at 37ºC of 2-7 days old females and marked by the progenitor cell marker escargot (esg) Gal4 line driving the expression of UAS GFP. Although esg is expressed only in the progenitor cells (ISCs and EBs), the amount of GFP produced in our experimental conditions was enough to be detected also in EEs and ECs in MARCM clones.

Genotypes

yw UAS flp ; esg Gal4 UAS-GFP/CyO; FRT82B Gal80/TM6b flies and *yw hsp70-flp; esg Gal4 UAS-GFP UAS-Ras^{V12}/Cyo; FRT82B Gal80/TM6b* were used as a driver lines to generate MARMC clones. These lines were crossed with *yw hsp70-flp;sp/Cyo; FRT82B/TM6b* flies and *yw hsp70-flp;UAS-Ras^{V12}/Cyo; FRT82B Apc2^{N175K}Apc^{Q8} /TM6b* flies to generate wild type, Apc, Ras and Apc Ras clones.

yw hsp70-flp; esg Gal4 UAS-GFP UAS-Ras^{V12}/Cyo; FRT82B Gal80/TM6b were crossed with *yw hsp70-flp;UAS-Tkv^{Q253}/Cyo; FRT82B Apc2^{N175K}Apc^{Q8} /TM6b*, *yw hsp70-flp; Sp/Cyo; FRT82B Apc2^{N175K}Apc^{Q8} UAS-Mirr RNAi /TM6b, yw hsp70-flp;UAS-Tkv^{DN}/Cyo; FRT82B Apc2^{N175K}Apc^{Q8}*, *yw hsp70-flp;UAS-Tkv^{DN}/Cyo; FRT82B Apc2^{N175K}Apc^{Q8} UAS Mirr RNAi* to generate the Apc Ras Tkv* and Apc Ras Mirr^{RNAi}, Apc Ras Tkv^{DN} and Apc Ras Tkv^{DN} Mirr^{RNAi} clones.

yw UAS flp ; esg Gal4 UAS-GFP/CyO; FRT82B Gal80/TM6b flies were crossed with *yw hsp70-flp;UAS-Tkv^{Q253}/Cyo; FRT82B/TM6b , yw hsp70-flp;sp/Cyo; FRT82B Mirr RNAi/TM6b* flies and *yw hsp70-flp;sp/Cyo; FRT82B UAS Mirr /TM6b* flies to generate Tkv*, Mirr RNAi and UAS Mirr clones.

yw hsp70-flp; esg Gal4 UAS-GFP/Cyo; Tub>Gal80^{ts}/TM6b were crossed with *w; UAS-Tkv^{Q253}/Cyo* or *w; Sp/CyO; UAS-Mirr RNAi/TM3* to express Tkv^{Q253} or Mirr RNAi in the progenitor cells. Adult flies were kept at 29ºC for 10 days to allow the expression of the UAS constructs. Apc2^{N175K} is a loss-of-function allele, Apc^{Q8} is a null allele, UAS-Ras^{V12} and UAS-Tkv^{Q253} are gain-of-function transgenes. Stocks were obtained form Bloomington Stock Center and VDRC and as a personal gifts.

Staining of *Drosophila* adult midguts

Adult female flies were dissected in PBS. All the digestive tract was removed and fixed in PBS and 4% electron microscopy grade paraformaldehyde (Polysciences, USA) for 35-45 minutes at room temperature. Samples were rinsed 3 times with PBS, 2% BSA, 0.1% Triton X-100 (PBT-BSA), incubated with the primary antibody overnight at 4°C and with the secondary antibody for 2 hours at room temperature. Finally, the samples were rinsed 3 times with PBT-BSA and mounted in DAPI-containing media (Vectashield, USA). All the steps were performed without mechanical agitation.

Antibodies

Primary antibodies mouse α-Pros (1:50), α-Dl (1:10), α-Dlg (1:250), α-Mmp1 (1:50), and α-Sn (1:50) were obtained from the Developmental Studies Hybridoma Bank (DSHB), rabbit α-PH3 (1:100) from Cell Signalling (USA), rabbit α-Pdm1 (1:1000) was a gift of Dr.Yang Xiaohang (Institute of Molecular and Cell Biology, Singapore), rabbit α-laminin (1:1000) was from Sigma (USA), rabbit α-Mirror (1:1000) was a gift of Dr. Helen McNeill (Samuel Lunenfeld Research Institute, Toronto), rat α-Ara/Caup (1:200). Secondary antibodies were from Invitrogen (USA). TRICT-conjugated Phalloidin (Sigma, USA) was used at 5µg/ml.

Image processing and quantifications

Images were obtained on a Leica SPE or Leica SP5 confocal microscopy and processed in Photoshop CS5 (Adobe, USA). GFP area was calculated using ImageJ 1.34s (Rasband, W.S., http://rsb.info.nih.gov/ij/). Statistical analysis and graphics were performed applying the Wilcoxon Signed-Ranks Test using R software package (R development Core Team). Differences were considered significative when $p<0.05$.

Intestinal physiology assays

Defecation assays were performed and quantified as previously described (Cognigni, Bailey, & Miguel-Aliaga, 2011). At least 20 flies of each genotype were monitored over the course of four weeks in fly vials with standard food at 25^{o}C. Once a week, they were individually transferred to clear plastic cuvettes containing the same food supplemented with 0.5% bromophenol blue for 72 hours. Digital images of the cuvette walls were obtained using an Epson Perfection 4990 Photo scanner. After each defecation assay, flies were transferred to food without the dye in order to monitor the dye's intestinal transit.

Cell purification and RNAi extraction and amplification

Drosophila midguts were dissected from control, Apc or Apc Ras flies four weeks after induction. In order to obtain single cell suspensions, samples were incubated in PBS containing 0,4mg/ml dispase (Gibco) for 15 min at 37ºC, syringed using a 27G needle and washed twice with PBS. After selecting for the viable population (propidium iodide negative), GFP^{+} cells were isolated by fluorescence activated cell sorting (FACS) using a FACSAria 2.0 (BD Biosciences) and RNA was extracted and amplified as recently described (Gonzalez-Roca et al., 2010).

Differential expression analysis

All microarray statistical analyses were performed using Bioconductor (Gentleman et al., 2004). Background correction, quantile normalization and median polish summarization was performed as implemented in Bioconductor's affy package (Gautier, Cope, Bolstad, & Irizarry, 2004).

For all samples with biological replicates (WT, APC, RAS and APC-RAS at 1 week and WT, APC and APC-RAS at 4 weeks), the Bioconductor's phenoTest package was used to find differentially expressed genes between groups of interest. Only genes with a Bayesian posterior probability of differential expression (PDE) > 0.95 and an absolute fold change value (FC) > 2 were considered as differentially expressed.

For finding differentially expressed genes between the individual RAS sample at 4 weeks and the rest of the groups, fold changes between the expression estimates for the RAS at 4 weeks sample and the mean expression estimates for each one of the other groups were computed after MA mean and variance normalization using the GAM method. An empirical Bayes partial density model was used to obtain Bayesian posterior probabilities of differential expression and again only genes with PDE>0.95 and |FC|>2 were considered as differentially expressed.

Gene Set Enrichment Analysis

The GSEA pre-ranked tool was used to perform Gene Set Enrichment Analysis (Subramanian et al., 2005) on Gene Ontology (Biological Process, Cellular Component and Molecular Function) and Kyoto Encyclopedia of Genes and Genomes (KEGG) gene sets.

All genes in the array were ranked by mean fold change at gene level for the APC-RAS vs WT at 1 week, APC-RAS vs WT at 4 weeks, APC vs WT at 1 week and RAS vs WT at 1 week comparisons, and the lists were used for performing the analyses. Gene sets were obtained from the Bioconductor GO and KEGG packages, and *Drosophila melanogaster* gene to gene set association information was retrieved from the Bioconductor annotation package for the Affymetrix GeneChip *Drosophila* 2.0 array. Gene sets were filtered to exclude from the Gene Set Enrichment Analysis those with more than 500 genes or less than 15. We used the GSEA pre-ranked algorithm using 1000 permutations and the weighted enrichment statistic. The gene sets showed in the list are those with a nominal p value <0,05.

Microarray data analysis

Venn diagrams were performed using the online application Oliveros, J.C. (2007) VENNY. *An interactive tool for comparing lists with Venn Diagrams,* http://bioinfogp.cnb.csic.es/tools/venny/index.html.

qPCR protocols and primers

Gene expression levels were assessed using Power Sybr Green quantitative PCR (Applied Biosystems) following the manufacturer's instructions. Actin 5C was used as an endogenous control for normalization and differences in target gene expression were determined using the StepOne 2.0 software (Applied Biosystems). All measurements were performed in triplicate from three independent sorting experiments. Primer pairs for each gene were the following:

Ara forward) GGCCAAAGATGAGACCAAAG
Ara reverse) GCTGATGATGATACGGATGG
Dad forward) TTTGAAACCAATAGGGCTGA
Dad reverse) TCACCGCAGATGACTAAAGTG
Dl forward) GAGCAAGTCGAGTGTCCAAA
Dl reverse) GCACCAACAAGCTCCTCAT
Fz3 forward) TGCTCTGCTCGTCTCTGTTT
Fz3 reverse) ATGCACAACTCGTGCTTCTC
Mad forward) GGAGACCTGTAATCGTCCGT
Mad reverse) GGCTCGCTATTCTCCTTCAC
Med forward) CTGCTCACTCACTCCCTGTG
Med reverse) CGGCATTAACTGATCCATTG
Mirror forward) CAACAGCTATGGCATGGATT
Mirror reverse) TCAGTCTTCTTCTCGCGTTG
Myo31DF forward) GATCCAGGTGAAGAGACGGT
Myo31DF reverse) TTCCAAACCATTGAGGATGA
Optix forward) TGGGCAACTTCAGGGAAC
Optix reverse) ACTTCTTTCGCACCCGATAC
Pro forward) CCGATGATCTGTTGATTGCT
Pro reverse) GGTACCTCAATGTGGTTATTGC
Put forward) CCACATCCTGATTGTTGAGC
Put reverse) GCATGGGCCTTCTTCTCTAC
Rho forward) CTCCATCATTGAGATTGCCA
Rho reverse) GACGATATTGAAGCCCAGGT
Sn forward) AGGATCTGCATAAGATCGCA
Sn reverse) CAGCTGCGTGGATCAATAAT

Stat92e forward) GTTGCGACTGGATCTCTGAC

Stat92e reverse) ATCTGCTTGAACAGGTGCAG

Tkv forward) AGACCAGAAATGGCACACAA

Tkv reverse) TTTCCTTCCGACATGTCATC

Bioinformatic search of regulatory transcription factors

The matScan software (Blanco, Messeguer, Smith, & Guigó, 2006) was used to scan promoter regions of 2000 nucleotides upstream of the genes of interest for possible binding sites for known transcription factors. Genomic coordinates were obtained by the biomaRt package of Bioconductor (Durinck et al., 2005) with the dm3 version of the *Drosophila melanogaster* genome. We used 123 position weight matrices (PWM) from the JASPAR database (Vlieghe et al., 2006). Results were filtered by the default value of the matScan software (hits above 80% of the maximum possible score value). To further refine the candidate hits, we performed a permutation test by randomly selecting 500 regions of 2000 nucleotides from the dm3 genome and repeating the analysis for all PWMs. We used a cutoff of 0.005 for the resulting p-values. Finally, we downloaded the evolutionary conservation track from UCSC (Fujita et al., 2011) for 14 species close to *Drosophila melanogaster* and filtered out hits with mean scores lower than 0.9. The matScan software was also used to scan promoter regions of 2000 nucleotides upstream of the main components of the TGF-b pathway (TGFBR1, TGFBR2, SMAD2, SMAD3, SMAD4, SMAD6, SMAD7) for possible binding sites for IRX transcription factors. Genomic coordinates were obtained by the biomaRt package of Bioconductor with the hg19 version of the Homo sapiens genome. We used 6 position weight matrices (PWM) for IRX genes from the uniProbe database. In particular, we found matrices for IRX2, IRX3 (2 matrices), IRX4, IRX5 and IRX6. Results were filtered using the default value set by matScan (hits above 80% of the maximum possible score). To further refine the candidate hits, we performed a permutation test by randomly selecting 1000 regions of 2000 nucleotides from the hg19 genome and repeating the analysis for all PWMs. We used a cutoff of 0.002 for the resulting p-values. Finally, we downloaded the evolutionary conservation track from UCSC for 46 species close to Homo sapiens and filtered out hits with mean conservation scores lower than 0.7.

Cell lines and transfections

Human adenocarcinoma cell lines from rectum (SW837), cervix (HeLa) or mammary gland (MDA-MB-231) were cultured under standard conditions in DMEM 10%FBS, and transfections were performed using PEI (polyethylenimine) reagent (Polysciences Inc.).

Irx knock down

Downregulation of human Irx3 or human Irx5 was achieved by transfecting HeLa or MDA cells with shRNA constructs from the MISSION TRC-Hs 1.0 shRNA library (clones TRCN0000016900 for Irx3 and TRCN0000018302 for Irx5). Cells transfected with a non-targeting shRNA (SHC002) were used as a control. Knock down efficiency was tested by quantitative RT-PCR.

Quantitative RT-PCR of human genes

All human qRT-PCRs were performed using TaqMan Gene Expression Assays (Applied Biosystems). Irx3: Hs01124217_g1, Irx5: Hs00373920_g1, Smad3: Hs00969210_m1. PPIA (Hs99999904_m1) and GAPDH (Hs99999905_m1) were used as endogenous controls for normalization.

TGF-β reporter assay

SW837 cells were cotransfected with the pCAGA-Luc12X Firefly luciferase TGF-β reporter (Dennler et al., 1998), the Renilla luciferase plasmid pRL-TK (Promega) and human Irx3 or human Irx5 cDNAs. 36h after transfection recombinant TGF-β was added to cells for 16h and luciferase activity was measured using the Dual Luciferase Reporter Assay System (Promega). TGF-β pathway activation was determined by normalizing the Firefly luciferase activity with Renilla luciferase activity.

Results

4. Results

1 Establishment and characterization of a colorectal cancer model in *Drosophila*

1.1 Co-activation of Wingless and Ras pathways induces overgrowths in the Drosophila adult midgut

Human colorectal cancer (CRC) usually starts with activating mutations in the Wnt signalling pathway that transform the normal epithelium to a benign adenoma. In 85% of CRC cases this activation is due to mutations that supress the activity of the Wnt negative regulator APC (Sancho, 2004). Further progression towards carcinoma is driven, in 50% of CRCs cases, by activating mutations in the K-RAS oncogene (Network, 2012). Despite the essential role of these two pathways in CRC little is known about which genes regulated by these pathways, play key roles in tumour progression and contribute to the cancer phenotype. In order to identify these key driver genes we decided to use the *Drosophila* adult midgut as an *in vivo* model system. Hence, we generated a CRC model by activating the same signalling pathways that drive CRC early progression. We induced MARCM GFP+ clones bearing mutations for both Apc genes present in the *Drosophila* genome, Apc and Apc2, and overexpressing the oncogenic form of Ras, Ras^{V12} (Apc-Ras clones). As controls, we generated wild-type clones; clones mutant for both Apc genes (Apc clones) and clones overexpressing Ras^{V12} (Ras clones). Of note, MARCM clones require a mitotic division in order to be generated. Therefore, they were generated specifically in the ISCs, the only dividing cells in the adult midgut. Finally, we decided to analyse the clones at one week and four weeks after clone induction in order to analyse the general progression of the clones.

We first noticed that flies bearing Apc-Ras clones show a lower survival rate than controls flies four weeks after clone induction (ACI) (Figure 17).

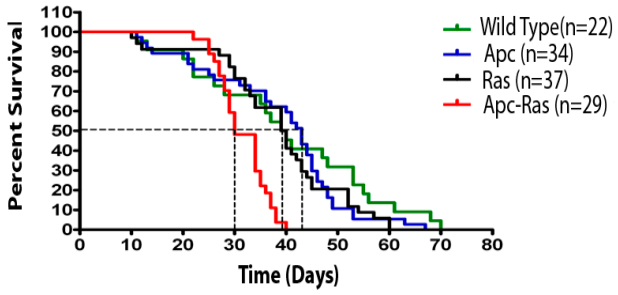

Figure 17. Fly survival after clone induction. At four weeks ACI Apc-Ras survival rate was reduced to a 50%. In contrast, control flies showed higher survival rates at this time point. Interestingly, none of the flies bearing Apc-Ras clones survived further than 40 days, while other genotypes could reach 60 or 70 days of maximal survival rate.

To start characterizing the clones we measured three physical parameters: clone number, clone size and clone distribution (Table 2). One week ACI, Apc-Ras clones were scattered along the gut and were similar in size to Apc clones, and slightly larger than WT or Ras clones. However, no dramatic differences were observed in clone number or distribution. Conversely, at four weeks ACI most of the Apc-Ras clones were dramatically enlarged and appeared mostly restricted to the most-anterior part of the anterior midgut, in contrast to wild type clones that remained small and scattered along the gut. Similarly, Apc clones slightly increased their size between one and four weeks ACI, but they did not suffer changes in clone number nor distribution. Of note, a small decrease in clone number could also be observed in wild type clones. We propose that this small decrease is due the disappearance of those clones that have been generated in the EB and not in the ISC during clone induction in the dividing ISC. All these unicellular transient clones cannot divide and consequently, they differentiate and die without descendants disappearing from the epithelia after some days. Finally, at four weeks ACI Ras clones had almost disappeared from the midgut epithelia, remaining just few of them mostly occupying the gastric region (Figures 18 and 19 and Table 2). In summary, four weeks ACI Apc-Ras clones showed a strong tendency to overgrowth and to be located in the most anterior part of the midgut while wild type and Apc clones remained small distributed homogeneously between the anterior and posterior midgut, but hardly present in gastric region. In contrast, Ras clones were mainly restricted to the gastric region. We propose that the observed effect on clone spatial restriction in Apc-Ras and Ras is reflecting regional differences in the adult midgut that are affecting clone survival.

Our results show that the co-activation of Wg and EGFR pathways in the adult midgut is enough to induce overgrowths that are never present in single-altered clones, indicating a synergic activity of both signalling pathways. Of note, this effect of Apc-Ras on midgut cell proliferation has been confirmed by a recent publication (Wang, 2013).

Genotype	Week ACI	n	Number of clones (num clones ± SD) A	M	P	Clone size (GFP⁺ area/domain area ± SD) A	M	P	Clone distribution (GFP⁺ area/total area ± SD) A	M	P
Wild Type	1	8	37,5±10,5	1,6±1,7	57,9±13,3	3,1±1,6	0,1±0,1	2,9±1,7	48,8±10,0	0,3±0,3	51,0±10,2
Apc	1	10	29,8±7,4	5,9±3,8	39,8±13,6	8,0±7,0	2,0±1,5	10,7±4,8	31,9±12,5	1,7±1,2	66,4±12,4
Ras	1	9	15,2±5,3	5,0±1,7	15,7±9,9	3,4±1,9	15,9±15,4	2,5±2,8	38,8±19,5	30,6±19,5	30,6±22,6
Apc-Ras	1	10	22,9±8,4	4,6±3,1	23,5±6,3	7,4±3,6	8,2±9,1	4,5±2,4	52,1±15,5	9,9±9,5	38,0±17,8
Wild Type	4	10	25,5±7,3	7,8±4,5	24,2±4,1	2,7±1,5	3,7±2,6	3,9±2,1	37,7±12,1	9,3±6,7	53,0±13,0
Apc	4	10	32,6±10,1	6,9±5,1	37,2±6,5	11,4±7,7	1,5±1,8	15,3±7,5	36,3±18,7	0,7±0,8	63,0±18,5
Ras	4	12	1,5±1,2	2,2±1,1	2,4±2,0	0,2±0,2	11,6±7,0	0,4±0,5	10,1±10,3	75,6±12,5	14,2±14,5
Apc-Ras	4	19	3,3±2,3	2,5±1,8	3,2±2,8	26,1±16,4	18,6±25,1	2,5±4,6	81,8±22,4	11,0±14,8	7,2±14,2

Table 2. Quantification of the number, size and distribution of the clones of the different genotypes analysed. (A) anterior midgut, (M) Fe/Cu domain, (P) posterior midgut. (ACI) after clone induction.

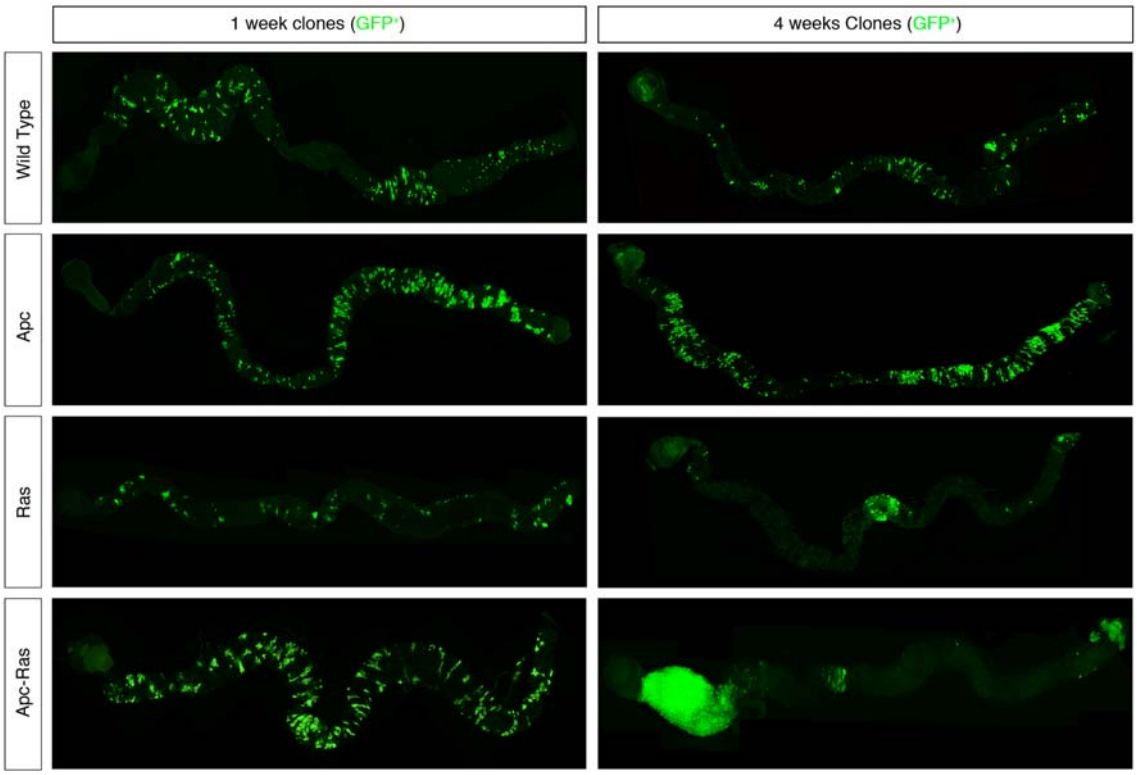

Figure 18. General overview of the MARMC clones in the adult midgut. In green clone cells induced by MARCM technique. Observe the dramatic grow of Apc-Ras clones at four weeks ACI.

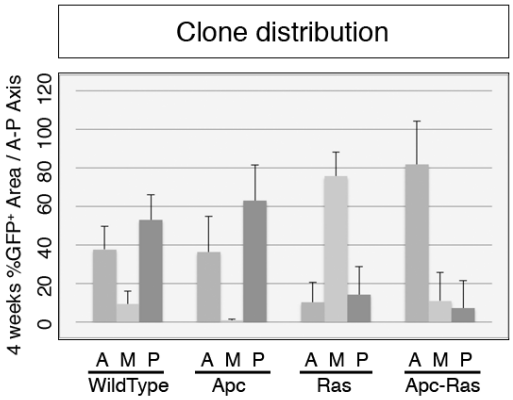

Figure 19. Clone distribution in the Adult midgut four weeks ACI.
The clones do not distribute uniformly through the gut at four weeks ACI. Wild Type and Apc clones distribute between anterior (A) and posterior (P) regions, but rarely in the central region (M). In contrast, Ras clones are mainly located in the central region. Apc-Ras clones are mainly located in the most anterior gut.

1.2 Ras-activated clones delaminate from the epithelia via activation of Cdc42

The increase of clone area observed during Apc-Ras clone progression correlated with an important reduction in clone number (Figure 20 and Table 2). In particular, the number of Apc-Ras clones was reduced from 23 one week ACI to 3.3 four weeks ACI in the anterior region (Table 2). Similarly, the number of Ras clones also decreased, although in this case correlated with a strong reduction of clonal area (Figure 20). Remarkably, this decrease on clone number was not observed in Wild Type or Apc clones (Figure 20).

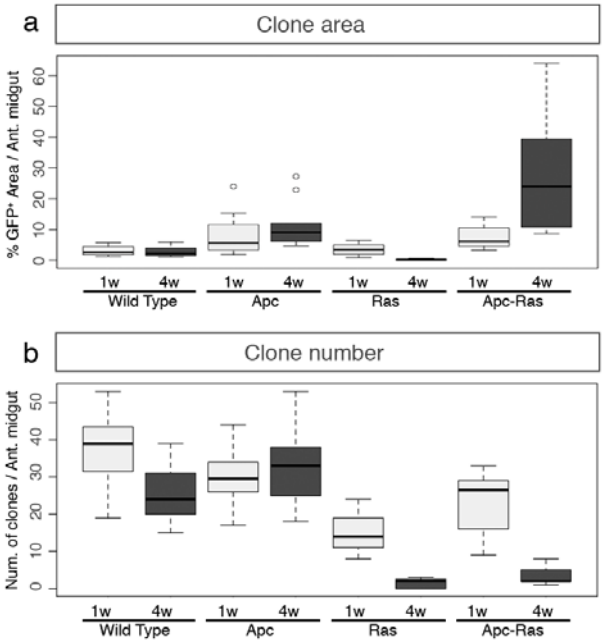

Figure 20. Clone size and number. a.- box-plot for the % GFP area in the anterior midgut. Observe the increase in Apc-Ras area**. b.-** Box-plot for the number of clones in the anterior midgut. Note the decrease of clone number at four weeks ACI in Ras and Apc-Ras guts.

In this context, we postulated the existence of a Ras^{V12}-driven mechanism in the adult midgut that would affect clone survival, inducing the disappearance of Ras^{V12}-expressing clones from the epithelia. We sought to determine which mechanism was driving this effect focusing in two alternative mechanisms: apoptosis or clone delamination, this last due to the results shown in previous reports about Ras^{V12}-induced cell delamination in mammals and *Drosophila* (Buchon, 2010; Hogan, 2009).

In order to analyse whether apoptosis was playing a role in the elimination of Ras^{V12}-expressing clones we used two different transgenes able to block apoptosis when over-expressed: UAS P35, a viral apoptosis inhibitor and UAS DIAP1, the *Drosophila* homolog of *Inhibitor of Apoptosis 1*. Four weeks ACI, guts containing Apc-

Ras clones over-expressing UAS P35 or UAS DIAP1 did not show differences with guts containing Apc-Ras clones alone, neither in number, size nor distribution (Figure 21), indicating that apoptosis does not play an essential role in the disappearance of Ras^{V12}-expressing clones.

We also analysed the putative role of cell delamination in Ras^{V12}-expressing clone disappearance. It has been shown in mammalian cell cultures that normal cells can sense Ras^{V12}-expressing cells and induce their extrusion from the cell monolayer (Hogan, 2009). Many proteins have been involved in this process, such as the RhoGTPase Cdc42, the ROCK complex or the adhesion protein E-Cadherin. As mentioned in the introduction, it has been shown that a similar mechanism could occur in the *Drosophila* adult midgut, where the activation of the EGFR pathway in the enterocytes induces their extrusion from the epithelia (Buchon, 2010). In order to analyse whether a similar mechanism could account for the decline in the number of Ras^{V12}-expressing clones, we used a transgene able to over-express $Cdc42^{N17}$ a dominant negative form of the RhoGTPase involved in the Ras-driven cell extrusion in mammals (Hogan, 2009). Interestingly, Apc-Ras clones over-expressing UAS $Cdc42^{N17}$ showed a delay in the disappearance of the number of clones. Three weeks ACI, when Apc-Ras clones have already disappeared from the posterior midgut, Apc-Ras-$Cdc42^{N17}$ clones were still present in the posterior midgut (Figure 21). These clones, however, mostly disappeared four weeks ACI, suggesting that UAS$Cdc42^{N17}$ is not strong enough to completely block the process or that other mechanisms might also play a role in this process.

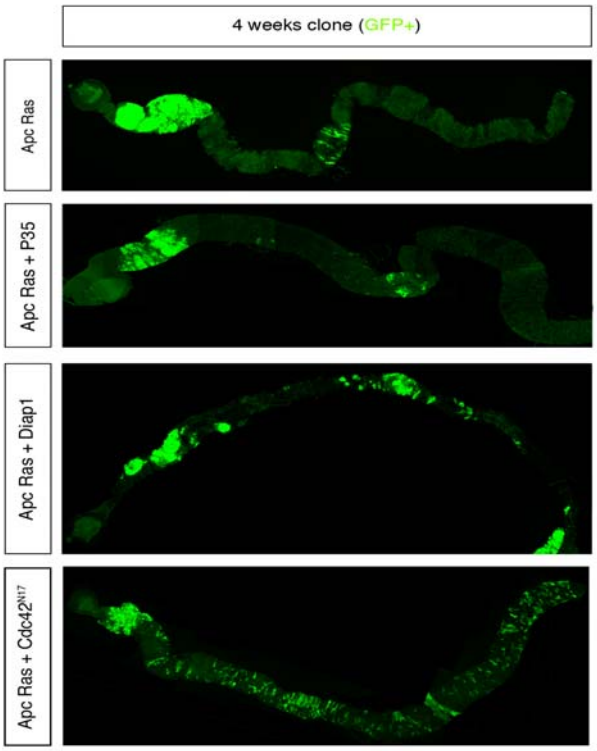

Figure 21. Clone disappearance by cell extrusion mediated by Cdc42. Four weeks ACI most of the clones in Apc-Ras have disappeared. A blockade in apoptosis by p35 or Diap1 does not block clone disappearance. Conversely, the addition of a dominant form of Cdc42, protein implicated in cell extrusion, can delay and eventually block clone disappearance.

Finally, we would like to point out that we have been able to observe some hints of Ras^{V12}-driven cell extrusion in the adult midgut. Ras^{V12}-expressing cells could be detected either on top or under the normal epithelial monolayer (Figure 22), suggesting events of apical or basal extrusion. These events occur very early after clone induction, being possible to observe them already at one day ACI. Although these results are preliminary, they indicate that cell extrusion could be a common event suffered for Ras^{V12}-expressing clones.

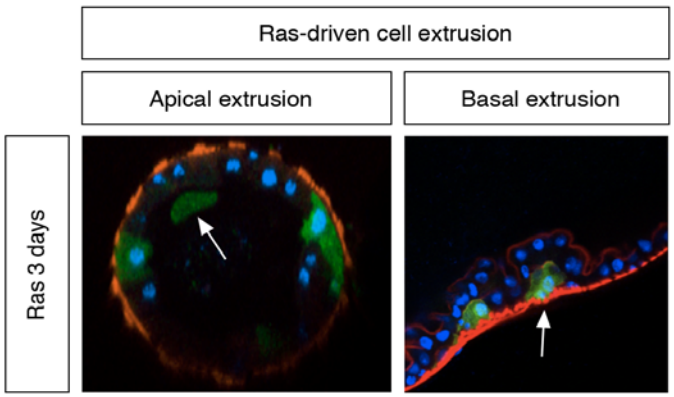

Figure 22. Cell delamination in Ras bearing clones. The arrows are marking cells that have been extruded apically (left) or basally (right)

In summary, some conclusions can be taken from these results. First, apoptosis is not essential in Ras^{V12}-expressing clone disappearance. Second, Cdc42 mediated-cell extrusion could play a role in Ras^{V12}-expressing clone elimination, as blockade of Cdc42 activity is enough to delay this process. The eventual delamination of the clones four weeks ACI could be due either to the weakness of the $Cdc42^{N17}$ allele or to the existence of other proteins that could partially rescue the activity of Cdc42. Finally, the Apc-Ras-UASCdc42^{N17} clones that survive in the posterior midgut do not over-proliferate, suggesting that regional differences may affect clone growth and progression.

1.3 Apc-Ras clones show many tumoural characteristics

1.3.1 Apc-Ras clones show an increased number of proliferative cells.

Apc-Ras clones usually progress to form very large overgrowths in the most anterior part of the gut, suggesting an increase in cell proliferation in comparison to control clones. Accordingly, a large number of Phospho-Histone 3 (PH3) positive cells, that marks specifically mitotic cells, were observed inside Apc-Ras clones (Figure 23). Conversely, none of the controls presented similar mitotic cell number. In WT conditions, an adult gut present around 5-20 cells (Jiang, 2009). Clearly, Apc-Ras clones present a strong increase in cell division rate. Of note, this increase seems to be clone-autonomous as all the PH3+ cells are inside the clone but not in the cells that surround the clone.

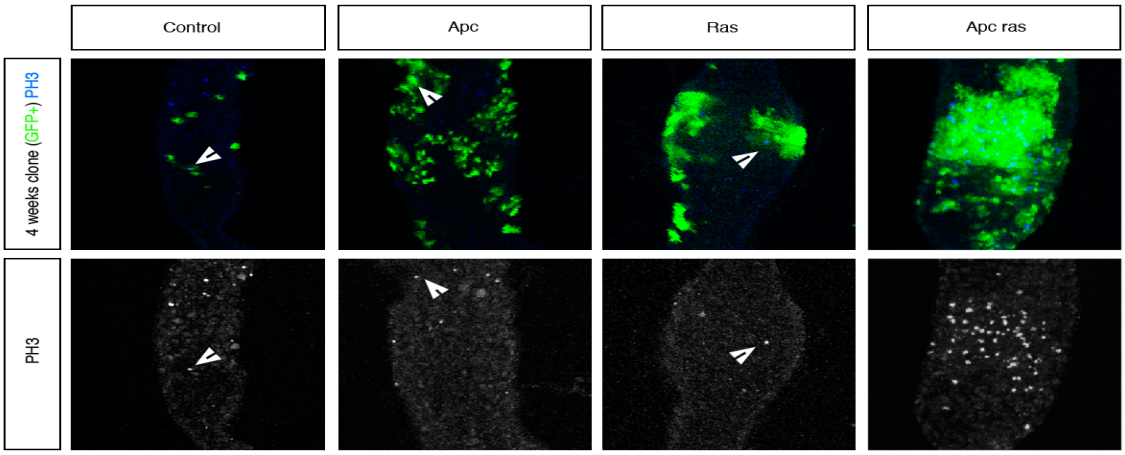

Figure 23. Cell proliferation in four weeks ACI MARMC clones. Cell proliferation is observed by Phospho-Histone 3 staining. Observe the concentration of PH3+ cells in Apc-Ras clones. Arrowheads: PH3+ cells.

This result demonstrates the strong mitogenic effect that the synergy of the Wg and EGFR pathways is able to generate in the adult midgut.

1.3.2 Apc-Ras clones show cell heterogeneity but a decrease in differentiated cell and ISC numbers.

It has been shown that human tumours present cell heterogeneity, where some of the tumoral cells differentiate as in the normal tissue (Merlos-Suárez, 2011). Usually, the degree of tissue dedifferentiation, commonly called dysplasia, is used as a general tumour grading system where low differentiation level corresponds to advanced tumour stages and poor prognosis (Cancer, 2010). To analyse whether Apc-Ras clones show cell heterogeneity, we labelled by immunostaining the differentiated cell types of the *Drosophila* adult midgut: the enterocytes (EC) and the enteroendocrine cells (EE). ECs can be identified by the expression of the POU Domain protein 1 (Pdm1, also known as nubbin) whereas EE cells express the transcription factor Prospero (Pros). We observed that Apc-Ras clones display cell heterogeneity, as they were positive for both differentiated cell types markers (Figure 24). Noticeably, and similarly to human tumours, Apc-Ras clones showed a remarkable reduction in the number of differentiated cells (Figure 24) suggesting that the process of differentiation is reduced in these clones. We reasoned that the clones could be formed mostly by intestinal stem cells (ISC), the only proliferative cells in the adult midgut but, surprisingly, few cells within the clone were positive for the ISC marker Delta (Dl) (Figure 25). In order to confirm these results and quantify the number of ISCs, ECs and EE cells within the clones, we sorted by FACS the GFP+ cells from Apc-Ras and control clones four weeks ACI. Quantitative (qPCR) analysis of the cDNA obtained from the sorted cells confirmed the immunostaining results, showing a clear reduction of the levels of Dl, Pros and the EC marker Myo31DF in Apc-Ras clones when compared to wild type and Apc clones (Figure 26). For technical reasons it was not possible to obtain enough GFP+ cells from Ras clones to perform the analysis. Taken together, these results demonstrate that ISC maintenance and the differentiation process are both altered in Apc-Ras clones, and open the question of which cell type is the major component of these clones.

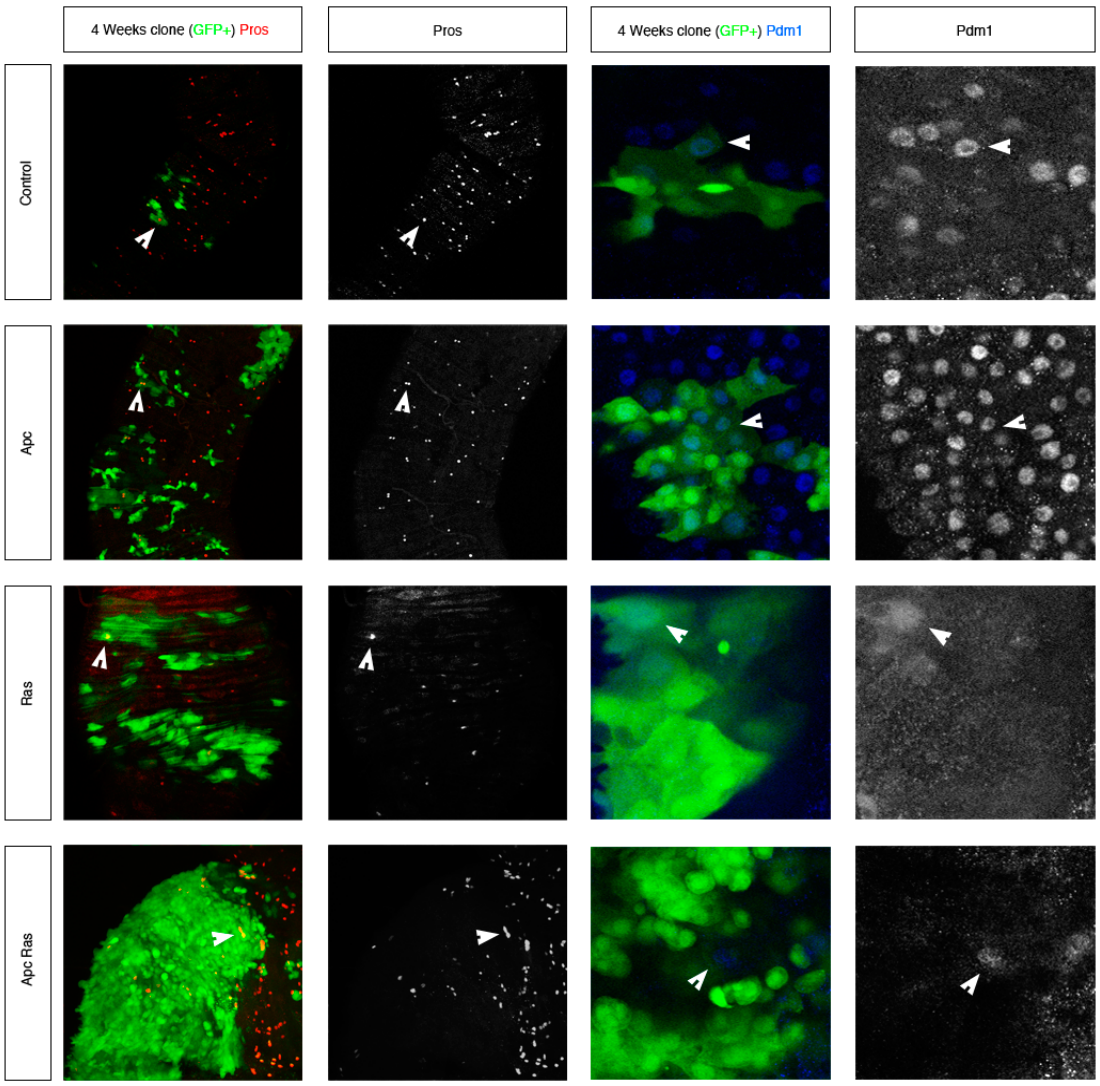

Figure 24. Differentiation state is compromised in Apc-Ras clones. WT and Apc show normal differentiation with approximately 80% of EC and 10% of EE. Apc-Ras clones show very strong reduced levels for both differentiation markers although some cells retain the ability for differentiate. Note that four Ras clones are located in a different and very specific region and the comparison cannot be adjusted.

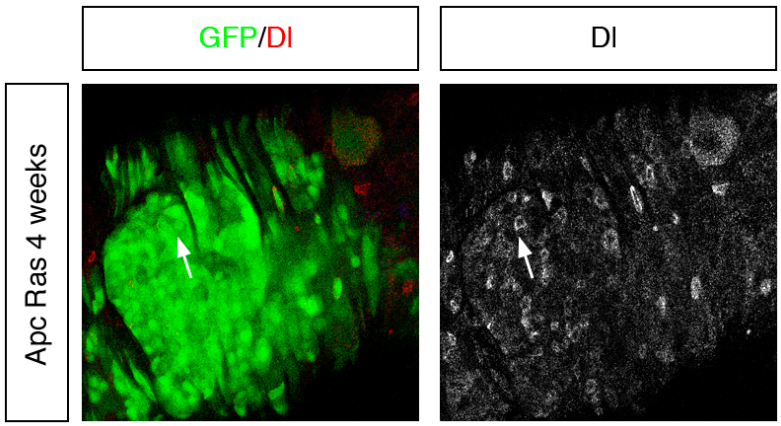

Figure 25. ISC presence in Apc-Ras clones. ISC are marked by the expression of high levels of Dl. Few cells inside express Dl suggesting that few cells inside Apc-Ras are ISC.

Of note, it has been described that despite Apc clones are hyperproliferative, cell differentiation is not altered (Lee, 2009; Lin, 2008). Accordingly, our results showed that in Apc clones the differentiation markers were similar to wild type clones (Figure 26). Moreover, Dl levels suffered a 2-fold increase, indicating an expansion of the number of ISCs as it has also been previously reported (Figure 26) (Lee, 2009; Lin, 2008). Together, these results confirmed the accuracy of the sorting protocol.

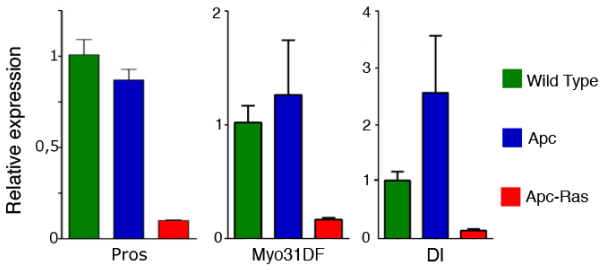

Figure 26. qPCR for cell fate markers in four weeks ACI clones. Quantifications for Prospero, Myo31DF -a marker of EC- and Dl -the marker for ISC-. Observe the reduction of all the 3 markers in Apc-Ras cells.

As aforementioned, only ISCs divide in the normal adult midgut. Therefore, in wild type conditions all PH3+ cells co-stain with Dl. Interestingly, inside Apc-Ras clones we observed a high number of cells PH3+ that are negative for Dl expression (Figure 27), suggesting that these aberrant cell types with proliferative capabilities, such as the *cancer stem cells* in human cancers, could be the cells responsible for the tumoral growth of Apc-Ras clones. We have named these cells EB-like, as they are progenitor cells but we do not have any evidence that divide asymmetrically or have any stem cell characteristics. Further studies are necessary to understand the nature of these EB-like cells.

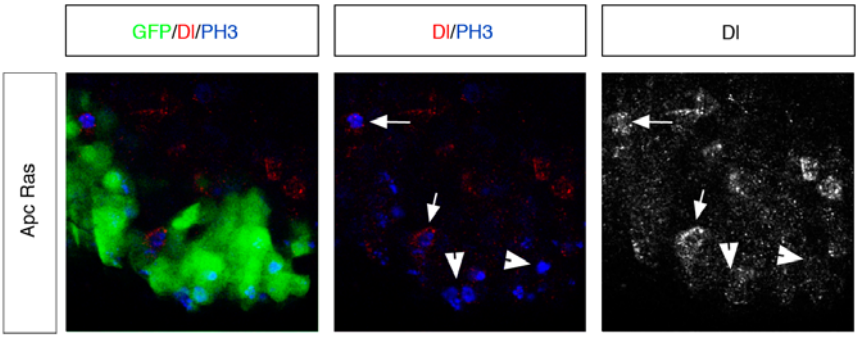

Figure 27. Dl- cells express division markers in Apc-Ras. In normal conditions all the PH3 cells. In Apc-Ras some PH3+ cells show reduce or null levels of ISC. Arrow: cells with high Dl Arrowhead: cells with low or null Dl

1.3.3 Epithelial tissue structure and cell polarity become disorganized in Apc-Ras clones

One of the main characteristics of human epithelial tumour cells is the loss of cell polarity (Wodarz, 2007). Cell polarity is a common property of epithelia and enables the cells to acquire a tight supracellular organization as well as to carry out specialized functions. The loss of cell polarity during cancer progression is associated with loss of cell adhesion and increased cell motility, both events linked to metastatic processes (Wodarz, 2007). Due to the critical role of the loss of epithelial characteristics during solid tumour progression we decided to analyse cell organization and polarity in Apc-Ras clones. We first analysed the adhesion protein DE-Cadherin (DE-Cad). DE-Cad is the principal component of the adherens junction, a cell-cell adhesion complex considered the limit between the apical and the basolateral membrane. The lack of E-Cad is frequent in advanced cancers and is associated with a migratory behaviour of the tumour cells (Wodarz, 2007). In Apc-Ras clones DE-Cad showed a membranal WT-like pattern in the cells located at the periphery of the clone, but was absent in the inner cells (Figure 28). We suggest that this pattern could reflect a difference between the cells that have lost DE-Cad and then acquire a pro-migratory behaviour (inner cells) and those with DE-Cad, less invasive, that remain in the surface of the midgut. However, we cannot exclude that this result would be an artefact due to the lack of antibody penetrance.

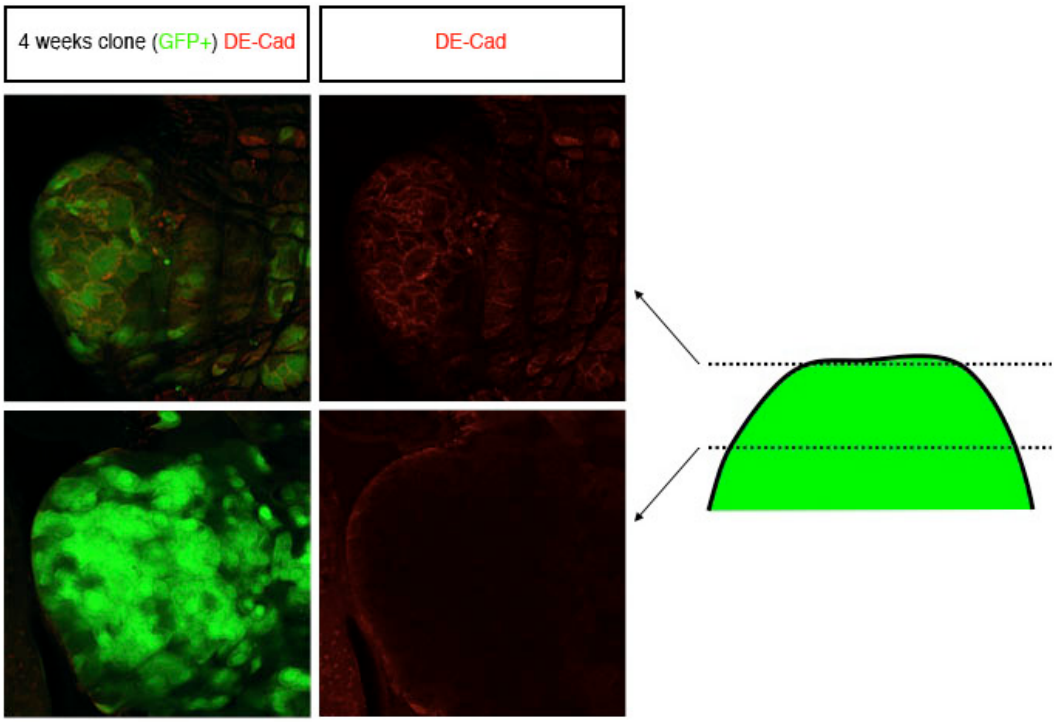

Figure 28. DE-Cadherin expression in Apc-Ras clones. The adhesion protein DE-Cadherin is the principal component of the adherens junction, the border between the apical and the basolateral membranes. In Apc-Ras cells DE-Cad expression can be observed in superficial cells (Top) but not in the inner mass (Bottom). On the right side, a scheme of the sections.

To further analyse epithelial integrity and polarity, we analysed the pattern of Discs large protein (Dlg). Dlg is a polarity protein that resides specifically in the lateral membrane of the epithelial cells both in *Drosophila* and Mammals, and contributes to maintain the polarity scaffold of the cells. In humans, the delocalization of Dlg has been reported as a clear symptom of loss of cell polarity during tumour formation (Wodarz, 2007). In wild type clones four weeks ACI, Dlg resided in the plasmatic membrane (Figure 29). In contrast, Dlg showed a diffused cytoplasmic staining in Apc-Ras clones, demonstrating a loss of cell polarity (Figure 29). Of note, Dlg staining was more diffuse in the inner cells within the clone than in the surface cells, where Dlg was mainly located in the membrane, suggesting that inner cells tend to be more depolarized than surface cells (Figure 29). In addition, Ras clones also showed Dlg delocalization indicating that the activation of the EGFR-Ras program is sufficient to induce loss of cell polarity in the midgut (Figure 29).

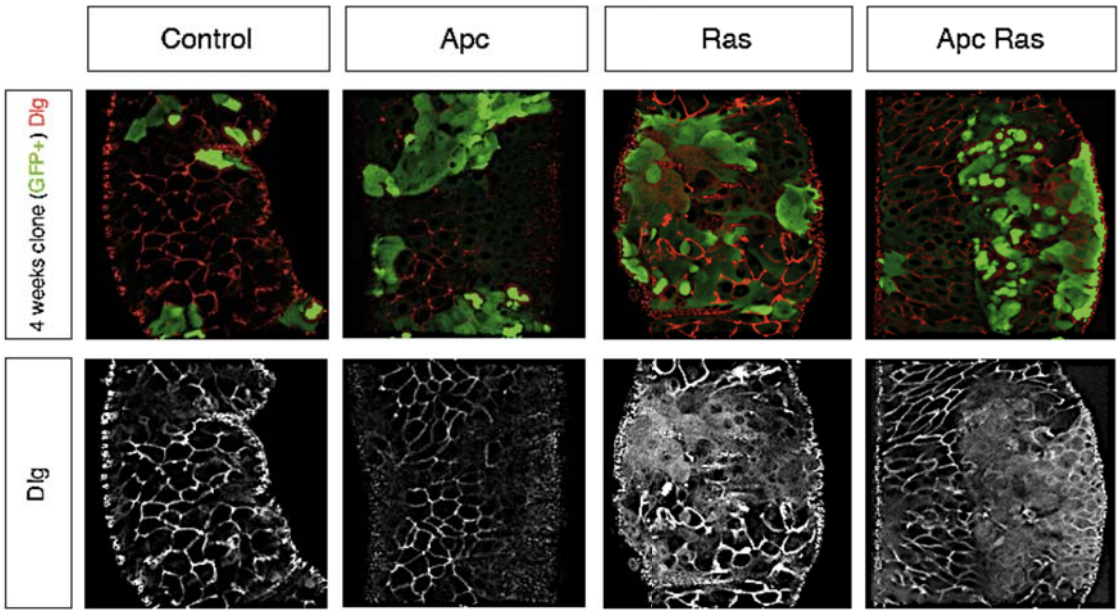

Figure 29. Activation of Ras-MAPK pathway induces cell depolarization in the adult midgut. Dlg is a membranal marker located in basolateral membrane in normal condition. The activation of Ras pathway alters the pattern of Dlg. The delocalization of Dlg is a clear sign of lack of cell polarity.

To confirm the loss of cell polarity and epithelial organization in Apc-Ras clones we analysed other markers as Armadillo (Arm) and Phalloidin. Arm, an essential transducer of the Wg pathway, is stabilized in the absence of Apc and, consequently, we observed an increase in the cytoplasmic staining of Arm in Apc-Ras clones (Figure

30). Arm is also an intracellular component of the adherens junction. In wild type epithelia, Arm is highly restricted to the apicolateral membrane of ISCs while the other cell types express lower levels of the protein (Figure 30) (Maeda, 2008). In Apc-Ras cells, however, Arm is localized around all cell membrane (Figure 30) suggesting that those cells have lost cell polarity.

We also analysed the pattern of the actin-binding molecule Phalloidin. In wild type conditions, Phalloidin accumulates in the apical side of the ECs, where microvilli reside (Figure X). In normal epithelia, therefore, Phalloidin staining lines parallel to the basal membrane marking the apical side of the ECs (Figure X, arrowhead). In Apc-Ras clones, however, we observed that this pattern has disappeared completely and the cells express homogeneous levels of Phalloidin (Figure 30, arrow), indicating that epithelial integrity and polarity was compromised.

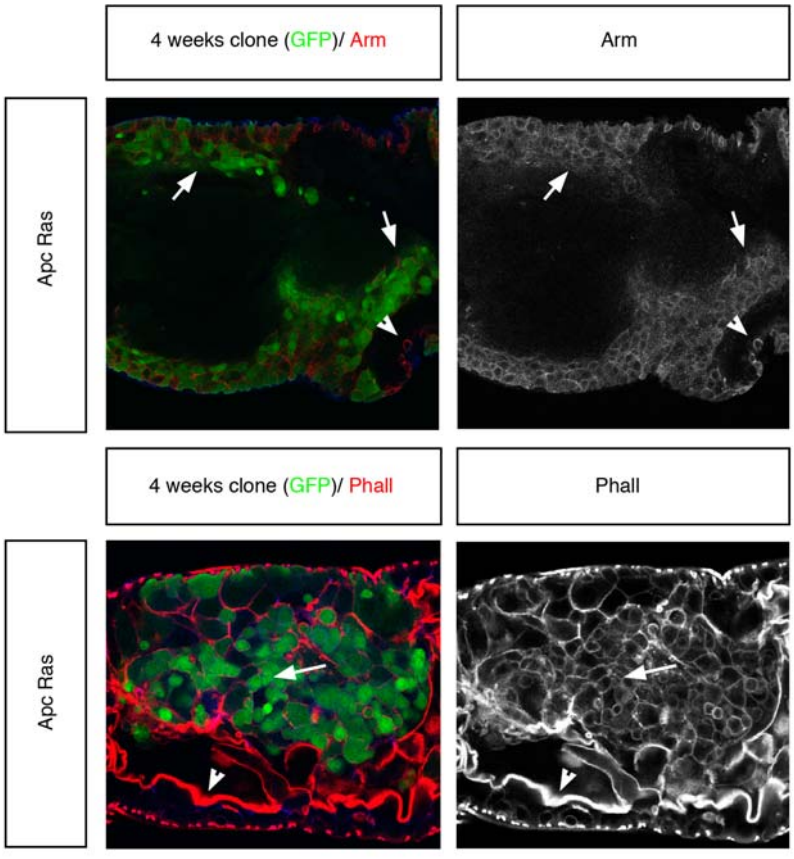

Figure 30. Arm and Phalloidin delocalization suggest severe tissue disorganization in Apc-Ras clones. Armadillo (Arm) shows a increased staining inside Apc-Ras clones as well as a uniform staining along the membrane (Arrow). Conversely, outside Apc-Ras clones Apc-Ras is mainly present in ISCs and not present in the basal side of the cells (Arrowhead). Phalloidin staining shows a stereotypic pattern in the midgut with a high accumulation in the apical side of the enterocytes due to the existence of the microvilli (Arrowhead). This pattern is lost in Apc-Ras clones where Phalloidin is uniformly expressed around the cells (Arrow). These two stainings reveal a severe degree of tissue disorganization inside Apc-Ras clones.

Finally, we analysed the microstructure of wild type guts and Apc-Ras clones by electron microscopy (EM). The wild type gut epithelium is composed by a monolayer of highly polarized cells with a clear apical surface full of small microvilli that form the apical brush border of the enterocytes, surrounded by longitudinal muscle fibres

essential for proper intestinal transit (Figure 31). The enterocytes are large poliploid cells with an apical nucleus that compose most of the epithelial layer. ISCs and EE cells are, in contrast, small and basally located (Figure 31). This epithelial organization was completely lost in Apc-Ras clones. We observed multilayering, with non-polarized cells detached from the basal membrane (Figure 31, arrowhead). We also observed muscle fibres surrounded by Apc-Ras cells (Figure 31, arrow) and the presence of multiple lumens (Figure 31, arrows), a common feature in human CRC tumours.

Taken together, our results show that the normal epithelial structure and organization was completely disrupted in Apc-Ras clones.

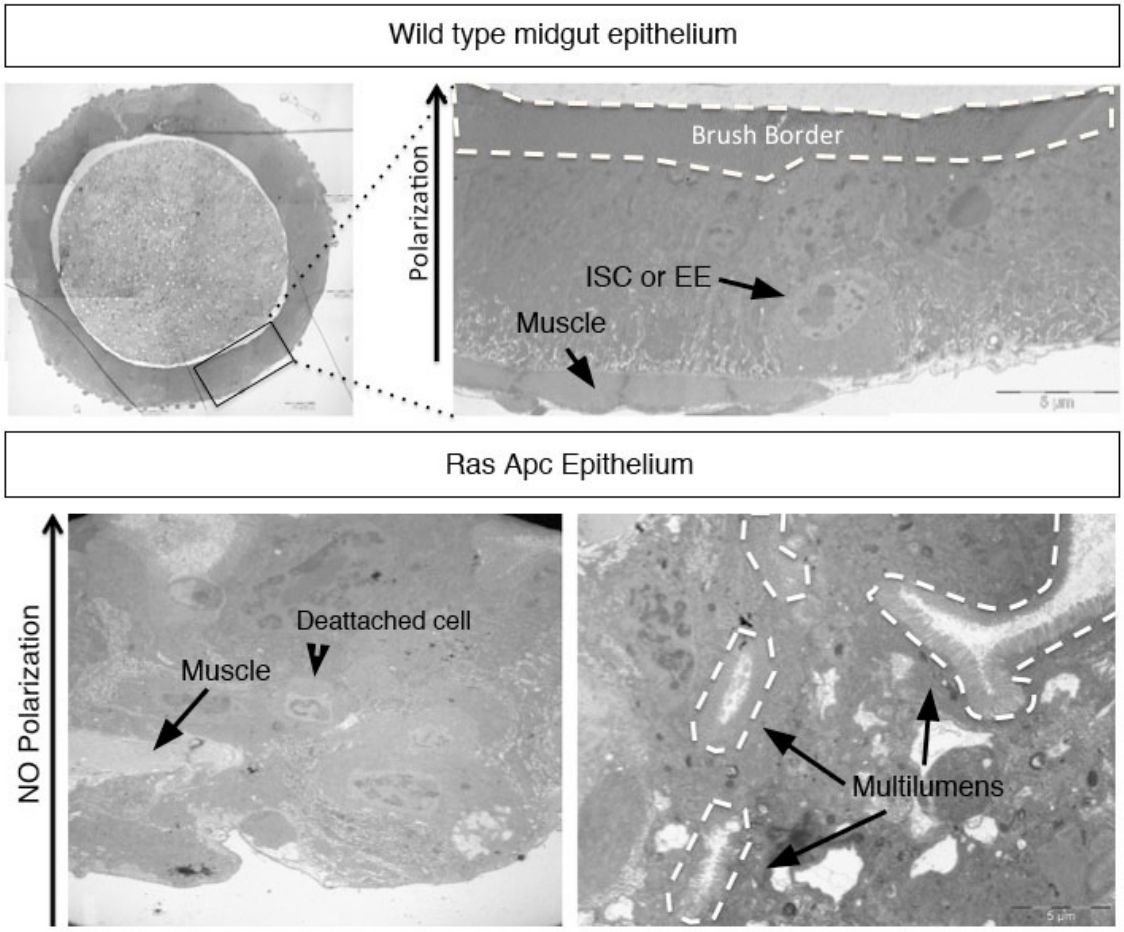

Figure 31. EM analysis reveals gross tissue defects and the apparition of multilumens. In WT midguts, the cells display as a stratified monolayer with an apical side towards the lumen and a basal side lying in the basal membrane. Only the EC reach the apical surface with their microvilli forming the brush border but ISC and EE remain protected from external aggressions. This pattern is completely altered in Apc-Ras clones with loss of epithelial polarity, tissue disorganization and the apparition of multilumens.

1.3.4 Apc-Ras cells express Singed, a migration-related protein used as a poor-prognosis tumoral marker

The different stages during tumour progression are associated with the expression of several proteins or tumoral markers. One of these proteins is Fascin, Singed (Sn) in *Drosophila* (Okenve-Ramos, 2013). The expression of Fascin has been described as a marker for advanced CRC (Hashimoto, 2006; Qualtrough, 2009) and has been identified as a direct target of β-catenin and Wnt signalling pathway activation during CRC progression (Vignjevic, 2007). Fascin is an actin-bundling protein associated with a migratory behaviour of cells (Qualtrough, 2009). In the wildtype *Drosophila* midgut, Sn is restricted to the tracheal cells that surround the midgut epithelium, but is never present in the gut epithelia (Figure 32). In Apc-Ras clones four weeks ACI we observed, however, a substantial upregulation of Sn expression by immunostaining (Figure 32). We confirmed this result by qPCR analysis that showed a 50 folds increase in Sn relative expression in Apc-Ras cells when compared to wild type cells four weeks ACI (Figure 33 and Annex 1). Interestingly, Sn expression was mostly restricted to the outer part of the Apc-Ras clones (Figure 32), a pattern also observed in human CRC (Vignjevic, 2007). Of note, Sn expression requires both Wg and EGFR pathways activity, as neither Apc nor Ras cells showed Sn expression.

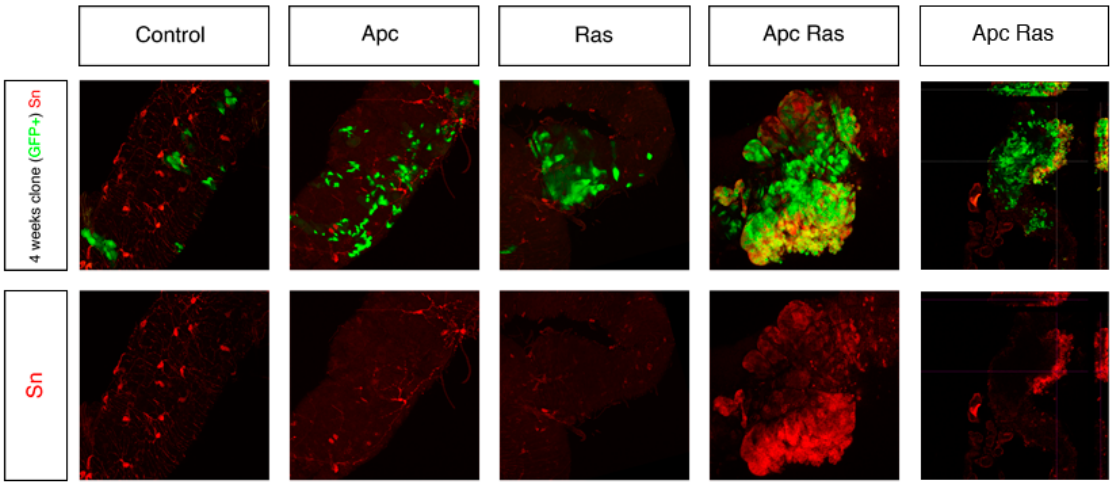

Figure 32 Apc-Ras cells in the leading edge overexpress the migration-related protein Singed. Singed is a essential protein for the correct formation of filopodia and migratory cell behaviour. In normal conditions Sn is restricted to the tracheal cells surrounding the midgut epithelium but Apc-Ras cells increase the levels of Sn expression inside the epithelium. Note in the last image that Sn expression is restricted to the outer section of the clone

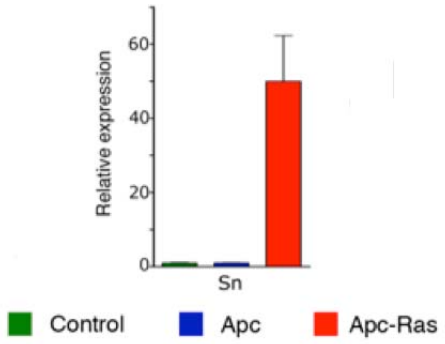

Figure 33. Sn expression levels by qPCR. Sn is not expressed in midgut epithelia in Wild type conditions. Conversely, Sn is highly upregulated in Apc-Ras cells.

In humans, Fascin expression correlates with poor prognosis and metastasis during tumour progression (Hashimoto, 2006). In order to analyse whether Sn expression play any role in tumour migration, we expressed a Sn RNAi construct in Apc-Ras clones. As we did not observe any effect, we were unable to conclude whether Sn does not participate in tumoral growth or migration or whether the RNAi was not efficient. Further work will be required to analyse the role of Sn upregulation in Apc-Ras clones.

1.3.5 Apc-Ras clone metastasis is not detectable.

Metastasis is the capability of tumour cells to migrate and generate secondary tumours in distant organs from the host (Hanahan, 2000). The metastatic process is linked to an advanced tumour state and to the acquisition of cell migration properties (Hanahan, 2011). We observed that 17% of Apc-Ras clones (n=111) were irregularly-shaped, grew opposite to the lumen and affected the surrounding muscular layers (Figure 34, up left). We also observed Apc-Ras clones moving on top of the surrounding wild type epithelia (Figure 34, up right) indicating a certain degree of cell migration ability. We were unable to detect, however, breaks in the basal membrane surrounding Apc-Ras clones, marked with the antibody against Laminin (Figure 34, middle). The basal membrane is an structure that separates the epithelium from the surrounding tissues, and its breaking is a clear sign of tumour invasion. Despite we have been unable to detect GFP+ cells or microtumours outside the gut, we can not exclude the possibility that solitary GFP+ cells are able of leave the tumour mass but are incapable to initiate metastatic tumours.

Of note, we also analysed the expression of the matrix metalloproteinase 1 (Mmp1), that is implicated in the degradation of the extracellular matrix and the basement membrane (Beaucher, 2007). Immunostaining experiments revealed the

absence of Mmp1 in Apc-Ras clones (Figure 34, bottom), in contradiction with microarray data that shows a 3,5 fold upregulation of Mmp1 in Apc-Ras cells when compared to wild type (Annex 1). We postulate that an internal post-transcriptional mechanism could block Mmp1 translation, avoiding the break of the basal membrane and the spread of Apc-Ras clones.

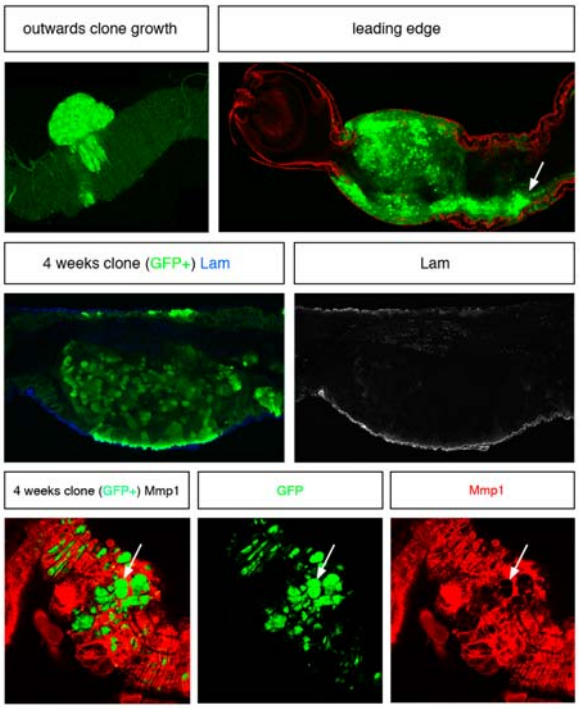

Figure 34. Apc-Ras clone show some invasive capabilities but not metastasis.
Up left. a small fraction of the clones (17%) grow towards the abdominal cavity. Up right. some clones show a loose attachment and migratory behaviour in top of the normal epithelia. Middle. Apc-Ras clones are not able to break the basal membrane, here marked by laminin antibody. Bottom. Apc-Ras clones show a strong reduction in Mmp1 antibody, a metalloproteinase responsible of breaking the extracellular matrix.

Finally, in order to further investigate the potential of Apc-Ras cells to colonize other tissues, we performed an allograft-based tumorigenicity assay. In this assay, a small piece of the tissue of interest is injected into the abdominal cavity of a host, in order to determine its growth potential. It has been shown that *Drosophila* tumours and normal proliferative tissues can survive and growth inside a host abdominal cavity (Gonzalez, 2013). In the case of tumours, they invade other parts of the host body, an effect apparent after ten-to-twenty days of the injection. Unfortunately, flies hosting pieces of Apc-Ras clones died two-to-five days after the injection, time not enough to observe significant overgrowths neither to determine their invasive abilities. We were able to observe, however, an slight growth of the injected Apc-Ras pieces (Figure 35), but further experiments will be required to analyse in detail its properties.

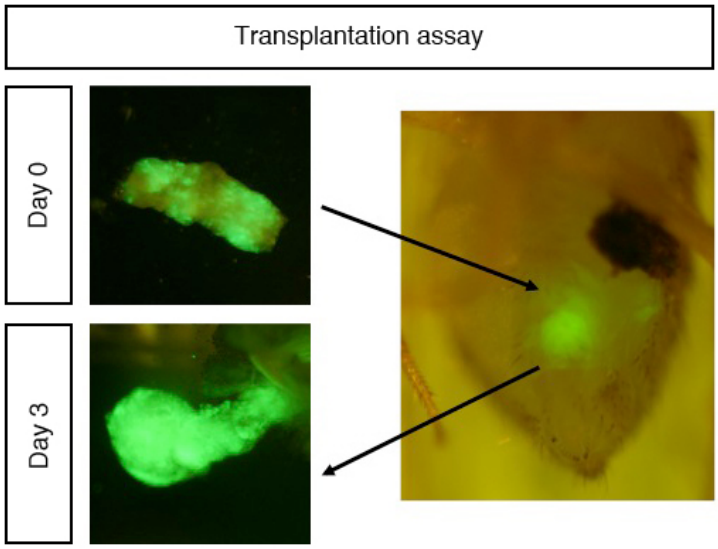

Figure 35. Allograft-based tumorigenecity assay in *Drosophila.* The injection of proliferative tissues in the *Drosophila* abdominal cavity is used as an assay to corroborate the tumoral potential of a certain proliferative tissue. In our case transplanted Apc-Ras clones can grow quickly but hosts die in a short time after transplantation making difficult to conclude anything about a putative metastatic potential.

1.4 Apc-Ras clones affect adult midgut physiology

**Experiments done in collaboration with Irene Miguel Aliaga laboratory (Department of Zoology, University of Cambridge).*

Drosophila is a commonly used model system for genetic or drug screenings, due to its powerful genetics and relatively low cost. In search for a test to analyse the tumour burden of flies bearing Apc-Ras clones that could be used for screens, we focused our attention in a recently developed *in vivo* method that determines the physiological state of the *Drosophila* adult midgut (Cognigni, 2011). We wondered whether this assay could help us to determine if Apc-Ras clones could affect normal midgut physiology. We used two different parameters to analyse the physiological state of the flies: Faecal output and Intestinal transit time. The number of faecal deposition was used as a simple readout of the physiological state of the adult gut. Interestingly, we observed that there was reduction on the number of depositions of Apc, Ras and Apc-Ras clones bearing flies, being the last ones the most affected (Figure 36, a). In addition we analysed the intestinal transit time to determine the efficiency of the digestive tract in food processing. To perform this assay, we quantified the number of flies that retain bromophenol-dyied food 24 hours after feeding. Flies bearing Apc-Ras clones showed a significant delay in food transit in comparison to control flies (Figure 36,b), being able to retain the dyed-food up to five days after feeding (Figure 36, c,d). We hypothesised that these physiological changes might be due, at least partially, to the lumen shrinkage that Apc-Ras clones provoke in the gut. Accordingly, the luminal space of guts containing Apc-Ras clones was dramatically reduced in comparison to guts containing wild type or Apc clones (Figure 37). Of note, Ras clones eventually

showed luminal shrinkage although the gastric region usually presents a very irregular tissue structure (Buchon, 2013). Moreover, the partial collapse of the luminal space in guts containing Apc-Ras clones could cause the short survival rate of the Apc-Ras flies by the obstruction of the gut lumen. This physiological assay, on top of demonstrating that Apc-Ras alters normal gut physiology, might be used as simple readout of the existence of tumours. Accordingly, easy anti-tumour drug screenings could be performed using the physiological gut state as a simple readout for the efficiency of the anti-tumour drug.

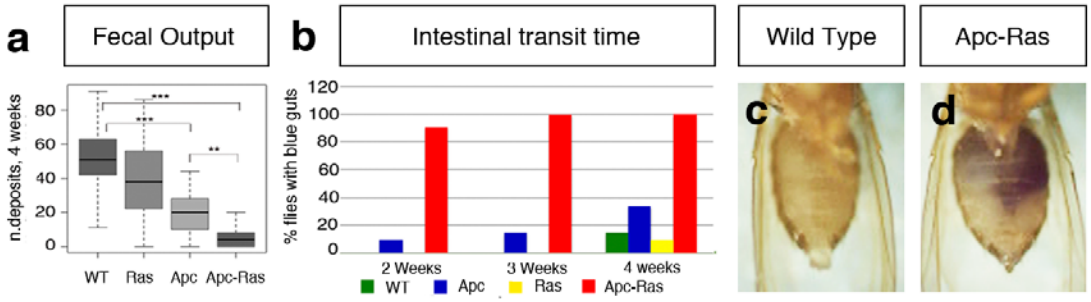

Figure 36. Apc-Ras affects the normal physiology of the adult midgut. a. the number of faecal deposits decrease progressively in Ras, Apc and Apc-Ras. b. Number of flies with blue guts 1 days after dye feeding. c. Abdomen of Wild type 5 days after dye feeding. d. Abdomen of Apc-Ras 5 days after dye feeding.

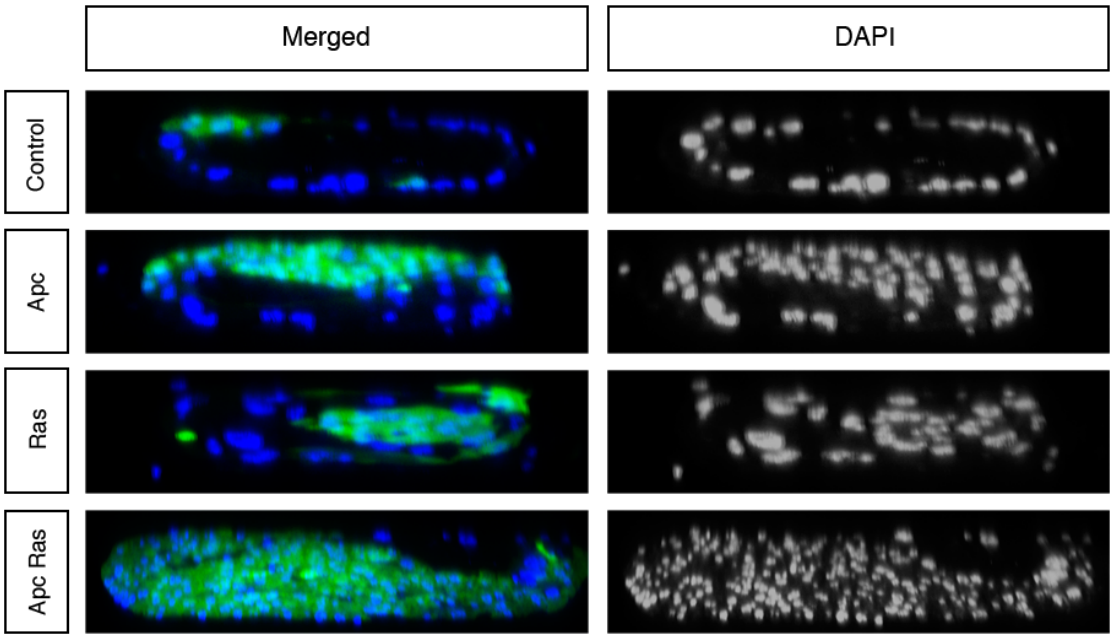

Figure 37. Transversal section of clone-bearing midguts. The WT section shows a monolayer of nuclei that forms the epithelium and delimits the lumen. The apparition of aberrant clones provokes the shrinkage of the luminal space due to the growth of the epithelium. In the case of Apc-Ras clone the luminal space occludes almost completely blocking the intestinal transit.

2 Transcriptional profiling of midgut clonal cells

One of the objectives of this work was to identify new genes involved in tumour formation and progression. To accomplish this objective, we performed a transcriptional profile analysis of Apc-Ras cells compared to wild type, Apc and Ras cells. We sorted by FACS the GFP^+ cells from guts bearing clones from each genotype one and four weeks ACI, and the mRNA obtained from the sorted cells was hybridized with Affymetrix 2.0 *Drosophila* genome arrays (see material and methods). The data obtained was analysed in collaboration with the IRB bioinformatics unit. After computational corrections (see mat & methods), the samples showed a low intra-group variation as samples clustered by genotype and time point variables (Figure 38, B).

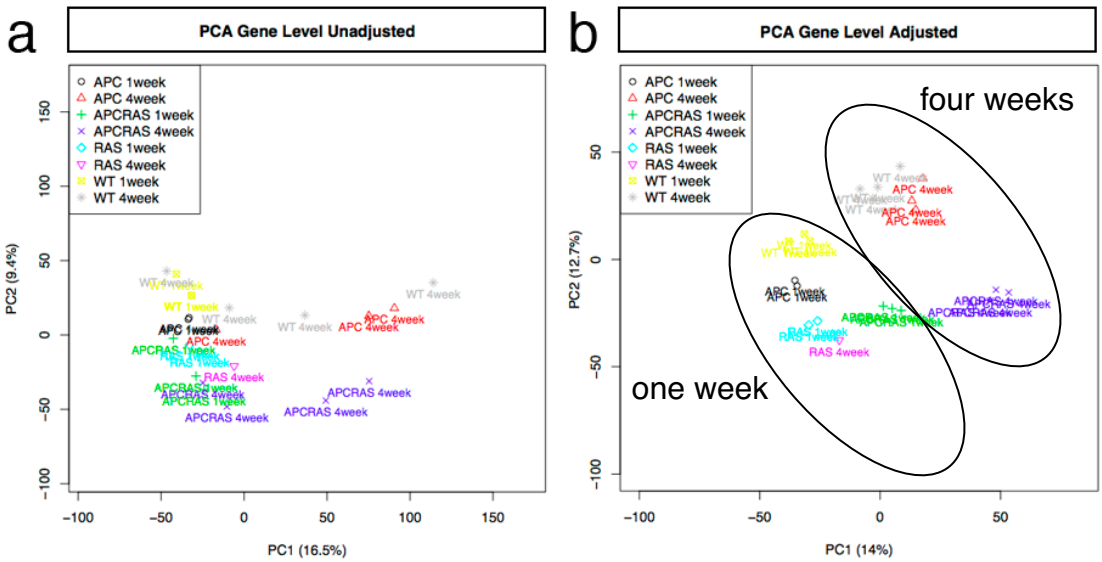

Figure 38. Principal component analysis (PCA) before (left) and after (right) adjustments. Observe the association of the different genotypes and time points into clusters after the PCA computational corrections. Note that Ras samples do not show time-point differences.

The microarray analysis showed that there were 882 differentially expressed genes (DEG) at one week ACI and 1217 DEG at four weeks ACI (Tables 3 and 4 and Annex 1 for DEG lists).

One week	Apc	Ras	Apc-Ras
Up	99	173	257
Down	150	212	326
Total	249	385	583

Four weeks	Apc	Ras	Apc-Ras
Up	60	382	389
Down	65	313	313
Total	125	695	702

Tables 3 and 4. Differential expressed genes in each genotype at one week and four weeks ACI

Venn diagrams comparing the three different conditions analysed (Apc vs WT, Ras vs WT and Apc-Ras vs WT) revealed a significant result: more than 50% of Apc-Ras DEG are specifically altered in Apc-Ras clones (Figure 39). These genes (315 at one week ACI and 433 at four weeks ACI) are not altered either in Apc nor Ras, indicating that the co-activation of both pathways must induce a synergic effect specifically altering the expression of genes that could be essential for Apc-Ras clone progression.

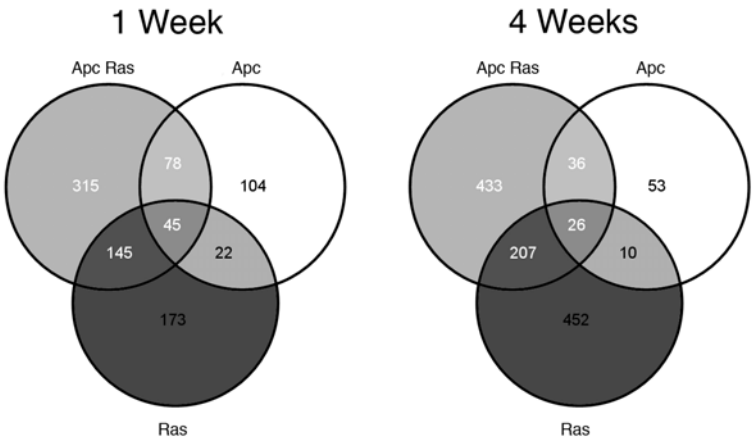

Figure 39. Venn diagrams comparing DEG in Apc,Ras and Apc-Ras conditions at one and four weeks ACI. Observe that more than 50% of Apc-Ras DEGs are specific of Apc-Ras condition.

Given these results, we can identify three different genetic programmes in Apc-Ras cells. First, the Wingless programme, that comprises those genes that depend on the activation of the Wingless pathway, and are present in Apc or Apc-Ras DEG lists. Second, the Ras programme, that includes all the target genes of the Ras-MAPK pathway and that are present in Ras and Apc-Ras DEG lists. And finally, a new Apc-Ras programme that comprises those genes that need the co-activation of both signalling pathways and are therefore altered only in Apc-Ras cells. These genes are the best candidates to play key driver roles and contribute to the tumoral phenotype of Apc-Ras clones, but an *in vivo* screen is necessary to analyse the functional relevance of each of these genes. In summary, the transcriptional profile analysis shows that there are significant transcriptional differences between WT and Apc-Ras cells, both at one week and four weeks ACI. These results also indicate that these differences are already partially present in Apc or Ras clones, albeit an important part of this DEG are Apc-Ras specific. A further analysis of the contribution of each program in Apc-Ras clone development will be essential to fully understand the process of tumour formation.

2.1 Functional analysis of Apc-Ras one week microarray data.

To identify genes with putative key roles in tumour development, we first performed a Gene Set Enrichment Analysis (GSEA). GSEA permits to determine if *a priori* defined gene sets (GO biological terms and KEGG terms) show significant differences between two biological samples. To perform this analysis we specifically used the data obtained from one week clones, as non-specific effects such the restricted spatial position of the clones or the activation of the senescence programs could affect the interpretation of four weeks clones. In our analysis, we first performed the GSEA of Apc-Ras clones vs wild type and then compared the results obtained with the GSEAs of Apc vs wild type and Ras vs wild type (Tables 5, 6, 7 and 8). Remarkably, we found that around the 60% of the significantly altered terms ($p<0,05$) in Apc-Ras clones were also altered in Apc or Ras conditions.

Focusing on the upregulated functions, Apc-Ras GSEA analysis revealed a high number of proliferation-related terms on the top positions (Table 5 and 6 and Figure 40). These terms, expected in a tumour-like condition, are already present in Apc and Ras conditions (Tables 5, 6 and Figure 40), both described previously as hyperproliferative (Buchon, 2010; Lee, 2009). Interestingly, however, 33% of the genes classified as proliferation-related genes were only up-regulated in Apc-Ras clones (Table 11). The GSEA analysis also revealed a significant upregulation of DNA mismatch repair terms in Apc-Ras clones (table 5,6 and Figure 40), possibly indicating that mechanisms of defence against new mutations could be activated in these high-proliferating cells to avoid an hypermutation state. Our analysis also showed an Apc-Ras-specific upregulation of terms related with migration (ex. *border follicle cell migration, glial cell migration and motor axon guidance*) as well as of terms related with cell adhesion and heterophilic cell adhesion. This could indicate the apparition of new cellular capabilities that would confer a different supracellular organization as well as a putative migratory behaviour to Apc-Ras cells. Finally, we also found many differences in the signalling and regulation of transcription cluster that could help us to identify signalling pathways that could play key roles in tumour progression (Table 5,6 and figure 40).

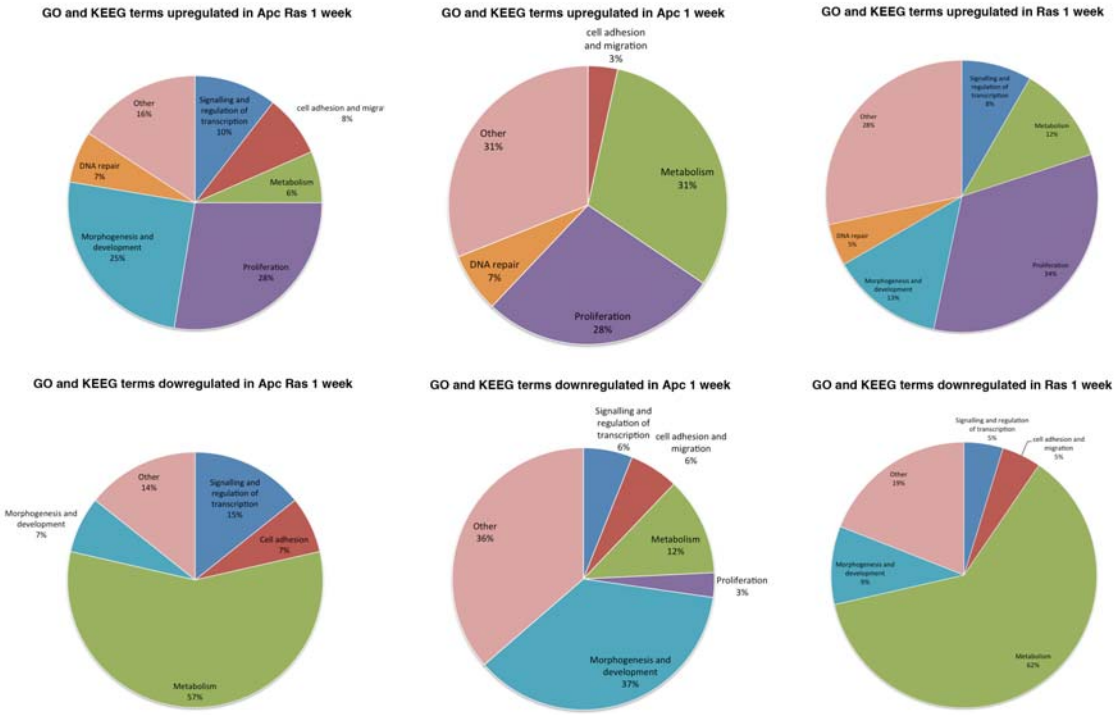

Figure 40. Apc-Ras GO term and KEGG term association by function. To facilitate the analysis we associate the GO and KEGG terms in functional groups. Left: Apc-Ras one week altered terms. Middle: Apc altered terms Right: Ras altered terms.

In the analysis of the downregulated terms, we found that most of them were metabolic processes such as *starch and sucrose metabolism, glycerolipid metabolism or fatty acid metabolism* (Table 7 and 8), suggesting that Apc-Ras cells could be losing part of their normal digestive functions. Also appeared altered some signalling and regulation of transcription terms, as the Jak-Stat signalling pathway (Tables 7 and 8), that could play essential roles blocking tumour progression. In summary, the GSEA analysis revealed that Apc-Ras cells one week ACI are involved manly in cell division and consequently can be activating the DNA mismatch repair programme to prevent further damage in the DNA. Remarkably, Apc-Ras cells express specific cell adhesion terms (Figure 40), indicating a certain degree of tissue compartmentalization between the Apc-Ras cells and the surrounding epithelium. Finally, Apc-Ras cells also present a reduction of catabolism-related terms suggesting a loss of the normal digestive functions probably by the loss of differentiated cells.

GO TERM NAME	NES	ALTERED IN APC	ALTERED IN RAS	ALTERED IN APC-RAS FOUR WEEKS ACI
GO0007049_CELL CYCLE	3.3616774	Yes	Yes	Yes
GO0007052_MITOTIC SPINDLE ORGANIZATION	3.0862541	Yes	Yes	Yes
GO0016203_MUSCLE ATTACHMENT	2.791168	Yes	No	Yes
GO0007067_MITOSIS	2.7904801	No	Yes	Yes
GO0007143_FEMALE MEIOSIS	2.7408538	No	Yes	No
GO0006974_RESPONSE TO DNA DAMAGE STIMULUS	2.6429095	No	Yes	Yes
GO0008283_CELL PROLIFERATION	2.5944138	Yes	Yes	No
GO0007517_MUSCLE ORGAN DEVELOPMENT	2.5907562	No	Yes	No
GO0007059_CHROMOSOME SEGREGATION	2.5621793	No	Yes	No
GO0000910_CYTOKINESIS	2.457602	Yes	Yes	Yes
GO0006508_PROTEOLYSIS	2.385885	Yes	Yes	No
GO0045214_SARCOMERE ORGANIZATION	2.3404906	No	No	Yes
GO0007346_REGULATION OF MITOTIC CELL CYCLE	2.326103	Yes	Yes	Yes
GO0016321_FEMALE MEIOSIS CHROMOSOME SEGREGATION	2.2933614	No	Yes	No
GO0007442_HINDGUT MORPHOGENESIS	2.265934	No	No	Yes
GO0008045_MOTOR AXON GUIDANCE	2.2347622	No	No	No
GO0007426_TRACHEAL OUTGROWTH, OPEN TRACHEAL SYSTEM	2.20226	No	No	Yes
GO0009987_CELLULAR PROCESS	2.1642485	No	Yes	No
GO0007435_SALIVARY GLAND MORPHOGENESIS	2.1383228	No	No	No
GO0030261_CHROMOSOME CONDENSATION	2.1280203	No	Yes	No
GO0007155_CELL ADHESION	2.1115284	No	No	No
GO0006342_CHROMATIN SILENCING	2.0863361	No	Yes	No
GO0007224_SMOOTHENED SIGNALING PATHWAY	2.0854273	No	No	Yes
GO0006260_DNA REPLICATION	2.073375	Yes	Yes	No
GO0055059_ASYMMETRIC NEUROBLAST DIVISION	2.0276892	No	Yes	No
GO0030036_ACTIN CYTOSKELETON ORGANIZATION	2.0259564	No	No	Yes
GO0007476_IMAGINAL DISC-DERIVED WING MORPHOGENESIS	1.9857954	No	No	No
GO0007422_PERIPHERAL NERVOUS SYSTEM DEVELOPMENT	1.9538825	No	Yes	No
GO0051533_POSITIVE REGULATION OF NFAT PROTEIN IMPORT INTO NUCLEUS	1.9269041	No	Yes	No
GO0006357_REGULATION OF TRANSCRIPTION FROM RNA POLYMERASE II PROMOTER	1.9219371	No	No	No
GO0008586_IMAGINAL DISC-DERIVED WING VEIN MORPHOGENESIS	1.9030036	No	No	No
GO0007088_REGULATION OF MITOSIS	1.8969175	No	Yes	No
GO0007298_BORDER FOLLICLE CELL MIGRATION	1.865676	No	No	No
GO0007629_FLIGHT BEHAVIOR	1.8445185	No	No	No
GO0006325_CHROMATIN ORGANIZATION	1.8383553	No	Yes	No
GO0000381_REGULATION OF ALTERNATIVE NUCLEAR MRNA SPLICING, VIA SPLICEOSOME	1.8092618	No	Yes	No
GO0048477_OOGENESIS	1.7889079	No	Yes	No
GO0048813_DENDRITE MORPHOGENESIS	1.78346	No	Yes	No
GO0007520_MYOBLAST FUSION	1.7582133	No	No	Yes
GO0035317_IMAGINAL DISC-DERIVED WING HAIR ORGANIZATION	1.756693	No	No	Yes
GO0042052_RHABDOMERE DEVELOPMENT	1.7470253	No	No	No
GO0006470_PROTEIN DEPHOSPHORYLATION	1.7415438	No	No	No
GO0007420_BRAIN DEVELOPMENT	1.7387389	No	Yes	No
GO0007076_MITOTIC CHROMOSOME CONDENSATION	1.730614	No	Yes	Yes
GO0000122_NEGATIVE REGULATION OF TRANSCRIPTION FROM RNA POLYMERASE II PROMOTER	1.7227821	No	No	No
GO0051225_SPINDLE ASSEMBLY	1.7221627	No	Yes	No
GO0001745_COMPOUND EYE MORPHOGENESIS	1.7137231	No	No	No
GO0008356_ASYMMETRIC CELL DIVISION	1.6897434	No	Yes	No
GO0008407_BRISTLE MORPHOGENESIS	1.6848693	No	No	Yes
GO0030717_KARYOSOME FORMATION	1.6745214	No	No	No
GO0042067_ESTABLISHMENT OF OMMATIDIAL PLANAR POLARITY	1.6683617	No	No	No
GO0016055_WNT RECEPTOR SIGNALING PATHWAY	1.6668079	No	No	No
GO0008347_GLIAL CELL MIGRATION	1.6644531	No	No	No
GO0000022_MITOTIC SPINDLE ELONGATION	1.6634221	No	No	No
GO0007474_IMAGINAL DISC-DERIVED WING VEIN SPECIFICATION	1.6628839	No	No	Yes

Table 5. Upregulated GO terms in Apc-Ras vs WT one week. Terms in bold letters are Apc-Ras specific.

KEGG TERM NAME	NES	ALTERED IN APC	ALTERED IN RAS	PRESENT IN FOUR WEEKS ACI APC-RAS
03030_DNA REPLICATION	3.5513563	Yes	Yes	Yes
03013_RNA TRANSPORT	3.139647	Yes	Yes	Yes
03430_MISMATCH REPAIR	2.9471028	Yes	Yes	Yes
03050_PROTEASOME	2.936774	Yes	Yes	Yes
03420_NUCLEOTIDE EXCISION REPAIR	2.8207977	Yes	Yes	Yes
03040_SPLICEOSOME	2.1824641	Yes	Yes	Yes
00240_PYRIMIDINE METABOLISM	2.1726103	Yes	Yes	No
03008_RIBOSOME BIOGENESIS IN EUKARYOTES	1.9845544	Yes	Yes	No
03018_RNA DEGRADATION	1.7332468	Yes	Yes	No
03020_RNA POLYMERASE	1.6781868	Yes	Yes	No
00970_AMINOACYL-TRNA BIOSYNTHESIS	1.6664301	Yes	Yes	No
04914_PROGESTERONE-MEDIATED OOCYTE MATURATION	2.2584085	No	Yes	No
03015_MRNA SURVEILLANCE PATHWAY	2.159989	No	Yes	No
03410_BASE EXCISION REPAIR	2.1017823	No	Yes	No
03440_HOMOLOGOUS RECOMBINATION	2.0927181	No	Yes	Yes
00514_OTHER TYPES OF O-GLYCAN BIOSYNTHESIS	**1.8505743**	**No**	**No**	**No**
00480_GLUTATHIONE METABOLISM	1.8375828	No	Yes	Yes
04630_JAK-STAT SIGNALING PATHWAY	**1.8002695**	**No**	**No**	**No**
03010_RIBOSOME	**1.738505**	**No**	**No**	**No**
00980_METABOLISM OF XENOBIOTICS BY CYTOCHROME P450	**1.7017028**	**No**	**No**	**Yes**
00982_DRUG METABOLISM - CYTOCHROME P450	**1.6760672**	**No**	**No**	**Yes**

Table 6. Upregulated KEGG terms in Apc-Ras vs WT one week. Terms in bold letters are Apc-Ras specific. The terms that are showed here are statistically significant, p<0,05

GO TERM NAME	NES	PRESENT IN APC	PRESENT IN RAS	PRESENT IN FOUR WEEKS ACI APC-RAS
GO0019991_SEPTATE JUNCTION ASSEMBLY	-1.970982	Yes	Yes	No
GO0035151_REGULATION OF TUBE SIZE, OPEN TRACHEAL SYSTEM	-1.7828428	Yes	Yes	No
GO0010552_POSITIVE REGULATION OF GENE-SPECIFIC TRANSCRIPTION FROM RNA POLYMERASE II PROMOTER	-1.7208349	**No**	**No**	**No**
GO0001666_RESPONSE TO HYPOXIA	-1.6825345	Yes	No	No

Table 7. Downregulated GO terms in Apc-Ras vs WT one week. Terms in bold letters are Apc-Ras specific. The terms that are showed here are statistically significant, p<0,05

KEGG TERM NAME	NES	PRESENT IN APC	PRESENT IN RAS	PRESENT IN FOUR WEEKS ACI APC-RAS
04080_NEUROACTIVE LIGAND-RECEPTOR INTERACTION	-2.5869153	Yes	Yes	Yes
00903_LIMONENE AND PINENE DEGRADATION	-2.4290464	Yes	Yes	No
00052_GALACTOSE METABOLISM	-2.3100536	Yes	Yes	Yes
00511_OTHER GLYCAN DEGRADATION	**-2.2585769**	**No**	**No**	**No**
00500_STARCH AND SUCROSE METABOLISM	-2.0782123	Yes	Yes	Yes
00280_VALINE, LEUCINE AND ISOLEUCINE DEGRADATION	-2.055848	No	Yes	Yes
00071_FATTY ACID METABOLISM	-1.9869841	No	Yes	No
01040_BIOSYNTHESIS OF UNSATURATED FATTY ACIDS	-1.9523745	No	Yes	No
00790_FOLATE BIOSYNTHESIS	**-1.8780128**	**No**	**No**	**No**
04142_LYSOSOME	-1.8545971	Yes	Yes	No
00561_GLYCEROLIPID METABOLISM	**-1.7696161**	**No**	**No**	**No**

Table 8. Downregulated KEGG terms in Apc-Ras vs WT one week. Terms in bold letters are Apc-Ras specific. The terms that are showed here are statistically significant, p<0,05

We next proceeded to cluster the Apc-Ras DEGs into different broad gene function groups (Annex 2 and figure 41). The functional clusters were created by their relevance in tumour development and by their use in similar analyses (Marisa, 2013; Sabates-Bellver, 2007). The classification terms used were: signalling and regulation of transcription, proliferation, metabolism, cell adhesion and polarity, proteolysis, genes with other functions and genes with unknown function (Figure 41). We did not observe remarkable differences between the DEG functions between Apc-Ras, Apc and Ras clones (Figure 41). Similarly to the GSEA analysis, all the functional groups were represented in a similar proportion between the three genotypes, suggesting that there are not extreme genetic differences between Apc-Ras, Apc and Ras clones one week ACI.

After the group of genes with other functions and unknown genes, the most represented group was metabolism, which includes all those genes involved in cell energetics and molecule biosynthesis. Most of the metabolic genes downregulated in Apc-Ras clones were those related with the normal digestive and catalytic functions of the gut such as carbohydrases, lipases and nitrogen metabolism enzymes, or genes related with proteolysis. This result suggests that Apc-Ras clones might be losing enterocytes and, therefore, losing most of the macromolecule catalytic metabolism.

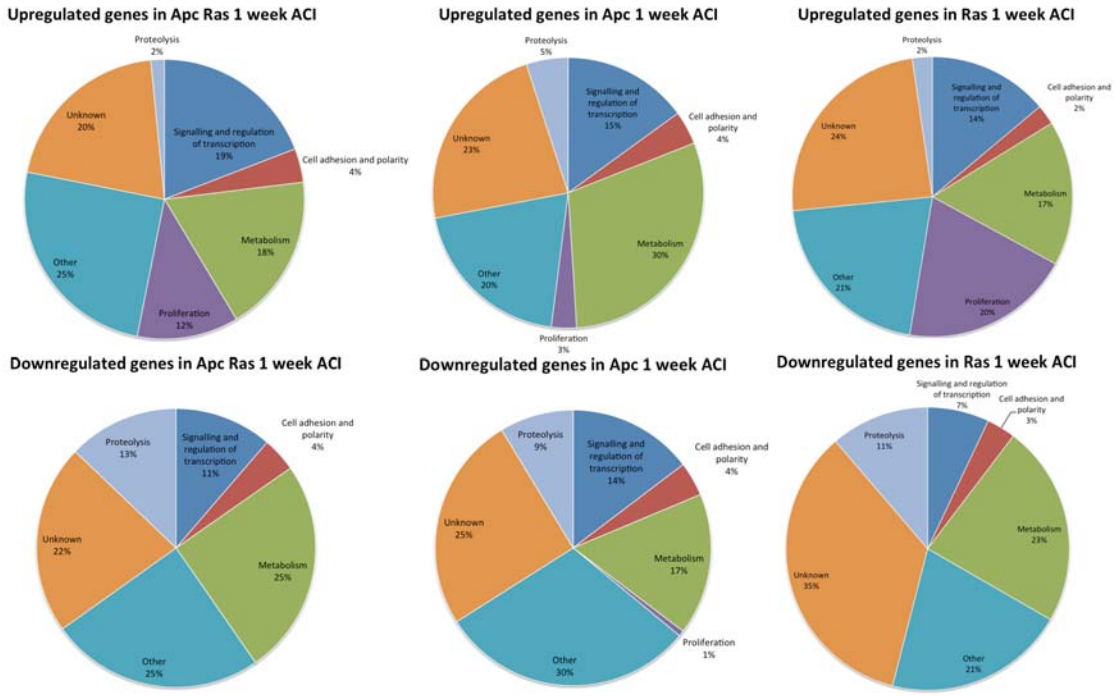

Figure 41. DEG functional clustering. To facilitate the interpretation of the analysis we clustered the genes into big functional groups. Left: Apc-Ras one week DEG. Middle: Apc one week DEG Right: Ras one week DEG.

Conversely, the metabolism group upregulated in Apc-Ras cells included genes involved in xenobiotic and drug metabolism (ex. Glutathione S-transferases) and the glycolysis pathway (ex.ImpL3, Pfk). The alteration of the xenobiotic metabolism by the upregulation of gluthatione-S-transferases (GSTs) has been implicated in cancer progression, although the effects of these alterations are still controversial. Glutathione is involved in several roles such antioxidation, maintenance of redox state and detoxification of xenobiotics and GST are enzymes that catalyse the conjugation of glutathione with several electrophiles that could act as carcinogens (Balendiran, 2004). On the other hand, alterations of glucose metabolism (Glycolysis, Krebs cycle and phosphorilative oxidation), the central energetic pathway of the cell, has been well established during tumour progression (Cairns, 2011).

Another highly represented group was signalling and regulation of transcription. Many diffusible signalling molecules were upregulated in Apc-Ras clones (Table 9), as *Hedgehog, Branchless* (*Drosophila* FGF) and *Pvf2* (one of the *Drosophila* PDGFs) suggesting a putative role of these pathways in tumour progression. Jak-Stat ligands as *Outstreched and Unpaired3* were also upregulated, although in this case the pathway essential effector Stat92E was downregulated, arguing for a possible non-autonomous role of the pathway on the surrounding wild type tissue. Remarkably, we also found many negative regulators of the EGFR pathway as *argos, sprouty, short gastrulation and kekkon1*. In contrast, EGFR itself and the negative regulator of the pathway *capicua* were downregulated. Main components of the Dpp pathway appeared also downregulated at Apc-Ras clones one week ACI, such as the receptor Whishful thinking (Wit) or the transducer Mother against Dpp (Mad) while a major negative regulator of the pathway, *short gastrulation*, appeared upregulated (Table 9). Remarkably, a strong downregulation of these and other core Dpp pathway components, as the receptors Thickveins (Tkv) and Punt (Put) and the transducer Medea (Med), was also observed four weeks ACI (Table 13). Dpp/TGF-β has been described as an anti-mitotic signal in the adult midgut as well as during human CRC progression (Guo, 2013; Markowitz, 1996). Therefore, the downregulation of these core components of the Dpp pathway may play a role regulating tumour progression, role that will be analysed in detail on sections 4.3 and 4.4. In summary, the alteration of all these signalling pathways suggest that Apc-Ras clones may secrete and interpret signals that could affect, either autonomously or non-autonomously, the growth of the tumour. In this way, Apc-Ras cells probably have acquired two of the cancer hallmarks: self-sufficiency in growth signals and evasion of anti-growth signals (Hanahan, 2011).

SYMBOL	SIGNALLING MOLECULE NAME	FUNCTION	FOLD CHANGE	ALTERED IN APC	ALTERED IN RAS
fz3	frizzled 3	Wnt pathway receptor binding	15.00427013	Yes	No
hh	**hedgehog**	**Hh pathway receptor binding**	**7.261660483**	**No**	**No**
os	**outstretched**	**Jak-Stat pathway receptor binding**	**7.09544671**	**No**	**No**
ImpL2	Ecdysone-inducible gene L2	Insulin-like peptide	6.673466435	Yes	Yes
kek1	**kekkon-1**	**Negative reg. Of EGFR pathway**	**4.215478997**	**No**	**No**
Pvf2	**PDGF- and VEGF-related factor 2**	**Positive reg. Of PDGF pathway**	**3.857345224**	**No**	**No**
bnl	**branchless**	**FGFR Binding**	**3.646069437**	**No**	**No**
rho	**rhomboid**	**Positive reg. Of EGFR pathway**	**3.543405024**	**No**	**No**
upd3	unpaired 3	Positive reg. Of Jak-Stat pathway	3.488887903	Yes	Yes
otk	**off-track**	**Negative reg. Of Wnt pathway**	**3.073974455**	**No**	**No**
sog	**short gastrulation**	**Negative reg. Of Dpp pathway**	**2.864924286**	**No**	**No**
CG3074	**CG3074 gene product from transcript CG3074-RB**	**Positive reg. Of Wnt pathway**	**2.8469727**	**No**	**No**
l(2)k16918	**Regulator of ephrin expression**	**Ephrin signalling regulator**	**2.839293311**	**No**	**No**
Wnt5	**Wnt oncogene analog 5**	**Positive reg. Of Wnt pathway**	**2.781043168**	**No**	**No**
piwi	**CG6122 gene product from transcript CG6122-RA**	**Piwi-mediated RNA regulation**	**2.583241331**	**No**	**No**
argos	**CG4531 gene product from transcript CG4531-RA**	**Negative reg. Of EGFR pathway**	**2.581679289**	**No**	**No**
sty	**sprouty**	**Negative reg. Of EGFR pathway**	**2.581116299**	**No**	**No**
pigs	**pickled eggs**	**Negative reg. Of Notch pathway**	**2.255176598**	**No**	**No**
Ote	Otefin	Positive reg. Of Dpp pathway	2.240992696	No	Yes
esc	extra sexcombs	Chromatin silencing	2.092992811	No	Yes
18w	18 wheeler	Toll-like receptor	2.046012497	No	Yes
Src42A	**Src oncogene at 42A**	**Tyrosine kinase activity**	**-2.093366953**	**No**	**No**
trk	**trunk**	**Torso receptor binding**	**-2.267846928**	**No**	**No**
Egfr	**Epidermal growth factor receptor**	**EGFR pathway receptor**	**-2.35975681**	**No**	**No**
CG11347	**DOR**	**Ecdysone signalling pathway receptor**	**-2.434290806**	**No**	**No**
spz	spatzle	Toll receptor binding	-2.752578319	No	Yes
wit	**wishful thinking**	**Positive reg. Of Dpp pathway**	**-2.782583759**	**No**	**No**
CG7431	**Tyramine receptor**	**G-Protein coupled receptor**	**-2.85669672**	**No**	**No**
CG17278	CG17278 gene product from transcript CG17278-RA	Negative reg. Of Wnt pathway	-3.222888014	Yes	No
bru-2	CG31763 gene product from transcript CG31763-RA	RNA binding	-7.577620188	Yes	Yes

Table 9. List of altered signalling molecules 1 week ACI most likely to be involved in Apc-Ras clone progression. In bold letters are presented those genes specific for Apc-Ras.

Moreover, several transcriptions factors showed significant transcriptional changes in Apc-Ras clones (Table 10). Remarkably, one of the top transcription factors upregulated was p53, a gene involved in most of human cancers. The upregulation of p53, that acts as a tumour supressor, could be blocking the growth of the Apc-Ras clones to later, more aggressive stages, although preliminary results expressing p53 RNAi in Apc-Ras clones did not show any increase in tumour growth (data not shown). Another transcription factor upregulated was the Iroquois family member Mirror, that usually acts as a transcriptional repressor and that our work has identified as a regulator of Dpp pathway components (see section 4.4). Another interesting example

was the opposite transcriptional alteration of two transcription factors involved in migration and epithelial-to-mesenchimal (EMT) transition, Snail and Serpent (Becker, 2007; Campbell, 2011; Carver, 2001). Remarkably, the most upregulated transcription factor, seven up, is the homolog of a recently described TGF-β pathway inhibitor during prostate cancer progression (Qin, 2013).

SYMBOL	TRANSCRIPTION FACTOR NAME	FOLD CHANGE	ALTERED IN APC	ALTERED IN RAS
svp	**seven up**	**19.06645304**	**No**	**No**
Lim3	CG10699 gene product from transcript CG10699-RB	9.793604962	Yes	No
drm	**drumstick**	**8.550712363**	**No**	**No**
slbo	**slow border cells**	**6.24673069**	**No**	**No**
mirr	**mirror**	**5.82772484**	**No**	**No**
CG7056	CG7056 gene product from transcript CG7056-RA	4.756159642	Yes	No
sob	**sister of odd and bowl**	**3.927942945**	**No**	**No**
dimm	dimmed	3.706700047	No	Yes
dmrt93B	doublesex-Mab related 93B	3.312553213	Yes	No
sna	snail	3.179396467	No	Yes
p53	**CG33336 gene product from transcript CG33336-RB**	**2.673639768**	**No**	**No**
lab	labial	2.609381973	No	Yes
jumu	jumeau	2.395581577	No	Yes
CG6854	CG6854 gene product from transcript CG6854-RC	2.009540722	No	Yes
Stat92E	**Signal-transducer and activator of transcription protein at 92E**	**-2.037937061**	**No**	**No**
sqz	**squeeze**	**-2.047744373**	**No**	**No**
cic	capicua	-2.197556027	Yes	No
srp	**serpent**	**-2.257803191**	**No**	**No**
Clk	**Clock**	**-2.330596469**	**No**	**No**
Pdp1	**PAR-domain protein 1**	**-2.453192158**	**No**	**No**
exex	**extra-extra**	**-2.620646717**	**No**	**No**
CG2678	**CG2678 gene product from transcript CG2678-RA**	**-2.666296599**	**No**	**No**
luna	CG33473 gene product from transcript CG33473-RB	-4.775750326	Yes	No
Mad	Mothers against dpp	-5.010461861	Yes	Yes
CG6129	CG6129 gene product from transcript CG6129-RD	-7.359329899	Yes	No

Table 10. List of transcription factors altered in Apc-Ras 1 week ACI. In bold letters are presented those genes specific for Apc-Ras.

Another functional group highly represented was proliferation-related genes (Table 11). Apc-Ras cells one week ACI show upregulated proliferation genes as the mitogenic protein String, the cyclin B, the Polo kinase and Mkp3. Interestingly, almost all the proliferation genes were shared by Apc-Ras and Ras gene list, suggesting that the proliferative potential of Apc-Ras clones derives mostly from the Ras programme. Remarkably, despite the hyperproliferation shown by Apc clones, we found few proliferation genes upregulated (Figure 41 and table 11). An exhaustive analysis of the DEG revealed, however, that most of the proliferation genes present in Apc-Ras and Ras clones were also upregulated in Apc clones, although below to the 2 fold

threshold. Most of those genes showed expression values between 1.5 and 1.99 in Apc clones.

SYMBOL	GENE NAME	FOLD CHANGE	ALTERED IN APC	ALTERED IN RAS
stg	string	6.340772953	No	Yes
Mkp3	Mitogen-activated protein kinase phosphatase 3	5.245907111	No	Yes
msd1	**mitotic spindle density 1**	**3.83081083**	**No**	**No**
CHKov1	CG10618 gene product from transcript CG10618-RB	2.941583189	Yes	No
CG7922	CG7922 gene product from transcript CG7922-RA	2.90429135	Yes	No
polo	CG12306 gene product from transcript CG12306-RA	2.622321497	No	Yes
cnn	centrosomin	2.56936913	No	Yes
cerv	**cervantes**	**2.486307629**	**No**	**No**
lds	**lodestar**	**2.405166306**	**No**	**No**
cmet	CENP-meta	2.399092734	No	Yes
pav	pavarotti	2.379322786	No	Yes
mad2	CG17498 gene product from transcript CG17498-RA	2.3520829	No	Yes
pim	pimples	2.333740413	No	Yes
sti	sticky	2.321856494	No	Yes
CycB	Cyclin B	2.276940483	No	Yes
mei-38	**meiotic 38**	**2.272755766**	**No**	**No**
RPA2	Replication protein A2	2.192309994	No	Yes
Z600	**CG17962 gene product from transcript CG17962-RA**	**2.178097689**	**No**	**No**
rod	**rough deal**	**2.15854999**	**No**	**No**
Cks30A	Cyclin-dependent kinase subunit 30A	2.138000341	No	Yes
cdc2	CG5363 gene product from transcript CG5363-RA	2.122547482	No	Yes
dmt	**dalmatian**	**2.114997335**	**No**	**No**
ial	IpII-aurora-like kinase	2.112008551	No	Yes
mod(mdg4)	**modifier of mdg4**	**2.085415586**	**No**	**No**
feo	fascetto	2.050834794	No	Yes
fzy	fizzy	2.041742535	No	Yes
borr	borealin-related	2.039979677	No	Yes
Klp61F	Kinesin-like protein at 61F	2.032112134	No	Yes
Incenp	**Inner centromere protein**	**2.025890343**	**No**	**No**
bora	aurora borealis	2.02338917	No	Yes

Table 11. List of proliferation-related genes altered in Apc-Ras 1 week ACI. In bold letters are presented those genes specific for Apc-Ras.

Finally, the group of cell adhesion and polarity genes includes a plethora of genes with diverse functions. None of the main genes related with cell adhesion (adherens junction/septate junction members) or polarity members were altered. In contrast, genes related with specific junctions or specialized tissues, mostly genes related with heterophilic cell-cell adhesion and muscle development, were altered (Table 12). This data suggest that specific junctions and differential adhesion levels could be formed between Apc-Ras cells. Similar scenarios have been observed in

mammals, where the differential expression of Ephrin member proteins between CRC and WT cells induce differential cell adhesion (Batlle, 2012). Interestingly, Reph, a intracellular regulator of the Ephrin pathway recently described (Dearborn, 2012), was upregulated in Apc-Ras cells. This Reph upregulation suggests a putative role of Ephrins in Apc-Ras progression that future work will have to determine.

SYMBOL	GENE NAME	FUNCTION	FOLD CHANGE	PRESENT IN APC	PRESENT IN RAS
kirre	kin of irre	heterophilic cell-cell adhesion	7.933765753	No	Yes
Tsp	**Thrombospondin**	**cell adhesion mediated by integrin**	**7.392953233**	**No**	**No**
Ama	Amalgam	cell adhesion	4.867243472	Yes	Yes
plx	**pollux**	**cell adhesion mediated by integrin**	**4.606497368**	**No**	**No**
rst	**roughest**	**homophilic cell adhesion**	**3.233328966**	**No**	**No**
Gli	**Gliotactin**	**septate junction assembly**	**2.107874468**	**No**	**No**
scrib	scribbled	septate junction assembly	2.021504174	No	Yes
btsz	bitesize	Cell adhesion and Polarity	-2.023985199	No	Yes
sinu	sinuous	septate junction assembly	-2.264987416	No	Yes
CG42256	**DSCam2**	**homophilic cell adhesion**	**-2.341181024**	**No**	**No**
CG42330	**DSCam4**	**homophilic cell adhesion**	**-2.617465202**	**No**	**No**

Table 12. List of cell adhesion genes most-likely to be involved in Apc-Ras progression. In bold letters are presented those genes specific for Apc-Ras.

In summary, the transcriptional analysis performed has identified many putative genes that could contribute to the initial steps of tumoral progression of Apc-Ras clones.

2.2 Apc-Ras transcriptomic changes during clone progression.

Tumour progression implies several changes in the tumour cells (Hanahan, 2011). Usually, small human tumours are well differentiated and resemble the normal surrounding tissue. In contrast, advanced tumours present lower levels of differentiation, aberrant cell types and gross tissue defects. Likewise, Apc-Ras clones one week ACI are small and do not show transcriptional changes of differentiation markers but four weeks ACI have grown to form mostly undifferentiated tumour masses. In order to analyse which are the transcriptional differences during the tumoral progression of Apc-Ras clones, we performed the transcriptional profile analysis of Apc-Ras clones four weeks ACI and compared both to Apc-Ras clones 1 week ACI and wild type clones four weeks ACI.

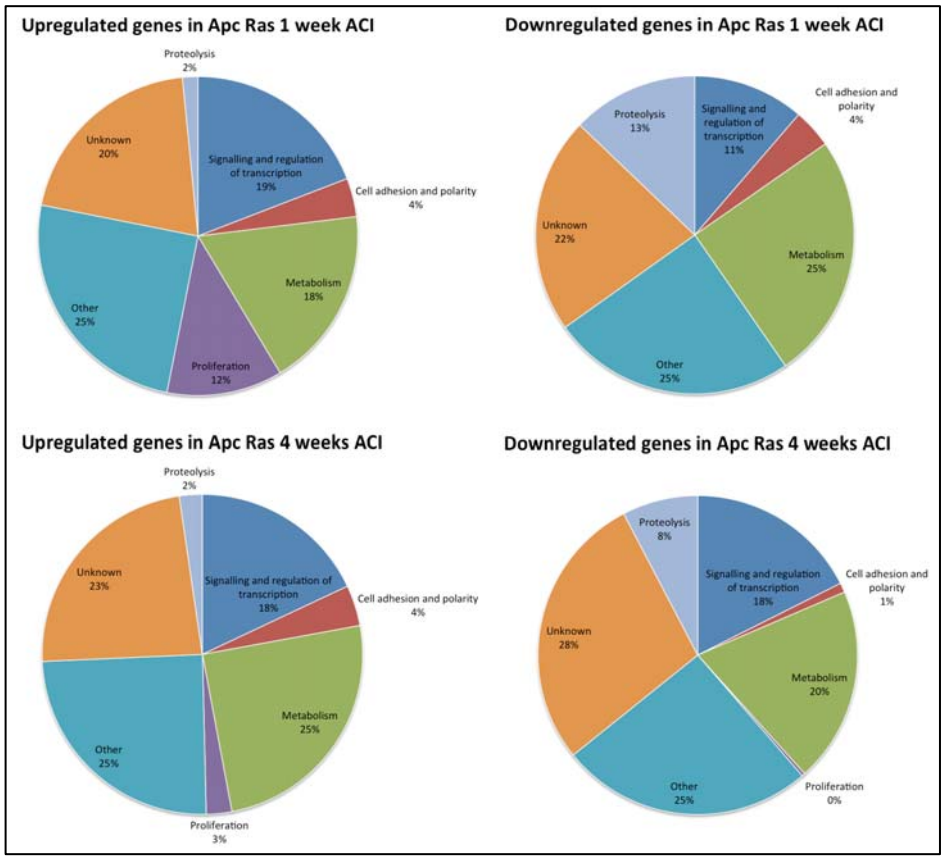

Figure 42.- DEG comparision by function between Apc-Ras one week and four weeks.

We observed few differences between Apc-Ras clones one and four weeks ACI at the overall functional analysis level (Figure 42). There was a slight decrease in the number of proliferation genes four weeks ACI, although most of those genes showed expression values between 1,5FC and 1,99FC. However, striking differences were observed at gene level (Table 43). Remarkably, if we compare the genes altered in Apc-Ras at one week ACI with those altered at four weeks we can observe that most of the genes are not shared between both conditions suggesting that most of the genes are important for the initiation or the progression of the clone but not essential during all the clone progression (Figure 43).

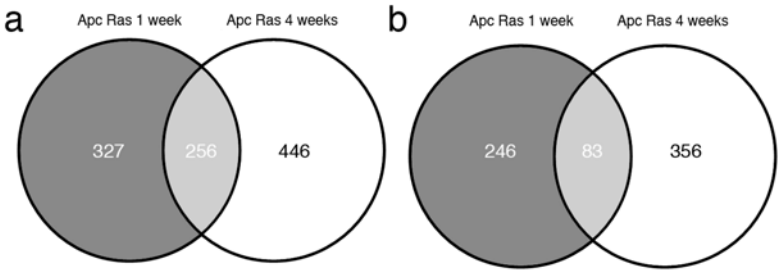

Figure 43.- Venn diagram of the DEG list of Apc-Ras vs WT at one week and four weeks ACI. Observe that there is a small overlapping of the gene lists. left: lists containing all the genes present in the comparisons Apc-Ras vs WT one week and four. Right: lists containing just those DEG specific of Apc-Ras vs WT and not present in Apc or Ras vs wt lists.

Our analysis suggests that few genes are essential during all the stages of Apc-Ras tumoral progression. Conversely, most of the genes identified seem to be implicated either in the initial or the late stages of the Apc-Ras clone development, but not both. We have to take into account, however, that the DEG may be due both to differential expression in tumour cells as well as to the different identity of the cells in later stages of tumour development. In any case, our results highlight several signalling molecules and transcription factors, specifically altered four weeks ACI, which could be contributing to the Apc-Ras phenotype (Table 13).

As previously shown by qPCR analysis, the Notch ligand Delta was downregulated in Apc-Ras clones four weeks ACI, confirming the accuracy of the transcriptional profile. The most striking alteration was the downregulation of many core components of the Dpp pathway: *Tkv, Punt, Dad and Mad*. Moreover, several negative regulators of the pathway appear upregulated in Apc-Ras clones four weeks ACI, such *Follistatin* or *Short Gastrulation* (Table 13). All together, these results suggest that the Dpp pathway could act as a tumour suppressor and, consequently, would need to be downregulated in order for the Apc-Ras clones to progress, a role that is characterized in section 3. Other signalling molecules that could also play a role in Apc-Ras clone progression were *Pvf3 (PVR/PDGF-like ligand), Crosveinless-2 (a short-range Dpp pathway modulator)* (Serpe, 2008), *Dawdle (Activin-like ligand)* (Parker, 2006), *Wengen (TNF-like ligand)* (Kauppila, 2003) *or Unpaired 2 (Jak-Stat receptor ligand)*. We also observed that the RTK receptor Torso and the Hedgehog receptor *Patched* were upregulated at four weeks ACI (Table 13), while their ligands, Trunk and Hedgehog, were upregulated already one week ACI (Table 9). It has been well established that Patched is itself a target gene of the Hh pathway, and therefore its upregulation four weeks ACI could be consequence of Hh pathway activity. At this time point it is not clear, however, whether the cells that produce Hh would be the same that respond to it, or whether Hh production and response could be identifying two different cell types within the tumour mass. In addition, the upregulation of the RTK Torso and its ligand, Trunk, is remarkably as they are mainly implicated in early embryo morphogenesis (Casanova, 1989) and Trunk has not been never detected in posterior stages of the development or adulthood (Flybase, 2013). We also found that the ligand Trim9 and the receptor Unc5 of the Netrin pathway, a pathway involved in chemotaxis and axon guidance, were downregulated, suggesting a putative role of Netrins in Apc-Ras clone progression and migration. Finally, many transcription factors also appeared altered, both upregulated and downregulated, specifically in Apc-Ras at four weeks

ACI, as Bicoid, a specific early embriogenesys TF (Flybase, 2013), or the Notch transducer elements Enhancer of Split HLHgamma and HLHm7 (Table 13).

SYMBOL	GENE NAME	FUNCTION	FOLD CHANGE	PRESENT IN APC	PRESENT IN RAS
daw	**dawdle**	**Activin receptor binding**	**11.28935441**	**No**	**No**
Pvf3	**PDGF- and VEGF-related factor 3**	**PDGF receptor binding**	**8.793451766**	**No**	**No**
cv-2	**crossveinless 2**	**BMP receptor binding**	**6.069136611**	**No**	**No**
nkd	naked cuticle	Negative reg. of Wg pathway	5.922401577	Yes	No
trbl	**tribbles**	**Ser/thr kinase activity**	**5.449337196**	**No**	**No**
upd2	unpaired 2	Positive reg. Of Jak-Stat Pathway	4.7088503	No	Yes
how	**held out wings**	**mRNA binding**	**4.14891398**	**No**	**No**
kek2	**kekkon-2**	**Negative reg. Of EGFR Pathway**	**3.91751577**	**No**	**No**
Fs	**Follistatin**	**Negative reg. of Dpp pathway**	**3.853888286**	**No**	**No**
CG9098	**CG9098 gene product from transcript CG9098-RA**	**Positive reg. Of EGFR Pathway**	**3.780634631**	**No**	**No**
wgn	**wengen**	**TNF receptor binding**	**3.731615761**	**No**	**No**
Gadd45	**CG11086 gene product from transcript CG11086-RA**	**Regulation of JNK Cascade**	**3.494298111**	**No**	**No**
br	**broad**	**Transcription factor activity**	**3.343049399**	**No**	**No**
tor	torso	Torso signalling receptor activity	2.779982693	No	Yes
Ets21C	Ets at 21C	Transcription factor activity	2.777494121	No	Yes
Vdup1	Vitamin D[[3]] up-regulated protein 1	Negative reg. of gene expression	2.419220589	No	Yes
Ack	**activated Cdc42 kinase**	**Tyrosine kinase activity**	**2.413170264**	**No**	**No**
loco	locomotion defects	GPCR Signalling transduction activity	2.396479485	No	Yes
alph	**alphabet**	**Ser/thr phosphatase activity**	**2.312203683**	**No**	**No**
rumi	**CG31152 gene product from transcript CG31152-RA**	**Negative reg. Of Notch pathway**	**2.230037406**	**No**	**No**
bcd	**bicoid**	**Transcription factor activity**	**2.202949952**	**No**	**No**
ptc	**patched**	**Hh signalling receptor binding activity**	**2.192396734**	**No**	**No**
Sox14	**Sox box protein 14**	**Transcription factor activity**	**2.137399874**	**No**	**No**
Traf4	TNF-receptor-associated factor 4	positive reg. of JNK signalling	2.115970219	No	Yes
Bin1	**Bicoid interacting protein 1**	**Transcription factor binding activity**	**2.11518772**	**No**	**No**
vnd	ventral nervous system defective	Transcription factor activity	-2.065131664	No	Yes
HLHm7	E(spl) region transcript m7	Transcription factor activity	-2.150092377	No	Yes
put	**punt**	**Dpp signalling receptor pathway**	**-2.1700446**	**No**	**No**
Trim9	**CG31721 gene product from transcript CG31721-RB**	**netrin-activated signaling pathway**	**-2.185090074**	**No**	**No**
Mitf	**CG17469 gene product from transcript CG17469-RA**	**Transcription factor activity**	**-2.326641693**	**No**	**No**
unc-5	**CG8166 gene product from transcript CG8166-RA**	**netrin receptor activity**	**-2.378782169**	**No**	**No**
oc	ocelliless	Transcription factor activity	-2.48575648	Yes	No
CG7497	CG7497 gene product from transcript CG7497-RB	GPCR	-2.493116099	No	Yes
Tkv	thickveins	Dpp signalling receptor activity	-2.547332924	No	Yes
jing	**CG9397 gene product from transcript CG9397-RI**	**Transcription factor activity**	**-2.606883709**	**No**	**No**
for	**foraging**	**cGMP-dependent protein kinase activity**	**-2.645799403**	**No**	**No**
Fer1	**48 related 1**	**Transcription factor activity**	**-2.864203007**	**No**	**No**
HLHmgamma	**E(spl) region transcript mgamma**	**Transcription factor activity**	**-3.123105635**	**No**	**No**
tap	**target of Poxn**	**Transcription factor activity**	**-3.25469998**	**No**	**No**
corto	**CG2530 gene product from transcript CG2530-RA**	**chromatin silencing**	**-3.282609841**	**No**	**No**
dally	division abnormally delayed	extracellular signalling regulation	-3.388524535	No	Yes

SYMBOL	GENE NAME	FUNCTION	FOLD CHANGE	PRESENT IN APC	PRESENT IN RAS
Dl	**Delta**	**Notch signalling receptor binding**	**-4.434625682**	**No**	**No**
Ptx1	**CG1447 gene product from transcript CG1447-RC**	**Transcription factor activity**	**-8.210966398**	**No**	**No**
Dad	**Daughters against dpp**	**Negative reg. of Dpp pathway**	**-14.32614306**	**No**	**No**

Table 13. List of signalling molecules and transcription factors specifically altered at four weeks ACI most-likely to be involved in Apc-Ras progression. In bold letters are presented those genes specific for Apc-Ras.

Another remarkable characteristic was the Apc-Ras four weeks ACI-specific upregulation of several cell adhesion molecules, as Fasciclin I, II and III (Table 14). This molecules act via homophilic adhesions and have been described as modulators of the axon guidance (Elkins, 1990; Grenningloh, 1991; Snow, 1989). Moreover, some of these cell markers are not usually expressed in the WT adult gut, such Fasciclin I that is expressed almost exclusively in the CNS during adulthood (Flybase, 2013). The presence of specific Fasciclins such Fas1 suggests that Apc-Ras cells could be creating new and specific adhesions between them. We suggest that these proteins could be playing an essential role in cell compartmentalization and tumour cell migration.

SYMBOL	GENE NAME	FUNCTION	FOLD CHANGE	PRESENT IN APC	PRESENT IN RAS
Fas1	**Fasciclin 1**	**homophilic cell adhesion**	**14.04296766**	**No**	**No**
Lac	**Lachesin**	**septate junction assembly**	**9.821146617**	**No**	**No**
Fas3	Fasciclin 3	homophilic cell adhesion	5.880977118	No	Yes
prc	**pericardin**	**cell adhesion and polarity**	**3.83475367**	**No**	**No**
kon	**kon-tiki**	**muscle attachment activity**	**2.990004351**	**No**	**No**
Anxb11	**Annexin B11**	**cell adhesion activity**	**2.381586397**	**No**	**No**
Fas2	**Fasciclin 2**	**homophilic cell adhesion**	**2.206758579**	**No**	**No**
CG31004	Mesh	smooth septate junction assembly	-2.126320714	No	Yes

Table 14. List of cell adhesion molecules specifically altered at 4 weeks ACI most-likely to be involved in Apc-Ras progression. In bold letters are presented those genes specific for Apc-Ras.

Finally, I would like to point out that some of the differential gene expression between Apc-Ras one week and four weeks ACI could be attributed to regional differences. As mentioned above, four weeks ACI clones are usually located in the most anterior part of the anterior midgut. Recently published papers demonstrated that gene expression changes along the midgut anteroposterior axis (Buchon, 2013; Marianes, 2013) and therefore some differential gene expression might be due to the spatial restriction of the Apc-Ras four weeks ACI clones.

Moreover, it should be considered that part of the transcriptional differences could be linked to the senescence of the host and its cells as well as to the change in cell type composition of the clones, that could be affecting dramatically Apc-Ras clone gene expression.

2.3 Apc-Ras cells reprogram their metabolism progressively to produce a Warburg effect phenotype

One of the most intriguing events during tumour progression is the metabolic switch that tumour cells suffer during the progression of the disease (Cairns, 2011). Normal cells obtain ATP metabolizing the glucose by glycolysis and use the final substrate, pyruvate, to enter into the chain of redox reactions known as Krebs cycle. The NADH created in the Krebs cycle is processed by a very energetic process called oxidative phosphorylation producing high quantity of ATP molecules (36 ATP molecules for each glucose molecule). In contrast, cancer cells uncouple the glycolysis from the oxidative phosphorylation. Instead, Pyruvate is processed into Lactate in a low-efficiency process (4 ATP molecules for each glucose molecule). This metabolic switch is known as Warburg effect (Figure 44), and still nowadays the reason for this metabolic switch is unknown (Bensinger, 2012; Cairns, 2011; Soga, 2013). However, in the last decade many results indicate that glucose metabolites could be used in biosynthetic pathways in order to create new molecules essential for a quick division of the tumour cells. New membranes, organelles and macromolecules should be created quicker than in normal conditions and the use of the glucose metabolism metabolites could supply the requirements of macromolecules (Cairns, 2011).

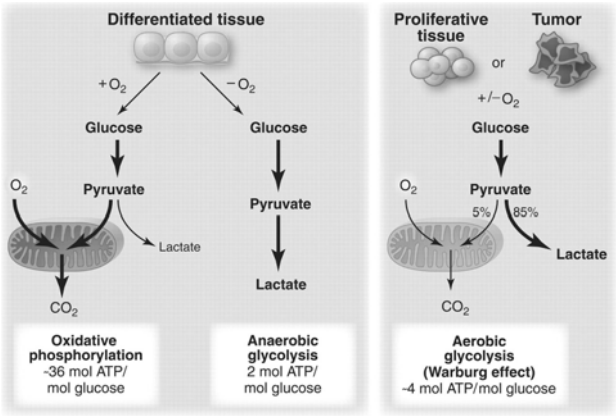

Figure 44. Warburg effect diagram. Differentiated cells use the oxidative phosphorylation to obtain large amounts of energy. Proliferative tissues or tumours use an inefficient aerobic glycolysis to produce less energy but useful to generate necessary macromolecules.

In order to determine whether Apc-Ras cells could be using the Warburg strategy, we analysed possible alterations on the GSEA terms involved in the main energetic metabolic pathway. As the Warburg effect is a process related with the size of the tumour that occurs while the tumour is progressing we compared the differential gene expression between Apc-Ras clones one and four weeks ACI. Interestingly, we observed that both Krebs cycle and oxidative phosphorylation were significantly

upregulated in one week Apc-Ras clones (Figure 45). Conversely, glycolysis and Pyruvate metabolism, both enhanced in Warburg effect-suffering cells, were significantly enhanced in four weeks Apc-Ras clones (Figure 45 and Annex 1 for relative gene expression and Annex 4 for each GSEA gene list).

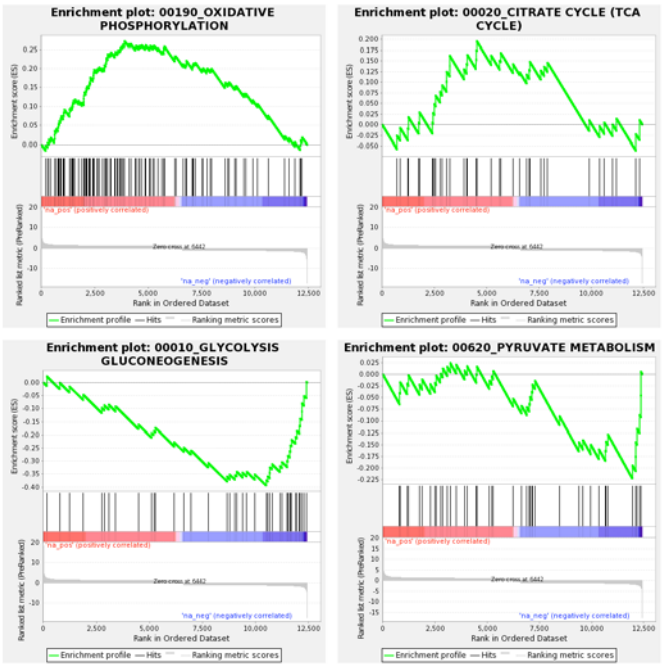

Figure 45. GSEA for the main metabolic pahways involved in energy production. GSEA analysis distributes all the genes by FC. The genes more upregulated in Apc-Ras one week ACI appear in the left side of the graphic while the most upregulated genes in Apc-Ras 4 weeks ACI appear in the right side of the graphic. Up: metabolic pathways upregulated in Apc-Ras one week vs Apc-Ras four weeks ACI.
Bottom: downregulated metabolic pathways in Apc-Ras one week vs Apc-Ras four weeks ACI. This metabolic shift towards glycolysis uncoupled from the oxidative phosphorilation is common in advance tumours.

Moreover, other glucose metabolic processes as pentose and glucoronate interconversions, fructose and mannose metabolism and starch and sucrose metabolism, linked to the cancer metabolic switch (Marisa, 2013), were also upregulated in Apc-Ras cells (Table 5 and 6) . The GSEA analysis also showed downregulation of the fatty acid metabolism (fatty acid metabolism, biosynthesis of unsaturated fatty acids, glycerolipid metabolism) that, together with the upregulation of nucleoside biosynthesis (pyrimidine metabolism), are metabolic changes linked to CRC progression (Maglietta, 2012). Finally, we also observed a high increase in the expression of genes related to Glutathione metabolism. Glutathione presence is related with reactive oxygen species (ROS) protection and its levels are elevated in many cancer tissues (Balendiran, 2004). In our model, Apc-Ras cells upregulate many glutathione-s-transferases, enzymes essential for proper glutathione metabolism and detoxification. This glutathione-s-transferases upregulation is linked with an upregulation of detoxification-related KEGG terms such as cytochrome P450 or drug metabolism. Together, these results show that glutathione and drug metabolism are upregulated in Apc-Ras cells, possibly to protect the cells from ROS. All these results

strongly suggest that dramatic changes in cell metabolism could be occurring in Apc-Ras cells.

2.4 A RNAi screening reveals key driver genes for Apc-Ras tumour progression.

Hundreds of genes show transcriptional alterations in a specific tumour, but few of them are implicated in the progression of the tumour. These genes are known as "tumour driver genes", in contrast to those that appear altered as a consequence of the tumorigenic process, the "passenger genes" (Ji, 2010). Genetic screenings are a very useful tool to discriminate and identify key driver genes. Hence, in order to identify those key driver genes during Apc-Ras clones progression, we decided to perform an *in vivo* RNAi screening in Apc-Ras clones. We used the RNAi technology to individually downregulate 246 candidate genes within Apc-Ras clones and identify those able to consistently modify their phenotype four weeks ACI. The candidate gene list included genes upregulated in Apc-Ras clones four weeks ACI, genes involved in human CRC progression and other handpicked putatively interesting genes (Annex 4). From the 246 genes analysed, we found 62 (25%) that changed the phenotype of Apc-Ras clones. We observed four main phenotypes; 1) guts with wild-type like clones (2 genes), 2) guts bearing very small anterior clones (25 genes), 3) guts with very small or unicellular scattered clones (33 genes) and 4) guts bearing clones invading the proventriculus (2 genes) (Table 15 and Figure 46).

Many positive genes from the screen are very promising. For example, Hedgehog, the morphogen of the Hedgehog signalling pathway seems essential for Apc-ras clone progression (Figure 46). With our results, Hedgehog pathway has emerged as an essential putative signalling pathway during Apc-Ras clone progression. By the identification of a substantive transcriptional upregulation of various members of the pathway during Apc-Ras clone progression and the essential role of Hedgehog in Apc-Ras clone growth, we can conclude that Hedgehog pathway is playing an essential role in tumour formation in the Adult *Drosophila* midgut.

number	Gene symbol	Viena RNAi	Selected by	Effect	Result
1	Aats-trp	107049	Up in Apc Ras	Yes	Small clones along the gut
12	atpalpha	12330	Others	Yes	Reduction anterior clone
13	bai	100612	Others	Yes	Invasion of the proventricle
20	Brwd3	110808	Others	Yes	Reduction anterior clone
22	b-tub at 56D	24138	Others	Yes	Small clones along the gut
23	bw	101584	Up in Apc Ras	Yes	Reduction anterior clone
26	cactin	106979	Up in Apc Ras	Yes	Small clones along the gut
30	CG1021	37336	Up in Apc Ras	Yes	Reduction anterior clone
33	CG10641	31308	Others	Yes	Small clones along the gut
36	CG10916	107518	Up in Apc Ras	Yes	Reduction anterior clone
38	CG11188	106977	Up in Apc Ras	Yes	Small clones along the gut
43	CG13623	110643	Up in Apc Ras	Yes	clones similar to wt
48	CG42666	103667	Up in Apc Ras	Yes	Small clones along the gut
54	CG17187	40051	Up in Apc Ras	Yes	Small clones along the gut
67	CG32138	34412	Others	Yes	Reduction anterior clone
69	CG32369	103923	Up in Apc Ras	Yes	Reduction anterior clone
72	CG34372	107979	Up in Apc Ras	Yes	Small clones along the gut
78	CG42321	107000	Others	Yes	Small clones along the gut
81	CG5273	107408	Up in Apc Ras	Yes	Small clones along the gut
86	CG6854	12762	Up in Apc Ras	Yes	Small clones along the gut
87	CG7044	27811	Up in Apc Ras	Yes	Reduction anterior clone
90	CG7188	110358	Up in Apc Ras	Yes	Small clones along the gut
92	CG7860	108281	Others	Yes	Small clones along the gut
96	CG9098	105144	Up in Apc Ras	Yes	Invasion of the proventricle
103	csk	102313	Up in Apc Ras	Yes	Small clones along the gut
118	eIF2B-delta	104403	Up in Apc Ras	Yes	Small clones along the gut
130	GB13F	100011	Others	Yes	Reduction anterior clone
131	gw	103581	Others	Yes	Small clones along the gut
134	hh	109454	Up in Apc Ras	Yes	Small clones along the gut
138	Hsc70-4	101734	Others	Yes	Small clones along the gut
139	lap2	2973	Others	Yes	Small clones along the gut
141	ImpL2	106543	Up in Apc Ras	Yes	Reduction anterior clone
145	jhamt	103958	Others	Yes	Small clones along the gut
158	loco	9248	Up in Apc Ras	Yes	Reduction anterior clone
160	Magu	106494	Others	Yes	Small clones along the gut
161	mct1	106773	Others	Yes	Small clones along the gut
162	Mmp1	101505	Up in Apc Ras	Yes	Reduction anterior clone
165	Myc	106066	Others	Yes	Small clones along the gut
168	nonA	26441	Others	Yes	Reduction anterior clone
170	oatp30B	22983	Others	Yes	Small clones along the gut
174	Pepck	20529	Up in Apc Ras	Yes	Reduction anterior clone
182	pros54	110659	Others	Yes	Reduction anterior clone
187	Pvr	105353	Up in Apc Ras	Yes	Small clones along the gut
189	RanGap	108264	Others	Yes	Small clones along the gut
194	RPA2	102306	Up in Apc Ras	Yes	Small clones along the gut
200	sens	106028	Others	Yes	Small clones along the gut
202	slik	43783	Others	Yes	Reduction anterior clone
203	slmb	34273	Others	Yes	Reduction anterior clone
204	slo (slowpoke)	104421	Others	Yes	Small clones along the gut
205	smo	108351	Others	Yes	Small clones along the gut
209	Spn5	28340	Up in Apc Ras	Yes	Reduction anterior clone
213	stc	47973	Others	Yes	Reduction anterior clone
225	mtSSB	107322	Others	Yes	Small clones along the gut
227	mt DNA helicase	108644	Others	Yes	Reduction anterior clone
229	sesB	48581	Others	Yes	Reduction anterior clone
230	Sod2	110547	Others	Yes	Reduction anterior clone
231	mt TFB2	107086	Others	Yes	Small clones along the gut
232	boi	3060	Others	Yes	Small clones along the gut
236	Dp110	107390	Others	Yes	clones similar to wt
239	E-cad	2781	Others	Yes	Reduction anterior clone
245	Mlh1	105425	Others	Yes	Reduction anterior clone
246	Msh6	108076	Others	Yes	Reduction anterior clone

Table 15. list of selected positive RNAi by phenotype.

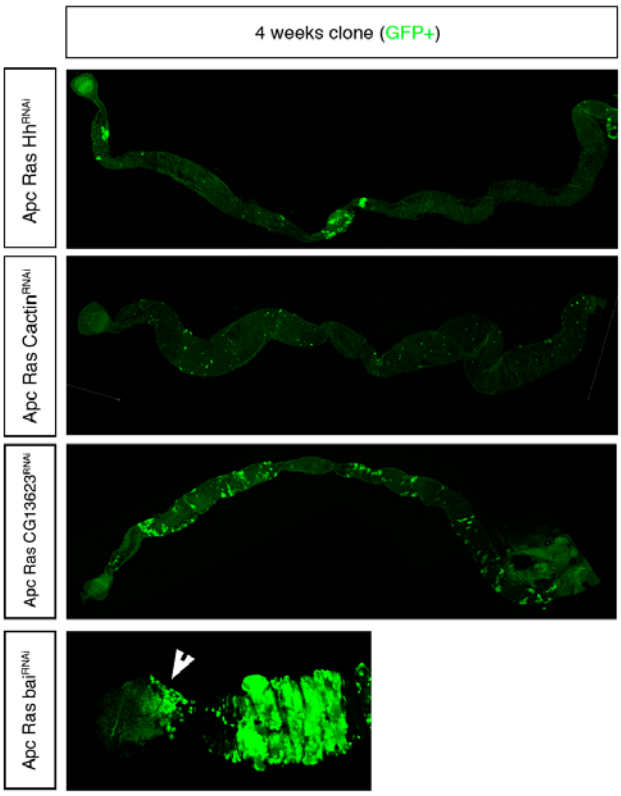

Figure 46. A RNAi screen allows to identify key genes for Apc-Ras clone progression. The depletion of Hh produces the shrinkage of Apc-Ras clones. The depletion of cactin produces produces the apparition of small clones scattered along the gut and the disappearance of the *typical* Apc-Ras anterior clone. Few RNAi such cg13623 RNAi produce the apparition of WT-like clones. Finally, two RNA (including bai) produce clones that can invade the proventriculus.

This screening has revealed 62 genes that seem to be essential during Apc-Ras tumour progression. These genes should be carefully analysed in further stages of the study to understand their role in tumour progression. For example, we want to identify which of these genes have a specific role in tumour formation and which of them are housekeeping genes essential for every cell to survive. Nowadays, a second re-screening is being performed to select those most promising genes to deeper analyse their contribution on Apc-Ras clone progression and normal gut homeostasis. Finally, this screening shows the usefulness of *Drosophila* in the identification of candidate genes by genetic screenings as a similar screening in mice would be much more difficult and time-consuming.

3 Dpp pathway signalling acts as a tumour suppressor during Apc-Ras clone progression

3.1 Apc-Ras clones show a transcriptional downregulation of core Dpp Pathway components.

TGF-β acts as a cytostatic signal during tumour progression (Ding, 2011; Elliott, 2005) and its activity is silenced during the adenoma-to-carcinoma transition (S. Markowitz, 2009). In *Drosophila*, the main homolog of the TGF-β superfamily signalling molecules is Decapentaplegic (Dpp). Dpp binds to a heterodimeric receptor (Tkv and Put), which transduces the signal through the Smad proteins (Mad and Med) to induce target gene expression. In the adult *Drosophila* midgut, Dpp has been recently described as an anti-mitogenic signal during normal homeostasis (Guo, 2013). Remarkably, Apc-Ras clones four weeks ACI show a transcriptional downregulation of many core components of the Dpp signalling pathway (Table 16). This transcriptional downregulation is similar to what occurs in CRC, where around a 20% of cases present mutations that inactivate the TGF-β signalling pathway (Network, 2012). This downregulation was not present in Apc-Ras clones one week ACI, neither in individual Apc or Ras clones (Table 16), indicating that this downregulation is Apc-Ras specific and depends on Apc-Ras clone progression. Moreover, the downregulation was seen in components related to Dpp reception, but not in Dpp production, indicating that the signal is specifically altered in the receptor cells.

Gene	Apc-Ras vs WT one week fold change		Apc-Ras vs WT four fold change	
Dpp	1,03		-1,14	
Tkv	-1,34		-2,54	(Ras -4,42)
Punt	-1.06		-2,17	
Mad	-5,01	(Apc -2,21 Ras -3,39)	-5,50	(Ras -11,01)
Med	1,23		1,27	
Dad	-1,91		-14,32	

Table 16. Fold changes of Dpp components in Apc-Ras. In parentheses those significant changes in other genotypes.

We confirmed the microarray data by qPCR analysis, that showed the downregulation of the receptors Tkv and Punt; the transducers Mad and Medea and the negative regulator and target gene of the pathway, Dad (Figure 47). These results

led us to hypothesize that Apc-Ras cells must be less responsive to the Dpp signalling. In this context, the downregulation of the target gene of the pathway Dad could suggest that Apc-Ras cells fail to respond to Dpp signalling when compared to WT cells.

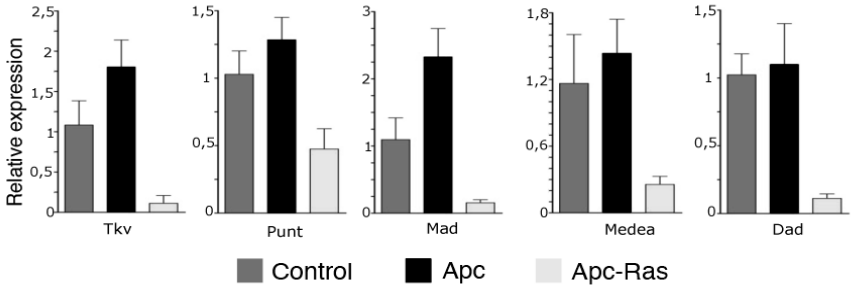

Figure 47. qPCR for Dpp components mRNA.
Observe the strong reduction of all the components in Apc-Ras 4 weeks ACI in comparison with Apc or WT samples. Ras mRNA was not possible to extract.

3.2 Dpp pathway transcriptional downregulation is essential for Apc-Ras clone progression

To analyze the functional role of Dpp in the progression of Apc-Ras clones, we activated the Dpp pathway by the expression of an activated form of its receptor Thickveins (UAS Tkv^{Act}) (Nellen, 1996) in Apc-Ras clones. Interestingly, the activation of the Dpp pathway in Apc-Ras clones was sufficient to block clone growth. Apc-Ras-Tkv* guts four weeks ACI showed a significant decrease in the size of the clones, as well as a strong reduction of the overall GFP+ area (Figure 48). This result suggests that Dpp pathway downregulation is essential for Apc-Ras clone progression. Accordingly to our results, the role of Dpp signalling pathway as a cytostatic signal in the *Drosophila* adult midgut has been recently described (Guo, 2013). In this report, clones with an active Dpp pathway showed a significant reduction in clone size, cell number and in the number of dividing, PH3+ cells when compared to WT clones. Accordingly, we generated clones expressing Tkv^{Act} and found that they were consistently smaller than WT clones at four weeks ACI (Figure 49 and Figure 18), indicating that Dpp pathway activation blocks clone growth. However, clones Apc-Ras-Tkv* usually contain PH3+ cells, indicating that although the capability of growth of Apc-Ras-Tkv* is clearly compromised (Figure 48), the ability of the Apc-Ras-Tkv*cells to divide is not completely blocked (Figure 49).

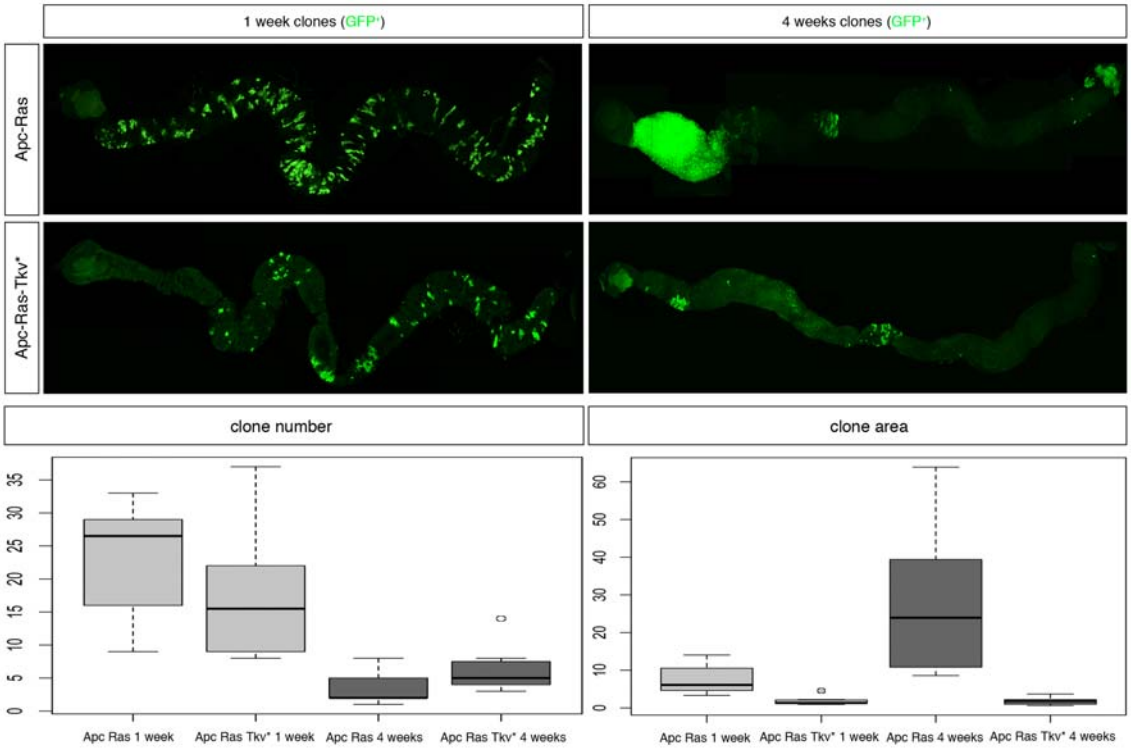

Figure 48. The silencing of Dpp signalling is essential for Apc-Ras clone progression. Up: overview of Apc-Ras and Apc-Ras-Tkv* at one week and four weeks ACI. Observe the difference in clone area at four between the two genotypes. Down: Quantifications of the clone area and clone number for Apc-Ras and Apc-Ras-Tkv* at one week and four weeks ACI

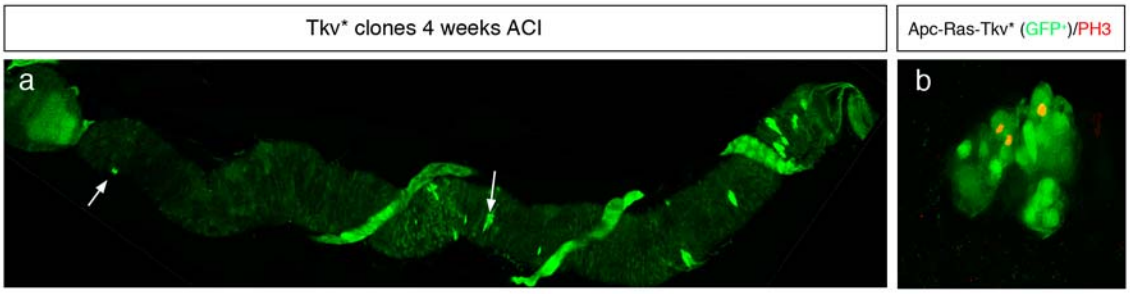

Figure 49. The overexpression of Dpp in the adult midgut provokes a reduction of clone growth but does not block completely the cell division. a. Clones bearing an active form of Tkv* are few and small in comparison with WT clones as previously reported (Guo, 2013). b. clones Apc-Ras-Tkv* are smaller in comparison with Apc-Ras clones but proliferative cells can be observed inside them.

3.3 Dpp signalling activation induces differentiation in Apc-Ras-Tkv clones and ectopic expression of differentiation markers in ISCs*

Our results showed that Apc-Ras-Tkv* clones were significantly smaller than Apc-Ras clones, indicating that Dpp signalling could act as a cytostatic signal during Apc-Ras clone progression. In this scenario, we wondered whether Dpp could be inducing ISC differentiation in Apc-Ras-Tkv* clones. The induction of ISC differentiation could be an indirect way to block cell proliferation, as differentiated cells cannot divide

in the adult midgut. Interestingly, in contrast to Apc-Ras clones, most of the cells in Apc-Ras-Tkv* clones four weeks ACI expressed the enterocyte marker Pdm1 (Figure 50). This result indicates that the activation of Dpp pathway in the Apc-Ras cells is sufficient to induce differentiation blocking, directly or indirectly, clone growth. Accordingly, we observed that the ectopic activation of the Dpp pathway in the ISCs, by the expression of UAS Tkv* in the progenitor esg+ cells is enough to induce the expression of the EC marker Pdm1 in all the ISCs (Figure 50). Conversely, clones mutant for Dpp in the adult midgut can differentiate properly (Guo, 2013). All together, these results suggest that ectopic activation of the Dpp pathway is enough to induce the expression of differentiation markers as Pdm1 but is dispensable for a correct differentiation.

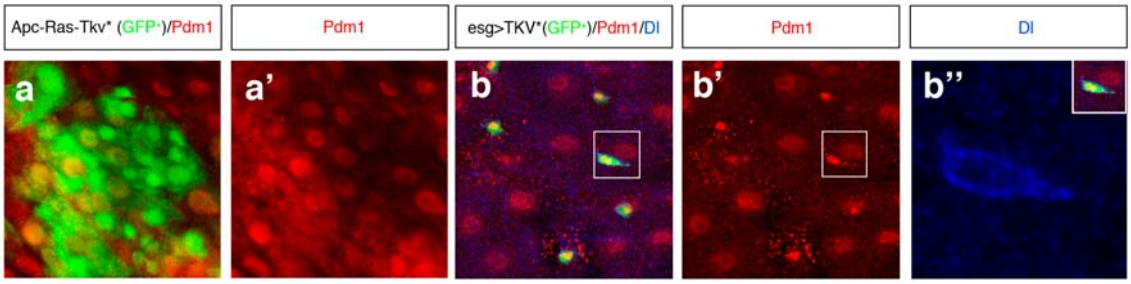

Figure 50. The overexpression of Dpp signalling induces cell differentiation in Apc-Ras cells and the expression of differentiation markers in the ISC. a. Apc-Ras-Tkv* clones present an increase of differentiated cells (Pdm1+) in comparison with Apc-Ras clones. b. The overexpression of the activated Tkv form (Tkv*) provokes the expression of a differentiation marker (Pdm1) in the ISCs (esg+/Dl+ cells).

4 Mirror is a repressor of Dpp signalling pathway during Apc-Ras clone progression

4.1 The transcription factor Mirror is upregulated in Apc-Ras cells and has putative binding sites in the core components of Dpp pathway.

As previously shown, many core components of the Dpp signalling pathway are transcriptionally downregulated in Apc-Ras cells. We sought to determine which mechanism could regulate this transcriptional downregulation, and we considered the possibility that a common negative regulator of transcription factor (TF) could be responsible for it. We searched for the existence of common binding sites in the promoter regions of the downregulated components of the Dpp pathway. In collaboration with the IRB bioinformatic unit, we analysed the 2000 kb upstream region of the transcription start point of the genes Tkv, Punt, Mad, Med and Dad. We found 70 known transcription factors with binding sites in these regions, interestingly, only 4 of these 70 were present in four of the five promoter regions analysed (Table 17 and Annex 5 for all the TF founded). These transcription factors were the three components of the Iroquois complex, Araucan, Caupolican and Mirror (Mirr), and the homeobox-containing gene Optix.

	Dad	Mad	Med	Put	Tkv	TOTAL
Araucan	2	1	0	1	3	7
Caupolican	2	1	0	1	3	7
Mirror	8	4	8	0	3	23
Optix	2	0	1	2	4	9

Table 17. Number of binding sites of selected TF on the promoter of the different Dpp pathway components.

To validate whether any of those TF was present in Apc-Ras clones we used two different approaches: 1) gene expression analysis by qPCR and microarray expression and 2) protein expression by immunostaining. The results indicated that only Mirr was increased in Apc-Ras by qPCR, microarray analysis and immunostaining (Figure 51 and Table 18). Araucan was slightly increased by qPCR but not by microarray neither immunostaining (Figure 51 and Table 18). Caupolican did not show a significant change in the microarray data or by immunostaining (qPCR was not performed by technical reasons) (Table 18). And finally, Optix expression was reduced in Apc-Ras clones when compared to WT clones and no change was detectable in the

microarray analysis (Figure 51 and Table 18). Therefore, Mirr is the only of these factors specifically upregulated in Apc-Ras clones, confirming Mirr as a bona fide candidate to be the common factor responsible of the transcriptional downregulation of the Dpp pathway components in Apc-Ras clones.

	Apc	Ras	Apc-Ras
Optix	1,029	-1,91	1,053
Araucan	-1,16	-1,13	1,15
Caupolican	-1,04	1,58	-1,088
Mirror	-1,09	1,85	**11,13**

Table 18. Gene expression levels for the selected TF in Apc, Ras and Apc-Ras transcriptome. Levels compared with wild type levels. Observe that Mirr is the only TF upregulated in Apc-Ras.

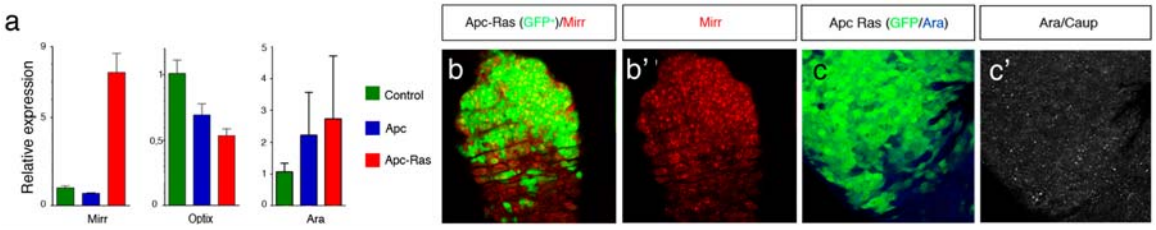

Figure 51. Mirr is overexpressed in Apc-Ras cells. a. qPCRs for Mirr, optix and Ara. b. immunostaining of Mirror in Apc-Ras clones. c. Immunostaining of Ara and Caup in Apc-Ras clones.

4.2 Mirror expression is essential for proper Apc-Ras clone progression

Mirr has been shown to act as a transcriptional repressor in many different contexts during *Drosophila* embryonic development (Andreu, 2012) and morphogenesis (Kehl, 1998; McNeill, 1997). To analyse whether Mirr has any role in Apc-Ras clone progression, we generated Apc-Ras clones overexpressing a RNAi for Mirr (Apc-Ras-Mirr^{RNAi}). The results showed that the reduction of Mirr expression in Apc-Ras clones was sufficient to reduce Apc-Ras clone growth (Figure 52). Apc-Ras-Mirr^{RNAi} clones one week ACI did not show significant differences with Apc-Ras clones neither in clone number, area nor distribution (Figure 52). However, four weeks ACI, the area occupied by Apc-Ras-Mirr^{RNAi} clones was reduced in comparison with Apc-Ras clones (Figure 52 a,d), demonstrating that Mirr is essential for Apc-Ras clone progression. In this context, the absence of Mirr in Apc-Ras clones (Apc-Ras-Mirr^{RNAi} clones) produced a similar effect to the activation of the Dpp pathway in Apc-Ras clones (Apc-Ras-Tkv* clones), corroborating the hypothesis that Mirr could be a transcriptional repressor of the Dpp pathway in Apc-Ras clones.

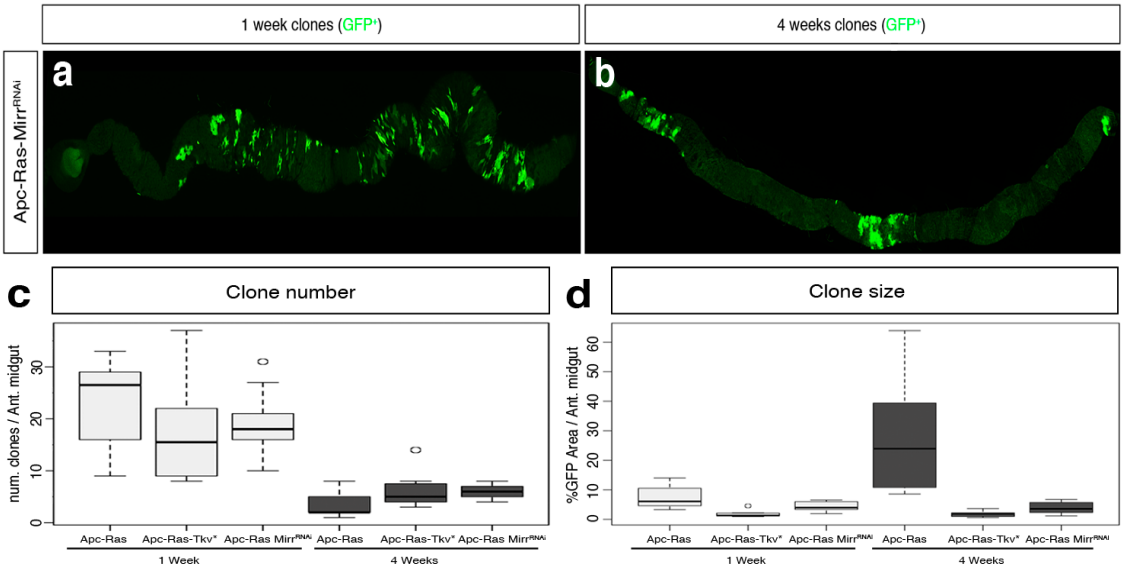

Figure 52. Mirr is essential for proper Apc-Ras clone progression. Up. Overview of Apc-Ras-MirrRNAi clones. Down. Quantifications of Apc-Ras, Apc-Ras-Tkv* and Apc-Ras-MirrRNAi clone area and number.

4.3 Mirror promotes Apc-Ras clone progression through downregulation of Dpp pathway.

We have shown that Mirr expression and Dpp pathway downregulation are both necessary events for the growth and progression of Apc-Ras clones. Additionally, a bioinformatic analysis has revealed that four core components of the Dpp pathway contain putative binding sites for Mirr in their promoter regions. Together, these results suggest that Mirr could repress the transcription of these core Dpp pathway components in Apc-Ras clones, reducing or eliminating their sensitivity to the tumour suppressor effect of Dpp. In order to demonstrate this possibility, we performed an epistatic analysis. We generated Apc-Ras clones expressing Mirr RNAi and a dominant negative form of Tkv (Tkv^{DN}) (Martin-Blanco, 2000), that blocks Dpp signalling (Apc-Ras-$Mirr^{RNAi}$-Tkv^{DN} clones). If MirrRNAi effect was not related to Dpp pathway downregulation, Apc-Ras-$Mirr^{RNAi}$-Tkv^{DN} clones would not grow, similarly to Apc-Ras-$Mirr^{RNAi}$. Conversely, if the effect of Mirr RNAi was mediated by the downregulation of the Dpp pathway, the absence of Mirr in a Tkv^{DN} background should not affect clone growth and, consequently, Apc-Ras-$Mirr^{RNAi}$-Tkv^{DN} clones would show a similar phenotype than Apc-Ras clones. And this was indeed the case, the size of the Apc-Ras-$Mirr^{RNAi}$-Tkv^{DN} clones was similar to Apc-Ras clones (Figure 53 a), demonstrating that the lack of growth seen in Apc-Ras-$Mirr^{RNAi}$ clones was due to the recovery of Dpp pathway activity, and therefore indicating that one of the roles of Mirr during Apc-Ras progression is the downregulation of the Dpp pathway. To confirm that Mirr represses

the Dpp pathway components at transcriptional levels, we extracted mRNA from Apc-Ras-Mirr^{RNAi} cells and measured the levels of the Dpp pathway components compared to WT, Apc and Apc-Ras cells. Although Tkv, Mad, Med and Dad had putative binding sites for Mirr in their promoters, only Mad and Med recovered their transcription levels in presence of Mirr RNAi (Figure 53 c). Mad levels were slightly increased while Med levels increased 4 FC in comparison to WT. Conversely, either Tkv nor Dad changed their transcriptional levels. Remarkably, Punt also showed restored transcriptional levels (Figure 53 c) despite the fact that we did not find putative Mirr binding site in its region in our bioinformatics analysis. This result could suggest an indirect regulation of the Dpp pathway by Mirr on top of the direct transcriptional repression or the existence of alternative binding sites for Mirr in Punt promoter.

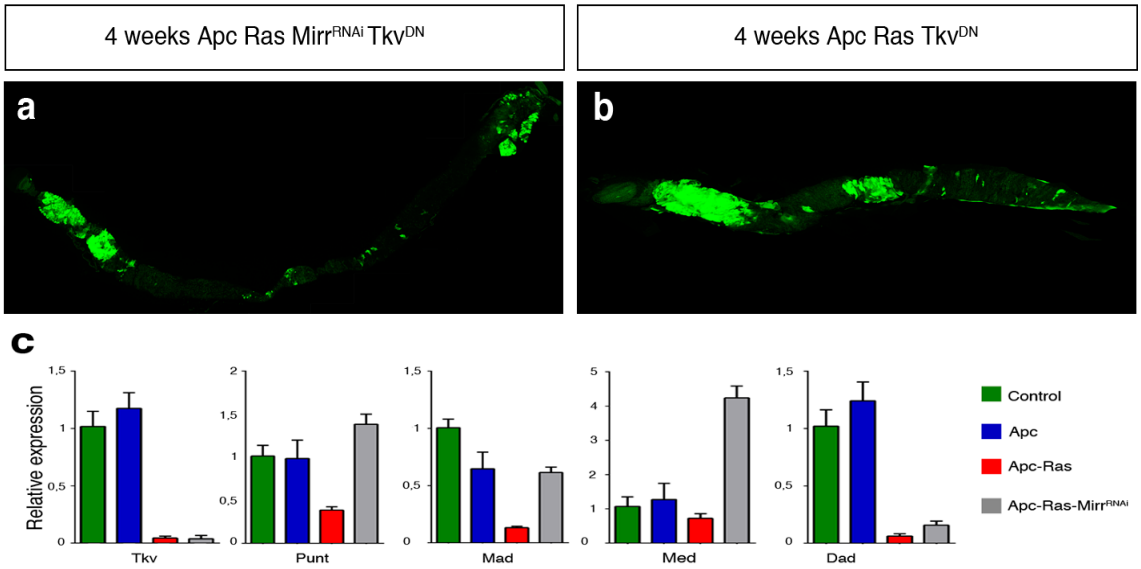

Figure 53. Mirror acts via silencing of the Dpp pathway. a. overview of Apc-Ras-MirrRNAi-TkvDN clones. The downregulation of Dpp blocks the effect of the RNAi against Mirror restoring the normal Apc-Ras growth rate. b. control Apc-Ras TkvDN. c. qPCR for the different components of the Dpp pathway. Observe the restoration of 3 of the silenced genes in Apc-Ras-MirrRNAi

4.4 Apc-Ras-Mirr^{RNAi} clones recover normal differentiation levels.

We demonstrated that Mirr, a transcriptional repressor highly upregulated in Apc-Ras clones, was essential for the transcriptional silencing of the Dpp pathway and, therefore, for the progression of these clones. We next sought to determine which were the cellular characteristics of the Apc-Ras-Mirr^{RNAi} clones. Interestingly, most of the cells within Apc-Ras-Mirr^{RNAi} clones were positive for the EC marker Pdm1 (Figure 54 a). Pdm1 expression, infrequent in Apc-Ras clones, suggests that the lack of Mirr in

Apc-Ras cells is sufficient to induce cell differentiation. To confirm this result, we measured the expression levels of the EE marker Prospero and the EC marker Myo31DF by qPCR. Pros and Myo31DF transcription was restored to WT levels in Apc-Ras-Mirr^{RNAi}, confirming that the lack of Mirr was enough to restore the differentiation in Apc-Ras clones. Surprisingly, the transcriptional levels of the ISC marker Delta were also increased, suggesting that Mirr expression can also impinge in ISC maintenance (Figure 54 b). These results demonstrate that Mirr expression negatively regulates the process of differentiation as well as ISC maintenance in Apc-Ras clones.

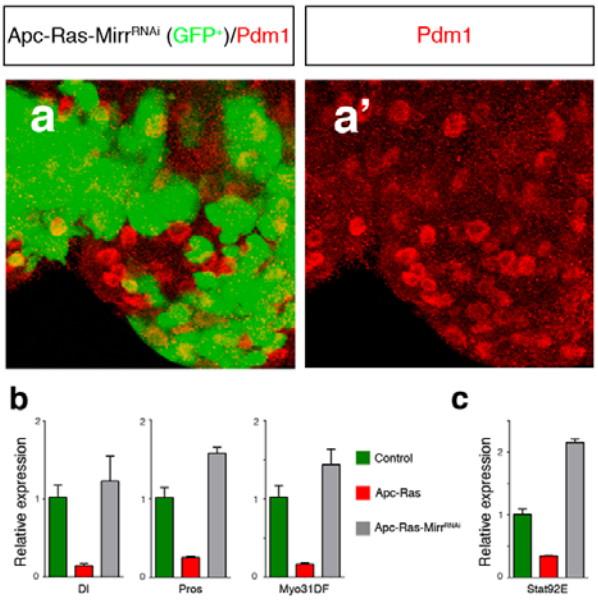

Figure 54. The depletion of Mirror in Apc-Ras cells provokes a restoration of the levels of cell differentiation
a. Apc-Ras-MirrRNAi clone showing a high number of differentiated cells (Pdm1) b. qPCR for the ISC marker Dl and the differentiation markers Pros and Myo31DF c. qPCR for the Jak-Stat effector Stat 92E.

4.5 Mirr downregulates Stat96E, an essential signal for differentiation in the Drosophila Adult midgut.

In 2010, Micchelli's lab demonstrated that Jak-Stat mutant cells in the midgut show strong defects on differentiation, as Jak-Stat mutant clones showed few or none differentiated cells. Moreover, Jak-Stat mutant clones frequently presented fewer ISCs (Beebe, 2010). They suggested that Jak-Stat mutant clones generate EB cells that fail to enter into differentiation resulting in EB-like containing small clones. This phenotype agrees with the defects in differentiation and ISC maintenance observed in Apc-Ras cells (Figure 24 and 25). Interestingly, the transcriptional levels of Stat92E, an essential Jak-Stat pathway transcription factor, were downregulated in Apc-Ras cells (Figure 54, c). Accordingly, the region 2000pb upstream of the Stat92E transcription start site had

putative Mirr binding sites as described in the bibliography (Bilioni, 2005). Stat92E downregulation suggests that Apc-Ras differentiation defects could be produced by a reduction of the Jak-Stat pathway activity in Apc-Ras cells.. In agreement, we measured the transcriptional levels of Stat92E in Apc-Ras-Mirr^{RNAi} cells and found a 2 FC increase compared to wild type levels (Figure 54, c). Together, these results suggest a possible role for Mirr reducing the differentiation in Apc-Ras clones through the inactivation of the Jak-Stat pathway due to the downregulation of Stat92E.

4.6 Mirror expression prevents differentiation in ISC and is essential for clone growth.

We have demonstrated that Mirr reduces the sensitivity to Dpp in Apc-Ras clones, promoting its growth and inhibiting differentiation. We next sought to determine which role has Mirr during normal gut homeostasis. We first analysed Mirr expression by means of MirrLacZ, a reporter of the endogenous expression of Mirr. MirrLacZ, was expressed in a narrow stripe in the proventriculus, anterior to the location where Apc-Ras clones usually develop (Figure 55). We also observed some cells expressing Mirr in the most anterior midgut, but this expression was very labile and infrequent. Mirr could not be detected in ISCs neither by immunostaining nor reporter expression. However, the expression of MirrRNAi in the ISCs induced the expression of the EC marker Pdm1 (Figure 55), similar to the phenotype observed after the forced activation of the Dpp pathway in ISCs (Figure 50). Moreover, four weeks ACI, clones expressing MirrRNAi were considerably smaller and fewer in number than wildtype clones, indicating that lack of Mirr critically compromises clone viability.

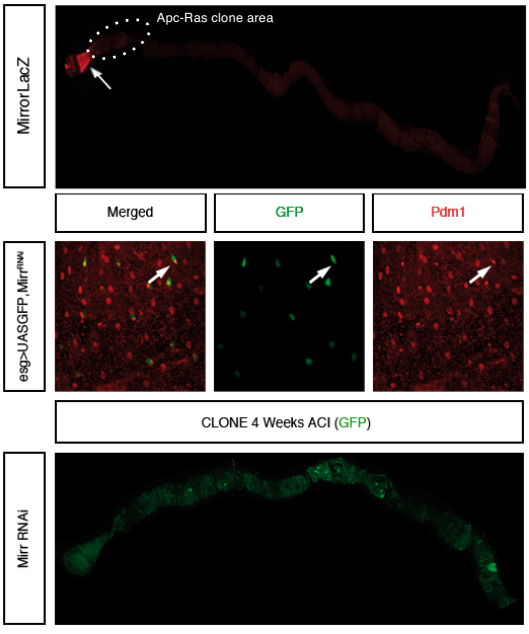

Figure 55. Mirror role during normal homeostasis. Up: Mirror LacZ expression. Note that Mirror is not detectable in the midgut. Middle: The expression of a MirrRNAi induces the expression of a differentiation marker (Pdm1) in the ISC. Bottom: clones bearing a MirrRNA are very small and few at four weeks ACI, suggesting that Mirr is essential for clone growth.

4.7 Mirror is conserved through evolution as a TGF-β signalling pathway repressor during CRC progression.

**Experiments performed in collaboration with Dra. Anna Merlos in Dr. Eduard Batlle's Laboratory.*

Once we observed the essential role of Mirr regulating the sensitivity to the Dpp pathway of Apc-Ras in the *Drosophila* adult midgut, we wondered whether this genetic interaction could be conserved in humans and play any role in CRC progression. Mirr belongs to the Iroquois complex that has three members very similar between them: Araucan, Caupolican and Mirror itself. In Humans, the Iroquois complex/IRX has 6 members (IRX 1-6) located in two clusters (Gómez-Skarmeta, 2002), but none of them can be adscript to an specific *Drosophila* counterpart. Nevertheless, the overall homology between complexes is high. Hence we searched for putative binding sites for all IRX proteins in the promoter regions of the core components of the TGF-β and BMP super family members. We analysed both pathways as Dpp pathway is the main homolog pathway for both TGF-β and BMP superfamily in *Drosophila*. We discovered the existence of putative binding sites for IRX in the Smad3 promoter (Mat&methods). Moreover these putative binding sites were conserved in 47 different species. Interestingly, it has been published that human adenoma show increased levels of IRX3 (Sabates-Bellver, 2007), and we found in the same samples that this upregulation correlates with a statistically significant downregulation of Smad3 (Figure 56, b). Interestingly, we also found that IRX3, and specially IRX5, were upregulated in mouse adenoma samples in comparison with normal surrounding tissue (Figure 56, a). We wondered whether IRX could regulate the transcriptional levels of Smad 3, similarly to the *Drosophila* model. We transfected shRNAs for IRX3 and IRX 5 in two different lines of human cancer cells (Hela and MDA) and observed that the reduction of IRX3 or IRX5 expression correlated with an increase in the transcriptional levels of Smad3 in both cell lines (Figure 56, c). Finally, we measured the response to TGF-β in SW837 cells, a human CRC cell line responsive to TGF-β signal, in absence or presence of IRX3 and IRX5 proteins. In both cases a strong reduction of the cellular response to TGF-β occurred, both in fold change and maximum activity assays when IRX3 or IRX5 were expressed in SW837 cells (Figure 56 d and e). All together, these preliminary results suggest that the role of Mirr regulating Dpp could be conserved in human CRC, where IRX proteins could be regulating TGF- β pathway activity. Therefore, the IRX

complex might be an important object of study to understand CRC progression. Interestingly, these results show clearly that transcriptional regulation of key driver genes could be occurring in cancer cells suggesting that not always the accumulation of mutations would be essential to silence or activate key signalling pathways during tumour progression.

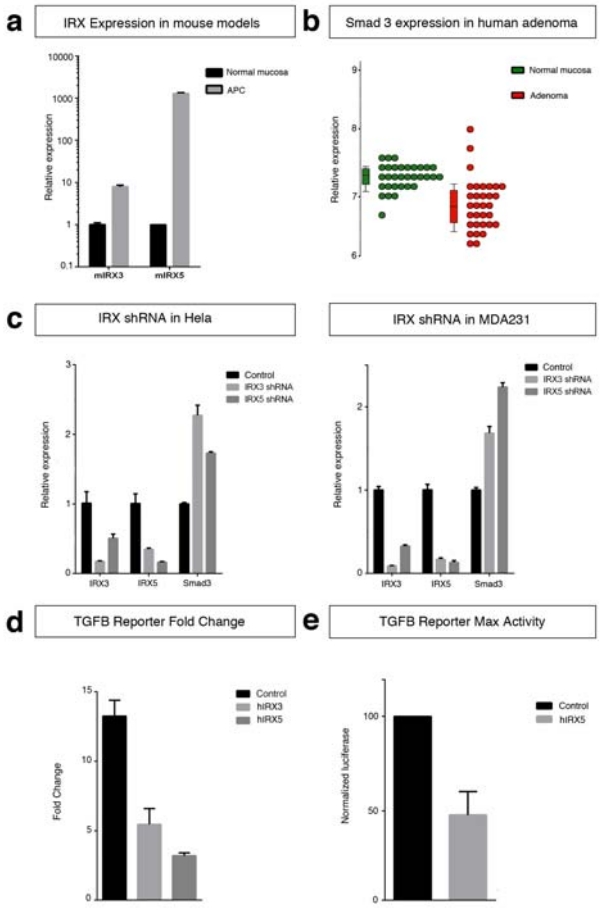

Figure 56. IRX role in TGF-β silencing. a. IRX3 and IRX5 levels are increased in Apc- guts. b. IRX3 expression correlates with Smad3 downregulation in CRC samples (Sabates-Bellver, 2007). c. The depletion of IRX3 or 5 induces an increase of Smad3 in HeLa and MDA321 cells. d and e. The transfection of IRX3 or IRX5 in cells responsive to TGF-β induces the reduction of the response of those cells to TGF-β.

Discussion

5. Discussion

The complete comprehension of the diverse genetic alterations and the genes that drive CRC progression is a keystone in cancer research. Among other functions, the identification of new genes implicated in the development of tumours is crucial to develop new and more accurate treatments against the disease. For that reason, during the last decades the generation of cancer animal models has emerged as an essential tool to discover those key driver genes essential in tumour initiation and progression. In this context, the main aim of this thesis has been to generate and characterize a *Drosophila* CRC model to understand the basic biology of the tumoral processes and identify new genes involved in tumour formation. In our model, the clonal co-activation of the Wingless and Ras pathways in the *Drosophila* adult midgut produce the formation of tumour-like clones in the most anterior part of the organ. These overgrowths show tumour characteristics such as loss of differentiation, loss of cell polarity and high proliferation. Interestingly, the transcriptional profiling of Apc-Ras cells revealed a transcriptional blockade of the TGF-β/Dpp signalling pathway among many other transcriptional changes. This blockade, essential for Apc-Ras clone progression, seems to be mediated by the transcriptional repressor Mirror, a TF highly expressed in Apc-Ras cells. Finally we have shown that Mirror could be a CRC driver gene, as two Mirror human homologs are expressed in CRC adenomas and they negatively affect the response of CRC cells to TGF-β. In summary, this work demonstrates the suitability of the use of *Drosophila* as a model organism to study tumour formation in an *in vivo* system and remarkably, opens several new questions that should be addressed carefully during the next years.

5.1 A mechanism of elimination of Ras^{V12} transformed cells exists along the animal kingdom

It is largely known the tumorigenic potential of Wingless/Wnt and Ras pathways both in humans and *Drosophila* (Jiang, 2011; Lee, 2009; Malumbres, 2003; Sancho, 2004; Segditsas, 2006). Accordingly to our results, transgenic mice bearing oncogenic mutations for Apc and Ras develop large invasive tumours (Luo, 2009; Sansom, 2006). Interestingly, although inactivating mutations in Apc cause the apparition of multiple small polyps along the small intestine (Moser, 1990; Zeineldin, 2013), the incidence of

oncogenic lesions in rodents with activating Ras mutations is very infrequent (Janssen, 2003).

Similarly, although in *Drosophila* Ras^{V12} clones have been described as hyperproliferative (Buchon, 2010; Jiang, 2011), in our conditions Ras^{V12}-bearing clones (Apc-Ras clones and Ras) tend to disappear from the epithelia during clone progression. Moreover, this Ras^{v12}-induced clone disappearance is not random and clones survive in specific positions. Four weeks ACI, Ras clones specifically locate in the gastric region whereas Apc-Ras clones developed in the most-anterior region of the midgut and in the gastric region. From this result three questions emerge: *Why Ras^{V12} bearing-clones disappear along time? Why Ras and Apc-Ras clones survive in specific regions of the gut? Can be established any parallelism between Drosophila and mice Ras^{v12} cell behaviour?*

The implication of K-RAS in the progression of CRC is well established (Fearon, 1990). Although this essential contribution, K-RAS mutations are detected in large adenomas and carcinomas but not in early adenomas, indicating that K-RAS mutations are not initial events of CRC. In addition, mice models demonstrated that K-RAS mutations are very inefficient creating tumours in mouse intestines but they boost the tumorigenic capabilities of APC-deleted cells in mice (Janssen, 2003; Luo, 2011). These results suggest that previous mutations in APC may be required to allow K-RAS mutations to produce a hyperproliferative effect in the gut. In *Drosophila*, we have demonstrated that Ras^{v12} expressing clones cannot progress and most of them disappear from the epithelia. This mechanism is independent of cell death process as the inhibition of apoptotic program cannot block the disappearance of Ras-activated clones. A previous report showed that the activation of the EGFR pathway is essential for damaged-cell delamination in the *Drosophila* midgut (Buchon, 2010). When an enterocyte is damaged, the EGFR pathway turns active in that cell and induces the delamination of that cell. Interestingly, the ectopic expression of the EGFR pathway in a non-damaged situation is sufficient to induce EC delamination. This result suggests that the physiological role of EGFR pathway in normal midgut cell turnover could explain why Ras^{V12} clones disappear from the epithelium. A possible molecular mechanism for the extrusion of Ras^{V12} cells has been also recently described in a mammalian *in vitro* cell culture assay. In this report, is shown that the interaction between surrounding normal cells and Ras^{V12} cells produce the extrusion of the last ones (Hogan, 2009). This mechanism is mediated by the ROCK complex; a complex

frequently involved in cell architecture and cell morphogenesis, and the GTPase CDC42 in the Ras^{V12} cells. Accordingly, we observed that delamination is occurring in Ras and Apc-Ras clones. Interestingly, the overexpression of a dominant negative form the kinase Cdc42 in Apc-Ras clones delays remarkably clone disappearance suggesting a critical role for Cdc42 in Ras^{V12} clone elimination. We suggest a conserved mechanism of Ras^{V12} forced delamination mediated by the interaction with surrounding normal cells. This mechanism could explain the infrequence of K-RAS tumours in rodents and the apparition of K-RAS mutations mid-late during CRC development as many of the K-RAS activated cells would disappear before any possibility of growth inside the host.

Interestingly, the extrusion of clones in the *Drosophila* midgut does not seem to be a random event. Ras-activated clones survive and grow in the gastric region. Similarly, Apc-Ras clones present a large and characteristic clone in the most anterior midgut. These regional differences are not recognizable at early stages of the clone progression and they start to appear after one week ACI suggesting that none of the zones is more susceptible for clone formation but for clone progression. These results suggest there are regions where it would exist a specific feature to promote clone growth. Specifically, Apc-Ras large clones appear in the most anterior region of the midgut. This region has been described as a delimited region with important anatomic and genetic differences (Buchon, 2013; Marianes, 2013; Shanbhag, 2009) that could be triggering Apc-Ras clone progression. Surprisingly and reinforcing this idea, although Apc-Ras $Cdc42^{DN}$ guts presented clones along the midgut at three weeks ACI, all the clones located outside the most anterior region could not grow as the ones located in the most-anterior region. This result demonstrates that something in the most anterior region, genetic/molecular or anatomic/physical, is essential for Apc-Ras clone progression although nowadays is totally unknown. In rodents, some regional differences have also been observed. In the most used mouse model for CRC, the Apc^{MIN} mice, the tumours develop exclusively in the small intestine while the large intestine remains unaffected. In contrast, the addition of different oncogenic alleles of K-RAS in a Apc^{MIN} background produce the apparition of large clones both in the small an in the large intestine (Luo, 2009, 2011). This result suggests a role of K-RAS not just in APC-deleted tumour growth but also in their specific site survival as the addition of K-RAS is enough to change the localization of the clones. Finally, in humans also exist differences in tumour site formation. Intestinal cancers occur mostly in the large intestine and some molecular differences exist between the clones that develop in the

right colon from those that arise in the transversal and left colon (Network, 2012). Interestingly, small intestine cancer are very infrequent, comprising less than a 2% of gastrointestinal malignancies (Zollinger, 1986). All this results reflect that regional differences are important for tumour progression in all the organisms. These differences are far from being understood and further studies should be performed to discover the causes of them.

5.2 Apc-Ras cells recapitulate many cellular changes associated to cancer cell transformation

Many cellular characteristics are linked to tumour cell transformation, such as loss of cell differentiation, loss of cell polarity or increased proliferation. These changes clearly reflect how the tumour cells lose the properties typical from the tissue of origin, particularly when the tumour arises in epithelium, a tissue with very specific cellular characteristics, as in the case of CRC. Apc-Ras clones show some of the common cellular changes associated to cell transformation. First of all, Apc-Ras clones showed high levels of cell proliferation. Moreover, as many advanced tumours, Apc-Ras clones showed a low rate of differentiated cells when compared to wild type clones. Although Apc-Ras cells could differentiate, demonstrated by Apc-Ras clone cell heterogeneity, the differentiation process is clearly compromised. Conversely, as reported in the bibliography, the overactivation of Wingless or Ras pathways do no alter dramatically the differentiation state of the clones (Jiang, 2009; Lee, 2009), indicating that is necessary the co-activation of the Wingless and Ras pathways to affect negatively the capacity of the EB to differentiate. Furthermore, Apc-Ras clone showed a reduction of the Dl positive cells, an ISC marker in the *Drosophila* midgut. This result discards the possibility that in Apc-Ras clones there is an increase in the number of ISC symmetric divisions, as that process would increase the number of ISC inside the clone. Some reports suggest that ISC with a low Dl staining could be the progenitors of the EE lineage (Micchelli, 2006; Ohlstein, 2007) but the hypothesis of an expansion of this type of ISC inside Apc-Ras clones could also be discarded as the number of EE inside Apc-Ras clones is dramatically reduced in Apc-Ras clones. Interestingly, the decrease of ISC, EC and EE indicates that most of the Apc-Ras cells are neither ISC nor differentiated cells. We hypothesized that these undifferentiated cells could acquire the capability of cell division. This was demonstrated by the existence of dividing non-Dl positive cells in Apc-Ras clones. These cells were not canonical ISC neither

differentiated cells and also were not canonical EB because they could not differentiate properly. To identify the real nature and the tumorigenic potential of the cells we should perform a one-cell allograft injection assay or cell culture to identify which Apc-Ras cells could initiate a tumour and which not. This experiment could reveal if Apc-Ras tumours follow a hierarchized pattern as happens in human CRC (Merlos-Suárez, 2011) with "Apc-Ras stem cells" capable of dividing and initiating a tumour in other hosts; progenitors, that can divide but cannot initiate a tumour; and differentiated cells.

Interestingly, a similar type of cells, neither ISC nor differentiated cells, have been observed in mutant clones for Jak-Stat pathway (Jiang, 2009). These clones have few Pdm1+, Pros+ and Dl+ cells resembling the cell fate phenotype of Apc-Ras clones. Accordingly to this results, Apc-Ras cells presented low transcriptional levels of Stat96E, the transducer of the Jak-Stat pathway, suggesting that the Jak-Stat pathway activity could be downregulated in the Apc-Ras cells. The TF Mirror could mediate this downregulation as the levels of Jak-Stat are restored to the normal levels in Apc-Ras $Mirr^{RNAi}$ clones. Hence, the downregulation of the Jak-Stat pathway can be one of the causes for altered cell differentiation in Apc-Ras clones. However, we cannot exclude other causes that block cell differentiation such as a rapid cell cycle that would prevent differentiation, or other effects associated to the activation of Wingless and Ras pathways. Finally, although the role of Jak-Stat pathway in CRC is far from being understood a recent publication suggest that the expression of STAT1 and STAT3 are good prognostic markers in colorectal carcinoma (Gordziel, 2013).

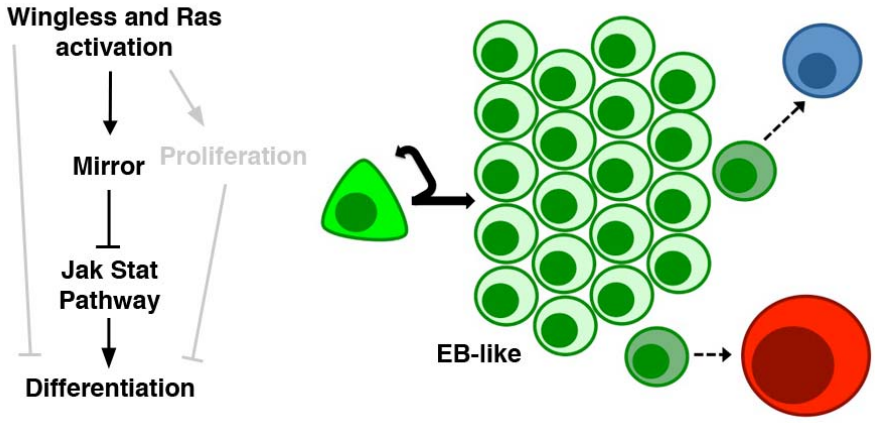

Figure 57. Model for the loss of differentiation phenotype of Apc-Ras clones. On the left: Genetic model. Apc-Ras will block differentiation by different ways, directly and indirectly. Mirror is a putative negative regulator of Jak-Stat pathway, a known differentiation factor in normal EB. On the right: hypothetic model of cell fate in Apc-Ras clones. In Apc-Ras ISC divide but EB cannot enter into differentiation process and start dividing creating a large pool of EB-like cells. Some cells can escape this blocking and eventually differentiate.

Other common characteristic of tumours that arise from epithelial tissues is loss of cell polarity. The epithelial cells present an apicobasal polarity composed by different clusters of proteins. The disruption of cell polarity has been linked to EMT transition and metastasis (Ellenbroek, 2007). Many cell adhesion and polarity proteins showed defects in Apc-Ras cells. The cell adhesion protein, DE-Cad, show defects on the cells residing in the inner mass of the Apc-Ras clones but no in the cells that reside in the surface. We suggested that this defects could be an artificial situation due to the lack of antibody penetrance inside the Apc-Ras clones. However, Apc-Ras cells show a increase on the transcriptional levels of the TF Snail, a known repressor of DE-Cad during cancer progression (Becker, 2007; Carver, 2001). Furthermore, Apc-Ras cells and also Ras cells show important levels of Disc Large (Dlg) delocalization. Mutations in many polarity proteins have been described in many cancers and most of the polarity proteins have been described as tumour suppressor genes (Ellenbroek, 2012). Among them, the most important complex seems to be the Dlg/Scrib complex. Scribble and Dlg have been reported as a very important tumour suppressor genes in *Drosophila* and a large number of *Drosophila* cancer models are based in mutant alleles for Scribble or Dlg (Wodarz, 2007). Interestingly, the deregulation of the Dlg/Scrib complex can alter the Hippo pathway, a known tumour-promoting signal, inducing the hyperproliferation of the affected cells.

In cancer diagnosis, many gene expression patterns, either negative or positive, are used as prognosis markers. One of these proteins is Fascin, an actin bundling protein overexpressed in some CRC tumours. Fascin expression correlates with the size of the tumour, the degree of tumour dysplasia and a poor prognosis diagnostic (Hashimoto, 2006; Qualtrough, 2009; Vignjevic, 2007). Also it has been shown that it can promote motility of adenoma cells *in vitro.* Interestingly*,* many Apc-Ras clones show an intense expression of Singed (Sn)*, the Drosophila* homolog for Fascin*.* Although Sn expression can suggest an increased motility of the cells and a pro-invasive behaviour of the cells, Apc-Ras cells cannot break the basement membrane. The Basement membrane is a layer where the epithelial cells anchor and acts as a mechanical barrier for those malignant cells that try to invade underlying tissues. Those malign tumours that have not break the basal membrane are called carcinoma *in situ.* Many proteins are necessary to break the basement membrane and among them the most important are the Matrix metalloproteases (MMPs). MMPs play an essential role in extracellular matrix degradation and are essential for the metastasis (Beaucher, 2007). Surprisingly, although Mmp1 expression is transcriptionally upregulated in Apc-

Ras, the protein expression is totally repressed in comparison with the normal tissue. This suggests a possible posttranscriptional regulation that could induce Mmp1 repression and the existence of a mechanism of defence against the spread of the clone.

All the aforementioned characteristics of Apc-Ras cells: High proliferation rate, loss of cell differentiation, loss of cell polarity and expression of motility-related proteins strongly suggest that *Drosophila* Apc-Ras cells behave as pre-invasive malignant cells. In summary, Apc-Ras clones recapitulates various features of a common Carcinoma *in situ* in humans corroborating that Apc-Ras clones are a good model to study mid-early stages of CRC in *Drosophila*.

5.3 Apc-Ras cells present a tumour-like transcriptional profile

Although the genetic background of cancer has been extensively studied, the underlying gene expression changes have been kept out of the focus in detriment of the *genetic mutational* of the tumour. However, during the last years many publications have tried to elucidate the main transcriptional changes that occur during the adenoma to carcinoma progression (Maglietta, 2012; Marisa, 2013; Network, 2012; Sabates-Bellver, 2007). In this scenario, we sought to determine the transcriptional alterations occurring in the Apc-Ras cells by a microarray analysis. Interestingly, around a 50% of the genes that appear transcriptionally altered in Apc-Ras are not present in Apc or Ras single mutants. These results indicate a critical synergic effect of the co-activation of Wg and EGFR/Ras, activating a specific program that cannot be activated without the simultaneous presence of both signals. How this synergic effect is performed is still an unknown question. Maybe some of the Apc-Ras specific genes present binding sites for Wg and Ras effectors in their promoters and need both inputs to be activated. This few genes could modify the expression of many downstream genes creating the specific Apc-Ras program. Other possible explanation could be that the co-activity of Apc-dependent proteins and Ras-dependent proteins also could produce the alteration of some genes that otherwise would remained unaltered. This result gives us an important message about why the accumulation of mutations is an event so relevant in cancer progression as this accumulation of mutation and therefore, the simultaneous alteration of different signalling pathways produce not just the activation of that genes dependent on a determinate signalling pathways but also those that need various genetic inputs simultaneously.

The main feature of Apc-Ras cells one week ACI is the upregulation of dozens of genes linked to division and related processes: *cytokinesis, mitotic spindle formation, cell cycle*, etc. This upregulation is partially already present in Apc and Ras suggesting that the proliferative signal in Apc-Ras comes from both signals. These transcriptional changes were expected as Apc-Ras, Apc and Ras clones present more dividing cells that Wild Type clones by immunostaining. Linked to this change there is a upregulation of GO terms and genes related with mismatch repair genes that suggest that an active replication of the DNA is held by Apc-Ras cells and the mechanisms of defence are consequently activated to prevent the additional DNA damage.

In addition, many changes can be observed in various metabolic pathways. Metabolism has emerged as one of the main players in cancer progression (Cairns, 2011; Soga, 2013). One of the main changes is the acquisition of a known metabolic pathway called aerobic glycolysis. The aerobic glycolysis or Warburg effect is the use of an inefficient glucose metabolism uncoupled from the electron transport chain. This metabolic change, that occurs frequently in advance tumours, produce less energy but the cell can use the glucose-derived metabolites to biosynthesize new macromolecules such membrane lipids and nucleotides to maintain a correct proliferation rate. In Apc-Ras clones we can observe an increase of the glycolysis and the pyruvate metabolism and a downregulation of the Krebs cycle and the oxidative phosphorylation that clearly suggest that Apc-Ras cells are using a kind of aerobic glycolysis pathway. Although the main causes and the functional relevance of this metabolic reprogramming are mainly unknown, several hypotheses have been postulated to explain the process. Some researchers have suggested that this process would be a response to hypoxia and oxidative stress conditions. The tumour would require larger amounts of oxygen and its lack would to produce the metabolic reprogram to avoid the oxidative stress generated by the lack of oxygen and hypoxia. Moreover, the intermediate metabolites of the Warburg effect would be used to create new molecules and membranes in a correct ratio to maintain the fast division cycle. Finally, some evidences have shown that cell metabolism would be heterogeneous inside tumours and a symbiotic relationship would be established inside them. The lactated formed in the Warburg metabolism-using cells would be secreted and captured by other cells that would transformed to pyruvate inside them to take benefit from it (Bensinger, 2012).

Many signalling pathways are altered in Apc-Ras transcriptional profile. The most compromised is the Dpp signalling pathway, which is going to be addressed in the next section. Other major signalling pathways appear altered, such as the

Hedgehog pathway. In Apc-Ras cells the morphogen Hedgehog as well as the receptor Patched appeared clearly upregulated. Interestingly, the absence of Hedgehog in Apc-Ras cells blocks the growth of the clone. This suggests a crucial role for Hedgehog during Apc-Ras clone progression. Unfortunately, the actual role of Hedgehog in the adult midgut remains still unknown and the role of Hedgehog pathway in CRC progression is still very unclear. Interestingly, the increase of Hedgehog and Patched in Apc-Ras clones suggests the possible existence of two different populations as it has been described that Hedgehog always is secreted from different cells to those ones that respond to it and express the receptor Patched. If this is true a paracrine relationship between two different subpopulations could be described inside a tumour-like clone. On the other hand, it is possible that in a non-homeostatic condition such Apc-Ras clones the same cells secrete and receive Hedgehog. In both cases, a genetic regulation of the Hedgehog pathway occurs in Apc-Ras cells. Hedgehog pathway seems to act as a growth signal in Apc-Ras clones and its autonomous upregulation in Apc-Ras cells indicates that the clones are sustaining independently their growth signals as happens in many human cancers (Hanahan, 2011). Also the effector of the Jak-Stat pathway, Stat92E, appeared silenced in Apc-Ras cells. This result suggest that Apc-Ras cells have silenced the Jak-Stat pathway, probably to block Jak-Stat-induced differentiation (Jiang, 2009). Conversely, various ligands for Jak-Stat are upregulated showing a paradox inside Apc-Ras clones. We suggest that although Apc-Ras cells are not responding to Jak-Stat signal, they send cytokines to promote ISC division in the surrounding normal cells inducing in this way a paracrine mitogenic effect.

Other group of genes that should be addressed in the future is the one that comprise the genes related with cell adhesion and polarity. Some genes related with specific types of cell adhesion are altered in Apc-Ras such as the regulator of Ephrin activity Reph. In humans it is known that Ephrins, a specific type of adhesion molecule and implicated in cell compartmentalization, play a role in CRC tumorigenesis indicating that the Ephrin pathway play an important during tumorigenic processes (Batlle, 2012). Moreover, the three Fasciclins present in *Drosophila*, are specifically upregulated in Apc-Ras cells. Two of the Fasciclins are not present in the *Drosophila* Midgut (Fas 1 and Fas 2) in normal conditions and are described as nervous system-specific (Flybase, 2013). Fasciclins have been extensively described as mediators of axon guidance (Elkins, 1990; Grenningloh, 1991; Snow, 1989) suggesting a putative role of them in cell migration. In summary, the expression of specific cell adhesion

molecules could reflect the compartmentalization between the Apc-Ras cells and the surrounding normal cells and this could be translated into different migratory effects.

Interestingly, an important change of the transcriptional profile can be observed between Apc-Ras cells at one week and four weeks ACI. More than 50% of the genes are Apc-Ras one-week-specific or Apc-Ras four-weeks specific. This suggests that most of the genes are not essential during all Apc-Ras clone progression but just in their initiation or their progression. This transcriptomic changes reflect a clear progression of Apc-Ras clones and could be explained by several reasons: tumour cell transformation, change of cell niche from the normal epithelia to a tumour environment, changes in cell proportions or clone aging. Most of these transcriptional changes correlate with those that are frequently observed in human samples and validate the *Drosophila CRC* model as an easy tool to investigate transcriptional changes along tumour progression. Now, a deep functional analysis of the altered genes in Apc-Ras should be performed to identify which of those transcriptionally altered genes have a real function in Apc-Ras progression, the so-called tumour driven genes. Until now, we have discovered almost 70 genes that are essential for the progression of Apc-Ras clones. The characterization of the role of those genes in Apc-Ras progression and in human samples will help to understand better the process of CRC tumorigenesis.

5.4 The Dpp signalling pathway acts as a tumour suppressor signal in the Adult Drosophila midgut

It is largely known the role of the Dpp/TGF-β signalling pathway as a cytostatic signal during the first stages of many cancers (Markowitz, 1996; Massagué, 2008). Genetic alterations in TGFBRII and Smad4 appear in 40% and 20% of CRCs respectively (Network, 2012). For that reason, when we observed a transcriptional repression of several Dpp components in Apc-Ras clones we thought that this transcriptional repression could have an important role in Apc-Ras clone progression. Interestingly, the forced activation of the Dpp signalling in Apc-Ras clones induced a very important shrinkage of Apc-Ras clones demonstrating that Dpp signal acts as a tumour suppressor signal and its silencing is essential for Apc-Ras clone growth. In the *Drosophila* midgut, the role of Dpp pathway is far from being completely understood. On one hand, it is clear that it has a cytostatic effect in the gut. Although this has been confirmed, contradictory results have been published in two recent papers about Dpp pathway and gut homeostasis. This cytostatic effect has been suggested to be

exclusively induced directly in the ISC (Guo, 2013) or via the EC response to Dpp (Li, 2013). By both ways, the depletion of the Dpp signalling increases the number of PH3 positive cells in the gut. Moreover, the overactivation of the pathway provokes a reduction in clone growth in comparison with wild type guts (Guo, 2013). Interestingly, ectopic Dpp activation in the ISC provokes the apparition of a differentiation marker in the ISC, Pdm1. This indicates that Dpp can be regulating in some way the differentiation of the EB. Although the new expression of Pdm1, this esg^{+} cells still express Dl marker suggesting that the differentiation is not completed. Those cells are simultaneously expressing ISC and EC markers demonstrating the aberrant fate of the cells.

It is known that in many systems, there is a tight and antagonistic relation between proliferation and differentiation (Casanova, 2012). Hence, Dpp can be acting as one of those many signalling pathways that regulate the balance between proliferatory fate – ISC– and differentiation –EC or EE– in the *Drosophila* adult midgut. In this sense, Dpp will act similarly to Notch, restricting ISC proliferation and promoting differentiation of the ISC. Conversely, the lack of Notch signalling produces the lack of EC and expansion of EEs while the depletion of Dpp signalling does not affect cell differentiation. Additionally, one of the firsts evidences that suggested us that Dpp was promoting differentiation was the restricted expression of Tkv, the receptor, in the EC (Figure X a). Despite of that, a reporter of the activity of the pathway, DadGFP, is expressed in other small cells that are not EC (Figure X b). This paradox also vaguely suggested in the bibliography, makes difficult to interpret the results and strongly demands a deeper characterization of the Dpp pathway by the scientific community. We hypothesized that others receptors for Dpp such Wishful Thinking (Wit) could be activating the pathway in the ISC.

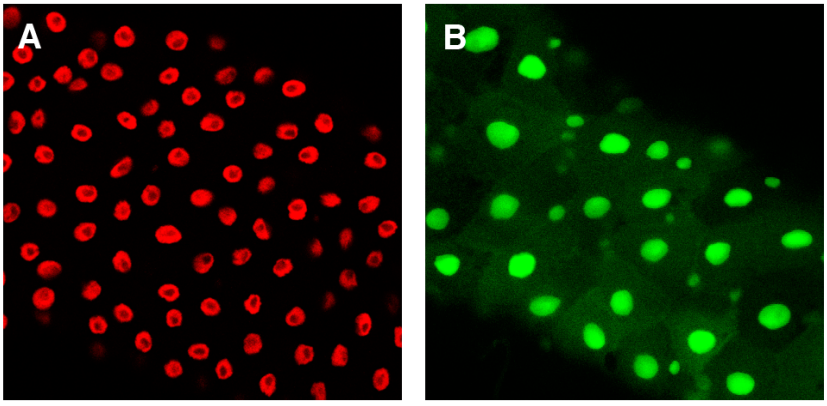

Figure 58. Paradox in Dpp signal transduction. There is a controversy on which are really the cells that respond to Dpp in the *Drosophila* adult midgut. The cells that express the Dpp receptor type II thick veins are only the EC but conversely, a reporter of the activity of the pathway reveals that other cells in the gut, by the size of the nuclei, respond to Dpp.

All the previous data suggests that Dpp signal could be an inductor of differentiation but not an essential signal for proper differentiation. In addition, it seems that the Dpp signal is activated in the adult midgut in response to injury (Guo, 2013). This response and Dpp activation counteracts the several proliferating signals that dying EC produce to renew the epithelium and avoid hyperproliferation. In this scenario, Apc-Ras cells via the downregulation of Dpp activation could surpass one of the growth barriers in the adult gut and divide without control. In summary, we propose that Dpp signal needs to be downregulated to permit Apc-Ras clone progression. This downregulation is necessary to eliminate the growth barrier that Dpp signal impose in the adult midgut. This growth barrier includes different roles such as reduction of proliferation ratio and induction of differentiation. Hence, it is obvious that the presence of this signal clearly counteract the tumorigenic effects of the activation of Wg and Ras signalling pathways and should be inactivated. This thesis also demonstrated the evolutionary conservation of the anti-tumorigenic role of TGF-β/Dpp during the first stages of the tumour development.

Many questions are still unsolved about the normal role of Dpp signal and about which are the sources and the cells that respond to Dpp. This problem probably is due to the fact that Dpp signal and pattern are very labile in the adult midgut. The different reports of the pathway (DadLacZ, DadGFP, Pmad antibodies…) analysed in the lab and in the different published reports are showing contradictory patterns and it is not clear which cells actually respond to Dpp. Further efforts are necessary to characterize the multiple roles and the pattern of Dpp signalling pathway in normal homeostasis and disease in *Drosophila*.

5.5 Mirror as a differentiation-repressor factor in the Drosophila midgut

It has been largely supported that genetic mutations are necessary and essential to activate or inactivate the core signalling pathways that control cancer development. However, the existence of transcriptional and other genetic regulations have been kept out of the focus in cancer research, probably due to the lack of efficient tools to look the levels of mRNA until the last decades. In this work we have shown that the transcriptional downregulation of the Dpp pathway during Apc-Ras clone progression is essential for Apc-Ras clone growth. This transcriptional downregulation

of the Dpp pathway in Apc-Ras cells play a similar role to the loss-of-function mutations of TGFBRII or Smad4 occasionally occurring after APC or K-RAS mutations during CRC progression. In both cases, the depletion of Dpp/TGF-β eliminates a growth barrier for tumour growth.

We have shown that a known transcription factor, Mirror, is specifically upregulated in Apc-Ras and acts as a transcriptional repressor of different members of the Dpp pathway reducing the responsiveness of Apc-Ras cells to Dpp. This data shows a clear example of the synergic activity of the activation of both pathways in the midgut cells. Mirror has been reported as a target gene of the EGFR pathway in the ovary (Andreu, 2012; Jordan, 2000). However, in our conditions the activation of EGFR pathways does not affect *mirror* transcriptional levels showing that Mirror expression requirements are different in different tissues. The expression of Mirror is essential for Apc-Ras clone progression as the elimination of Mirror in Apc-Ras cells reduces clone growth. Importantly, an epistasis analysis has shown that Mirror mainly acts through the repression of Dpp pathway in Apc-Ras cells. Hence, Mirror central role in Apc-Ras cells seems to be the repression of Dpp components. But what is the functional relevance of this regulation?

If Dpp acts as an inductor of differentiation in the adult gut as mentioned before, Mirror would act as a repressor of differentiation. This suggests that Mirror can be a kind of stemness maintenance gene. Unfortunately, the expression of Mirror in the gut, by a lacZ reporter, is restricted to a stripe in the transition between the proventriculus and the anterior midgut and it is not detected in ISC or other cells in the midgut. Despite of that, very recent microarray results from the lab point to a differential expression of Mirror between ISC and EB, suggesting that Mirror can be present in the ISC. Additionally, the expression of an RNAi against Mirror in the ISC produce a partial differentiation of many ISC and clones bearing a Mirror RNAi have an important reduction in size. This data suggest that although Mirror cannot be detected in the ISC, functional levels of Mirror are present in those cells. Further experiments are necessary to validate this hypothesis, but Mirror can be acting in the ISC as a stemness factor. Mirror would be repressing Dpp pathway in the ISC and preventing in this way, ISC differentiation. Accordingly, in Apc-Ras cells the expression of Mirror will have a similar role blocking cell differentiation and maintaining a proliferative fate for Apc-Ras cells. In this scenario there is a third actor that can be contributing actively to the Apc-Ras phenotype: the Jak-Stat pathway. As previously mentioned, Mirror seems to be repressing the effector of the pathway, Stat92E, in Apc-Ras cells. In addition, the

differentiation failure showed in Apc-Ras clones mimics the Jak-Stat loss-of-function clones (Jiang, 2009; Lin, 2010). Jak-Stat signalling seems to have a dual role in the adult midgut. On one hand, the Jak-Stat pathway promotes division in the ISC. Conversely, Jak-Stat promotes differentiation in the EB. The regulation of this dual role is still completely unknown. In this scenario, we propose that Mirror acts in Apc-Ras cells downregulating Dpp and Jak-Stat pathways repressing differentiation and division. In the normal gut and in homeostatic conditions, most of the ISC are quiescent. In this case, Mirror would be repressing both pathways to prevent differentiation and additionally Jak-Stat-induced proliferation. The process of division on the ISC would decrease Mirror levels by an unknown mechanism, permitting the activation of both pathways and consequently, the induction of the differentiation in the resulting EB.

In summary, we suggest that Mirror can be present in the ISC repressing differentiation by silencing one or more pathways. This model supports the theory that stem cells are not cells with stemness-inducing factors but cells containing differentiation-repressing proteins (Casanova, 2012). Finally, It should be take in consideration that Apc-Ras cells are altering many genes and pathways in Apc-Ras cells and although we are presenting Mirror as a central factor, probably many other genes are contributing to Apc-Ras clone progression.

5.6 The role of IRX proteins during CRC progression.

Our work has demonstrated that the transcriptional downregulation of various Dpp pathway components is essential for proper Apc-Ras clone progression. This data correlates with some CRC cases where TGFBRII and Smad4 present loss-of-function mutation. Interestingly, although these mutations are just present in around 20-30% of CRC (Network, 2012), a large proportion of CRC are resistant to TGF-β. Looking at the role of Mirror as a repressor transcription factor of the Dpp signalling pathway, we wondered if the homologous protein to Mirror in human has any role in CRC progression. IRX proteins have been vaguely linked to oncogenic processes in previous reports. IRX1 and IRX4 have been documented as tumour suppressors of prostate and gastric cancer (Guo, 2010; Nguyen, 2012) whereas IRX5 have been linked to the control of cell cycle and apoptosis in prostate cancer (Myrthue, 2008). This work nicely showed that the downregulation of IRX3 or IRX5 in human HeLa cells produces an increase of Smad 3, the effector of the TGF-β, in those cells suggesting a Smad3-repressing role of IRX proteins. In addition, the repression of IRX3 or IRX5 in

cells responsive to TGF-β produces a significant decrease of the levels of response of those cells to TGF-β. These results clearly points to a repressor role of IRX proteins on the TGF-β pathway and this suggests that IRX proteins can be playing a central role on the repression of the TGF-β induced growth barrier during CRC.

With all the previous results, we present a model where the simultaneous activation of Wg/Wnt and EGFR/RAS produce the accumulation of Mirror/IRX in the cells leading to a decrease of the ability to response to TGF-β (Figure X). Probably, this situation is a transient situation where the IRX expression allows the cells to persist in a TGF-β rich context and gives time to them to accumulate mutations that will impair completely the response to TGF-β. This model shows that genetics mutations are not always necessary to silence or activate a signalling pathway during tumour progression and transcriptional changes inside the tumour are also critical in cancer. Similar results has been reported recently by the identification of COUP-TFII as a transcriptional silencer of the TGF-β-induced growth barrier during prostate cancer (Qin, 2013). Interestingly, the most upregulated gene in Apc-Ras cells is Seven Up, the *Drosophila* homolog of COUP-TFII. This suggests a putative conserved role of Seven Up/COUP-TFII in tumorigenesis. Also this data reinforces the idea of focusing on the study of the different transcription factors altered in Apc-Ras. Transcription Factors can control the transcriptional levels of many genes and most of them can be essential for Apc-Ras tumorigenesis.

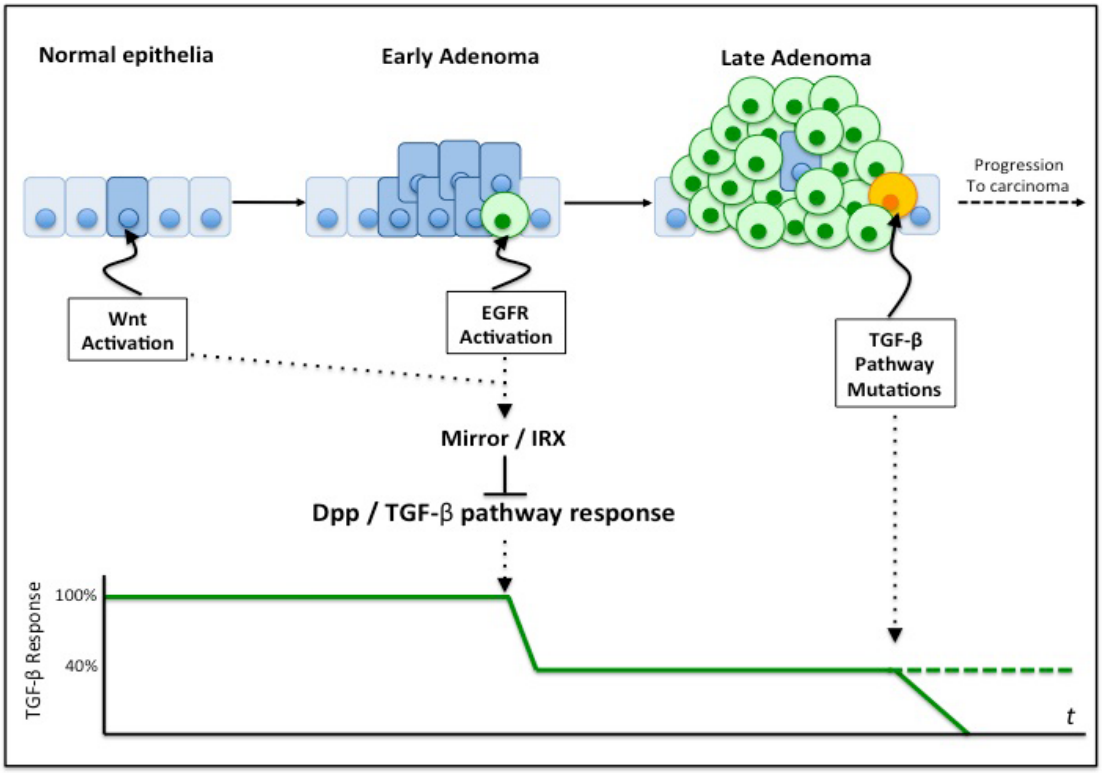

Figure 59. Model for IRX role during CRC progression. IRX proteins will act as silencers of TGF-β signalling pathway reducing the growth barrier imposed by this signal. This silencing would help the cells to maintain their proliferative capabilities to further accumulate mutations on the pathway. There is the possibility that this IRX expression would explain those CRC cases that are not responsive to TGF-β but do not show mutations in members of the pathway.

Final discussion: Is the Drosophila midgut a good model to study CRC?

"The limitations of D. melanogaster as a model system to study cancer are many and substantial, but it also has important advantages. By being conscious of the limitations but exploiting the advantages, studies in D. melanogaster will contribute to understanding cancer across different fronts (Gonzalez, 2013)." This sentence extracted from a cancer review written by Cayetano Gonzalez reflects perfectly how I see *Drosophila* after this work. *Drosophila* has many disadvantatges and it is difficult if not impossible to study some of the sistemic effects implicated in cancer such as inflammatory or immune responses. However, our *Drosophila* CRC model resembles at a high extend the properties of CRC cells and many results have demonstrate the suitability of this model. In future studies this model can give us valuable information about the nature and behaviour of the tumour cells and also strong candidate genes to validate in upper organisms. For this reason, I strongly encourage the scientific

communitiy to accept *Drosophila* cancer models as simple and useful tools to investigate the basic aspects of tumour biology and cancer disease.

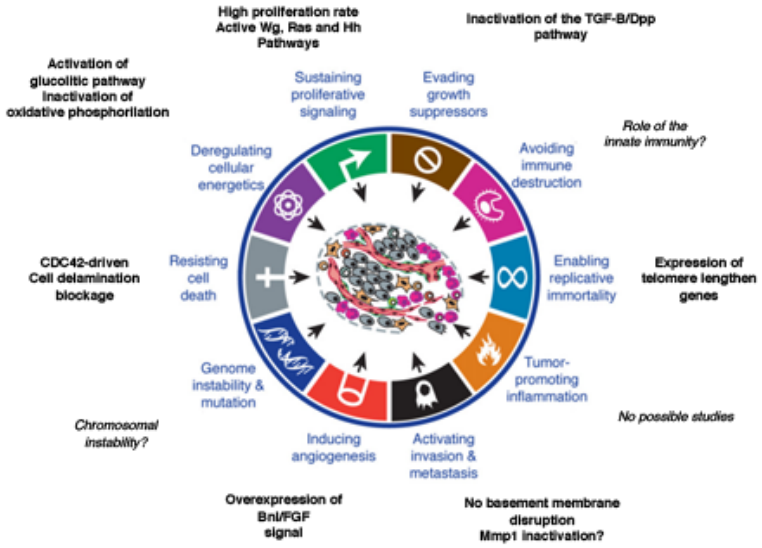

Figure 60. Evidences of Hallmarks of cancer in Apc-Ras model. In bold letters those results that show a putative link to a specific hallmark. In italic letters those hallmarks not without any evidence in Apc-Ras model.

Conclusions

6. Conclusions

According to the results, our conclusions are:

1. The clonal co-activation of Wg and EGFR pathways induces the apparition of tumour-like overgrowths in the *Drosophila* adult midgut.

2. The expression of Ras^{v12} induces the extrusion of most of the clones by the activation of the protein Cdc42.

3. Apc-Ras clones are hyperproliferative and present loss of cell differentiation, loss of cell polarity and overall tissue disorganization.

4. Apc-Ras clones are not metastatic.

5. Apc-Ras clones alter normal physiology of the adult midgut reducing the number of faecal depositions and making slower the intestinal transit.

6. The transcriptional profile of Apc-Ras cells revels a synergic activity of the activation of Wg and EGFR pathways with genes specifically altered in Apc-Ras clones but not altered in single-altered clones.

7. Apc Ras clones profile is rich in proliferation genes and signalling molecules, and present metabolic alterations similar to the ones occurring during human CRC progression.

8. Apc-Ras cells present a transcriptional silencing of the components of the Dpp signalling pathway.

9. The transcriptional silencing of the Dpp pathway in Apc-Ras cells is essential for proper Apc-Ras clone progression.

10. The activation of Dpp pathway in Apc-Ras cells induces a blockade in clone growth and an increase of differentiated cells.

11. The transcription factor Mirror is upregulated in Apc-Ras cells and is the protein responsible of the transcriptional silencing of the Dpp pathway.

12. The expression of Mirror is essential for Apc-Ras clone progression.

13. The absence of Mirror in Apc-Ras cells produces a decrease of clone area and restores normal cell differentiation.

14. Mirror regulates negatively the levels of Stat92E in Apc-Ras cells.

15. IRX3 and IRX5 are upregulated in colon adenomas and their expression negatively correlates with the responsiveness of SW837 cells to TGF-β treatment.

References

Andreu, M. J., González-Pérez, E., Ajuria, L., Samper, N., González-Crespo, S., Campuzano, S., & Jiménez, G. (2012). Mirror represses pipe expression in follicle cells to initiate dorsoventral axis formation in Drosophila. *Development (Cambridge, England)*, *139*(6), 1110–4. doi:10.1242/dev.076562

Apidianakis, Y., & Rahme, L. G. (2011). Drosophila melanogaster as a model for human intestinal infection and pathology. *Disease models & mechanisms*, *4*(1), 21–30. doi:10.1242/dmm.003970

Arbouzova, N. I., & Zeidler, M. P. (2006). JAK/STAT signalling in Drosophila: insights into conserved regulatory and cellular functions. *Development (Cambridge, England)*, *133*(14), 2605–16. doi:10.1242/dev.02411

Baker, S. J., Preisinger, A. C., Jessup, J. M., Paraskeva, C., Markowitz, S., Willson, J. K., … Vogelstein, B. (1990). p53 gene mutations occur in combination with 17p allelic deletions as late events in colorectal tumorigenesis. *Cancer research*, *50*(23), 7717–22. Retrieved from http://www.ncbi.nlm.nih.gov/pubmed/2253215

Baldus, S. E., Schaefer, K.-L., Engers, R., Hartleb, D., Stoecklein, N. H., & Gabbert, H. E. (2010). Prevalence and heterogeneity of KRAS, BRAF, and PIK3CA mutations in primary colorectal adenocarcinomas and their corresponding metastases. *Clinical cancer research : an official journal of the American Association for Cancer Research*, *16*(3), 790–9. doi:10.1158/1078-0432.CCR-09-2446

Balendiran, G. (2004). The role of glutathione in cancer. *Cell biochemistry and …*, (August), 343–352. doi:10.1027/cbf.1149

Bardin, A. J., Perdigoto, C. N., Southall, T. D., Brand, A. H., & Schweisguth, F. (2010). Transcriptional control of stem cell maintenance in the Drosophila intestine. *Development (Cambridge, England)*, *137*(5), 705–14. doi:10.1242/dev.039404

Batlle, E., & Wilkinson, D. G. (2012). Molecular mechanisms of cell segregation and boundary formation in development and tumorigenesis. *Cold Spring Harbor perspectives in biology*, *4*(1), a008227. doi:10.1101/cshperspect.a008227

Beaucher, M., Hersperger, E., Page-McCaw, A., & Shearn, A. (2007). Metastatic ability of Drosophila tumors depends on MMP activity. *Developmental biology*, *303*(2), 625–34. doi:10.1016/j.ydbio.2006.12.001

Becker, K.-F., Rosivatz, E., Blechschmidt, K., Kremmer, E., Sarbia, M., & Höfler, H. (2007). Analysis of the E-cadherin repressor Snail in primary human cancers. *Cells, tissues, organs*, *185*(1-3), 204–12. doi:10.1159/000101321

Beebe, K., Lee, W.-C., & Micchelli, C. a. (2010). JAK/STAT signaling coordinates stem cell proliferation and multilineage differentiation in the Drosophila intestinal stem cell lineage. *Developmental biology*, *338*(1), 28–37. doi:10.1016/j.ydbio.2009.10.045

Bensinger, S. J., & Christofk, H. R. (2012). New aspects of the Warburg effect in cancer cell biology. *Seminars in cell & developmental biology*, *23*(4), 352–61. doi:10.1016/j.semcdb.2012.02.003

Bienz, M., & Clevers, H. (2000). Linking Colorectal Cancer to Wnt Signaling Review. *Cell*, *103*, 311–320. Retrieved from http://defaye.arnaud.free.fr/cours/M2/CAOD/supp2.pdf

Bilioni, A., Craig, G., Hill, C., & McNeill, H. (2005). Iroquois transcription factors recognize a unique motif to mediate transcriptional repression in vivo. *Proceedings of the National Academy of Sciences of the United States of America*, *102*(41), 14671–6. doi:10.1073/pnas.0502480102

Biteau, B., Hochmuth, C. E., & Jasper, H. (2008). JNK activity in somatic stem cells causes loss of tissue homeostasis in the aging Drosophila gut. *Cell stem cell*, *3*(4), 442–55. doi:10.1016/j.stem.2008.07.024

Biteau, B., & Jasper, H. (2011). EGF signaling regulates the proliferation of intestinal stem cells in Drosophila. *Development (Cambridge, England)*, *138*(6), 1045–55. doi:10.1242/dev.056671

Blanco, E., Messeguer, X., Smith, T. F., & Guigó, R. (2006). Transcription factor map alignment of promoter regions. *PLoS computational biology*, *2*(5), e49. doi:10.1371/journal.pcbi.0020049

Bond, D., & Foley, E. (2012). Autocrine platelet-derived growth factor-vascular endothelial growth factor receptor-related (Pvr) pathway activity controls intestinal stem cell proliferation in the adult Drosophila midgut. *The Journal of biological chemistry*, *287*(33), 27359–70. doi:10.1074/jbc.M112.378018

Bray, S. J. (2006). Notch signalling: a simple pathway becomes complex. *Nature reviews. Molecular cell biology*, *7*(9), 678–89. doi:10.1038/nrm2009

Buchon, N., & Broderick, N. (2009). Invasive and indigenous microbiota impact intestinal stem cell activity through multiple pathways in Drosophila. *Genes & …*, 2333–2344. doi:10.1101/gad.1827009.tion

Buchon, N., Broderick, N. A., Kuraishi, T., & Lemaitre, B. (2010). Drosophila EGFR pathway coordinates stem cell proliferation and gut remodeling following infection. *BMC biology*, *8*(1), 152. doi:10.1186/1741-7007-8-152

Buchon, N., Osman, D., David, F. P. a, Boquete, J.-P., Deplancke, B., & Lemaitre, B. (2013). Morphological and Molecular Characterization of Adult Midgut Compartmentalization in Drosophila. *Cell reports*, 1–14. doi:10.1016/j.celrep.2013.04.001

Cairns, R. A., Harris, I. S., & Mak, T. W. (2011). Regulation of cancer cell metabolism. *Nature reviews. Cancer*, *11*(2), 85–95. doi:10.1038/nrc2981

Calon, A., Espinet, E., Palomo-Ponce, S., Tauriello, D. V. F., Iglesias, M., Céspedes, M. V., … Batlle, E. (2012). Dependency of colorectal cancer on a TGF-β-driven program in stromal cells for metastasis initiation. *Cancer cell*, *22*(5), 571–84. doi:10.1016/j.ccr.2012.08.013

Campbell, K., Whissell, G., Franch-Marro, X., Batlle, E., & Casanova, J. (2011). Specific GATA factors act as conserved inducers of an endodermal-EMT. *Developmental cell*, *21*(6), 1051–61. doi:10.1016/j.devcel.2011.10.005

Cancer, A. J. C. on. (2010). *AJCC Cancer Staging Manual.* (7th ed.). NY.

Carver, E. A., Jiang, R., Lan, Y., Oram, K. F., & Gridley, T. (2001). The mouse snail gene encodes a key regulator of the epithelial-mesenchymal transition. *Molecular and cellular biology*, *21*(23), 8184–8. doi:10.1128/MCB.21.23.8184-8188.2001

Casanova, J, & Struhl, G. (1989). Localized surface activity of torso, a receptor tyrosine kinase, specifies terminal body pattern in Drosophila. *Genes & development*, *3*(12B), 2025–38. Retrieved from http://www.ncbi.nlm.nih.gov/pubmed/2560750

Casanova, Jordi. (2012). Stemness as a cell default state. *EMBO reports*, *13*(5), 396–7. doi:10.1038/embor.2012.47

Choi, N. H., Lucchetta, E., & Ohlstein, B. (2011). Nonautonomous regulation of Drosophila midgut stem cell proliferation by the insulin-signaling pathway. *Proceedings of the National Academy of Sciences of the United States of America*, *108*(46), 18702–7. doi:10.1073/pnas.1109348108

Cognigni, P., Bailey, A. P., & Miguel-Aliaga, I. (2011). Enteric neurons and systemic signals couple nutritional and reproductive status with intestinal homeostasis. *Cell metabolism*, *13*(1), 92–104. doi:10.1016/j.cmet.2010.12.010

Cordero, J. B., Stefanatos, R. K., Scopelliti, A., Vidal, M., & Sansom, O. J. (2012). Inducible progenitor-derived Wingless regulates adult midgut regeneration in Drosophila. *The EMBO journal*, *31*(19), 3901–17. doi:10.1038/emboj.2012.248

Cordero, J., Stefanatos, R., & Myant, K. (2012). Non-autonomous crosstalk between the Jak/Stat and Egfr pathways mediates Apc1-driven intestinal stem cell hyperplasia in the Drosophila adult midgut. *Development (Cambridge, England)*, *139*(24), 4524–35. doi:10.1242/dev.078261

Dearborn, R. E., Dai, Y., Reed, B., Karian, T., Gray, J., & Kunes, S. (2012). Reph, a regulator of Eph receptor expression in the Drosophila melanogaster optic lobe. *PloS one*, *7*(5), e37303. doi:10.1371/journal.pone.0037303

Dennler, S., Itoh, S., Vivien, D., ten Dijke, P., Huet, S., & Gauthier, J. M. (1998). Direct binding of Smad3 and Smad4 to critical TGF beta-inducible elements in the promoter of human plasminogen activator inhibitor-type 1 gene. *The EMBO journal*, *17*(11), 3091–100. doi:10.1093/emboj/17.11.3091

Ding, Z., Wu, C.-J., Chu, G. C., Xiao, Y., Ho, D., Zhang, J., … DePinho, R. A. (2011). SMAD4-dependent barrier constrains prostate cancer growth and metastatic progression. *Nature*, *470*(7333), 269–73. doi:10.1038/nature09677

Durinck, S., Moreau, Y., Kasprzyk, A., Davis, S., De Moor, B., Brazma, A., & Huber, W. (2005). BioMart and Bioconductor: a powerful link between biological databases and microarray data analysis. *Bioinformatics (Oxford, England)*, *21*(16), 3439–40. doi:10.1093/bioinformatics/bti525

Elkins, T., Hortsch, M., Bieber, A. J., Snow, P. M., & Goodman, C. S. (1990). Drosophila fasciclin I is a novel homophilic adhesion molecule that along with fasciclin III can mediate cell sorting. *The Journal of cell biology*, *110*(5), 1825–32. Retrieved from http://www.pubmedcentral.nih.gov/articlerender.fcgi?artid=2200178&tool=pmcentrez&rendertype=abstract

Ellenbroek, S. I. J., Iden, S., & Collard, J. G. (2012). Cell polarity proteins and cancer. *Seminars in cancer biology*, *22*(3), 208–15. doi:10.1016/j.semcancer.2012.02.012

Elliott, R., & Blobe, G. (2005). Role of transforming growth factor Beta in human cancer. *Journal of Clinical Oncology*, *23*(9), 2078–93. doi:10.1200/JCO.2005.02.047

Fearon, E. R. (2011). Molecular genetics of colorectal cancer. *Annual review of pathology*, *6*, 479–507. doi:10.1146/annurev-pathol-011110-130235

Fearon, E., & Vogelstein, B. (1990). A genetic model for colorectal tumorigenesis. *Cell*, *61*, 759–767. Retrieved from http://www.charite.de/idz/ag_hanski/download/Fearon and Vogelstein.pdf

Foulds, L. (1954). The experimental study of tumor progression: a review. *Cancer research*, *14*(5), 327–39. Retrieved from http://www.ncbi.nlm.nih.gov/pubmed/13160960

Fox, D. T., & Spradling, A. C. (2009). The Drosophila hindgut lacks constitutively active adult stem cells but proliferates in response to tissue damage. *Cell stem cell*, *5*(3), 290–7. doi:10.1016/j.stem.2009.06.003

Fujita, P. A., Rhead, B., Zweig, A. S., Hinrichs, A. S., Karolchik, D., Cline, M. S., … Kent, W. J. (2011). The UCSC Genome Browser database: update 2011. *Nucleic acids research*, *39*(Database issue), D876–82. doi:10.1093/nar/gkq963

Gautier, L., Cope, L., Bolstad, B. M., & Irizarry, R. A. (2004). affy--analysis of Affymetrix GeneChip data at the probe level. *Bioinformatics (Oxford, England)*, *20*(3), 307–15. doi:10.1093/bioinformatics/btg405

Gentleman, R. C., Carey, V. J., Bates, D. M., Bolstad, B., Dettling, M., Dudoit, S., … Zhang, J. (2004). Bioconductor: open software development for computational biology and bioinformatics. *Genome biology*, *5*(10), R80. doi:10.1186/gb-2004-5-10-r80

Gómez-Skarmeta, J. L., & Modolell, J. (2002). Iroquois genes: genomic organization and function in vertebrate neural development. *Current Opinion in Genetics & Development*, *12*(4), 403–408. doi:10.1016/S0959-437X(02)00317-9

Gonzalez, C. (2013). Drosophila melanogaster: a model and a tool to investigate malignancy and identify new therapeutics. *Nature reviews. Cancer*, *13*(3), 172–83. doi:10.1038/nrc3461

Gonzalez-Roca, E., Garcia-Albéniz, X., Rodriguez-Mulero, S., Gomis, R. R., Kornacker, K., & Auer, H. (2010). Accurate expression profiling of very small cell populations. (S. Huang, Ed.)*PloS one*, *5*(12), e14418. doi:10.1371/journal.pone.0014418

Gordziel, C., Bratsch, J., Moriggl, R., Knösel, T., & Friedrich, K. (2013). Both STAT1 and STAT3 are favourable prognostic determinants in colorectal carcinoma. *British journal of cancer*, *109*(1), 138–46. doi:10.1038/bjc.2013.274

Goulas, S., Conder, R., & Knoblich, J. A. (2012). The Par complex and integrins direct asymmetric cell division in adult intestinal stem cells. *Cell stem cell*, *11*(4), 529–40. doi:10.1016/j.stem.2012.06.017

Grady, W. M., Myeroff, L. L., Swinler, S. E., Rajput, A., Thiagalingam, S., Lutterbaugh, J. D., … Markowitz, S. (1999). Mutational inactivation of transforming growth factor beta receptor type II in microsatellite stable colon cancers. *Cancer research*, *59*(2), 320–4. Retrieved from http://www.ncbi.nlm.nih.gov/pubmed/9927040

Grenningloh, G., Rehm, E. J., & Goodman, C. S. (1991). Genetic analysis of growth cone guidance in Drosophila: fasciclin II functions as a neuronal recognition molecule. *Cell*, *67*(1), 45–57. Retrieved from http://www.ncbi.nlm.nih.gov/pubmed/1913818

Guo, X., Liu, W., Pan, Y., Ni, P., Ji, J., Guo, L., … Yu, Y. (2010). Homeobox gene IRX1 is a tumor suppressor gene in gastric carcinoma. *Oncogene*, *29*(27), 3908–20. doi:10.1038/onc.2010.143

Guo, Z., Driver, I., & Ohlstein, B. (2013). Injury-induced BMP signaling negatively regulates Drosophila midgut homeostasis. *The Journal of cell biology*, *201*(6), 945–61. doi:10.1083/jcb.201302049

Häcker, U., Nybakken, K., & Perrimon, N. (2005). Heparan sulphate proteoglycans: the sweet side of development. *Nature reviews. Molecular cell biology*, *6*(7), 530–41. doi:10.1038/nrm1681

Hanahan, D, & Weinberg, R. A. (2000). The hallmarks of cancer. *Cell*, *100*(1), 57–70. Retrieved from http://eutils.ncbi.nlm.nih.gov/entrez/eutils/elink.fcgi?dbfrom=pubmed&id=10647931&retmode=ref&cmd=prlinks

Hanahan, Douglas, & Weinberg, R. A. (2011). Hallmarks of cancer: the next generation. *Cell*, *144*(5), 646–674. Retrieved from http://www.ncbi.nlm.nih.gov/pubmed/21376230

Hashimoto, Y., Skacel, M., Lavery, I. C., Mukherjee, A. L., Casey, G., & Adams, J. C. (2006). Prognostic significance of fascin expression in advanced colorectal cancer: an immunohistochemical study of colorectal adenomas and adenocarcinomas. *BMC cancer*, *6*(1), 241. doi:10.1186/1471-2407-6-241

Hegan, P. S., Mermall, V., Tilney, L. G., & Mooseker, M. S. (2007). Roles for Drosophila melanogaster myosin IB in maintenance of enterocyte brush-border structure and resistance to the bacterial pathogen Pseudomonas entomophila. *Molecular biology of the cell*, *18*(11), 4625–36. doi:10.1091/mbc.E07-02-0191

Hochmuth, C. E., Biteau, B., Bohmann, D., & Jasper, H. (2011). Redox regulation by Keap1 and Nrf2 controls intestinal stem cell proliferation in Drosophila. *Cell stem cell*, *8*(2), 188–99. doi:10.1016/j.stem.2010.12.006

Hogan, C., Dupré-Crochet, S., Norman, M., Kajita, M., Zimmermann, C., Pelling, A. E., … Fujita, Y. (2009). Characterization of the interface between normal and transformed epithelial cells. *Nature cell biology*, *11*(4), 460–7. doi:10.1038/ncb1853

Janssen, K. P. (2003). Murine models of colorectal cancer: studying the role of oncogenic K-ras. *Cellular and molecular life sciences : CMLS*, *60*(3), 495–506. Retrieved from http://www.ncbi.nlm.nih.gov/pubmed/12737309

Jass, J. R. (2007). Classification of colorectal cancer based on correlation of clinical, morphological and molecular features. *Histopathology*, *50*(1), 113–30. doi:10.1111/j.1365-2559.2006.02549.x

Ji, X., Tang, J., Halberg, R., Busam, D., Ferriera, S., Peña, M. M. O., … Zhao, S. (2010). Distinguishing between cancer driver and passenger gene alteration candidates via cross-species comparison: a pilot study. *BMC cancer*, *10*(1), 426. doi:10.1186/1471-2407-10-426

Jiang, H., & Edgar, B. A. (2009). EGFR signaling regulates the proliferation of Drosophila adult midgut progenitors. *Development*, *136*(3), 483–493. Retrieved from http://eutils.ncbi.nlm.nih.gov/entrez/eutils/elink.fcgi?dbfrom=pubmed&id=19141677&retmode=ref&cmd=prlinks

Jiang, H., Grenley, M. O., Bravo, M.-J., Blumhagen, R. Z., & Edgar, B. A. (2011). EGFR/Ras/MAPK signaling mediates adult midgut epithelial homeostasis and regeneration in Drosophila. *Cell stem cell*, *8*(1), 84–95. doi:10.1016/j.stem.2010.11.026

Jiang, H., Patel, P., & Kohlmaier, A. (2009). Cytokine/Jak/Stat signaling mediates regeneration and homeostasis in the Drosophila midgut. *Cell*, *137*(7), 1343–1355. doi:10.1016/j.cell.2009.05.014.Cytokine/Jak/Stat

Jordan, K. C., Clegg, N. J., Blasi, J. A., Morimoto, A. M., Sen, J., Stein, D., … Ruohola-Baker, H. (2000). The homeobox gene mirror links EGF signalling to embryonic dorso-ventral axis formation through notch activation. *Nature genetics*, *24*(4), 429–33. doi:10.1038/74294

Karpowicz, P., Perez, J., & Perrimon, N. (2010). The Hippo tumor suppressor pathway regulates intestinal stem cell regeneration. *Development (Cambridge, England)*, *137*(24), 4135–45. doi:10.1242/dev.060483

Kauppila, S., Maaty, W. S. A., Chen, P., Tomar, R. S., Eby, M. T., Chapo, J., … Chaudhary, P. M. (2003). Eiger and its receptor, Wengen, comprise a TNF-like system in Drosophila. *Oncogene*, *22*(31), 4860–7. doi:10.1038/sj.onc.1206715

Kehl, B. T., Cho, K. O., & Choi, K. W. (1998). mirror, a Drosophila homeobox gene in the Iroquois complex, is required for sensory organ and alula formation.

Development (Cambridge, England), *125*(7), 1217–27. Retrieved from http://www.ncbi.nlm.nih.gov/pubmed/9477320

Lee, S.-H., Park, J.-S., Kim, Y.-S., Chung, H.-Y., & Yoo, M.-A. (2012). Requirement of matrix metalloproteinase-1 for intestinal homeostasis in the adult Drosophila midgut. *Experimental cell research*, *318*(5), 670–81. doi:10.1016/j.yexcr.2012.01.004

Lee, W.-C., Beebe, K., Sudmeier, L., & Micchelli, C. A. (2009). Adenomatous polyposis coli regulates Drosophila intestinal stem cell proliferation. *Development*, *136*(13), 2255–2264. Retrieved from http://eutils.ncbi.nlm.nih.gov/entrez/eutils/elink.fcgi?dbfrom=pubmed&id=19502486&retmode=ref&cmd=prlinks

Levy, L., & Hill, C. S. (2006). Alterations in components of the TGF-beta superfamily signaling pathways in human cancer. *Cytokine & growth factor reviews*, *17*(1-2), 41–58. doi:10.1016/j.cytogfr.2005.09.009

Li, H., Qi, Y., & Jasper, H. (2013). Dpp signaling determines regional stem cell identity in the regenerating adult Drosophila gastrointestinal tract. *Cell reports*, *4*(1), 10–8. doi:10.1016/j.celrep.2013.05.040

Li, W., Zhu, T., & Guan, K.-L. (2004). Transformation potential of Ras isoforms correlates with activation of phosphatidylinositol 3-kinase but not ERK. *The Journal of biological chemistry*, *279*(36), 37398–406. doi:10.1074/jbc.M405730200

Li, Z., Zhang, Y., Han, L., Shi, L., & Lin, X. (2013). Trachea-derived dpp controls adult midgut homeostasis in Drosophila. *Developmental cell*, *24*(2), 133–43. doi:10.1016/j.devcel.2012.12.010

Lin, G, Xu, N., & Xi, R. (2008). Paracrine Wingless signalling controls self-renewal of Drosophila intestinal stem cells. *Nature*. Retrieved from http://www.nature.com/nature/journal/vaop/ncurrent/full/nature07329.html

Lin, Guonan, Xu, N., & Xi, R. (2010). Paracrine unpaired signaling through the JAK/STAT pathway controls self-renewal and lineage differentiation of drosophila intestinal stem cells. *Journal of molecular cell biology*, *2*(1), 37–49. doi:10.1093/jmcb/mjp028

Liu, W., Singh, S., & Hou, S. (2010). JAK-STAT is restrained by Notch to control cell proliferation of the Drosophila intestinal stem cells. *Journal of cellular biochemistry*, *109*(5), 992–999. doi:10.1002/jcb.22482.JAK-STAT

Luo, F., Brooks, D. G., Ye, H., Hamoudi, R., Poulogiannis, G., Patek, C. E., … Arends, M. J. (2009). Mutated K-ras(Asp12) promotes tumourigenesis in Apc(Min) mice more in the large than the small intestines, with synergistic effects between K-ras and Wnt pathways. *International journal of experimental pathology*, *90*(5), 558–74. doi:10.1111/j.1365-2613.2009.00667.x

Luo, F., Poulogiannis, G., Ye, H., Hamoudi, R., & Arends, M. J. (2011). Synergism between K-rasVal12 and mutant Apc accelerates murine large intestinal tumourigenesis. *Oncology reports*, *26*(1), 125–33. doi:10.3892/or.2011.1288

Maeda, K., Takemura, M., Umemori, M., & Adachi-Yamada, T. (2008). E-cadherin prolongs the moment for interaction between intestinal stem cell and its progenitor cell to ensure Notch signaling in adult Drosophila midgut. *Genes to cells : devoted to molecular & cellular mechanisms*, *13*(12), 1219–27. doi:10.1111/j.1365-2443.2008.01239.x

Maglietta, R., Liuzzi, V. C., Cattaneo, E., Laczko, E., Piepoli, A., Panza, A., … Ancona, N. (2012). Molecular pathways undergoing dramatic transcriptomic changes during tumor development in the human colon. *BMC cancer*, *12*, 608. doi:10.1186/1471-2407-12-608

Malumbres, M., & Barbacid, M. (2003). RAS oncogenes: the first 30 years. *Nature reviews. Cancer*, *3*(6), 459–65. doi:10.1038/nrc1097

Marianes, A., & Spradling, A. C. (2013a). Physiological and stem cell compartmentalization within the Drosophila midgut. *eLife*, *2*, e00886. doi:10.7554/eLife.00886

Marianes, A., & Spradling, A. C. (2013b). Physiological and stem cell compartmentalization within the Drosophila midgut. *eLife*, *2*, e00886. doi:10.7554/eLife.00886

Marisa, L., de Reyniès, A., Duval, A., Selves, J., Gaub, M. P., Vescovo, L., … Boige, V. (2013). Gene Expression Classification of Colon Cancer into Molecular Subtypes: Characterization, Validation, and Prognostic Value. (C. Kemp, Ed.)*PLoS Medicine*, *10*(5), e1001453. doi:10.1371/journal.pmed.1001453

Markowitz, S., & Bertagnolli, M. (2009). Molecular basis of colorectal cancer. *New England Journal of …*, 2449–2460. Retrieved from http://www.nejm.org/doi/full/10.1056/NEJMra0804588

Markowitz, S. D., & Roberts, A. B. (1996). Tumor suppressor activity of the TGF-beta pathway in human cancers. *Cytokine & growth factor reviews*, *7*(1), 93–102. Retrieved from http://www.ncbi.nlm.nih.gov/pubmed/8864357

Martin-Blanco, E., Pastor-Pareja, J. C., & Garcia-Bellido, A. (2000). JNK and decapentaplegic signaling control adhesiveness and cytoskeleton dynamics during thorax closure in Drosophila. *Proceedings of the National Academy of Sciences*, *97*(14), 7888–7893. doi:10.1073/pnas.97.14.7888

Massagué, J. (2008). TGFb in cancer. *Cell*, *134*(2), 215–230. doi:10.1016/j.cell.2008.07.001.TGF

McNeill, H., Yang, C. H., Brodsky, M., Ungos, J., & Simon, M. A. (1997). mirror encodes a novel PBX-class homeoprotein that functions in the definition of the dorsal-ventral border in the Drosophila eye. *Genes & development*, *11*(8), 1073–82. Retrieved from http://www.ncbi.nlm.nih.gov/pubmed/9136934

Merlos-Suárez, A., Barriga, F. M., Jung, P., Iglesias, M., Céspedes, M. V., Rossell, D., … Batlle, E. (2011). The Intestinal Stem Cell Signature Identifies Colorectal Cancer Stem Cells and Predicts Disease Relapse. *Cell Stem Cell*, *8*(5), 511–524.

Retrieved from http://www.sciencedirect.com/science/article/pii/S193459091100110X

Micchelli, C. A. (2012). The origin of intestinal stem cells in Drosophila. *Developmental dynamics : an official publication of the American Association of Anatomists*, *241*(1), 85–91. doi:10.1002/dvdy.22759

Micchelli, C. A., & Perrimon, N. (2006). Evidence that stem cells reside in the adult Drosophila midgut epithelium. *Nature*, *439*(7075), 475–479. Retrieved from http://eutils.ncbi.nlm.nih.gov/entrez/eutils/elink.fcgi?dbfrom=pubmed&id=16340959&retmode=ref&cmd=prlinks

Mortimer, N. T., & Moberg, K. H. (2009). Regulation of Drosophila embryonic tracheogenesis by dVHL and hypoxia. *Developmental biology*, *329*(2), 294–305. doi:10.1016/j.ydbio.2009.03.001

Moser, A. R., Pitot, H. C., & Dove, W. F. (1990). A dominant mutation that predisposes to multiple intestinal neoplasia in the mouse. *Science (New York, N.Y.)*, *247*(4940), 322–4. Retrieved from http://www.ncbi.nlm.nih.gov/pubmed/2296722

Myrthue, A., Rademacher, B. L. S., Pittsenbarger, J., Kutyba-Brooks, B., Gantner, M., Qian, D. Z., & Beer, T. M. (2008). The iroquois homeobox gene 5 is regulated by 1,25-dihydroxyvitamin D3 in human prostate cancer and regulates apoptosis and the cell cycle in LNCaP prostate cancer cells. *Clinical cancer research : an official journal of the American Association for Cancer Research*, *14*(11), 3562–70. doi:10.1158/1078-0432.CCR-07-4649

Nellen, D., Burke, R., Struhl, G., & Basler, K. (1996). Direct and Long-Range Action of a DPP Morphogen Gradient. *Cell*, *85*(3), 357–368. Retrieved from http://www.sciencedirect.com/science/article/pii/S0092867400811149

Network, C. G. A. (2012). Comprehensive molecular characterization of human colon and rectal cancer. *Nature*, *487*(7407), 330–337. Retrieved from http://eutils.ncbi.nlm.nih.gov/entrez/eutils/elink.fcgi?dbfrom=pubmed&id=22810696&retmode=ref&cmd=prlinks

Nguyen, H. H., Takata, R., Akamatsu, S., Shigemizu, D., Tsunoda, T., Furihata, M., … Nakagawa, H. (2012). IRX4 at 5p15 suppresses prostate cancer growth through the interaction with vitamin D receptor, conferring prostate cancer susceptibility. *Human molecular genetics*, *21*(9), 2076–85. doi:10.1093/hmg/dds025

Ohlstein, B., & Spradling, A. (2006). The adult Drosophila posterior midgut is maintained by pluripotent stem cells. *Nature*, *439*(7075), 470–474. Retrieved from http://eutils.ncbi.nlm.nih.gov/entrez/eutils/elink.fcgi?dbfrom=pubmed&id=16340960&retmode=ref&cmd=prlinks

Ohlstein, B., & Spradling, A. (2007). Multipotent Drosophila intestinal stem cells specify daughter cell fates by differential notch signaling. *Science*, *315*(5814), 988–992. Retrieved from http://eutils.ncbi.nlm.nih.gov/entrez/eutils/elink.fcgi?dbfrom=pubmed&id=17303754&retmode=ref&cmd=prlinks

Parker, L., Ellis, J. E., Nguyen, M. Q., & Arora, K. (2006). The divergent TGF-beta ligand Dawdle utilizes an activin pathway to influence axon guidance in Drosophila. *Development (Cambridge, England)*, *133*(24), 4981–91. doi:10.1242/dev.02673

Qin, J., Wu, S.-P., Creighton, C. J., Dai, F., Xie, X., Cheng, C.-M., … Tsai, S. Y. (2013). COUP-TFII inhibits TGF-β-induced growth barrier to promote prostate tumorigenesis. *Nature*, *493*(7431), 236–40. doi:10.1038/nature11674

Qualtrough, D., Singh, K., Banu, N., Paraskeva, C., & Pignatelli, M. (2009). The actin-bundling protein fascin is overexpressed in colorectal adenomas and promotes motility in adenoma cells in vitro. *British journal of cancer*, *101*(7), 1124–9. doi:10.1038/sj.bjc.6605286

Rajagopalan, H., Bardelli, A., Lengauer, C., Kinzler, K. W., Vogelstein, B., & Velculescu, V. E. (2002). Tumorigenesis: RAF/RAS oncogenes and mismatch-repair status. *Nature*, *418*(6901), 934. doi:10.1038/418934a

Ren, F., Wang, B., Yue, T., Yun, E.-Y., Ip, Y. T., & Jiang, J. (2010). Hippo signaling regulates Drosophila intestine stem cell proliferation through multiple pathways. *Proceedings of the National Academy of Sciences of the United States of America*, *107*(49), 21064–9. doi:10.1073/pnas.1012759107

Rowan, a J., Lamlum, H., Ilyas, M., Wheeler, J., Straub, J., Papadopoulou, a, … Tomlinson, I. P. (2000). APC mutations in sporadic colorectal tumors: A mutational "hotspot" and interdependence of the "two hits". *Proceedings of the National Academy of Sciences of the United States of America*, *97*(7), 3352–7. Retrieved from http://www.pubmedcentral.nih.gov/articlerender.fcgi?artid=16243&tool=pmcentrez&rendertype=abstract

Royet, J. (2011). Epithelial homeostasis and the underlying molecular mechanisms in the gut of the insect model Drosophila melanogaster. *Cellular and molecular life sciences : CMLS*, *68*(22), 3651–60. doi:10.1007/s00018-011-0828-x

Sabates-Bellver, J., Van der Flier, L. G., de Palo, M., Cattaneo, E., Maake, C., Rehrauer, H., … Marra, G. (2007). Transcriptome profile of human colorectal adenomas. *Molecular cancer research : MCR*, *5*(12), 1263–75. doi:10.1158/1541-7786.MCR-07-0267

Salomon, R. N., & Jackson, F. R. (2008). Tumors of testis and midgut in aging flies. *Fly*, *2*(6), 265–8. Retrieved from http://www.ncbi.nlm.nih.gov/pubmed/19077545

Sancho, E., Batlle, E., & Clevers, H. (2004). Signaling pathways in intestinal development and cancer. *Annual review of cell and developmental biology*, *20*, 695–723. doi:10.1146/annurev.cellbio.20.010403.092805

Sansom, O. J., Meniel, V., Wilkins, J. A., Cole, A. M., Oien, K. A., Marsh, V., … Clarke, A. R. (2006). Loss of Apc allows phenotypic manifestation of the transforming properties of an endogenous K-ras oncogene in vivo. *Proceedings of the National Academy of Sciences of the United States of America*, *103*(38), 14122–7. doi:10.1073/pnas.0604130103

Schubbert, S., Shannon, K., & Bollag, G. (2007). Hyperactive Ras in developmental disorders and cancer. *Nature reviews. Cancer*, *7*(4), 295–308. doi:10.1038/nrc2109

Segditsas, S., & Tomlinson, I. (2006). Colorectal cancer and genetic alterations in the Wnt pathway. *Oncogene*, *25*(57), 7531–7. doi:10.1038/sj.onc.1210059

Serpe, M., Umulis, D., Ralston, A., Chen, J., Olson, D. J., Avanesov, A., … Blair, S. S. (2008). The BMP-binding protein Crossveinless 2 is a short-range, concentration-dependent, biphasic modulator of BMP signaling in Drosophila. *Developmental cell*, *14*(6), 940–53. doi:10.1016/j.devcel.2008.03.023

Seto, E. S., & Bellen, H. J. (2004). The ins and outs of Wingless signaling. *Trends in Cell Biology*, *14*(1), 45–53. doi:10.1016/j.tcb.2003.11.004

Shanbhag, S., & Tripathi, S. (2009). Epithelial ultrastructure and cellular mechanisms of acid and base transport in the Drosophila midgut. *The Journal of experimental biology*, *212*(Pt 11), 1731–44. doi:10.1242/jeb.029306

Shaw, R. L., Kohlmaier, A., Polesello, C., Veelken, C., Edgar, B. A., & Tapon, N. (2010). The Hippo pathway regulates intestinal stem cell proliferation during Drosophila adult midgut regeneration. *Development (Cambridge, England)*, *137*(24), 4147–58. doi:10.1242/dev.052506

Shilo, B. (2003). Signaling by the Drosophila epidermal growth factor receptor pathway during development. *Experimental Cell Research*, *284*(1), 140–149. doi:10.1016/S0014-4827(02)00094-0

Singh, S. R., Zeng, X., Zheng, Z., & Hou, S. X. (2011). The adult Drosophila gastric and stomach organs are maintained by a multipotent stem cell pool at the foregut/midgut junction in the cardia (proventriculus). *Cell Cycle*, *10*(7), 1109–1120. doi:10.4161/cc.10.7.14830

Snow, P. M., Bieber, A. J., & Goodman, C. S. (1989). Fasciclin III: a novel homophilic adhesion molecule in Drosophila. *Cell*, *59*(2), 313–23. Retrieved from http://www.ncbi.nlm.nih.gov/pubmed/2509076

Soga, T. (2013). Cancer metabolism: key players in metabolic reprogramming. *Cancer science*, *104*(3), 275–81. doi:10.1111/cas.12085

Staley, B. K., & Irvine, K. D. (2010). Warts and Yorkie mediate intestinal regeneration by influencing stem cell proliferation. *Current biology : CB*, *20*(17), 1580–7. doi:10.1016/j.cub.2010.07.041

Strand, M., & Micchelli, C. A. (2011). Quiescent gastric stem cells maintain the adult Drosophila stomach. *Proceedings of the National Academy of Sciences of the United States of America*, *108*(43), 17696–701. doi:10.1073/pnas.1109794108

Subramanian, A., Tamayo, P., Mootha, V. K., Mukherjee, S., Ebert, B. L., Gillette, M. A., … Mesirov, J. P. (2005). Gene set enrichment analysis: a knowledge-based approach for interpreting genome-wide expression profiles. *Proceedings of the*

National Academy of Sciences of the United States of America, *102*(43), 15545–50. doi:10.1073/pnas.0506580102

Takashima, S., Mkrtchyan, M., Younossi-Hartenstein, A., Merriam, J. R., & Hartenstein, V. (2008). The behaviour of Drosophila adult hindgut stem cells is controlled by Wnt and Hh signalling. *Nature*, *454*(7204), 651–5. doi:10.1038/nature07156

Van de Wetering, M., Sancho, E., Verweij, C., de Lau, W., Oving, I., Hurlstone, A., … Clevers, H. (2002). The beta-catenin/TCF-4 complex imposes a crypt progenitor phenotype on colorectal cancer cells. *Cell*, *111*(2), 241–50.

Veenstra, J. A., Agricola, H.-J., & Sellami, A. (2008). Regulatory peptides in fruit fly midgut. *Cell and tissue research*, *334*(3), 499–516. doi:10.1007/s00441-008-0708-3

Vignjevic, D., Schoumacher, M., Gavert, N., Janssen, K.-P., Jih, G., Laé, M., … Robine, S. (2007). Fascin, a novel target of beta-catenin-TCF signaling, is expressed at the invasive front of human colon cancer. *Cancer research*, *67*(14), 6844–53. doi:10.1158/0008-5472.CAN-07-0929

Vlieghe, D., Sandelin, A., De Bleser, P. J., Vleminckx, K., Wasserman, W. W., van Roy, F., & Lenhard, B. (2006). A new generation of JASPAR, the open-access repository for transcription factor binding site profiles. *Nucleic acids research*, *34*(Database issue), D95–7. doi:10.1093/nar/gkj115

Wang, C., Zhao, R., Huang, P., Yang, F., Quan, Z., Xu, N., & Xi, R. (2013). APC loss-induced intestinal tumorigenesis in Drosophila: Roles of Ras in Wnt signaling activation and tumor progression. *Developmental biology*, *378*(2), 122–40.

Wilkins, J. A., & Sansom, O. J. (2008). C-Myc is a critical mediator of the phenotypes of Apc loss in the intestine. *Cancer research*, *68*(13), 4963–6. doi:10.1158/0008-5472.CAN-07-5558

Wodarz, A., & Näthke, I. (2007). Cell polarity in development and cancer. *Nature cell biology*, *9*(9), 1016–24. doi:10.1038/ncb433

Wu, J. S., & Luo, L. (2006). A protocol for mosaic analysis with a repressible cell marker (MARCM) in Drosophila. *Nature protocols*, *1*(6), 2583–9.

Xu, N., Wang, S. Q., Tan, D., Gao, Y., Lin, G., & Xi, R. (2011). EGFR, Wingless and JAK/STAT signaling cooperatively maintain Drosophila intestinal stem cells. *Developmental biology*, *354*(1), 31–43. doi:10.1016/j.ydbio.2011.03.018

Zeineldin, M., & Neufeld, K. L. (2013). More than two decades of Apc modeling in rodents. *Biochimica et biophysica acta*, *1836*(1), 80–9. doi:10.1016/j.bbcan.2013.01.001

Zollinger, R. M. (1986). Primary neoplasms of the small intestine. *American journal of surgery*, *151*(6), 654–8. Retrieved from http://www.ncbi.nlm.nih.gov/pubmed/2424326

Annexes

Annex 1. Differentially expressed genes in Apc vs WT 1 week ACI comparison

symbol	genename	APC vs WT 1week FC	APC vs WT 1week PDE	APC vs WT REJ
tau	CG31057 gene product from transcript CG31057-RA	41.31519613	0.999992208	1
CG7900	CG7900 gene product from transcript CG7900-RB	24.29849663	0.999888175	1
fz3	frizzled 3	8.244020773	0.999158661	1
CG15695	CG15695 gene product from transcript CG15695-RA	7.58365295	0.998085571	1
CG30502	CG30502 gene product from transcript CG30502-RB	7.03683735	0.993022888	1
CG18173	CG18173 gene product from transcript CG18173-RA	6.937383059	0.999928278	1
CG5630	CG5630 gene product from transcript CG5630-RB	6.813726064	0.998017685	1
CG6283	CG6283 gene product from transcript CG6283-RA	6.729710584	0.999851036	1
tw	Protein O-mannosyltransferase 2	6.688665834	0.995593903	1
CG31058	CG31058 gene product from transcript CG31058-RA	6.299701874	0.999719849	1
CG5630	CG5630 gene product from transcript CG5630-RB	6.04437328	0.999989229	1
nub	nubbin	5.394569283	0.969398529	1
CG7922	CG7922 gene product from transcript CG7922-RA	5.179181599	0.999993123	1
CG10140	CG10140 gene product from transcript CG10140-RA	5.065279432	0.999585393	1
slow	slowdown	4.844857872	0.9992463	1
CG7056	CG7056 gene product from transcript CG7056-RA	4.737984472	0.999694977	1
CG4250	CG4250 gene product from transcript CG4250-RA	4.530927977	0.984539354	1
CG18765	CG18765 gene product from transcript CG18765-RB	4.349734795	0.954642211	1
CG14877	CG14877 gene product from transcript CG14877-RA	4.172166366	0.999252225	1
CG17124	CG17124 gene product from transcript CG17124-RB	4.159055309	0.962888246	1
CG1942	CG1942 gene product from transcript CG1942-RA	4.061659836	0.999965379	1
Takl1	Tak1-like 1	4.054979313	0.982304286	1
CG11899	CG11899 gene product from transcript CG11899-RA	3.989663718	0.998150575	1
CG31344	CG31344 gene product from transcript CG31344-RA	3.734615878	0.996656061	1
upd3	unpaired 3	3.674246635	0.998329103	1
CG17124	CG17124 gene product from transcript CG17124-RB	3.673728686	0.999474587	1
upd3	unpaired 3	3.509483059	0.997899041	1
CG6045	CG6045 gene product from transcript CG6045-RA	3.383959879	0.999931497	1
CG3397	CG3397 gene product from transcript CG3397-RA	3.381180304	0.997026926	1
Npc2e	Niemann-Pick type C-2e	3.209986232	0.992814253	1
CG10154	CG10154 gene product from transcript CG10154-RA	3.17601887	0.973981248	1
Dbi	Diazepam-binding inhibitor	3.14320858	0.957936202	1
Ugt86Di	CG6658 gene product from transcript CG6658-RA	3.112365653	0.997015556	1
CHKov1	CG10618 gene product from transcript CG10618-RB	3.094698187	0.999981916	1
CG17930	CG17930 gene product from transcript CG17930-RA	3.072604769	0.976829368	1
CG5958	CG5958 gene product from transcript CG5958-RA	2.973130971	0.988357021	1
CG31809	CG31809 gene product from transcript CG31809-RB	2.968358757	0.999676733	1
NijA	Ninjurin A	2.948087475	0.988702668	1
Lim3	CG10699 gene product from transcript CG10699-RB	2.914221959	0.963363805	1
ASPP	Ankyrin-repeat, SH3-domain, and Proline-rich-region Protein	2.900372165	0.974046543	1
spri	sprint	2.884412292	0.974331405	1
CG15347	CG15347 gene product from transcript CG15347-RA	2.865184094	0.998368733	1
CG17109	CG17109 gene product from transcript CG17109-RA	2.811828907	0.984566954	1
CG6579	CG6579 gene product from transcript CG6579-RB	2.792509287	0.999111595	1
CG7142	CG7142 gene product from transcript CG7142-RA	2.750434307	0.958701796	1
Mtl	Mig-2-like	2.712852286	0.999988493	1
Ets21C	Ets at 21C	2.708210953	0.999785137	1
Nmdmc	NAD-dependent methylenetetrahydrofolate dehydrogenase	2.697983558	0.997724229	1
CG32365	CG32365 gene product from transcript CG32365-RA	2.674975585	0.99701066	1
fu12	CG17608 gene product from transcript CG17608-RA	2.65309389	0.999997455	1
Ama	Amalgam	2.636591239	0.991360501	1
CG1753	CG1753 gene product from transcript CG1753-RA	2.605780011	0.985855077	1
CG3348	CG3348 gene product from transcript CG3348-RA	2.589480211	0.999940416	1
CG11686	CG11686 gene product from transcript CG11686-RA	2.589374043	0.995688925	1
rtet	tetracycline resistance	2.554062601	0.979046052	1
exu	exuperantia	2.544191046	0.999312511	1
dmrt93B	doublesex-Mab related 93B	2.534396872	0.999702902	1
CG18746	CG18746 gene product from transcript CG18746-RA	2.527919031	0.989216522	1
Oseg4	CG2069 gene product from transcript CG2069-RA	2.521210601	0.999628758	1
CG11318	CG11318 gene product from transcript CG11318-RA	2.480069271	0.998042087	1
Gfat1	Glutamine:fructose-6-phosphate aminotransferase 1	2.475236047	0.960856775	1
alpha-Est3	alpha-Esterase-3	2.44174008	0.992107166	1

Annex 1. Differentially expressed genes in Apc vs WT 1 week ACI comparison

symbol	genename	APC vs WT 1week FC	APC vs WT 1week PDE	APC vs WT REJ
CG14820	CG14820 gene product from transcript CG14820-RA	2.435747074	0.995697585	1
ImpL2	Ecdysone-inducible gene L2	2.42557371	0.993479612	1
CG31705	CG31705 gene product from transcript CG31705-RA	2.377161751	0.964225708	1
CG13511	CG13511 gene product from transcript CG13511-RA	2.371622801	0.997310446	1
CG8051	CG8051 gene product from transcript CG8051-RA	2.359077766	0.998902207	1
nAcRbeta-21C	nicotinic acetylcholine receptor beta 21C	2.354353196	0.967552656	1
CG14879	CG14879 gene product from transcript CG14879-RB	2.315788523	0.996106651	1
CG14528	CG14528 gene product from transcript CG14528-RA	2.310823372	0.97485271	1
CG13321	CG13321 gene product from transcript CG13321-RA	2.301653916	0.991766852	1
CG4973	CG4973 gene product from transcript CG4973-RA	2.298757731	0.983590224	1
CG5916	CG5916 gene product from transcript CG5916-RA	2.296003347	0.974125787	1
CG4860	CG4860 gene product from transcript CG4860-RA	2.293283503	0.989258233	1
CG9150	CG9150 gene product from transcript CG9150-RB	2.284261551	0.96478018	1
Pole2	CG10489 gene product from transcript CG10489-RA	2.282020018	0.999915317	1
beat-Ib	beaten path Ib	2.254041347	0.990734091	1
CG10062	CG10062 gene product from transcript CG10062-RA	2.226650356	0.999980935	1
CG3655	CG3655 gene product from transcript CG3655-RB	2.219146675	0.996172336	1
CG33080	CG33080 gene product from transcript CG33080-RA	2.218210462	0.972481163	1
CG9184	CG9184 gene product from transcript CG9184-RB	2.211852245	0.9855355	1
CG7593	CG7593 gene product from transcript CG7593-RA	2.207504549	0.976633643	1
glob1	globin 1	2.152767777	0.998890311	1
Tsp42Ef	Tetraspanin 42Ef	2.150764652	0.996217938	1
CG15127	CG15127 gene product from transcript CG15127-RA	2.1495742	0.969218191	1
CG5011	CG5011 gene product from transcript CG5011-RA	2.143831783	0.999839005	1
CG6981	CG6981 gene product from transcript CG6981-RB	2.127780381	0.954770962	1
CG42565	CG42565 gene product from transcript CG42565-RA	2.126285801	0.962496855	1
ltd	lightoid	2.110292353	0.951020079	1
fry	furry	2.10371149	0.999667985	1
CG10641	CG10641 gene product from transcript CG10641-RA	2.095480268	0.968246174	1
ImpL3	Ecdysone-inducible gene L3	2.08268422	0.961238068	1
CG6610	CG6610 gene product from transcript CG6610-RA	2.081718575	0.992040126	1
GstE10	Glutathione S transferase E10	2.061679663	0.986998126	1
CG31004	CG31004 gene product from transcript CG31004-RC	2.040379528	0.958890997	1
CG7995	CG7995 gene product from transcript CG7995-RC	2.021792729	0.990670053	1
CG4836	CG4836 gene product from transcript CG4836-RC	2.019559194	0.999664714	1
Tsp2A	Tetraspanin 2A	2.017128238	0.995688106	1
Cad96Ca	CG10244 gene product from transcript CG10244-RA	2.016086508	0.998571481	1
Ndae1	Na[+]-driven anion exchanger 1	2.009170188	0.97379902	1
CG4781	CG4781 gene product from transcript CG4781-RA	2.00518428	0.994563754	1
edl	ETS-domain lacking	2.004622637	0.989762204	1
CG7713	CG7713 gene product from transcript CG7713-RA	-2.002919271	0.994323173	-1
Cirl	CG8639 gene product from transcript CG8639-RC	-2.003494644	0.966142035	-1
Eip63E	Ecdysone-induced protein 63E	-2.005982856	0.986708254	-1
CG12766	CG12766 gene product from transcript CG12766-RA	-2.011298093	0.983278127	-1
CG14253	CG14253 gene product from transcript CG14253-RB	-2.014815734	0.996162812	-1
cic	capicua	-2.026661111	0.999544863	-1
CG17186	CG17186 gene product from transcript CG17186-RA	-2.032635501	0.999983958	-1
mamo	maternal gene required for meiosis	-2.034024616	0.971331799	-1
Dh	Diuretic hormone	-2.046770747	0.988837362	-1
Cenp-C	CG31258 gene product from transcript CG31258-RA	-2.047021917	0.99856794	-1
CG10858	CG10858 gene product from transcript CG10858-RB	-2.054317817	0.97008726	-1
CG11342	CG11342 gene product from transcript CG11342-RA	-2.065810124	0.999116715	-1
CG9384	CG9384 gene product from transcript CG9384-RA	-2.066637617	0.958283235	-1
CG12868	CG12868 gene product from transcript CG12868-RB	-2.073455167	0.991181427	-1
CG17646	CG17646 gene product from transcript CG17646-RB	-2.074896723	0.985913718	-1
Mical	Molecule interacting with CasL	-2.084540353	0.999282657	-1
Grip	Glutamate receptor binding protein	-2.086936268	0.960360362	-1
CG2991	CG2991 gene product from transcript CG2991-RA	-2.088108836	0.998695698	-1
CG5267	CG5267 gene product from transcript CG5267-RA	-2.09073149	0.997531363	-1
Sema-1a	CG18405 gene product from transcript CG18405-RD	-2.096839749	0.999465906	-1
CG9005	CG9005 gene product from transcript CG9005-RB	-2.098387966	0.99523175	-1
CG1969	CG1969 gene product from transcript CG1969-RB	-2.099341623	0.993637625	-1

Annex 1. Differentially expressed genes in Apc vs WT 1 week ACI comparison

symbol	genename	APC vs WT 1week FC	APC vs WT 1week PDE	APC vs WT REJ
Cyp9b1	Cytochrome P450-9b1	-2.116913475	0.998309814	-1
CG1304	CG1304 gene product from transcript CG1304-RA	-2.118495806	0.987670282	-1
osp	outspread	-2.123876159	0.996277993	-1
MESK2	Misexpression suppressor of KSR 2	-2.128249661	0.999921966	-1
crb	crumbs	-2.144622292	0.974773663	-1
CG3308	CG3308 gene product from transcript CG3308-RA	-2.14736531	0.990446302	-1
Nrx-IV	Neurexin IV	-2.149194306	0.975065071	-1
CG31288	CG31288 gene product from transcript CG31288-RA	-2.152510165	0.983147019	-1
siz	schizo	-2.159930428	0.996107949	-1
sut4	sugar transporter 4	-2.163200811	0.994632262	-1
CG5316	CG5316 gene product from transcript CG5316-RC	-2.171169604	0.999987195	-1
CG3301	CG3301 gene product from transcript CG3301-RB	-2.208965414	0.986992749	-1
Argk	Arginine kinase	-2.212440671	0.962300786	-1
CG10663	CG10663 gene product from transcript CG10663-RB	-2.21248816	0.998471212	-1
Mad	Mothers against dpp	-2.216575401	0.992769959	-1
mamo	maternal gene required for meiosis	-2.225867109	0.970510565	-1
RhoGEF3	CG42378 gene product from transcript CG42378-RI	-2.231103391	0.978468208	-1
SP1173	CG10121 gene product from transcript CG10121-RC	-2.24221401	0.973394377	-1
Cyp9f2	CG11466 gene product from transcript CG11466-RB	-2.243676871	0.997711395	-1
CG17637	CG17637 gene product from transcript CG17637-RA	-2.245196646	0.998240164	-1
CG30015	CG30015 gene product from transcript CG30015-RA	-2.250580416	0.996727468	-1
CG6834	CG6834 gene product from transcript CG6834-RA	-2.252214256	0.980720313	-1
rib	ribbon	-2.255372153	0.988128631	-1
pkaap	CG4132 gene product from transcript CG4132-RA	-2.256550991	0.988918751	-1
CG34401	CG34401 gene product from transcript CG34401-RA	-2.257669695	0.998973114	-1
Cyp6a9	Cytochrome P450-6a9	-2.264878973	0.986855407	-1
CG4680	CG4680 gene product from transcript CG4680-RA	-2.271931824	0.975534441	-1
Gel	Gelsolin	-2.276423559	0.971305683	-1
Gr85a	Gustatory receptor 85a	-2.287294904	0.9999168	-1
Jon74E	Jonah 74E	-2.29010106	0.982435553	-1
CG6484	CG6484 gene product from transcript CG6484-RA	-2.296832159	0.969712982	-1
CG6108	CG6108 gene product from transcript CG6108-RA	-2.299992788	0.99426707	-1
CG14691	CG14691 gene product from transcript CG14691-RA	-2.330311721	0.999210847	-1
CG5646	CG5646 gene product from transcript CG5646-RA	-2.342765948	0.964679656	-1
sick	sickie	-2.346974887	0.997778289	-1
Atet	ABC transporter expressed in trachea	-2.352194678	0.989209137	-1
Cbl	CG7037 gene product from transcript CG7037-RB	-2.367433703	0.99263512	-1
unk	unkempt	-2.378670944	0.973715296	-1
Sema-5c	Semaphorin-5c	-2.379836709	0.991590611	-1
slif	slimfast	-2.39079425	0.999879185	-1
mod(mdg4)	modifier of mdg4	-2.400523622	0.999975643	-1
CG14740	CG14740 gene product from transcript CG14740-RA	-2.408955091	0.996854869	-1
CG8008	CG8008 gene product from transcript CG8008-RB	-2.424987406	0.998449666	-1
ect	ectodermal	-2.427886411	0.99249793	-1
CG14314	CG14314 gene product from transcript CG14314-RA	-2.431669421	0.99846746	-1
CG14408	CG14408 gene product from transcript CG14408-RA	-2.434423293	0.999941845	-1
CG15152	CG15152 gene product from transcript CG15152-RA	-2.440517346	0.979879218	-1
CG5455	CG5455 gene product from transcript CG5455-RA	-2.442807968	0.981366835	-1
mex1	midgut expression 1	-2.454712043	0.993950495	-1
CG1600	CG1600 gene product from transcript CG1600-RA	-2.475588556	0.998301259	-1
CG4325	CG4325 gene product from transcript CG4325-RA	-2.478391717	0.997829567	-1
CalpA	Calpain-A	-2.488156868	0.989828817	-1
CG32352	CG32352 gene product from transcript CG32352-RB	-2.538518324	0.990305218	-1
Apc	APC-like	-2.542890399	0.99858596	-1
btl	breathless	-2.549681253	0.994004467	-1
pyd	polychaetoid	-2.558020554	0.996172966	-1
sick	sickie	-2.58592423	0.998508924	-1
CG12991	CG12991 gene product from transcript CG12991-RA	-2.596744603	0.989728116	-1
CG2813	CG2813 gene product from transcript CG2813-RA	-2.600271098	0.973999804	-1
chrb	charybde	-2.612915615	0.974697983	-1
CG5254	CG5254 gene product from transcript CG5254-RA	-2.629025554	0.985841995	-1
CG9468	CG9468 gene product from transcript CG9468-RA	-2.658918201	0.975065502	-1

Annex 1. Differentially expressed genes in Apc vs WT 1 week ACI comparison

symbol	genename	APC vs WT 1week FC	APC vs WT 1week PDE	APC vs WT REJ
dnt	doughnut on 2	-2.687499186	0.997601348	-1
CG7997	CG7997 gene product from transcript CG7997-RB	-2.689923945	0.990047582	-1
CG32450	CG32450 gene product from transcript CG32450-RA	-2.735732589	0.997894242	-1
Ten-m	Tenascin major	-2.744209576	0.985577368	-1
CG7678	CG7678 gene product from transcript CG7678-RA	-2.777358315	0.996609229	-1
CG6527	CG6527 gene product from transcript CG6527-RA	-2.781655195	0.951561803	-1
Fps85D	Fps oncogene analog	-2.789347241	0.999536416	-1
CG10877	CG10877 gene product from transcript CG10877-RA	-2.795981101	0.984200978	-1
CG6006	CG6006 gene product from transcript CG6006-RC	-2.806095047	0.993846976	-1
CG32264	CG32264 gene product from transcript CG32264-RH	-2.834286714	0.999354338	-1
Npc2d	Niemann-Pick type C-2d	-2.858950804	0.985905522	-1
vkg	viking	-2.887172871	0.996226295	-1
clumsy	CG8681 gene product from transcript CG8681-RB	-2.911375218	0.992512556	-1
beat-IIIc	CG15138 gene product from transcript CG15138-RA	-2.940416582	0.989271349	-1
CG13492	CG13492 gene product from transcript CG13492-RC	-2.95182165	0.996878501	-1
capu	cappuccino	-2.976296575	0.99388992	-1
CG31763	CG31763 gene product from transcript CG31763-RA	-2.999811538	0.996493645	-1
CG3734	CG3734 gene product from transcript CG3734-RA	-3.018779467	0.999816464	-1
CG12194	CG12194 gene product from transcript CG12194-RA	-3.025303048	0.998436735	-1
CG3301	CG3301 gene product from transcript CG3301-RB	-3.030218375	0.999846214	-1
Cg25C	Collagen type IV	-3.048654137	0.999268104	-1
CG4377	CG4377 gene product from transcript CG4377-RA	-3.077370057	0.964053211	-1
Gr43b	CG1339 gene product from transcript CG1339-RA	-3.08023841	0.997894339	-1
CG12057	CG12057 gene product from transcript CG12057-RA	-3.080360516	0.969354095	-1
Gdh	Glutamate dehydrogenase	-3.083409932	0.992868968	-1
CG32355	CG32355 gene product from transcript CG32355-RA	-3.084422704	0.999802993	-1
nrv2	nervana 2	-3.115148209	0.99111053	-1
CG5568	CG5568 gene product from transcript CG5568-RA	-3.115696971	0.996955947	-1
luna	CG33473 gene product from transcript CG33473-RB	-3.136752871	0.999862654	-1
Pde6	Phosphodiesterase 6	-3.156392621	0.950923128	-1
CG11155	CG11155 gene product from transcript CG11155-RA	-3.159594164	0.99996054	-1
CG6129	CG6129 gene product from transcript CG6129-RD	-3.178856172	0.998092456	-1
lambdaTry	CG12350 gene product from transcript CG12350-RA	-3.18282947	0.970618085	-1
CG14626	CG14626 gene product from transcript CG14626-RA	-3.2609185	0.972726289	-1
CG14691	CG14691 gene product from transcript CG14691-RA	-3.34426339	0.994495212	-1
Bace	beta-site APP-cleaving enzyme	-3.387295172	0.971882482	-1
unc-104	CG8566 gene product from transcript CG8566-RB	-3.408550757	0.971977823	-1
Gr64a	Gustatory receptor 64a	-3.492182414	0.951912653	-1
CG8093	CG8093 gene product from transcript CG8093-RA	-3.619653533	0.984635967	-1
Jon99Fi	Jonah 99Fi	-3.641613517	0.966069661	-1
Mef2	Myocyte enhancer factor 2	-3.773308618	0.999351136	-1
CG11155	CG11155 gene product from transcript CG11155-RA	-3.905761808	0.990682375	-1
Jon65Aii	Jonah 65Aii	-3.926730779	0.993652197	-1
Gyc-89Da	Guanylyl cyclase at 89Da	-4.049872241	0.999443275	-1
luna	CG33473 gene product from transcript CG33473-RB	-4.050666391	0.998789923	-1
mira	miranda	-4.188129737	0.979384986	-1
CG5107	CG5107 gene product from transcript CG5107-RA	-4.231535521	0.967125304	-1
beat-IIa	beaten path IIa	-4.258892511	0.999994575	-1
Jon25Biii	Jonah 25Biii	-4.290038447	0.973614988	-1
CG17278	CG17278 gene product from transcript CG17278-RA	-4.310078249	0.988961801	-1
CG6490	CG6490 gene product from transcript CG6490-RB	-4.357239679	0.999922011	-1
CG4678	CG4678 gene product from transcript CG4678-RE	-4.369296473	0.992837272	-1
CG12026	CG12026 gene product from transcript CG12026-RB	-4.371122257	0.999988135	-1
Caps	Calcium activated protein for secretion	-4.609032942	0.984751608	-1
CG7966	CG7966 gene product from transcript CG7966-RA	-4.687325753	0.997462638	-1
pros	prospero	-4.707130807	0.961473443	-1
CG3301	CG3301 gene product from transcript CG3301-RB	-4.864031765	0.997401062	-1
CG12374	CG12374 gene product from transcript CG12374-RA	-4.990290326	0.995004261	-1
CG14741	CG14741 gene product from transcript CG14741-RB	-5.1265686	0.999447927	-1
CG6043	CG6043 gene product from transcript CG6043-RG	-5.204954183	0.999989627	-1
CG15629	CG15629 gene product from transcript CG15629-RA	-5.428469278	0.997106521	-1
CG11068	CG11068 gene product from transcript CG11068-RA	-5.525406248	0.998750967	-1

Annex 1. Differentially expressed genes in Apc vs WT 1 week ACI comparison

symbol	genename	APC vs WT 1week FC	APC vs WT 1week PDE	APC vs WT REJ
CG13315	CG13315 gene product from transcript CG13315-RA	-5.541897543	0.9928918	-1
stl	stall	-5.654134772	0.996877408	-1
CG4462	CG4462 gene product from transcript CG4462-RA	-5.660446162	0.999232701	-1
CG2082	CG2082 gene product from transcript CG2082-RC	-5.759282177	0.985194706	-1
CG2082	CG2082 gene product from transcript CG2082-RC	-6.101154584	0.990031795	-1
tomboy20	CG14690 gene product from transcript CG14690-RA	-6.380651689	0.999925059	-1
CG10960	CG10960 gene product from transcript CG10960-RC	-6.479417037	0.999901377	-1
Jon65Ai	Jonah 65Ai	-6.679338149	0.974788438	-1
LvpL	Larval visceral protein L	-6.81724637	0.953720399	-1
CG10472	CG10472 gene product from transcript CG10472-RA	-9.774311374	0.975886182	-1
CG17145	CG17145 gene product from transcript CG17145-RA	-13.47878445	0.990665448	-1
CG15186	CG15186 gene product from transcript CG15186-RA	-16.71690198	0.999996589	-1

Annex 1. Differentially expressed genes in Ras vs WT 1 week ACI comparison

symbol	genename	RAS vs WT 1week FC	RAS vs WT 1week PDE	RAS vs WT REJ
CG14743	CG14743 gene product from transcript CG14743-RA	12.67016307	0.991391502	1
GstD2	Glutathione S transferase D2	12.18903842	0.999911336	1
lab	labial	11.38153068	0.999285086	1
ImpL2	Ecdysone-inducible gene L2	7.513945068	0.999935474	1
ferrochelatase	CG2098 gene product from transcript CG2098-RC	6.215579111	0.992407145	1
CG3635	CG3635 gene product from transcript CG3635-RB	6.130206281	0.997248713	1
CG4726	CG4726 gene product from transcript CG4726-RA	5.996733071	0.999720079	1
CG14545	CG14545 gene product from transcript CG14545-RA	5.462133518	0.99809504	1
CG33494	CG33494 gene product from transcript CG33494-RA	5.189341417	0.996820903	1
CG6330	CG6330 gene product from transcript CG6330-RB	5.047337007	0.99781903	1
Pal	Peptidyl-alpha-hydroxyglycine-alpha-amidating lyase	4.589239341	0.992834403	1
CG10947	CG10947 gene product from transcript CG10947-RC	4.571488153	0.999356835	1
stg	string	4.520083275	0.991766167	1
CG3348	CG3348 gene product from transcript CG3348-RA	4.410010217	0.999975293	1
7B2	CG1168 gene product from transcript CG1168-RB	4.278363184	0.991292463	1
ImpL3	Ecdysone-inducible gene L3	4.260371925	0.998710723	1
CG34253	CG34253 gene product from transcript CG34253-RA	3.877606817	0.9953356	1
kirre	kin of irre	3.78450354	0.987222934	1
Mkp3	Mitogen-activated protein kinase phosphatase 3	3.739273459	0.999398584	1
CG5514	CG5514 gene product from transcript CG5514-RC	3.66644078	0.984233039	1
Tret1-1	Trehalose transporter 1-1	3.665752001	0.976866376	1
NtR	CG6698 gene product from transcript CG6698-RA	3.645689468	0.999922885	1
Ir94a	Ionotropic receptor 94a	3.49436531	0.997079834	1
CG13248	CG13248 gene product from transcript CG13248-RA	3.462280607	0.991255843	1
CG14869	CG14869 gene product from transcript CG14869-RB	3.426528286	0.99821725	1
chp	chaoptic	3.307583681	0.994563218	1
dimm	dimmed	3.269136194	0.964374601	1
CG42390	CG42390 gene product from transcript CG42390-RB	3.243842323	0.99907702	1
CG13117	CG13117 gene product from transcript CG13117-RA	3.237432162	0.997647196	1
Cyp6a2	Cytochrome P450-6a2	3.234634237	0.977404702	1
AdoR	Adenosine receptor	3.148472276	0.968959524	1
Tsp42Eg	Tetraspanin 42Eg	3.146355472	0.952335181	1
CG14297	CG14297 gene product from transcript CG14297-RA	3.136153763	0.997579396	1
GstD5	Glutathione S transferase D5	3.113346302	0.978093911	1
spz	spatzle	3.086617466	0.999580984	1
CG14294	CG14294 gene product from transcript CG14294-RA	3.084566957	0.970620064	1
fas	faint sausage	3.037636509	0.955706151	1
DNaseII	Deoxyribonuclease II	3.03535072	0.96394177	1
Mcm10	Sensitized chromosome inheritance modifier 19	2.956631707	0.99513217	1
MtnD	Metallothionein D	2.948543863	0.966918487	1
mud	mushroom body defect	2.937059946	0.983673773	1
l(2)01810	lethal (2) 01810	2.915313571	0.95871269	1
wus	wurst	2.906305193	0.996461663	1
exu	exuperantia	2.886835201	0.999964529	1
polo	CG12306 gene product from transcript CG12306-RA	2.8819565	0.9999792	1
CG14695	CG14695 gene product from transcript CG14695-RA	2.875606944	0.996280869	1
Mkp3	Mitogen-activated protein kinase phosphatase 3	2.862373946	0.999764354	1
CG8486	CG8486 gene product from transcript CG8486-RE	2.847537421	0.976686358	1
cmet	CENP-meta	2.847341632	0.99999999	1
brp	bruchpilot	2.838028084	0.988496549	1
shu	shutdown	2.836760034	0.998393339	1
Chd3	CG9594 gene product from transcript CG9594-RA	2.835329683	0.999806591	1
CG4771	CG4771 gene product from transcript CG4771-RA	2.828777594	0.996507563	1
Cyp6d2	CG4373 gene product from transcript CG4373-RA	2.807419641	0.96582879	1
Cks30A	Cyclin-dependent kinase subunit 30A	2.749761507	0.999332621	1
spn-E	spindle E	2.748409875	0.956051908	1
AcCoAS	Acetyl Coenzyme A synthase	2.748061216	0.991369192	1
CycB	Cyclin B	2.745520302	0.99980449	1
mad2	CG17498 gene product from transcript CG17498-RA	2.711011645	0.999988138	1
dgt3	dim gamma-tubulin 3	2.710666198	0.999203016	1
CG14006	CG14006 gene product from transcript CG14006-RA	2.709464571	0.986799373	1
CG13407	CG13407 gene product from transcript CG13407-RA	2.705583325	0.988179833	1

Annex 1. Differentially expressed genes in Ras vs WT 1 week ACI comparison

symbol	genename	RAS vs WT 1week FC	RAS vs WT 1week PDE	RAS vs WT REJ
HP4	Heterochromatin protein 4	2.680329092	0.991667942	1
bora	aurora borealis	2.66561407	0.999999812	1
CG2053	CG2053 gene product from transcript CG2053-RA	2.63298723	0.97755446	1
sti	sticky	2.626987075	0.999690203	1
Mmp2	Matrix metalloproteinase 2	2.624409826	0.998559501	1
CG31898	CG31898 gene product from transcript CG31898-RA	2.615034035	0.998088728	1
sip2	septin interacting protein 2	2.613547261	0.999967851	1
CG7224	CG7224 gene product from transcript CG7224-RB	2.609493203	0.9967458	1
fzy	fizzy	2.608801165	0.990450506	1
Pen	Pendulin	2.595191587	0.99904526	1
CG9576	CG9576 gene product from transcript CG9576-RA	2.578743923	0.972195773	1
Ret	Ret oncogene	2.57096953	0.99829985	1
sofe	sister of feo	2.556601068	0.999983586	1
Ote	Otefin	2.555692518	0.999207364	1
pav	pavarotti	2.545123189	0.99985637	1
cdc2	CG5363 gene product from transcript CG5363-RA	2.528807939	0.999364067	1
upd3	unpaired 3	2.512178318	0.990872631	1
Ir94c	Ionotropic receptor 94c	2.496876281	0.998878533	1
PH4alphaEFB	prolyl-4-hydroxylase-alpha EFB	2.496051401	0.991942801	1
CG3523	CG3523 gene product from transcript CG3523-RA	2.453114114	0.97099963	1
CG1358	CG1358 gene product from transcript CG1358-RD	2.432748262	0.996971448	1
Mcm2	Minichromosome maintenance 2	2.427094481	0.993557634	1
futsch	CG34387 gene product from transcript CG34387-RC	2.426701617	0.994952385	1
RPA2	Replication protein A2	2.417003526	0.999450846	1
Pfk	Phosphofructokinase	2.40559918	0.997418451	1
Tsp96F	Tetraspanin 96F	2.392291792	0.991464013	1
CG6114	CG6114 gene product from transcript CG6114-RA	2.386325862	0.964030158	1
CG9008	CG9008 gene product from transcript CG9008-RA	2.383468753	0.999973433	1
sna	snail	2.373104674	0.996813897	1
CG32758	CG32758 gene product from transcript CG32758-RA	2.372029471	0.998066642	1
CG5630	CG5630 gene product from transcript CG5630-RB	2.369069712	0.999299331	1
18w	18 wheeler	2.368802995	0.998745562	1
GstD9	Glutathione S transferase D9	2.358199416	0.999830824	1
CG11634	CG11634 gene product from transcript CG11634-RA	2.355959692	0.999893143	1
ncd	non-claret disjunctional	2.347375198	0.9992562	1
CG1942	CG1942 gene product from transcript CG1942-RA	2.345428111	0.997651592	1
CG14591	CG14591 gene product from transcript CG14591-RD	2.340740008	0.960210263	1
CG33145	CG33145 gene product from transcript CG33145-RA	2.32693163	0.999488039	1
Ac78C	Adenylyl cyclase 78C	2.325621186	0.986688662	1
GstE10	Glutathione S transferase E10	2.312195529	0.982723325	1
CG2909	CG2909 gene product from transcript CG2909-RA	2.299132264	0.997146691	1
CG30022	CG30022 gene product from transcript CG30022-RB	2.298342648	0.991135241	1
alph	alphabet	2.292203067	0.995704658	1
asp	abnormal spindle	2.290823363	0.998687168	1
tum	tumbleweed	2.281524434	0.99783427	1
Pole2	CG10489 gene product from transcript CG10489-RA	2.279171144	0.999966157	1
Gr39a	Gustatory receptor 39a	2.276966752	0.989244362	1
CG6465	CG6465 gene product from transcript CG6465-RA	2.27435249	0.962506752	1
jumu	jumeau	2.273421586	0.997856587	1
pim	pimples	2.272772337	0.996902126	1
feo	fascetto	2.260856826	0.993833368	1
CG30022	CG30022 gene product from transcript CG30022-RB	2.255354515	0.986631651	1
upd3	unpaired 3	2.251268922	0.979777232	1
InR	Insulin-like receptor	2.250102876	0.999933886	1
CG3036	CG3036 gene product from transcript CG3036-RA	2.243222126	0.996175462	1
CG13565	CG13565 gene product from transcript CG13565-RA	2.240768386	0.998076037	1
BthD	BthD selenoprotein	2.237652993	0.997310278	1
CG10420	CG10420 gene product from transcript CG10420-RA	2.232771083	0.984690128	1
cnn	centrosomin	2.226706317	0.99636711	1
Aplip1	APP-like protein interacting protein 1	2.22449602	0.999984019	1
WRNexo	WRN exonuclease	2.211336659	0.979927518	1
CG13599	CG13599 gene product from transcript CG13599-RA	2.209446778	0.999654347	1

Annex 1. Differentially expressed genes in Ras vs WT 1 week ACI comparison

symbol	genename	RAS vs WT 1week FC	RAS vs WT 1week PDE	RAS vs WT REJ
CG11318	CG11318 gene product from transcript CG11318-RA	2.207831603	0.995781344	1
spel1	spellchecker1	2.198294691	0.990791978	1
CG12112	CG12112 gene product from transcript CG12112-RA	2.187769526	0.999599528	1
sprt	sprite	2.186292186	0.99623992	1
Dgp-1	CG5729 gene product from transcript CG5729-RA	2.183515561	0.999912988	1
CG8247	CG8247 gene product from transcript CG8247-RB	2.178602067	0.988085553	1
Nnf1a	CG13434 gene product from transcript CG13434-RA	2.176340773	0.981981504	1
Klp67A	Kinesin-like protein at 67A	2.172134618	0.999906807	1
CG10722	CG10722 gene product from transcript CG10722-RA	2.168751782	0.994522768	1
CG2017	CG2017 gene product from transcript CG2017-RA	2.168750036	0.99769731	1
chn	charlatan	2.164885886	0.966019262	1
Klp61F	Kinesin-like protein at 61F	2.162287177	0.999949868	1
esc	extra sexcombs	2.159393962	0.997544569	1
pch2	CG31453 gene product from transcript CG31453-RA	2.159102806	0.999758107	1
CG7730	CG7730 gene product from transcript CG7730-RC	2.154255863	0.960776405	1
wun2	wunen-2	2.152796904	0.982197854	1
CG6854	CG6854 gene product from transcript CG6854-RC	2.144094945	0.99734757	1
CG31272	CG31272 gene product from transcript CG31272-RA	2.141219026	0.974955412	1
CG4822	CG4822 gene product from transcript CG4822-RB	2.139943698	0.965919812	1
CG9752	CG9752 gene product from transcript CG9752-RA	2.138655052	0.972619389	1
CG18213	CG18213 gene product from transcript CG18213-RA	2.134221104	0.998079357	1
CG14050	CG14050 gene product from transcript CG14050-RA	2.133294363	0.990767079	1
SP1173	CG10121 gene product from transcript CG10121-RC	2.121723119	0.952136718	1
CycA	Cyclin A	2.11135722	0.999995884	1
CG7593	CG7593 gene product from transcript CG7593-RA	2.101595329	0.973158493	1
msd5	mitotic spindle density 5	2.098490165	0.999728784	1
CG2680	CG2680 gene product from transcript CG2680-RB	2.08016343	0.999901065	1
bw	brown	2.075888427	0.9901452	1
CG33290	CG33290 gene product from transcript CG33290-RA	2.075244833	0.997608416	1
Ant2	Adenine nucleotide translocase 2	2.075186933	0.994507155	1
CG8173	CG8173 gene product from transcript CG8173-RA	2.072403013	0.995944507	1
CG16734	CG16734 gene product from transcript CG16734-RD	2.063057626	0.994298522	1
dpa	disc proliferation abnormal	2.062551358	0.978272952	1
scrib	scribbled	2.061304986	0.998755394	1
borr	borealin-related	2.05737685	0.999587497	1
CG4674	CG4674 gene product from transcript CG4674-RA	2.04707742	0.985294959	1
Ras85D	Ras oncogene at 85D	2.045796813	0.998541334	1
Mcm6	Minichromosome maintenance 6	2.043682301	0.997477699	1
Kaz1-ORFB	CG1220 gene product from transcript CG1220-RE	2.042365577	0.999859366	1
CG11120	CG11120 gene product from transcript CG11120-RA	2.036930805	0.969480212	1
Invadolysin	CG3953 gene product from transcript CG3953-RA	2.032057736	0.998714209	1
CG34007	CG34007 gene product from transcript CG34007-RA	2.031971241	0.9858083	1
CG17267	CG17267 gene product from transcript CG17267-RA	2.031834556	0.999562768	1
CG10641	CG10641 gene product from transcript CG10641-RA	2.03149574	0.973255419	1
CG33483	CG33483 gene product from transcript CG33483-RB	2.028238327	0.970069899	1
tyn	trynity	2.02750949	0.995310242	1
Ama	Amalgam	2.027143338	0.957440241	1
ial	IpIl-aurora-like kinase	2.023587117	0.999139593	1
gwl	greatwall	2.018879768	0.998397746	1
Tsp33B	Tetraspanin 33B	2.016854169	0.998698497	1
CG30020	CG30020 gene product from transcript CG30020-RA	2.010619822	0.99710808	1
CG34253	CG34253 gene product from transcript CG34253-RA	2.007357481	0.99507634	1
RnrL	Ribonucleoside diphosphate reductase large subunit	2.001413447	0.965578164	1
CG15729	CG15729 gene product from transcript CG15729-RA	-2.002510878	0.969624585	-1
CG34394	CG34394 gene product from transcript CG34394-RD	-2.009771524	0.998962169	-1
Rala	Ras-related protein	-2.01494703	0.999815428	-1
CG42554	CG42554 gene product from transcript CG42554-RA	-2.019231423	0.980598166	-1
CG34347	CG34347 gene product from transcript CG34347-RB	-2.021088393	0.987354139	-1
CG9003	CG9003 gene product from transcript CG9003-RD	-2.030630383	0.966336293	-1
CG10737	CG10737 gene product from transcript CG10737-RS	-2.034288461	0.985592644	-1
CG10283	CG10283 gene product from transcript CG10283-RB	-2.036320853	0.99982167	-1
CG10737	CG10737 gene product from transcript CG10737-RS	-2.040778141	0.974332093	-1

Annex 1. Differentially expressed genes in Ras vs WT 1 week ACI comparison

symbol	genename	RAS vs WT 1week FC	RAS vs WT 1week PDE	RAS vs WT REJ
spir	spire	-2.044321295	0.988685452	-1
kel	kelch	-2.04520475	0.994918623	-1
CG8066	CG8066 gene product from transcript CG8066-RA	-2.047988211	0.96537325	-1
CG2211	CG2211 gene product from transcript CG2211-RA	-2.052903454	0.966040919	-1
spir	spire	-2.054061981	0.979584246	-1
Eip75B	Ecdysone-induced protein 75B	-2.064380576	0.999207184	-1
Timp	Tissue inhibitor of metalloproteases	-2.071897728	0.999995372	-1
smi35A	smell impaired 35A	-2.087925699	0.972910726	-1
tamo	CG4057 gene product from transcript CG4057-RA	-2.089385062	0.996084529	-1
dnc	dunce	-2.093975874	0.996064291	-1
CG1718	CG1718 gene product from transcript CG1718-RA	-2.094966967	0.981518725	-1
alpha-Est8	alpha-Esterase-8	-2.097304669	0.980971106	-1
CG12200	CG12200 gene product from transcript CG12200-RA	-2.09798044	0.993313177	-1
CG1637	CG1637 gene product from transcript CG1637-RC	-2.1002483	0.997514128	-1
cry	cryptochrome	-2.101226882	0.997576176	-1
CG18067	CG18067 gene product from transcript CG18067-RA	-2.106116936	0.964947726	-1
CG3303	CG3303 gene product from transcript CG3303-RA	-2.106187984	0.998374601	-1
CG7970	CG7970 gene product from transcript CG7970-RA	-2.110450955	0.968981642	-1
CG15210	CG15210 gene product from transcript CG15210-RA	-2.111742718	0.988140886	-1
CAP	CG18408 gene product from transcript CG18408-RI	-2.111777004	0.975823035	-1
KCNQ	KCNQ potassium channel	-2.11682282	0.995844829	-1
CG42367	CG42367 gene product from transcript CG42367-RB	-2.118563647	0.964593612	-1
iotaTry	iotaTrypsin	-2.121500141	0.972520635	-1
ptr	proximal to raf	-2.130236876	0.990553975	-1
Dat	Dopamine N acetyltransferase	-2.132885425	0.999436546	-1
CG7083	CG7083 gene product from transcript CG7083-RA	-2.140509942	0.994949269	-1
CG34349	CG34349 gene product from transcript CG34349-RC	-2.142823216	0.999960392	-1
Spn4	Serine protease inhibitor 4	-2.146007246	0.999290757	-1
CG12214	CG12214 gene product from transcript CG12214-RB	-2.14619721	0.978015748	-1
Megalin	CG42611 gene product from transcript CG42611-RA	-2.146596437	0.999636907	-1
CG30463	CG30463 gene product from transcript CG30463-RB	-2.152234251	0.970813864	-1
CG6765	CG6765 gene product from transcript CG6765-RA	-2.15544334	0.968730247	-1
Cyp9b1	Cytochrome P450-9b1	-2.158298599	0.998723985	-1
CG17010	CG17010 gene product from transcript CG17010-RA	-2.159289647	0.969584508	-1
E23	Early gene at 23	-2.164207233	0.986725984	-1
CG6792	CG6792 gene product from transcript CG6792-RA	-2.170041864	0.998447532	-1
dnr1	defense repressor 1	-2.178834688	0.997852334	-1
CG4653	CG4653 gene product from transcript CG4653-RA	-2.181382998	0.990399908	-1
Cyp6a13	CG2397 gene product from transcript CG2397-RA	-2.183899342	0.974698528	-1
CG5455	CG5455 gene product from transcript CG5455-RA	-2.191079446	0.96386704	-1
olf186-M	CG14489 gene product from transcript CG14489-RA	-2.191357171	0.995153364	-1
CG11155	CG11155 gene product from transcript CG11155-RA	-2.194831571	0.999674477	-1
CG31454	CG31454 gene product from transcript CG31454-RA	-2.200438922	0.996402196	-1
CG34401	CG34401 gene product from transcript CG34401-RA	-2.20518758	0.999995851	-1
osp	outspread	-2.20900334	0.995090086	-1
sinu	sinuous	-2.215904749	0.972731072	-1
Best1	Bestrophin 1	-2.223933125	0.998494839	-1
sick	sickie	-2.224691139	0.995473259	-1
Hnf4	Hepatocyte nuclear factor 4	-2.226182733	0.982185048	-1
Spn4	Serine protease inhibitor 4	-2.249120523	0.995550454	-1
CG3301	CG3301 gene product from transcript CG3301-RB	-2.25112881	0.993917104	-1
CG18745	CG18745 gene product from transcript CG18745-RA	-2.25407055	0.997244988	-1
Sclp	CG2471 gene product from transcript CG2471-RA	-2.26417216	0.959310519	-1
Cyp6a19	CG10243 gene product from transcript CG10243-RA	-2.280427032	0.984616502	-1
CG13321	CG13321 gene product from transcript CG13321-RA	-2.294538114	0.974747469	-1
CG6484	CG6484 gene product from transcript CG6484-RA	-2.298679592	0.969979749	-1
CG1637	CG1637 gene product from transcript CG1637-RC	-2.302713792	0.997649556	-1
CG32352	CG32352 gene product from transcript CG32352-RB	-2.305238912	0.973622804	-1
CG1427	CG1427 gene product from transcript CG1427-RC	-2.305531234	0.984558652	-1
smp-30	Senescence marker protein-30	-2.305677896	0.958930263	-1
clumsy	CG8681 gene product from transcript CG8681-RB	-2.32481981	0.977040824	-1
CG6967	CG6967 gene product from transcript CG6967-RD	-2.332640862	0.996198359	-1

Annex 1. Differentially expressed genes in Ras vs WT 1 week ACI comparison

symbol	genename	RAS vs WT 1week FC	RAS vs WT 1week PDE	RAS vs WT REJ
btsz	bitesize	-2.34320144	0.993874921	-1
CG1637	CG1637 gene product from transcript CG1637-RC	-2.356821642	0.999853878	-1
Tsp29Fb	Tetraspanin 29Fb	-2.363066832	0.993932866	-1
CG1304	CG1304 gene product from transcript CG1304-RA	-2.364488309	0.992325321	-1
CG32521	CG32521 gene product from transcript CG32521-RA	-2.366174705	0.961229118	-1
CG3902	CG3902 gene product from transcript CG3902-RA	-2.370957452	0.992719055	-1
Ahcy89E	Adenosylhomocysteinase 89E	-2.38882246	0.989040742	-1
CG31875	CG31875 gene product from transcript CG31875-RC	-2.393537088	0.98765069	-1
ect	ectodermal	-2.399059222	0.999249734	-1
CG32219	CG32219 gene product from transcript CG32219-RA	-2.400925774	0.991832191	-1
CG10249	CG10249 gene product from transcript CG10249-RJ	-2.400935887	0.989471021	-1
Megalin	CG42611 gene product from transcript CG42611-RA	-2.41360382	0.99281543	-1
Cyp6a17	CG10241 gene product from transcript CG10241-RA	-2.41521451	0.999921682	-1
CAH2	Carbonic anhydrase 2	-2.425538078	0.961424274	-1
CG8952	CG8952 gene product from transcript CG8952-RA	-2.430461241	0.965270784	-1
CG8788	CG8788 gene product from transcript CG8788-RA	-2.454110195	0.974449437	-1
CG14120	CG14120 gene product from transcript CG14120-RA	-2.468606269	0.999289577	-1
CG6357	CG6357 gene product from transcript CG6357-RA	-2.476278501	0.988509837	-1
CG6108	CG6108 gene product from transcript CG6108-RA	-2.491931893	0.984443207	-1
stl	stall	-2.492967382	0.976514555	-1
CG11426	CG11426 gene product from transcript CG11426-RA	-2.501678191	0.991890231	-1
Ugt86Dh	CG4772 gene product from transcript CG4772-RA	-2.505098844	0.998511257	-1
CG4752	CG4752 gene product from transcript CG4752-RA	-2.505236154	0.980498927	-1
CG30154	CG30154 gene product from transcript CG30154-RA	-2.507076544	0.997796154	-1
CG3277	CG3277 gene product from transcript CG3277-RC	-2.512235975	0.975879579	-1
CG1146	CG1146 gene product from transcript CG1146-RB	-2.532794275	0.991612342	-1
fus	fusilli	-2.540474073	0.999877227	-1
CG15673	CG15673 gene product from transcript CG15673-RB	-2.555011624	0.959750346	-1
Tsp42Eq	Tetraspanin 42Eq	-2.565693559	0.997161438	-1
CG34269	CG34269 gene product from transcript CG34269-RA	-2.567948584	0.998341496	-1
spheroide	CG9675 gene product from transcript CG9675-RA	-2.571989959	0.960933888	-1
CG18748	CG18748 gene product from transcript CG18748-RB	-2.579516845	0.998366674	-1
stv	starvin	-2.584616626	0.997943144	-1
kar	karmoisin	-2.588127482	0.998982162	-1
aay	astray	-2.60254529	0.999630551	-1
Npc2d	Niemann-Pick type C-2d	-2.622909653	0.974981767	-1
Damm	Death associated molecule related to Mch2	-2.628452605	0.982582501	-1
CG12374	CG12374 gene product from transcript CG12374-RA	-2.631060081	0.956558101	-1
TotB	Turandot B	-2.643140854	0.987337825	-1
CG14740	CG14740 gene product from transcript CG14740-RA	-2.657121739	0.980614121	-1
alpha-Est5	alpha-Esterase-5	-2.662473568	0.979969724	-1
CG14741	CG14741 gene product from transcript CG14741-RB	-2.680910896	0.992510967	-1
Cyp6d5	CG3050 gene product from transcript CG3050-RA	-2.681186295	0.991769661	-1
CG3726	CG3726 gene product from transcript CG3726-RA	-2.683114153	0.998563284	-1
Pkg21D	cGMP-dependent protein kinase 21D	-2.685015346	0.961049128	-1
CG6834	CG6834 gene product from transcript CG6834-RA	-2.705161726	0.992419932	-1
CG14629	CG14629 gene product from transcript CG14629-RA	-2.706037531	0.967677884	-1
CG30460	CG30460 gene product from transcript CG30460-RE	-2.709811976	0.996454629	-1
CG9555	CG9555 gene product from transcript CG9555-RB	-2.71167897	0.993004227	-1
MESR3	Misexpression suppressor of ras 3	-2.712096785	0.993220824	-1
CG31076	CG31076 gene product from transcript CG31076-RA	-2.719657849	0.996265312	-1
hig	hikaru genki	-2.725433152	0.99986964	-1
Jheh1	Juvenile hormone epoxide hydrolase 1	-2.737738485	0.999531796	-1
CG18747	CG18747 gene product from transcript CG18747-RB	-2.743295038	0.964189675	-1
CG1681	CG1681 gene product from transcript CG1681-RA	-2.746477576	0.991510259	-1
beat-IIIc	CG15138 gene product from transcript CG15138-RA	-2.755986018	0.977759035	-1
Dscam	Down syndrome cell adhesion molecule	-2.763740463	0.99280269	-1
CG7678	CG7678 gene product from transcript CG7678-RA	-2.765872841	0.997084226	-1
CG13829	CG13829 gene product from transcript CG13829-RA	-2.767069571	0.986504731	-1
CG9084	CG9084 gene product from transcript CG9084-RB	-2.770235639	0.993882267	-1
CG15629	CG15629 gene product from transcript CG15629-RA	-2.78857777	0.964184285	-1
rgn	regeneration	-2.798143626	0.991723267	-1

Annex 1. Differentially expressed genes in Ras vs WT 1 week ACI comparison

symbol	genename	RAS vs WT 1week FC	RAS vs WT 1week PDE	RAS vs WT REJ
fok	fledgling of Klp38B	-2.799615414	0.998781099	-1
Megalin	CG42611 gene product from transcript CG42611-RA	-2.800655645	0.992685246	-1
CG34401	CG34401 gene product from transcript CG34401-RA	-2.807054352	0.999670922	-1
CG16749	CG16749 gene product from transcript CG16749-RA	-2.81973037	0.950729655	-1
Menl-2	CG7969 gene product from transcript CG7969-RE	-2.821795896	0.956321274	-1
CG7992	CG7992 gene product from transcript CG7992-RA	-2.826855684	0.999796973	-1
capu	cappuccino	-2.837311192	0.993833025	-1
sick	sickie	-2.84180231	0.999641466	-1
Jheh3	Juvenile hormone epoxide hydrolase 3	-2.851732486	0.95280126	-1
CG4893	CG4893 gene product from transcript CG4893-RA	-2.853602995	0.999584905	-1
Doa	Darkener of apricot	-2.890503846	0.999993237	-1
bru-2	bruno-2	-2.902910239	0.995483538	-1
CG12992	CG12992 gene product from transcript CG12992-RB	-2.903276048	0.995476077	-1
CG7470	CG7470 gene product from transcript CG7470-RA	-2.903282832	0.99992295	-1
Jon65Aii	Jonah 65Aii	-2.907344114	0.982562594	-1
Ac76E	Adenylyl cyclase 76E	-2.91553116	0.999984834	-1
CG15309	CG15309 gene product from transcript CG15309-RA	-2.924589113	0.991897809	-1
Cg25C	Collagen type IV	-2.976775222	0.999034628	-1
CG8693	CG8693 gene product from transcript CG8693-RA	-2.977934857	0.954147254	-1
Ddr	Discoidin domain receptor	-2.977945724	0.957608495	-1
CG32687	CG32687 gene product from transcript CG32687-RA	-3.01550788	0.996821176	-1
CG8834	CG8834 gene product from transcript CG8834-RB	-3.021447329	0.977445162	-1
Ugt35a	UDP-glycosyltransferase 35a	-3.05171831	0.999763665	-1
CG15422	CG15422 gene product from transcript CG15422-RA	-3.063819077	0.980782489	-1
Gr43b	CG1339 gene product from transcript CG1339-RA	-3.127678127	0.998038323	-1
CG12991	CG12991 gene product from transcript CG12991-RA	-3.141840128	0.991567186	-1
Cyp9f2	CG11466 gene product from transcript CG11466-RB	-3.17180638	0.999693598	-1
Chit	Chitinase-like	-3.211984381	0.998645584	-1
MtnA	Metallothionein A	-3.230878533	0.999849322	-1
Grip	Glutamate receptor binding protein	-3.272991767	0.995435615	-1
CG14968	CG14968 gene product from transcript CG14968-RB	-3.281251283	0.999774938	-1
CG11241	CG11241 gene product from transcript CG11241-RB	-3.317863613	0.999890447	-1
CG2556	CG2556 gene product from transcript CG2556-RA	-3.324173668	0.999994529	-1
CG15674	CG15674 gene product from transcript CG15674-RA	-3.34183883	0.999997739	-1
CG2930	CG2930 gene product from transcript CG2930-RD	-3.347871336	0.994268056	-1
CG34406	CG34406 gene product from transcript CG34406-RA	-3.378110688	0.999887875	-1
CG10650	CG10650 gene product from transcript CG10650-RA	-3.399899458	0.999895756	-1
CG34198	CG34198 gene product from transcript CG34198-RA	-3.406363397	0.998208386	-1
CG15152	CG15152 gene product from transcript CG15152-RA	-3.491277003	0.999506202	-1
CG16996	CG16996 gene product from transcript CG16996-RA	-3.524876514	0.98923785	-1
Tsp42Er	Tetraspanin 42Er	-3.556054044	0.999845992	-1
Ect4	CG34373 gene product from transcript CG34373-RD	-3.562220466	0.996548418	-1
Argk	Arginine kinase	-3.578432755	0.988689103	-1
CG9380	CG9380 gene product from transcript CG9380-RC	-3.596750187	0.997451366	-1
Mad	Mothers against dpp	-3.596752286	0.999809426	-1
CG7997	CG7997 gene product from transcript CG7997-RB	-3.602030056	0.997535771	-1
CG4462	CG4462 gene product from transcript CG4462-RA	-3.631649098	0.988640648	-1
CG5011	CG5011 gene product from transcript CG5011-RA	-3.675708589	0.999994819	-1
CG10858	CG10858 gene product from transcript CG10858-RB	-3.736437023	0.998478901	-1
CG12560	CG12560 gene product from transcript CG12560-RB	-3.761832151	0.999704781	-1
Cyp6a9	Cytochrome P450-6a9	-3.778561733	0.999445551	-1
CG32264	CG32264 gene product from transcript CG32264-RH	-3.780565946	0.999870244	-1
CG8093	CG8093 gene product from transcript CG8093-RA	-3.95806684	0.965292211	-1
Cyp6w1	CG8345 gene product from transcript CG8345-RA	-3.968085003	0.958619396	-1
CG9568	CG9568 gene product from transcript CG9568-RA	-3.975574894	0.99949621	-1
CG4678	CG4678 gene product from transcript CG4678-RE	-4.00889423	0.997276969	-1
CG5804	CG5804 gene product from transcript CG5804-RA	-4.055813805	0.990086998	-1
CG10157	CG10157 gene product from transcript CG10157-RA	-4.058706705	0.990495856	-1
CG10911	CG10911 gene product from transcript CG10911-RA	-4.088539372	0.971939248	-1
CG30049	CG30049 gene product from transcript CG30049-RA	-4.273546691	0.96747525	-1
CG7966	CG7966 gene product from transcript CG7966-RA	-4.279121826	0.999726461	-1
etaTry	etaTrypsin	-4.281615185	0.996739701	-1

Annex 1. Differentially expressed genes in Ras vs WT 1 week ACI comparison

symbol	genename	RAS vs WT 1week FC	RAS vs WT 1week PDE	RAS vs WT REJ
Ugt86Dj	CG15902 gene product from transcript CG15902-RA	-4.297498216	0.998637973	-1
mex1	midgut expression 1	-4.316747976	0.993952552	-1
Npc2e	Niemann-Pick type C-2e	-4.325288506	0.998344073	-1
CG16997	CG16997 gene product from transcript CG16997-RB	-4.399440441	0.997965186	-1
CG31763	CG31763 gene product from transcript CG31763-RA	-4.436532746	0.999461948	-1
CG12464	CG12464 gene product from transcript CG12464-RA	-4.44359907	0.954407918	-1
CG13284	CG13284 gene product from transcript CG13284-RA	-4.641926736	0.950149678	-1
CG13492	CG13492 gene product from transcript CG13492-RC	-4.65456299	0.99941737	-1
CG9673	CG9673 gene product from transcript CG9673-RA	-4.676177533	0.999990984	-1
Irc	Immune-regulated catalase	-4.776309077	0.966451632	-1
CG12910	CG12910 gene product from transcript CG12910-RA	-4.928709826	0.999811163	-1
CG3301	CG3301 gene product from transcript CG3301-RB	-5.136587411	0.999991117	-1
CG10877	CG10877 gene product from transcript CG10877-RA	-5.139782388	0.997908991	-1
CG6043	CG6043 gene product from transcript CG6043-RG	-5.503070457	0.999990157	-1
CG34176	CG34176 gene product from transcript CG34176-RA	-5.589503946	0.999995891	-1
CG9380	CG9380 gene product from transcript CG9380-RC	-5.857756904	0.999140156	-1
Cyp4e2	Cytochrome P450-4e2	-5.907128779	0.997699136	-1
CG15255	CG15255 gene product from transcript CG15255-RA	-6.152980662	0.996612883	-1
CG31198	CG31198 gene product from transcript CG31198-RA	-6.241845111	0.990419827	-1
lambdaTry	CG12350 gene product from transcript CG12350-RA	-6.408689421	0.991628209	-1
CG4377	CG4377 gene product from transcript CG4377-RA	-6.649614943	0.985041274	-1
CG2082	CG2082 gene product from transcript CG2082-RC	-6.764840224	0.983038059	-1
CG10472	CG10472 gene product from transcript CG10472-RA	-6.816567429	0.965256735	-1
CG32407	CG32407 gene product from transcript CG32407-RA	-8.463528649	0.996625781	-1
CG3301	CG3301 gene product from transcript CG3301-RB	-9.042672084	0.999574521	-1
CG5246	CG5246 gene product from transcript CG5246-RA	-9.244498858	0.999934216	-1
be	ben	-10.94437963	0.998959864	-1
CG2082	CG2082 gene product from transcript CG2082-RC	-12.71581939	0.993164567	-1
LvpL	Larval visceral protein L	-13.61758228	0.997459845	-1
CG4363	CG4363 gene product from transcript CG4363-RA	-13.87242863	0.986669558	-1

Annex 1. Differentially expressed genes in Apc Ras vs WT 1 week ACI comparison

symbol	genename	APC RAS vs WT 1week FC	APC RAS vs WT 1week PDE	APC RAS vs WT REJ
svp	seven up	19.06645304	0.998274351	1
tw	Protein O-mannosyltransferase 2	18.18928401	0.999579029	1
fz3	frizzled 3	15.00427013	0.999917429	1
svp	seven up	11.12175479	0.965490108	1
LysX	Lysozyme X	10.76853614	0.999473174	1
l(2)01810	lethal (2) 01810	9.829470564	0.99839975	1
CG30359	CG30359 gene product from transcript CG30359-RA	9.814621258	0.979383154	1
Lim3	CG10699 gene product from transcript CG10699-RB	9.793604962	0.999712301	1
CG7900	CG7900 gene product from transcript CG7900-RB	9.098810132	0.999556046	1
CG14526	CG14526 gene product from transcript CG14526-RB	8.837821	0.99224239	1
sn	singed	8.612470594	0.999698801	1
drm	drumstick	8.550712363	0.994716321	1
CG3348	CG3348 gene product from transcript CG3348-RA	8.074320504	0.99999999	1
GstD2	Glutathione S transferase D2	8.010877361	0.999999773	1
kirre	kin of irre	7.933765753	0.999148689	1
tau	CG31057 gene product from transcript CG31057-RA	7.476293273	0.999987888	1
Tsp	Thrombospondin	7.392953233	0.999999255	1
hh	hedgehog	7.261660483	0.999857351	1
CG5630	CG5630 gene product from transcript CG5630-RB	7.199284824	0.999999744	1
os	outstretched	7.09544671	0.999866503	1
CG10140	CG10140 gene product from transcript CG10140-RA	6.957993051	1	1
blot	bloated tubules	6.911772046	0.966216741	1
ImpL2	Ecdysone-inducible gene L2	6.673466435	0.999944623	1
CG17119	CG17119 gene product from transcript CG17119-RA	6.607731764	0.999918077	1
mp	multiplexin	6.501395166	0.995815595	1
CG13117	CG13117 gene product from transcript CG13117-RA	6.433091869	1	1
CG4726	CG4726 gene product from transcript CG4726-RA	6.367737	0.999891116	1
stg	string	6.340772953	0.999841538	1
CG14545	CG14545 gene product from transcript CG14545-RA	6.309860002	0.998951007	1
slbo	slow border cells	6.24673069	0.997003657	1
mirr	mirror	5.82772484	0.999551761	1
CG13654	CG13654 gene product from transcript CG13654-RA	5.784203535	0.953467525	1
Mkp3	Mitogen-activated protein kinase phosphatase 3	5.245907111	0.99982941	1
Hk	Hyperkinetic	5.241850717	0.961575232	1
CG11192	CG11192 gene product from transcript CG11192-RB	5.199843835	0.991686524	1
DNaseII	Deoxyribonuclease II	5.181418548	0.994911329	1
Ama	Amalgam	4.867243472	0.999928519	1
CG15829	CG15829 gene product from transcript CG15829-RA	4.859232861	0.998224908	1
CG6330	CG6330 gene product from transcript CG6330-RB	4.850249158	0.999146574	1
CG7056	CG7056 gene product from transcript CG7056-RA	4.756159642	0.999947178	1
CG3635	CG3635 gene product from transcript CG3635-RB	4.722666978	0.9957814	1
CG17930	CG17930 gene product from transcript CG17930-RA	4.697973533	0.999975335	1
plx	pollux	4.606497368	0.999766247	1
mirr	mirror	4.480024078	0.95005939	1
CG12702	CG12702 gene product from transcript CG12702-RA	4.380168289	0.998025092	1
CG34319	CG34319 gene product from transcript CG34319-RA	4.372555591	0.979097911	1
exu	exuperantia	4.362966047	0.999999962	1
CG10725	CG10725 gene product from transcript CG10725-RB	4.2737516	0.975510348	1
CG5621	CG5621 gene product from transcript CG5621-RA	4.265499473	0.99698983	1
kek1	kekkon-1	4.215478997	0.98107046	1
CG10641	CG10641 gene product from transcript CG10641-RA	4.183657533	0.999892184	1
rtet	tetracycline resistance	4.090438427	0.994563981	1
mp	multiplexin	3.985124632	0.999795595	1
sob	sister of odd and bowl	3.927942945	0.992767541	1
Pvf2	PDGF- and VEGF-related factor 2	3.857345224	0.977087394	1
GstD5	Glutathione S transferase D5	3.83222039	0.992391257	1
msd1	mitotic spindle density 1	3.83081083	1	1
CG16995	CG16995 gene product from transcript CG16995-RA	3.755180926	0.999068846	1
CG18594	CG18594 gene product from transcript CG18594-RA	3.742063234	0.998158168	1
CG12483	CG12483 gene product from transcript CG12483-RA	3.739267624	0.999710542	1
dimm	dimmed	3.706700047	0.975892019	1
ImpL3	Ecdysone-inducible gene L3	3.651276332	0.996743717	1

Annex 1. Differentially expressed genes in Apc Ras vs WT 1 week ACI comparison

symbol	genename	APC RAS vs WT 1week FC	APC RAS vs WT 1week PDE	APC RAS vs WT REJ
bnl	branchless	3.646069437	0.999989488	1
CG17124	CG17124 gene product from transcript CG17124-RB	3.63578331	0.999903875	1
CG13248	CG13248 gene product from transcript CG13248-RA	3.565864763	0.990125632	1
Gr94a	Gustatory receptor 94a	3.552231599	0.999982071	1
rho	rhomboid	3.543405024	0.99361805	1
Ir	Inwardly rectifying potassium channel	3.539498744	0.979565371	1
Ugt86Di	CG6658 gene product from transcript CG6658-RA	3.504399966	0.999832543	1
upd3	unpaired 3	3.488887903	0.998193213	1
Naam	Nicotinamide amidase	3.460544653	0.999998012	1
Mmp2	Matrix metalloproteinase 2	3.394291755	0.999966183	1
fred	friend of echinoid	3.385407448	0.963973029	1
Rh2	Rhodopsin 2	3.376268087	0.978578018	1
CG42390	CG42390 gene product from transcript CG42390-RB	3.342007872	0.999868973	1
CG34372	CG34372 gene product from transcript CG34372-RC	3.341962608	0.980558655	1
dmrt93B	doublesex-Mab related 93B	3.312553213	0.999999777	1
CG11686	CG11686 gene product from transcript CG11686-RA	3.30881611	0.999996242	1
CG30502	CG30502 gene product from transcript CG30502-RB	3.270830514	0.967228352	1
Tret1-1	Trehalose transporter 1-1	3.243704003	0.955565294	1
CG15828	CG15828 gene product from transcript CG15828-RC	3.242386492	0.986730396	1
Mkp3	Mitogen-activated protein kinase phosphatase 3	3.23582462	0.999900078	1
rst	roughest	3.233328966	0.994909709	1
CG5630	CG5630 gene product from transcript CG5630-RB	3.202573799	0.999964033	1
fax	failed axon connections	3.188996933	0.999990391	1
sna	snail	3.179396467	0.999781287	1
CG34372	CG34372 gene product from transcript CG34372-RC	3.116163138	0.985908996	1
otk	off-track	3.073974455	0.964911784	1
Dgp-1	CG5729 gene product from transcript CG5729-RA	3.050502608	0.999999819	1
Ilp6	Insulin-like peptide 6	3.037988623	0.999763769	1
ferrochelatase	CG2098 gene product from transcript CG2098-RC	2.998682927	0.954355238	1
Cpr66D	Cuticular protein 66D	2.987363096	0.970965369	1
CG17744	CG17744 gene product from transcript CG17744-RA	2.957372395	0.998036311	1
CHKov1	CG10618 gene product from transcript CG10618-RB	2.941583189	0.999987641	1
CG7922	CG7922 gene product from transcript CG7922-RA	2.90429135	0.999999347	1
CG15818	CG15818 gene product from transcript CG15818-RA	2.883597728	0.99992931	1
upd3	unpaired 3	2.879960996	0.99737826	1
CG33275	CG33275 gene product from transcript CG33275-RA	2.879445639	0.999999925	1
sog	short gastrulation	2.864924286	0.999008186	1
spel1	spellchecker1	2.856575447	0.999244775	1
CG10154	CG10154 gene product from transcript CG10154-RA	2.848509962	0.977376852	1
CG3074	CG3074 gene product from transcript CG3074-RB	2.8469727	0.999999114	1
CG13405	CG13405 gene product from transcript CG13405-RA	2.843839628	0.95506952	1
l(2)k16918	lethal (2) k16918	2.839293311	0.999422043	1
CG13631	CG13631 gene product from transcript CG13631-RA	2.8386157	0.997105335	1
Rbp9	RNA-binding protein 9	2.817991672	0.995287657	1
CG4860	CG4860 gene product from transcript CG4860-RA	2.793658752	0.997475855	1
CG14294	CG14294 gene product from transcript CG14294-RA	2.791162484	0.989129287	1
Wnt5	Wnt oncogene analog 5	2.781043168	0.999754001	1
CG10947	CG10947 gene product from transcript CG10947-RC	2.763154621	0.999440095	1
CG5390	CG5390 gene product from transcript CG5390-RA	2.759108961	0.999978167	1
scf	supercoiling factor	2.752054209	0.992617468	1
spri	sprint	2.737624251	0.999980781	1
CG10924	CG10924 gene product from transcript CG10924-RA	2.734070075	0.983975819	1
CG7224	CG7224 gene product from transcript CG7224-RB	2.732704064	0.99988299	1
CG42825	CG42825 gene product from transcript CG42825-RA	2.732374873	0.999995223	1
Ant2	Adenine nucleotide translocase 2	2.724278065	0.999999669	1
CG9009	CG9009 gene product from transcript CG9009-RB	2.70534458	0.999999977	1
CG17929	CG17929 gene product from transcript CG17929-RB	2.704713143	0.991055074	1
CG6610	CG6610 gene product from transcript CG6610-RA	2.702681511	0.999966707	1
WASp	CG1520 gene product from transcript CG1520-RA	2.699274891	0.993914177	1
slow	slowdown	2.697280769	0.997756868	1
CG3397	CG3397 gene product from transcript CG3397-RA	2.687287448	0.996646258	1
CG5958	CG5958 gene product from transcript CG5958-RA	2.682086964	0.999146498	1

Annex 1. Differentially expressed genes in Apc Ras vs WT 1 week ACI comparison

symbol	genename	APC RAS vs WT 1week FC	APC RAS vs WT 1week PDE	APC RAS vs WT REJ
p53	CG33336 gene product from transcript CG33336-RB	2.673639768	0.999528181	1
CG31344	CG31344 gene product from transcript CG31344-RA	2.656920871	0.989629215	1
Tg	Transglutaminase	2.644502819	0.972784565	1
polo	CG12306 gene product from transcript CG12306-RA	2.622321497	0.999999339	1
CG30022	CG30022 gene product from transcript CG30022-RB	2.619558901	0.993001937	1
wus	wurst	2.618453286	0.999949827	1
CG7593	CG7593 gene product from transcript CG7593-RA	2.610557595	0.996955728	1
lab	labial	2.609381973	0.992520303	1
Ir94a	Ionotropic receptor 94a	2.603069251	0.999668366	1
CG17304	CG17304 gene product from transcript CG17304-RA	2.598818566	0.981007777	1
piwi	CG6122 gene product from transcript CG6122-RA	2.583241331	0.998284796	1
argos	CG4531 gene product from transcript CG4531-RA	2.581679289	0.999950079	1
sty	sprouty	2.581116299	0.999905057	1
CG34259	CG34259 gene product from transcript CG34259-RB	2.570899109	0.988907636	1
cnn	centrosomin	2.56936913	0.998790296	1
krimp	krimper	2.566298542	0.997861775	1
Pfk	Phosphofructokinase	2.559993154	0.998531719	1
CG42389	CG42389 gene product from transcript CG42389-RE	2.546753425	0.999996193	1
CG3036	CG3036 gene product from transcript CG3036-RA	2.534410046	0.998582846	1
Tsp96F	Tetraspanin 96F	2.53050689	0.998143895	1
rgn	regeneration	2.525461015	0.984720123	1
NtR	CG6698 gene product from transcript CG6698-RA	2.50263254	0.999918765	1
CG14297	CG14297 gene product from transcript CG14297-RA	2.49231601	0.997570624	1
cerv	cervantes	2.486307629	0.972344637	1
CG32652	CG32652 gene product from transcript CG32652-RA	2.482695195	0.99251585	1
CG15745	CG15745 gene product from transcript CG15745-RB	2.472677882	0.999996278	1
alpha-Est3	alpha-Esterase-3	2.463059931	0.987921014	1
CG5399	CG5399 gene product from transcript CG5399-RA	2.459397824	0.998730367	1
CG7194	CG7194 gene product from transcript CG7194-RA	2.445135484	0.999870242	1
Cad96Ca	CG10244 gene product from transcript CG10244-RA	2.43795343	0.999993177	1
Ppn	Papilin	2.412309036	0.999958587	1
lds	lodestar	2.405166306	0.986503701	1
cmet	CENP-meta	2.399092734	1	1
jumu	jumeau	2.395581577	0.998622638	1
CG10527	CG10527 gene product from transcript CG10527-RA	2.390018901	0.996759894	1
GstS1	Glutathione S transferase S1	2.379431332	0.980641982	1
pav	pavarotti	2.379322786	0.999922103	1
CG32758	CG32758 gene product from transcript CG32758-RA	2.374794982	0.9999998	1
Ndae1	Na[+]-driven anion exchanger 1	2.371483535	0.998257988	1
GstD9	Glutathione S transferase D9	2.360335473	0.999852185	1
mad2	CG17498 gene product from transcript CG17498-RA	2.3520829	0.999999743	1
CG10420	CG10420 gene product from transcript CG10420-RA	2.351297813	0.991691963	1
pim	pimples	2.333740413	0.997637532	1
ec	echinus	2.328651514	0.999837373	1
CG10943	CG10943 gene product from transcript CG10943-RA	2.32502107	0.97251971	1
sti	sticky	2.321856494	0.999913502	1
CG9184	CG9184 gene product from transcript CG9184-RB	2.31993173	0.994238867	1
CG17119	CG17119 gene product from transcript CG17119-RA	2.318710055	0.998085637	1
CG7149	CG7149 gene product from transcript CG7149-RA	2.318341776	0.999700044	1
CG30269	CG30269 gene product from transcript CG30269-RA	2.312528934	0.993540929	1
Duox	Dual oxidase	2.305974697	0.999668919	1
CG10555	CG10555 gene product from transcript CG10555-RA	2.299144577	0.999992318	1
CG31058	CG31058 gene product from transcript CG31058-RA	2.295788616	0.982429041	1
mthl8	methuselah-like 8	2.293712898	0.999267354	1
CG12713	CG12713 gene product from transcript CG12713-RA	2.282353629	0.991563699	1
Ir94c	Ionotropic receptor 94c	2.279314063	0.999991571	1
CycB	Cyclin B	2.276940483	0.999618913	1
CG13599	CG13599 gene product from transcript CG13599-RA	2.273278774	0.999942858	1
mei-38	meiotic 38	2.272755766	0.990116069	1
pigs	pickled eggs	2.255176598	0.999989942	1
CG1529	CG1529 gene product from transcript CG1529-RA	2.25431711	0.981501954	1
Gap1	GTPase-activating protein 1	2.251101188	0.998618669	1

Annex 1. Differentially expressed genes in Apc Ras vs WT 1 week ACI comparison

symbol	genename	APC RAS vs WT 1week FC	APC RAS vs WT 1week PDE	APC RAS vs WT REJ
Pect	Phosphoethanolamine cytidylyltransferase	2.242011874	0.99985601	1
Ote	Otefin	2.240992696	0.99899291	1
CG34372	CG34372 gene product from transcript CG34372-RC	2.239953075	0.99863925	1
Pen	Pendulin	2.231179513	0.999777175	1
CG9917	CG9917 gene product from transcript CG9917-RA	2.219727282	0.999914404	1
Gfat1	Glutamine:fructose-6-phosphate aminotransferase 1	2.206479947	0.995850629	1
CG14204	CG14204 gene product from transcript CG14204-RA	2.204009791	0.990255052	1
sprt	sprite	2.202828094	0.9990622	1
CG15739	CG15739 gene product from transcript CG15739-RA	2.202358969	0.994363898	1
CG17264	CG17264 gene product from transcript CG17264-RA	2.201446403	0.991652521	1
shu	shutdown	2.197896694	0.999870144	1
Os-C	CG3250 gene product from transcript CG3250-RC	2.1975482	0.999625365	1
RPA2	Replication protein A2	2.192309994	0.999741421	1
edl	ETS-domain lacking	2.189711948	0.998642906	1
Gap1	GTPase-activating protein 1	2.188687117	0.99421812	1
CG4674	CG4674 gene product from transcript CG4674-RA	2.187723401	0.997051225	1
CG4267	CG4267 gene product from transcript CG4267-RA	2.186766023	0.960330347	1
CG34261	CG34261 gene product from transcript CG34261-RA	2.178286262	0.999273915	1
Z600	CG17962 gene product from transcript CG17962-RA	2.178097689	0.999996645	1
CG31145	CG31145 gene product from transcript CG31145-RC	2.177765293	0.971137648	1
Def	Defensin	2.175456732	0.978833693	1
wun2	wunen-2	2.166593884	0.999429991	1
Cht4	Chitinase 4	2.166477292	0.99651186	1
rod	rough deal	2.15854999	0.999987839	1
eys	eyes shut	2.139103847	0.997585369	1
Cks30A	Cyclin-dependent kinase subunit 30A	2.138000341	0.999638439	1
CG7730	CG7730 gene product from transcript CG7730-RC	2.129276009	0.986562248	1
dbr	debra	2.126811457	0.988326447	1
CG2100	CG2100 gene product from transcript CG2100-RB	2.124941774	0.994088821	1
cdc2	CG5363 gene product from transcript CG5363-RA	2.122547482	0.998651658	1
PH4alphaEFB	prolyl-4-hydroxylase-alpha EFB	2.121385363	0.993642095	1
CG7800	CG7800 gene product from transcript CG7800-RA	2.119335484	0.959840581	1
Idgf4	Imaginal disc growth factor 4	2.115411506	0.999983357	1
dmt	dalmatian	2.114997335	0.999995401	1
CG30022	CG30022 gene product from transcript CG30022-RB	2.112798185	0.99023023	1
CG13623	CG13623 gene product from transcript CG13623-RA	2.11227748	0.999769928	1
ial	Ipll-aurora-like kinase	2.112008551	0.999986313	1
rols	rolling pebbles	2.109965054	0.995844104	1
fne	found in neurons	2.108084483	0.999997666	1
Gli	Gliotactin	2.107874468	0.998597108	1
CG17715	CG17715 gene product from transcript CG17715-RA	2.107695037	0.999523127	1
CG10098	CG10098 gene product from transcript CG10098-RA	2.106867938	0.999951812	1
CG33275	CG33275 gene product from transcript CG33275-RA	2.106251596	0.996675617	1
CG12370	CG12370 gene product from transcript CG12370-RB	2.10475769	0.995752654	1
bw	brown	2.0999507	0.99224418	1
cenB1A	centaurin beta 1A	2.097044764	0.999996807	1
CG34372	CG34372 gene product from transcript CG34372-RC	2.094741988	0.978351747	1
esc	extra sexcombs	2.092992811	0.998454853	1
mod(mdg4)	modifier of mdg4	2.085415586	0.999938463	1
sip2	septin interacting protein 2	2.082201048	0.999968117	1
CG1792	CG1792 gene product from transcript CG1792-RA	2.081151589	0.999876261	1
CHKov2	CG10675 gene product from transcript CG10675-RA	2.079900448	0.965724138	1
Cad96Cb	CG13664 gene product from transcript CG13664-RC	2.07073311	0.9993763	1
Spn5	Serine protease inhibitor 5	2.05911142	0.991854125	1
Tsp42Ei	Tetraspanin 42Ei	2.058986298	0.993743689	1
CG13822	CG13822 gene product from transcript CG13822-RA	2.058637738	0.981301044	1
CG42565	CG42565 gene product from transcript CG42565-RA	2.058220787	0.982430319	1
Elongin-B	Elongin B	2.051961576	0.999938762	1
CG10638	CG10638 gene product from transcript CG10638-RA	2.05155883	0.999999691	1
feo	fascetto	2.050834794	0.997101455	1
Arc2	CG13941 gene product from transcript CG13941-RA	2.046268547	0.993590718	1
18w	18 wheeler	2.046012497	0.999823255	1

Annex 1. Differentially expressed genes in Apc Ras vs WT 1 week ACI comparison

symbol	genename	APC RAS vs WT 1week FC	APC RAS vs WT 1week PDE	APC RAS vs WT REJ
fzy	fizzy	2.041742535	0.995207773	1
CG33221	CG33221 gene product from transcript CG33221-RA	2.040737948	0.983250912	1
borr	borealin-related	2.039979677	0.999935939	1
Tsp	Thrombospondin	2.039472622	0.999999749	1
nec	necrotic	2.037439291	0.999685606	1
Klp61F	Kinesin-like protein at 61F	2.032112134	0.999986659	1
CG42458	CG42458 gene product from transcript CG42458-RA	2.031228573	0.999999979	1
CG17816	CG17816 gene product from transcript CG17816-RE	2.027754045	0.994913606	1
Tsp42Ej	Tetraspanin 42Ej	2.026735734	0.994789277	1
Incenp	Inner centromere protein	2.025890343	0.999989519	1
bora	aurora borealis	2.02338917	0.999999908	1
scrib	scribbled	2.021504174	0.999967212	1
CG6310	CG6310 gene product from transcript CG6310-RA	2.017812225	0.991430228	1
CG42254	CG42254 gene product from transcript CG42254-RB	2.014545493	0.999849173	1
CG14869	CG14869 gene product from transcript CG14869-RB	2.011257566	0.958139581	1
pch2	CG31453 gene product from transcript CG31453-RA	2.010822099	0.999850846	1
CG3630	CG3630 gene product from transcript CG3630-RA	2.01060586	0.999853742	1
CG6854	CG6854 gene product from transcript CG6854-RC	2.009540722	0.998735125	1
CG17272	CG17272 gene product from transcript CG17272-RA	2.004742053	0.999873832	1
Epac	CG34392 gene product from transcript CG34392-RC	2.004145132	0.999784019	1
Ras85D	Ras oncogene at 85D	2.001436623	0.998773394	1
CG4973	CG4973 gene product from transcript CG4973-RA	2.000726846	0.978196322	1
CG31530	CG31530 gene product from transcript CG31530-RA	2.000563562	0.990962936	1
CG3225	CG3225 gene product from transcript CG3225-RA	-2.00357172	0.971704627	-1
m1	E(spl) region transcript m1	-2.004205546	0.985703926	-1
CG33523	CG33523 gene product from transcript CG33523-RD	-2.004365083	0.999064495	-1
CG11155	CG11155 gene product from transcript CG11155-RA	-2.010003758	0.999538344	-1
CG34347	CG34347 gene product from transcript CG34347-RB	-2.0125931	0.997379797	-1
mthl10	methuselah-like 10	-2.014991304	0.998200946	-1
CG6490	CG6490 gene product from transcript CG6490-RB	-2.017861307	0.9994917	-1
ptr	proximal to raf	-2.020005486	0.999140391	-1
btsz	bitesize	-2.023985199	0.999573551	-1
CG34401	CG34401 gene product from transcript CG34401-RA	-2.028545764	0.999999998	-1
CG8008	CG8008 gene product from transcript CG8008-RB	-2.02964396	0.999969911	-1
CG30088	CG30088 gene product from transcript CG30088-RB	-2.03069768	0.954574795	-1
CG30344	CG30344 gene product from transcript CG30344-RA	-2.03460507	0.999996779	-1
Stat92E	Signal-transducer ANDactivator of transcription at 92E	-2.037937061	0.999970624	-1
dnr1	defense repressor 1	-2.03923664	0.999726113	-1
CG6126	CG6126 gene product from transcript CG6126-RA	-2.040647345	0.999999998	-1
CG18622	CG18622 gene product from transcript CG18622-RA	-2.042283858	0.999991481	-1
CG12071	CG12071 gene product from transcript CG12071-RB	-2.042366162	0.982059099	-1
ste24b	ste24b prenyl protease type I	-2.044834425	0.999904769	-1
CG3332	CG3332 gene product from transcript CG3332-RB	-2.045501402	0.957607271	-1
sqz	squeeze	-2.047744373	0.99969341	-1
Doa	Darkener of apricot	-2.052696451	0.999989681	-1
Ten-m	Tenascin major	-2.052806785	0.983210497	-1
Cad89D	CG14900 gene product from transcript CG14900-RB	-2.053378845	0.998998264	-1
CG1399	CG1399 gene product from transcript CG1399-RD	-2.058166174	0.999908556	-1
CG18747	CG18747 gene product from transcript CG18747-RB	-2.060043829	0.984161588	-1
Spn4	Serine protease inhibitor 4	-2.060975081	0.998996782	-1
Mct1	Monocarboxylate transporter 1	-2.063336636	0.983341377	-1
Or33a	Odorant receptor 33a	-2.064454371	0.97903419	-1
Cyp6g2	CG8859 gene product from transcript CG8859-RA	-2.067304289	0.999908364	-1
Spn3	Serine protease inhibitor 3	-2.067415287	0.999955981	-1
CG33177	CG33177 gene product from transcript CG33177-RA	-2.073234252	0.999999996	-1
CG10863	CG10863 gene product from transcript CG10863-RA	-2.074372715	0.999956337	-1
Zasp66	Z band alternatively spliced PDZ-motif protein 66	-2.075011004	0.969549617	-1
CG15605	CG15605 gene product from transcript CG15605-RA	-2.075954811	0.989567719	-1
CG5599	CG5599 gene product from transcript CG5599-RA	-2.078545002	0.999865033	-1
CG14691	CG14691 gene product from transcript CG14691-RA	-2.080420461	0.999999811	-1
CG3835	CG3835 gene product from transcript CG3835-RB	-2.083954587	0.997999179	-1
CG12910	CG12910 gene product from transcript CG12910-RA	-2.092046819	0.992196144	-1

Annex 1. Differentially expressed genes in Apc Ras vs WT 1 week ACI comparison

symbol	genename	APC RAS vs WT 1week FC	APC RAS vs WT 1week PDE	APC RAS vs WT REJ
CG10494	CG10494 gene product from transcript CG10494-RA	-2.092744821	0.999963181	-1
CG14471	CG14471 gene product from transcript CG14471-RB	-2.093366953	0.999984464	-1
CG32450	CG32450 gene product from transcript CG32450-RA	-2.093594246	0.999127513	-1
MESK2	Misexpression suppressor of KSR 2	-2.096432656	0.999938757	-1
CG8788	CG8788 gene product from transcript CG8788-RA	-2.099354887	0.995614453	-1
CG15547	CG15547 gene product from transcript CG15547-RA	-2.102497185	0.990900417	-1
CG3308	CG3308 gene product from transcript CG3308-RA	-2.102623952	0.999222198	-1
CG6108	CG6108 gene product from transcript CG6108-RA	-2.10386484	0.99783999	-1
CG34360	CG34360 gene product from transcript CG34360-RA	-2.111794129	0.999968932	-1
iotaTry	iotaTrypsin	-2.113758538	0.991323515	-1
Ucp4B	CG18340 gene product from transcript CG18340-RA	-2.115077825	0.960992906	-1
CG4020	CG4020 gene product from transcript CG4020-RA	-2.116765622	0.987936298	-1
sba	six-banded	-2.117209109	0.99977935	-1
aay	astray	-2.117922301	0.99959101	-1
CG7083	CG7083 gene product from transcript CG7083-RA	-2.122727238	0.996261779	-1
CG10737	CG10737 gene product from transcript CG10737-RS	-2.123724165	0.972298362	-1
btsz	bitesize	-2.123765068	0.999890847	-1
CG6928	CG6928 gene product from transcript CG6928-RB	-2.124465796	0.999995131	-1
CG1724	CG1724 gene product from transcript CG1724-RA	-2.133003124	0.952893058	-1
CG1637	CG1637 gene product from transcript CG1637-RC	-2.133993931	0.997245982	-1
Ect4	CG34373 gene product from transcript CG34373-RD	-2.134784831	0.997478254	-1
Glycogenin	CG9480 gene product from transcript CG9480-RA	-2.135322251	0.99998343	-1
CG31710	CG31710 gene product from transcript CG31710-RA	-2.15154711	0.99989499	-1
CG30460	CG30460 gene product from transcript CG30460-RE	-2.152304261	0.98916497	-1
CG1722	CG1722 gene product from transcript CG1722-RA	-2.153475067	0.997057468	-1
CG3301	CG3301 gene product from transcript CG3301-RB	-2.156072303	0.998794892	-1
CG31087	CG31087 gene product from transcript CG31087-RA	-2.161324356	0.999999928	-1
CG32352	CG32352 gene product from transcript CG32352-RB	-2.16143012	0.986361004	-1
CG15534	CG15534 gene product from transcript CG15534-RA	-2.163700357	0.990121639	-1
Ugt35a	UDP-glycosyltransferase 35a	-2.188586014	0.999970305	-1
cic	capicua	-2.197556027	0.999999997	-1
CG5255	CG5255 gene product from transcript CG5255-RA	-2.198953504	0.99134598	-1
CG5568	CG5568 gene product from transcript CG5568-RA	-2.200582638	0.997611412	-1
CG18404	CG18404 gene product from transcript CG18404-RA	-2.202597285	0.991156997	-1
CG33346	CG33346 gene product from transcript CG33346-RB	-2.204433028	0.951069082	-1
CG31431	CG31431 gene product from transcript CG31431-RA	-2.205590026	0.999944254	-1
Sry-alpha	Serendipity alpha	-2.206184183	0.999971508	-1
CG12992	CG12992 gene product from transcript CG12992-RB	-2.208776741	0.997670855	-1
Tango13	Transport and Golgi organization 13	-2.209496167	0.999921023	-1
CG5770	CG5770 gene product from transcript CG5770-RA	-2.210237127	0.975653089	-1
Muc68Ca	Mucin 68Ca	-2.212392548	0.957051595	-1
Acp62F	Accessory gland peptide 62F	-2.214635026	0.998917927	-1
Ptr	Ptc-related	-2.215307344	0.978220726	-1
CG3259	CG3259 gene product from transcript CG3259-RA	-2.215404875	0.999987906	-1
Lectin-galC1	Galactose-specific C-type lectin	-2.224778934	0.985503516	-1
bru-2	bruno-2	-2.233909591	0.999996251	-1
Dat	Dopamine N acetyltransferase	-2.238840835	0.999957585	-1
gukh	GUK-holder	-2.239591407	0.979687693	-1
CG30460	CG30460 gene product from transcript CG30460-RE	-2.242505159	0.991169702	-1
CG7970	CG7970 gene product from transcript CG7970-RA	-2.248107408	0.999869223	-1
CG42330	CG42330 gene product from transcript CG42330-RH	-2.248803646	0.999995243	-1
CG4723	CG4723 gene product from transcript CG4723-RA	-2.254090187	0.999952605	-1
CG32055	CG32055 gene product from transcript CG32055-RA	-2.254162781	0.999986341	-1
Gyc-89Db	Guanylyl cyclase at 89Db	-2.25429736	0.955607574	-1
CG2556	CG2556 gene product from transcript CG2556-RA	-2.256440734	0.999991435	-1
srp	serpent	-2.257803191	0.9882787	-1
CG4325	CG4325 gene product from transcript CG4325-RA	-2.26061089	0.999665173	-1
CG15465	CG15465 gene product from transcript CG15465-RA	-2.263342186	0.999986404	-1
sinu	sinuous	-2.264987416	0.992874492	-1
trk	trunk	-2.267846928	0.99973145	-1
Gr89a	Gustatory receptor 89a	-2.268571892	0.994473312	-1
CG1315	CG1315 gene product from transcript CG1315-RA	-2.277503597	0.995120123	-1

Annex 1. Differentially expressed genes in Apc Ras vs WT 1 week ACI comparison

symbol	genename	APC RAS vs WT 1week FC	APC RAS vs WT 1week PDE	APC RAS vs WT REJ
CG10283	CG10283 gene product from transcript CG10283-RB	-2.281457017	0.999996354	-1
CG13607	CG13607 gene product from transcript CG13607-RC	-2.289327604	0.987869878	-1
CG33281	CG33281 gene product from transcript CG33281-RA	-2.298585735	0.967361669	-1
CG8834	CG8834 gene product from transcript CG8834-RB	-2.304220236	0.99819488	-1
CG17855	CG17855 gene product from transcript CG17855-RA	-2.304684135	0.999997055	-1
CG9664	CG9664 gene product from transcript CG9664-RB	-2.313580922	0.999853021	-1
MESK2	Misexpression suppressor of KSR 2	-2.315915882	0.99972712	-1
CG9527	CG9527 gene product from transcript CG9527-RA	-2.31851877	0.998501554	-1
Clk	Clock	-2.330596469	0.997492999	-1
Fhos	CG42610 gene product from transcript CG42610-RC	-2.331118548	0.963939717	-1
CG6283	CG6283 gene product from transcript CG6283-RA	-2.33547327	0.999995598	-1
CG9914	CG9914 gene product from transcript CG9914-RA	-2.33595425	0.986774951	-1
CG42367	CG42367 gene product from transcript CG42367-RB	-2.337962909	0.973098118	-1
CG42256	CG42256 gene product from transcript CG42256-RH	-2.341181024	0.978806333	-1
CG30154	CG30154 gene product from transcript CG30154-RA	-2.345184823	0.997839269	-1
CG8837	CG8837 gene product from transcript CG8837-RA	-2.346330291	0.999999073	-1
Takr86C	Tachykinin-like receptor at 86C	-2.35154783	0.999999993	-1
CG16781	CG16781 gene product from transcript CG16781-RA	-2.356778642	0.992278629	-1
Egfr	Epidermal growth factor receptor	-2.35975681	0.999998166	-1
ect	ectodermal	-2.36171969	0.999970607	-1
CS-2	Chitin synthase 2	-2.371825938	0.999968443	-1
CG13325	CG13325 gene product from transcript CG13325-RA	-2.374352724	0.999727415	-1
CG42321	CG42321 gene product from transcript CG42321-RM	-2.376632722	0.999930742	-1
sut4	sugar transporter 4	-2.38689246	0.999678082	-1
pain	painless	-2.390160422	0.999938218	-1
kar	karmoisin	-2.396544448	0.999998154	-1
hig	hikaru genki	-2.397925421	0.999985042	-1
CG34376	CG34376 gene product from transcript CG34376-RB	-2.400102783	0.995850244	-1
olf186-M	CG14489 gene product from transcript CG14489-RA	-2.40145315	0.998771996	-1
Jon44E	Jonah 44E	-2.402224838	0.993929127	-1
GlcT-1	CG6437 gene product from transcript CG6437-RA	-2.402347692	0.999131553	-1
CG4928	CG4928 gene product from transcript CG4928-RA	-2.411811174	0.97353688	-1
laza	lazaro	-2.412094611	0.999697928	-1
CG32521	CG32521 gene product from transcript CG32521-RA	-2.42547498	0.999985477	-1
kappaTry	CG12388 gene product from transcript CG12388-RB	-2.426317807	0.996407548	-1
CG3344	CG3344 gene product from transcript CG3344-RA	-2.433593705	0.961039695	-1
CG11347	CG11347 gene product from transcript CG11347-RE	-2.434290806	0.986016331	-1
CG5254	CG5254 gene product from transcript CG5254-RA	-2.439286536	0.991585403	-1
CG15117	CG15117 gene product from transcript CG15117-RA	-2.442880307	0.999999205	-1
Atet	ABC transporter expressed in trachea	-2.444597209	0.998650044	-1
CG4653	CG4653 gene product from transcript CG4653-RA	-2.448980261	0.999142568	-1
Pdp1	PAR-domain protein 1	-2.453192158	0.999775944	-1
CG30116	CG30116 gene product from transcript CG30116-RC	-2.455071934	0.986223538	-1
Mes2	CG11100 gene product from transcript CG11100-RB	-2.466317279	0.999814786	-1
CG34406	CG34406 gene product from transcript CG34406-RA	-2.473037413	0.999511475	-1
CG3288	CG3288 gene product from transcript CG3288-RA	-2.474192517	0.999999173	-1
CG10170	CG10170 gene product from transcript CG10170-RA	-2.478726112	0.996397303	-1
cry	cryptochrome	-2.482135595	0.999770082	-1
Sln	Silnoon	-2.499929225	0.965316294	-1
CG32850	CG32850 gene product from transcript CG32850-RA	-2.50069085	0.994161163	-1
dnt	doughnut on 2	-2.502520883	0.999794935	-1
CG34347	CG34347 gene product from transcript CG34347-RB	-2.503240867	0.99997087	-1
CG9673	CG9673 gene product from transcript CG9673-RA	-2.5128631	0.999914351	-1
CG9498	CG9498 gene product from transcript CG9498-RA	-2.516392029	0.995991198	-1
beat-IIIc	CG15138 gene product from transcript CG15138-RA	-2.542367589	0.996326056	-1
Cyp6a19	CG10243 gene product from transcript CG10243-RA	-2.544158523	0.997622145	-1
Prestin	CG5485 gene product from transcript CG5485-RA	-2.54675921	0.999978382	-1
CG8678	CG8678 gene product from transcript CG8678-RA	-2.55080352	0.999840953	-1
RpS7	Ribosomal protein S7	-2.552829938	0.998415524	-1
CG8952	CG8952 gene product from transcript CG8952-RA	-2.576598316	0.976092136	-1
CG34401	CG34401 gene product from transcript CG34401-RA	-2.577526486	0.999667596	-1
Cyp4ac2	CG17970 gene product from transcript CG17970-RB	-2.578835085	0.998347824	-1

Annex 1. Differentially expressed genes in Apc Ras vs WT 1 week ACI comparison

symbol	genename	APC RAS vs WT 1week FC	APC RAS vs WT 1week PDE	APC RAS vs WT REJ
CG6018	CG6018 gene product from transcript CG6018-RA	-2.582399354	0.998085063	-1
Npc2d	Niemann-Pick type C-2d	-2.586817541	0.961518713	-1
CG14856	CG14856 gene product from transcript CG14856-RA	-2.604534311	0.999143876	-1
Cyp6d5	CG3050 gene product from transcript CG3050-RA	-2.610715794	0.997993048	-1
CG31102	CG31102 gene product from transcript CG31102-RA	-2.616977714	0.999957236	-1
CG42330	CG42330 gene product from transcript CG42330-RH	-2.617465202	0.999976958	-1
exex	extra-extra	-2.620646717	0.999947342	-1
CG11342	CG11342 gene product from transcript CG11342-RA	-2.628652394	0.999879652	-1
CG5932	CG5932 gene product from transcript CG5932-RA	-2.629413365	0.983487477	-1
osp	outspread	-2.65043888	0.999888327	-1
IM10	Immune induced molecule 10	-2.661106215	0.999969719	-1
CG2678	CG2678 gene product from transcript CG2678-RA	-2.666296599	0.994964671	-1
a	arc	-2.671543427	0.997453521	-1
sick	sickie	-2.675955372	0.99988857	-1
CG12766	CG12766 gene product from transcript CG12766-RA	-2.685396339	0.999887722	-1
CG13829	CG13829 gene product from transcript CG13829-RA	-2.69252043	0.993640244	-1
CG16965	CG16965 gene product from transcript CG16965-RB	-2.709134031	0.985700603	-1
Doa	Darkener of apricot	-2.721259336	0.999999939	-1
CG16749	CG16749 gene product from transcript CG16749-RA	-2.724589999	0.991107511	-1
Jheh3	Juvenile hormone epoxide hydrolase 3	-2.742896709	0.996596406	-1
fus	fusilli	-2.743539511	0.999953374	-1
CG17186	CG17186 gene product from transcript CG17186-RA	-2.744798483	0.999999969	-1
spz	spatzle	-2.752578319	0.99994382	-1
CG31198	CG31198 gene product from transcript CG31198-RA	-2.756859451	0.984944756	-1
zetaTry	zetaTrypsin	-2.759401633	0.993347805	-1
unc-104	CG8566 gene product from transcript CG8566-RB	-2.761432211	0.995344893	-1
CG9743	CG9743 gene product from transcript CG9743-RA	-2.761961788	0.999991809	-1
CG3544	CG3544 gene product from transcript CG3544-RA	-2.781845505	0.980399243	-1
wit	wishful thinking	-2.782583759	0.994500865	-1
Cyp6a23	CG10242 gene product from transcript CG10242-RA	-2.78258961	0.993172892	-1
CDase	Ceramidase	-2.797743549	0.997269648	-1
CG32264	CG32264 gene product from transcript CG32264-RH	-2.800174403	0.999811526	-1
CG16732	CG16732 gene product from transcript CG16732-RB	-2.801898688	0.999988767	-1
Cyp9b1	Cytochrome P450-9b1	-2.813243208	0.999819436	-1
CG32407	CG32407 gene product from transcript CG32407-RA	-2.829378403	0.993379593	-1
MtnC	Metallothionein C	-2.848916939	0.999969842	-1
sick	sickie	-2.849936724	0.999996645	-1
Cbl	CG7037 gene product from transcript CG7037-RB	-2.852149278	0.999240754	-1
PGRP-SC2	CG14745 gene product from transcript CG14745-RA	-2.853492986	0.979164009	-1
CG7431	CG7431 gene product from transcript CG7431-RA	-2.85669672	0.998048475	-1
Jon65Aiii	Jonah 65Aiii	-2.863450345	0.995361923	-1
Cyp4ac1	CG14032 gene product from transcript CG14032-RA	-2.868911137	0.999983433	-1
CG14120	CG14120 gene product from transcript CG14120-RA	-2.875207341	0.99978714	-1
CG13917	CG13917 gene product from transcript CG13917-RB	-2.891449077	0.999638699	-1
CG8713	CG8713 gene product from transcript CG8713-RA	-2.930469358	0.997487441	-1
Cyp6a9	Cytochrome P450-6a9	-2.937495298	0.999748405	-1
HdacX	Histone deacetylase X	-2.937903079	0.999999897	-1
CG42269	CG42269 gene product from transcript CG42269-RE	-2.9384821	0.99861869	-1
CG15611	CG15611 gene product from transcript CG15611-RB	-2.953751801	0.999290714	-1
CG18869	CG18869 gene product from transcript CG18869-RA	-2.959257891	0.999881018	-1
Fps85D	Fps oncogene analog	-2.965787626	0.99997797	-1
CG1681	CG1681 gene product from transcript CG1681-RA	-3.001437878	0.998281444	-1
CG15255	CG15255 gene product from transcript CG15255-RA	-3.020475935	0.99950333	-1
CG13492	CG13492 gene product from transcript CG13492-RC	-3.020803333	0.999183501	-1
CG32444	CG32444 gene product from transcript CG32444-RA	-3.025152149	0.9958687	-1
CG1637	CG1637 gene product from transcript CG1637-RC	-3.025774227	0.999989447	-1
CG15186	CG15186 gene product from transcript CG15186-RA	-3.042934606	0.999757407	-1
CG14375	CG14375 gene product from transcript CG14375-RA	-3.063236509	0.990107573	-1
CG14740	CG14740 gene product from transcript CG14740-RA	-3.070025244	0.999947502	-1
CG14691	CG14691 gene product from transcript CG14691-RA	-3.077367799	0.996359112	-1
CG30283	CG30283 gene product from transcript CG30283-RB	-3.106240018	0.986018493	-1
CG8093	CG8093 gene product from transcript CG8093-RA	-3.115126886	0.993251763	-1

Annex 1. Differentially expressed genes in Apc Ras vs WT 1 week ACI comparison

symbol	genename	APC RAS vs WT 1week FC	APC RAS vs WT 1week PDE	APC RAS vs WT REJ
CG7997	CG7997 gene product from transcript CG7997-RB	-3.139328652	1	-1
CG31076	CG31076 gene product from transcript CG31076-RA	-3.149125857	0.999975427	-1
CG33099	CG33099 gene product from transcript CG33099-RA	-3.149725633	0.99991784	-1
CG30345	CG30345 gene product from transcript CG30345-RA	-3.151585776	0.999999936	-1
CG33127	CG33127 gene product from transcript CG33127-RA	-3.156607083	0.998012872	-1
CG9509	CG9509 gene product from transcript CG9509-RA	-3.16138462	0.998885145	-1
CG6206	CG6206 gene product from transcript CG6206-RA	-3.166850345	0.98805822	-1
CG10877	CG10877 gene product from transcript CG10877-RA	-3.177065344	0.992549488	-1
Tsp42Eq	Tetraspanin 42Eq	-3.188240337	0.999437233	-1
m-cup	mann-cup	-3.19191883	0.999992379	-1
CG10912	CG10912 gene product from transcript CG10912-RA	-3.199741512	0.9716257	-1
CG4678	CG4678 gene product from transcript CG4678-RE	-3.215087806	0.99839854	-1
CG17278	CG17278 gene product from transcript CG17278-RA	-3.222888014	0.967206647	-1
Grip	Glutamate receptor binding protein	-3.22624334	0.998402844	-1
CG10168	CG10168 gene product from transcript CG10168-RA	-3.226647919	0.999936407	-1
CG30049	CG30049 gene product from transcript CG30049-RA	-3.243634653	0.983885787	-1
CG8693	CG8693 gene product from transcript CG8693-RA	-3.254787857	0.984444457	-1
Ih	I[[h]] channel	-3.2751832	0.999595456	-1
CG2201	CG2201 gene product from transcript CG2201-RA	-3.278954786	0.999967321	-1
CG13827	CG13827 gene product from transcript CG13827-RA	-3.28155843	0.999762754	-1
CG10051	CG10051 gene product from transcript CG10051-RA	-3.287618349	0.99855709	-1
CG34198	CG34198 gene product from transcript CG34198-RA	-3.289868552	0.999999058	-1
beat-IIa	beaten path IIa	-3.290682645	0.999998051	-1
CG9896	CG9896 gene product from transcript CG9896-RA	-3.296113522	0.989079711	-1
CG16782	CG16782 gene product from transcript CG16782-RA	-3.29651197	0.966199031	-1
Cyp9f2	CG11466 gene product from transcript CG11466-RB	-3.29883411	0.999892045	-1
CG11155	CG11155 gene product from transcript CG11155-RA	-3.306900142	0.997264723	-1
CG3277	CG3277 gene product from transcript CG3277-RC	-3.317035265	0.999501444	-1
CG6527	CG6527 gene product from transcript CG6527-RA	-3.323653343	0.99337202	-1
CG33514	CG33514 gene product from transcript CG33514-RA	-3.326223432	0.989430224	-1
CG15309	CG15309 gene product from transcript CG15309-RA	-3.354780829	0.999720865	-1
Ahcy89E	Adenosylhomocysteinase 89E	-3.355434708	0.999616979	-1
CG9747	CG9747 gene product from transcript CG9747-RA	-3.379545005	0.988085357	-1
CG7470	CG7470 gene product from transcript CG7470-RA	-3.391726207	0.999998904	-1
CG11241	CG11241 gene product from transcript CG11241-RB	-3.404654379	0.999998965	-1
fok	fledgling of Klp38B	-3.412995577	0.999962736	-1
Cyp6w1	CG8345 gene product from transcript CG8345-RA	-3.413130977	0.978214231	-1
alphaTry	alphaTrypsin	-3.42079335	0.999294973	-1
CG1637	CG1637 gene product from transcript CG1637-RC	-3.446027871	0.999957877	-1
etaTry	etaTrypsin	-3.455923097	0.999997198	-1
CG34376	CG34376 gene product from transcript CG34376-RB	-3.45958855	0.999957376	-1
CG31286	CG31286 gene product from transcript CG31286-RB	-3.464932666	0.999746859	-1
CG9989	CG9989 gene product from transcript CG9989-RA	-3.513025983	0.999892454	-1
Jon99Fi	Jonah 99Fi	-3.528032378	0.988670013	-1
CG7678	CG7678 gene product from transcript CG7678-RA	-3.60363882	0.999779758	-1
CG33514	CG33514 gene product from transcript CG33514-RA	-3.604639508	0.997339515	-1
CG10477	CG10477 gene product from transcript CG10477-RA	-3.636889383	0.975788381	-1
CG16986	CG16986 gene product from transcript CG16986-RA	-3.645739783	0.996680742	-1
epsilonTry	epsilonTrypsin	-3.702984504	0.988654202	-1
vkg	viking	-3.861408427	0.999537061	-1
CG11878	CG11878 gene product from transcript CG11878-RA	-3.91299748	0.995579708	-1
smp-30	Senescence marker protein-30	-3.941107832	0.995315343	-1
CG14253	CG14253 gene product from transcript CG14253-RB	-3.94318849	0.999999985	-1
CG8997	CG8997 gene product from transcript CG8997-RA	-3.956923691	0.996196388	-1
Cyp12a4	CG6042 gene product from transcript CG6042-RA	-3.963977134	0.992755767	-1
Pkg21D	cGMP-dependent protein kinase 21D	-4.012514468	0.997492958	-1
CG14741	CG14741 gene product from transcript CG14741-RB	-4.018694117	0.999112462	-1
CG9463	CG9463 gene product from transcript CG9463-RA	-4.023001066	0.988673563	-1
Calx	Na/Ca-exchange protein	-4.042082708	0.999953377	-1
CG7953	CG7953 gene product from transcript CG7953-RA	-4.09921527	0.999999997	-1
stl	stall	-4.139248877	0.999558685	-1
CG7298	CG7298 gene product from transcript CG7298-RA	-4.162428845	0.96895236	-1

Annex 1. Differentially expressed genes in Apc Ras vs WT 1 week ACI comparison

symbol	genename	APC RAS vs WT 1week FC	APC RAS vs WT 1week PDE	APC RAS vs WT REJ
CG32521	CG32521 gene product from transcript CG32521-RA	-4.165921934	0.999364715	-1
CG30043	CG30043 gene product from transcript CG30043-RA	-4.204832307	0.993138889	-1
luna	CG33473 gene product from transcript CG33473-RB	-4.297824453	0.999997897	-1
CG9468	CG9468 gene product from transcript CG9468-RA	-4.351305335	0.99892592	-1
CG16997	CG16997 gene product from transcript CG16997-RB	-4.358698563	0.997804727	-1
CG10663	CG10663 gene product from transcript CG10663-RB	-4.358992203	0.999999979	-1
CG6484	CG6484 gene product from transcript CG6484-RA	-4.374471091	0.996882844	-1
CG10559	CG10559 gene product from transcript CG10559-RB	-4.39424869	0.981164482	-1
CG10472	CG10472 gene product from transcript CG10472-RA	-4.527965581	0.958818959	-1
CG10621	CG10621 gene product from transcript CG10621-RA	-4.532151714	0.999756405	-1
Gyc-89Da	Guanylyl cyclase at 89Da	-4.610172769	0.999999898	-1
betaTry	betaTrypsin	-4.685639192	0.999686401	-1
CG6006	CG6006 gene product from transcript CG6006-RC	-4.727876828	0.999975418	-1
CG3301	CG3301 gene product from transcript CG3301-RB	-4.729719424	0.999999898	-1
luna	CG33473 gene product from transcript CG33473-RB	-4.775750326	0.999944269	-1
CG12057	CG12057 gene product from transcript CG12057-RA	-4.781875476	0.998798599	-1
Cg25C	Collagen type IV	-4.825524704	0.999877625	-1
CG30090	CG30090 gene product from transcript CG30090-RA	-4.863858215	0.99636265	-1
CG12464	CG12464 gene product from transcript CG12464-RA	-4.889808491	0.959668379	-1
CG9466	CG9466 gene product from transcript CG9466-RA	-5.00481916	0.993906678	-1
Mad	Mothers against dpp	-5.010461861	0.999954683	-1
Tsp42Er	Tetraspanin 42Er	-5.060279778	0.999981733	-1
CG8661	CG8661 gene product from transcript CG8661-RA	-5.157102728	0.99837836	-1
CG5506	CG5506 gene product from transcript CG5506-RA	-5.51032711	0.999929595	-1
CG11068	CG11068 gene product from transcript CG11068-RA	-5.552573059	0.999974485	-1
Jon25Biii	Jonah 25Biii	-5.617442362	0.996227387	-1
CG17633	CG17633 gene product from transcript CG17633-RA	-5.670415071	0.999644113	-1
CG18180	CG18180 gene product from transcript CG18180-RA	-5.70544714	0.999991673	-1
CG15531	CG15531 gene product from transcript CG15531-RB	-5.866256622	0.999803202	-1
CG4377	CG4377 gene product from transcript CG4377-RA	-6.021206876	0.99979438	-1
CG3301	CG3301 gene product from transcript CG3301-RB	-6.243975745	0.999425032	-1
Mip	Myoinhibiting peptide precursor	-6.307957863	0.968498343	-1
CG15629	CG15629 gene product from transcript CG15629-RA	-6.499139442	0.999605008	-1
tomboy20	CG14690 gene product from transcript CG14690-RA	-6.627165039	0.999988706	-1
LvpH	Larval visceral protein H	-6.697758039	0.997868458	-1
Jon65Aii	Jonah 65Aii	-6.719187339	0.999040643	-1
CG12026	CG12026 gene product from transcript CG12026-RB	-6.870935547	0.999999956	-1
CG4462	CG4462 gene product from transcript CG4462-RA	-6.940925176	0.999924685	-1
CG5246	CG5246 gene product from transcript CG5246-RA	-6.941070661	0.999983296	-1
CG6043	CG6043 gene product from transcript CG6043-RG	-6.951726035	0.999999897	-1
be	ben	-7.168185459	0.996673115	-1
CG6129	CG6129 gene product from transcript CG6129-RD	-7.359329899	0.999969554	-1
Jon99Ci	Jonah 99Ci	-7.557904878	0.96488078	-1
CG31763	CG31763 gene product from transcript CG31763-RA	-7.577620188	0.999962586	-1
CG6295	CG6295 gene product from transcript CG6295-RA	-7.763407728	0.983963019	-1
Bace	beta-site APP-cleaving enzyme	-8.013710552	0.999454642	-1
Jon74E	Jonah 74E	-8.073414687	0.999905949	-1
CG5107	CG5107 gene product from transcript CG5107-RA	-8.363804478	0.997246351	-1
CG6006	CG6006 gene product from transcript CG6006-RC	-8.484896293	0.999563226	-1
CG9360	CG9360 gene product from transcript CG9360-RA	-9.374719419	0.9981047	-1
CG34040	CG34040 gene product from transcript CG34040-RA	-9.63859957	0.992416181	-1
CG12374	CG12374 gene product from transcript CG12374-RA	-10.21732337	0.999077964	-1
Jon65Ai	Jonah 65Ai	-10.36357776	0.997190447	-1
CG17145	CG17145 gene product from transcript CG17145-RA	-10.71263032	0.999999933	-1
CG5804	CG5804 gene product from transcript CG5804-RA	-14.83971653	0.999755811	-1
CG34386	CG34386 gene product from transcript CG34386-RC	-15.92995967	0.969390223	-1
CG2082	CG2082 gene product from transcript CG2082-RC	-19.24590073	0.999861772	-1
Ast-C	Allatostatin C	-19.87087114	0.956110367	-1
CG4363	CG4363 gene product from transcript CG4363-RA	-20.7767971	0.999206017	-1
CG2082	CG2082 gene product from transcript CG2082-RC	-21.16634434	0.999756936	-1

Annex 1. Differentially expressed genes in Apc Ras vs WT 4 weeks ACI comparison

symbol	genename	APC RAS vs WT 4week FC	APC RAS vs WT 4week PDE	APC RAS vs WT REJ
svp	seven up	59.41494545	0.999999893	1
sn	singed	51.0046812	0.999999816	1
Tsp	Thrombospondin	26.81143393	0.999934975	1
slbo	slow border cells	20.96653571	0.999968769	1
hh	hedgehog	16.07787061	0.999999903	1
tw	Protein O-mannosyltransferase 2	15.34745511	0.999999949	1
ImpL2	Ecdysone-inducible gene L2	14.29456666	0.999999154	1
Fas1	Fasciclin 1	14.04296766	0.998328509	1
Cad96Ca	CG10244 gene product from transcript CG10244-RA	13.61025654	0.999726795	1
CG3348	CG3348 gene product from transcript CG3348-RA	13.42857001	0.99999981	1
fz3	frizzled 3	13.0155895	0.99999988	1
sog	short gastrulation	12.60487262	0.999991499	1
svp	seven up	12.57938391	0.999983773	1
dmrt93B	doublesex-Mab related 93B	12.12059269	0.999999366	1
Gr94a	Gustatory receptor 94a	11.50387499	0.999760683	1
daw	dawdle	11.28935441	0.99924122	1
mirr	mirror	11.12928585	0.999688208	1
CG17119	CG17119 gene product from transcript CG17119-RA	10.43990419	0.999990751	1
kek1	kekkon-1	10.35088152	0.99999759	1
Idgf4	Imaginal disc growth factor 4	10.25302048	0.994704837	1
CG14526	CG14526 gene product from transcript CG14526-RB	10.21770907	0.999867149	1
Duox	Dual oxidase	10.11845249	0.99999213	1
Lac	Lachesin	9.821146617	0.991459024	1
blot	bloated tubules	9.359321159	0.998668499	1
CG5630	CG5630 gene product from transcript CG5630-RB	9.215303806	0.999967746	1
CG14545	CG14545 gene product from transcript CG14545-RA	8.943513912	0.998727078	1
CG6330	CG6330 gene product from transcript CG6330-RB	8.875012451	0.999973396	1
Pvf3	PDGF- and VEGF-related factor 3	8.793451766	0.994205098	1
CG7056	CG7056 gene product from transcript CG7056-RA	8.462966987	0.999956196	1
CG4726	CG4726 gene product from transcript CG4726-RA	8.418811019	0.999965998	1
p53	CG33336 gene product from transcript CG33336-RB	8.219050076	0.999907805	1
CG5630	CG5630 gene product from transcript CG5630-RB	7.999741854	0.999997899	1
CG13117	CG13117 gene product from transcript CG13117-RA	7.795650068	0.999877354	1
Ugt86Di	CG6658 gene product from transcript CG6658-RA	7.569427563	0.99999952	1
Lim3	CG10699 gene product from transcript CG10699-RB	7.55984518	0.999999002	1
kirre	kin of irre	7.480690886	0.999985595	1
GstD2	Glutathione S transferase D2	7.415281785	0.990524915	1
CG30359	CG30359 gene product from transcript CG30359-RA	7.391170065	0.99970441	1
CG32280	CG32280 gene product from transcript CG32280-RA	7.31563587	0.999511233	1
CG11897	CG11897 gene product from transcript CG11897-RA	7.309140843	0.999989199	1
bnl	branchless	7.286999891	0.967329768	1
Mmp2	Matrix metalloproteinase 2	7.221017157	0.999792254	1
Pepck	Phosphoenolpyruvate carboxykinase	7.17203602	0.996536801	1
Dgp-1	CG5729 gene product from transcript CG5729-RA	7.096251054	0.999965131	1
CG33494	CG33494 gene product from transcript CG33494-RA	6.965049337	0.999623803	1
CG14302	CG14302 gene product from transcript CG14302-RA	6.701989635	0.999727949	1
upd3	unpaired 3	6.633201681	0.999901587	1
CG13631	CG13631 gene product from transcript CG13631-RA	6.606635126	0.99798732	1
GstE9	Glutathione S transferase E9	6.551312138	0.999177997	1
Pvf3	PDGF- and VEGF-related factor 3	6.497433906	0.999639778	1
mirr	mirror	6.316511973	0.999819546	1
CG5390	CG5390 gene product from transcript CG5390-RA	6.274792414	0.981025097	1
CG42575	CG42575 gene product from transcript CG42575-RA	6.078652941	0.996370645	1
cv-2	crossveinless 2	6.069136611	0.999886666	1
CG10420	CG10420 gene product from transcript CG10420-RA	5.938471424	0.999951059	1
nkd	naked cuticle	5.922401577	0.999386261	1
CG3397	CG3397 gene product from transcript CG3397-RA	5.88550522	0.999933707	1
Fas3	Fasciclin 3	5.880977118	0.999709573	1
CG5621	CG5621 gene product from transcript CG5621-RA	5.78410449	0.992453506	1
CG30022	CG30022 gene product from transcript CG30022-RB	5.57306191	0.999999636	1
CG33275	CG33275 gene product from transcript CG33275-RA	5.545961513	0.999641126	1
CG14743	CG14743 gene product from transcript CG14743-RA	5.543615562	0.998697079	1

Annex 1. Differentially expressed genes in Apc Ras vs WT 4 weeks ACI comparison

symbol	genename	APC RAS vs WT 4week FC	APC RAS vs WT 4week PDE	APC RAS vs WT REJ
Pvf2	PDGF- and VEGF-related factor 2	5.539294939	0.999300401	1
Spn5	Serine protease inhibitor 5	5.514220914	0.999931068	1
trbl	tribbles	5.449337196	0.999820564	1
l(3)02640	lethal (3) 02640	5.439661672	0.999998575	1
Ama	Amalgam	5.433242024	0.999410688	1
upd3	unpaired 3	5.364200484	0.999964253	1
CG32037	CG32037 gene product from transcript CG32037-RA	5.237921483	0.993723212	1
rho	rhomboid	5.221494527	0.997961226	1
CG13654	CG13654 gene product from transcript CG13654-RA	5.17122114	0.999400797	1
CG7900	CG7900 gene product from transcript CG7900-RB	5.154735855	0.999828792	1
ImpL3	Ecdysone-inducible gene L3	5.115668449	0.999999796	1
Naam	Nicotinamide amidase	5.066169086	0.999997503	1
CG17119	CG17119 gene product from transcript CG17119-RA	5.055607256	0.9994516	1
bnl	branchless	5.044805683	0.995513822	1
CG4630	CG4630 gene product from transcript CG4630-RA	5.019587025	0.983407491	1
magu	CG2264 gene product from transcript CG2264-RD	5.003129766	0.999431413	1
CG42458	CG42458 gene product from transcript CG42458-RA	4.979643214	0.999820665	1
Cyp6a20	CG10245 gene product from transcript CG10245-RB	4.947115134	0.998099122	1
rtet	tetracycline resistance	4.905535198	0.999996644	1
amd	alpha methyl dopa-resistant	4.858735751	0.998627874	1
CG10527	CG10527 gene product from transcript CG10527-RA	4.836185152	0.999996799	1
nahoda	CG12781 gene product from transcript CG12781-RA	4.788321308	0.999953718	1
spri	sprint	4.76518201	0.999214905	1
upd2	unpaired 2	4.7088503	0.988542511	1
blow	blown fuse	4.612618905	0.999993257	1
CG33080	CG33080 gene product from transcript CG33080-RA	4.563819982	0.997531335	1
sna	snail	4.529845711	0.998500018	1
Tsp	Thrombospondin	4.466862322	0.999998047	1
sprt	sprite	4.439244978	0.999929627	1
wus	wurst	4.402214388	0.99999426	1
Mkp3	Mitogen-activated protein kinase phosphatase 3	4.397774247	0.999976348	1
CG32036	CG32036 gene product from transcript CG32036-RC	4.38970318	0.977711022	1
Pfk	Phosphofructokinase	4.343013087	0.999944919	1
CG11825	CG11825 gene product from transcript CG11825-RA	4.240504501	0.998992082	1
CG5644	CG5644 gene product from transcript CG5644-RA	4.212399529	0.998985585	1
CG30022	CG30022 gene product from transcript CG30022-RB	4.212016187	0.999986896	1
how	held out wings	4.14891398	0.999999668	1
CG8486	CG8486 gene product from transcript CG8486-RE	4.051597808	0.999858123	1
Arc2	CG13941 gene product from transcript CG13941-RA	4.043515646	0.99989784	1
plx	pollux	4.036850771	0.998549619	1
svp	seven up	3.989126765	0.993981666	1
GstD9	Glutathione S transferase D9	3.970986509	0.999994623	1
kek2	kekkon-2	3.91751577	0.983180008	1
CG6854	CG6854 gene product from transcript CG6854-RC	3.906205151	0.999966927	1
how	held out wings	3.891164327	0.999643871	1
pk	prickle	3.888346946	0.999990068	1
CG10140	CG10140 gene product from transcript CG10140-RA	3.863897585	0.983331682	1
Fs	Follistatin	3.853888286	0.998013273	1
DNaseII	Deoxyribonuclease II	3.852951259	0.983210273	1
prc	pericardin	3.83475367	0.971803205	1
Lsd-1	Lipid storage droplet-1	3.809614991	0.99993748	1
spri	sprint	3.782580095	0.996016114	1
CG9098	CG9098 gene product from transcript CG9098-RA	3.780634631	0.988840465	1
CHKov1	CG10618 gene product from transcript CG10618-RB	3.768276963	0.999942182	1
alpha4GT2	CG5878 gene product from transcript CG5878-RB	3.758334037	0.998676903	1
CG8028	CG8028 gene product from transcript CG8028-RA	3.752757457	0.999983017	1
wgn	wengen	3.731615761	0.99757368	1
CG34372	CG34372 gene product from transcript CG34372-RC	3.729253189	0.985294711	1
CG2017	CG2017 gene product from transcript CG2017-RA	3.69683721	0.999999759	1
bwa	brain washing	3.695314203	0.999683551	1
Aph-4	Alkaline phosphatase 4	3.687313314	0.99585266	1
CG7188	CG7188 gene product from transcript CG7188-RA	3.671098583	0.998422208	1

Annex 1. Differentially expressed genes in Apc Ras vs WT 4 weeks ACI comparison

symbol	genename	APC RAS vs WT 4week FC	APC RAS vs WT 4week PDE	APC RAS vs WT REJ
Fs	Follistatin	3.659460057	0.977194724	1
Tret1-1	Trehalose transporter 1-1	3.65402012	0.999310751	1
sty	sprouty	3.645918783	0.998465876	1
Mmp1	Matrix metalloproteinase 1	3.615879373	0.987521737	1
CG31055	CG31055 gene product from transcript CG31055-RA	3.605420997	0.950566791	1
form3	formin 3	3.556089962	0.999897565	1
CG7130	CG7130 gene product from transcript CG7130-RA	3.547908071	0.999796699	1
CG31918	CG31918 gene product from transcript CG31918-RA	3.531242602	0.999662801	1
CHKov2	CG10675 gene product from transcript CG10675-RA	3.517264912	0.998414349	1
slow	slowdown	3.514845887	0.998838803	1
rols	rolling pebbles	3.508602819	0.999645689	1
rpr	reaper	3.503114485	0.950824706	1
Gadd45	CG11086 gene product from transcript CG11086-RA	3.494298111	0.999709528	1
Mkp3	Mitogen-activated protein kinase phosphatase 3	3.473238645	0.999358402	1
mp	multiplexin	3.468450941	0.95518314	1
CG17124	CG17124 gene product from transcript CG17124-RB	3.461163593	0.979835978	1
Mmp2	Matrix metalloproteinase 2	3.40977423	0.999102232	1
CG8303	CG8303 gene product from transcript CG8303-RB	3.403382091	0.97430157	1
CG3074	CG3074 gene product from transcript CG3074-RB	3.361540286	0.999988761	1
CG2065	CG2065 gene product from transcript CG2065-RA	3.343304318	0.997539125	1
br	broad	3.343049399	0.999497881	1
CG3523	CG3523 gene product from transcript CG3523-RA	3.332798672	0.999673497	1
CG11060	CG11060 gene product from transcript CG11060-RA	3.325262598	0.999924584	1
CG9389	CG9389 gene product from transcript CG9389-RA	3.316524855	0.998582345	1
RPA2	Replication protein A2	3.302248522	0.99999934	1
PQBP-1	Poly-glutamine tract binding protein 1	3.281765232	0.99881246	1
CG11381	CG11381 gene product from transcript CG11381-RA	3.269726527	0.998163955	1
bw	brown	3.265498593	0.979815389	1
GstE10	Glutathione S transferase E10	3.265384535	0.999849084	1
CG9150	CG9150 gene product from transcript CG9150-RB	3.254538345	0.997653374	1
CG32138	CG32138 gene product from transcript CG32138-RA	3.254143708	0.999877421	1
CG14339	CG14339 gene product from transcript CG14339-RA	3.253295066	0.999621937	1
CG18190	CG18190 gene product from transcript CG18190-RB	3.252920294	0.998341696	1
scf	supercoiling factor	3.248010364	0.999999466	1
AcCoAS	Acetyl Coenzyme A synthase	3.247249256	0.999994256	1
CG7922	CG7922 gene product from transcript CG7922-RA	3.244455487	0.999989972	1
CG13800	CG13800 gene product from transcript CG13800-RB	3.237916633	0.998221281	1
Alr	Augmenter of liver regeneration	3.234292651	0.999985699	1
CG14626	CG14626 gene product from transcript CG14626-RA	3.195324869	0.995196051	1
Cyp6a2	Cytochrome P450-6a2	3.183268149	0.998492359	1
CG10641	CG10641 gene product from transcript CG10641-RA	3.173897252	0.999954528	1
drm	drumstick	3.168759676	0.999955532	1
l(2)01810	lethal (2) 01810	3.153359584	0.96274853	1
CG15097	CG15097 gene product from transcript CG15097-RC	3.146773584	0.999989755	1
GstE6	Glutathione S transferase E6	3.126440995	0.999931758	1
CG10802	CG10802 gene product from transcript CG10802-RA	3.065549968	0.999085982	1
CG32483	CG32483 gene product from transcript CG32483-RA	3.064339287	0.990939458	1
nec	necrotic	3.033041532	0.999979752	1
edl	ETS-domain lacking	3.030251511	0.999974021	1
NtR	CG6698 gene product from transcript CG6698-RA	3.028422741	0.99384433	1
CG7632	CG7632 gene product from transcript CG7632-RA	3.024698521	0.999685586	1
Ir	Inwardly rectifying potassium channel	3.016406242	0.999777659	1
Gr63a	Gustatory receptor 63a	3.009450769	0.997658627	1
rst	roughest	3.006005635	0.999322376	1
p53	CG33336 gene product from transcript CG33336-RB	2.992980969	0.999531997	1
kon	kon-tiki	2.990004351	0.95425922	1
CG8034	CG8034 gene product from transcript CG8034-RA	2.981683198	0.999690386	1
Nmdmc	NAD methylenetetrahydrofolate dehydrogenase	2.964838607	0.999678807	1
CG10638	CG10638 gene product from transcript CG10638-RA	2.962106264	0.999960256	1
CG3788	CG3788 gene product from transcript CG3788-RB	2.951188336	0.999152195	1
CG30273	CG30273 gene product from transcript CG30273-RA	2.945858454	0.999841971	1
Tsp33B	Tetraspanin 33B	2.93782454	0.997553604	1

Annex 1. Differentially expressed genes in Apc Ras vs WT 4 weeks ACI comparison

symbol	genename	APC RAS vs WT 4week FC	APC RAS vs WT 4week PDE	APC RAS vs WT REJ
Tim17a1	CG10090 gene product from transcript CG10090-RA	2.933164161	0.962919268	1
Cyp28d1	CG10833 gene product from transcript CG10833-RA	2.92602741	0.996284608	1
CG7145	CG7145 gene product from transcript CG7145-RD	2.924898623	0.999701369	1
otk	off-track	2.895661739	0.997742351	1
CG42365	CG42365 gene product from transcript CG42365-RA	2.892572472	0.999079245	1
CG42588	CG42588 gene product from transcript CG42588-RA	2.885838475	0.99999661	1
Spn43Ab	Serine protease inhibitor 43Ab	2.881724861	0.999958565	1
Fas3	Fasciclin 3	2.876247727	0.998527106	1
CG8964	CG8964 gene product from transcript CG8964-RA	2.874535848	0.999436377	1
Lrt	Leucine-rich tendon-specific protein	2.87395257	0.992700547	1
CG1021	CG1021 gene product from transcript CG1021-RE	2.854917416	0.998194587	1
sty	sprouty	2.854010328	0.999992896	1
CG4096	CG4096 gene product from transcript CG4096-RB	2.85202378	0.988644964	1
Mmp1	Matrix metalloproteinase 1	2.847566595	0.986364665	1
CG11000	CG11000 gene product from transcript CG11000-RB	2.839475156	0.999357221	1
CG12014	CG12014 gene product from transcript CG12014-RA	2.8272541	0.994239919	1
SP1173	CG10121 gene product from transcript CG10121-RC	2.824722975	0.996470685	1
CG9731	CG9731 gene product from transcript CG9731-RA	2.813585284	0.999262747	1
CG6608	CG6608 gene product from transcript CG6608-RB	2.812846151	0.997878191	1
Def	Defensin	2.811294551	0.999939532	1
GstD5	Glutathione S transferase D5	2.810599619	0.977650397	1
CG2004	CG2004 gene product from transcript CG2004-RA	2.795997155	0.99977351	1
tor	torso	2.779982693	0.979667633	1
Ets21C	Ets at 21C	2.777494121	0.990154007	1
CG10163	CG10163 gene product from transcript CG10163-RA	2.776514355	0.995518242	1
CG11710	CG11710 gene product from transcript CG11710-RA	2.774529509	0.99995415	1
HspB8	CG14207 gene product from transcript CG14207-RB	2.773934361	0.999973422	1
ec	echinus	2.772519896	0.955360096	1
GluClalpha	CG7535 gene product from transcript CG7535-RG	2.768320618	0.997629638	1
CG30384	CG30384 gene product from transcript CG30384-RA	2.764298835	0.999715332	1
KrT95D	Krueppel target at 95D	2.757392278	0.994676074	1
CG2909	CG2909 gene product from transcript CG2909-RA	2.745343331	0.999909605	1
Gap1	GTPase-activating protein 1	2.725066458	0.999939284	1
Hexo2	Hexosaminidase 2	2.701752416	0.999995975	1
CG32369	CG32369 gene product from transcript CG32369-RA	2.682647472	0.998574259	1
CG32252	CG32252 gene product from transcript CG32252-RA	2.681086097	0.999993774	1
GstE7	Glutathione S transferase E7	2.679331885	0.999835433	1
cactin	CG1676 gene product from transcript CG1676-RA	2.656457983	0.998992223	1
Cyp6d2	CG4373 gene product from transcript CG4373-RA	2.656422582	0.971352667	1
Prosbeta2R2	Proteasome beta2R2 subunit	2.646056583	0.996445183	1
CG10154	CG10154 gene product from transcript CG10154-RA	2.643655958	0.989048785	1
psd	palisade	2.626795572	0.999934285	1
CG42588	CG42588 gene product from transcript CG42588-RA	2.621354235	0.999994511	1
rempA	reduced mechanoreceptor potential A	2.620409969	0.998925936	1
CG10916	CG10916 gene product from transcript CG10916-RA	2.610064382	0.999984251	1
CG13681	CG13681 gene product from transcript CG13681-RA	2.601795504	0.995623977	1
Nmnat	Nicotinamide mononucleotide adenylyltransferase	2.592055116	0.996894037	1
mthl5	methuselah-like 5	2.591494643	0.999767377	1
ninaB	neither inactivation nor afterpotential B	2.577719339	0.993666441	1
Sp7	Serine protease 7	2.576276141	0.987789499	1
vari	varicose	2.563768264	0.991886405	1
CG11382	CG11382 gene product from transcript CG11382-RB	2.561142547	0.999609324	1
CG14695	CG14695 gene product from transcript CG14695-RA	2.557948854	0.999764638	1
CG13623	CG13623 gene product from transcript CG13623-RA	2.549577867	0.999845381	1
CG5080	CG5080 gene product from transcript CG5080-RB	2.545745819	0.996154868	1
CG13594	CG13594 gene product from transcript CG13594-RA	2.544172323	0.999963406	1
CG10725	CG10725 gene product from transcript CG10725-RB	2.541001959	0.974509508	1
CG1792	CG1792 gene product from transcript CG1792-RA	2.539784194	0.999203905	1
CG10433	CG10433 gene product from transcript CG10433-RA	2.529280264	0.981085019	1
CG31676	CG31676 gene product from transcript CG31676-RA	2.516075335	0.981263396	1
CG3714	CG3714 gene product from transcript CG3714-RC	2.51299334	0.97474125	1
Tsp42Ej	Tetraspanin 42Ej	2.50378022	0.99592098	1

Annex 1. Differentially expressed genes in Apc Ras vs WT 4 weeks ACI comparison

symbol	genename	APC RAS vs WT 4week FC	APC RAS vs WT 4week PDE	APC RAS vs WT REJ
dgt2	dim gamma-tubulin 2	2.494796878	0.999790952	1
CG4945	CG4945 gene product from transcript CG4945-RA	2.488010572	0.978711433	1
CG6499	CG6499 gene product from transcript CG6499-RB	2.483599363	0.994475856	1
CG3635	CG3635 gene product from transcript CG3635-RB	2.483040784	0.997734971	1
Mekk1	CG7717 gene product from transcript CG7717-RB	2.482528424	0.999974866	1
Cpr66D	Cuticular protein 66D	2.480047616	0.99987716	1
Ugt86Dd	CG6633 gene product from transcript CG6633-RB	2.478115159	0.991870522	1
CG42390	CG42390 gene product from transcript CG42390-RB	2.465409552	0.980885136	1
CG12483	CG12483 gene product from transcript CG12483-RA	2.461029151	0.964205135	1
Spn43Ad	Serpin 43Ad	2.45896098	0.999997824	1
Sodh-2	Sorbitol dehydrogenase-2	2.454074883	0.999821521	1
CG7272	CG7272 gene product from transcript CG7272-RA	2.448782856	0.99999932	1
CG2076	CG2076 gene product from transcript CG2076-RA	2.448475296	0.999571659	1
PhKgamma	Phosphorylase kinase gamma	2.438853426	0.98303626	1
wun2	wunen-2	2.437381207	0.99995656	1
Irbp	Inverted repeat-binding protein	2.437213325	0.999999469	1
Vdup1	Vitamin D[[3]] up-regulated protein 1	2.419220589	0.996063247	1
CG18193	CG18193 gene product from transcript CG18193-RA	2.418215222	0.99984565	1
bw	brown	2.414980667	0.984988421	1
Ack	CG14992 gene product from transcript CG14992-RA	2.413170264	0.998637984	1
CG8252	CG8252 gene product from transcript CG8252-RA	2.410479577	0.987070252	1
CG13407	CG13407 gene product from transcript CG13407-RA	2.409944095	0.975149509	1
Obp44a	CG2297 gene product from transcript CG2297-RA	2.408270955	0.974029602	1
RhoGEF3	CG42378 gene product from transcript CG42378-RI	2.40416658	0.999486056	1
CG9641	CG9641 gene product from transcript CG9641-RA	2.404068465	0.999511594	1
loco	locomotion defects	2.396479485	0.999954822	1
Hex-A	Hexokinase A	2.386520651	0.9989959	1
Anxb11	Annexin B11	2.381586397	0.99931922	1
e	ebony	2.378704796	0.999846961	1
CG8740	CG8740 gene product from transcript CG8740-RD	2.374849983	0.997778223	1
CG1882	CG1882 gene product from transcript CG1882-RA	2.3690919	0.998077846	1
CG4674	CG4674 gene product from transcript CG4674-RA	2.369063881	0.975980341	1
ferrochelatase	CG2098 gene product from transcript CG2098-RC	2.364815354	0.997231336	1
CG13784	CG13784 gene product from transcript CG13784-RC	2.363893745	0.984919566	1
Jhl-26	Juvenile hormone-inducible protein 26	2.36089902	0.999223501	1
CG6005	CG6005 gene product from transcript CG6005-RA	2.358024803	0.996328506	1
B4	CG9239 gene product from transcript CG9239-RA	2.35482729	0.999938859	1
CG6084	CG6084 gene product from transcript CG6084-RB	2.348145975	0.999822658	1
CG13659	CG13659 gene product from transcript CG13659-RA	2.34688823	0.998436816	1
CG33275	CG33275 gene product from transcript CG33275-RA	2.344697129	0.971743726	1
CG10700	CG10700 gene product from transcript CG10700-RA	2.343495865	0.999882673	1
GstS1	Glutathione S transferase S1	2.33689364	0.959697931	1
Pgi	Phosphoglucose isomerase	2.336264818	0.998341628	1
CG17187	CG17187 gene product from transcript CG17187-RA	2.33488133	0.999933061	1
CG9773	CG9773 gene product from transcript CG9773-RA	2.334061058	0.999859417	1
CG7069	CG7069 gene product from transcript CG7069-RA	2.329422258	0.987581175	1
CG5535	CG5535 gene product from transcript CG5535-RC	2.326141911	0.998733706	1
CG16853	CG16853 gene product from transcript CG16853-RA	2.321286597	0.99724863	1
argos	CG4531 gene product from transcript CG4531-RA	2.319975067	0.977677341	1
CG10738	CG10738 gene product from transcript CG10738-RD	2.317537747	0.995549453	1
CG13360	CG13360 gene product from transcript CG13360-RA	2.315757981	0.99342764	1
CG13032	CG13032 gene product from transcript CG13032-RA	2.314078409	0.979766034	1
alph	alphabet	2.312203683	0.9935645	1
CG42588	CG42588 gene product from transcript CG42588-RA	2.30446136	0.99979415	1
Ku80	CG18801 gene product from transcript CG18801-RA	2.295313081	0.999999855	1
CG42588	CG42588 gene product from transcript CG42588-RA	2.293548242	0.999970586	1
CG11188	CG11188 gene product from transcript CG11188-RA	2.28939924	0.999322529	1
sob	sister of odd and bowl	2.285571647	0.995154792	1
Pgm	Phosphogluconate mutase	2.283200185	0.998279313	1
Cht12	CG30293 gene product from transcript CG30293-RA	2.281149598	0.987309793	1
CG1890	CG1890 gene product from transcript CG1890-RA	2.274594276	0.993254686	1
Alas	Aminolevulinate synthase	2.273341206	0.993909506	1

Annex 1. Differentially expressed genes in Apc Ras vs WT 4 weeks ACI comparison

symbol	genename	APC RAS vs WT 4week FC	APC RAS vs WT 4week PDE	APC RAS vs WT REJ
RpL28	Ribosomal protein L28	2.268032131	0.999058683	1
ferrochelatase	CG2098 gene product from transcript CG2098-RC	2.263402213	0.980588141	1
Corp	Companion of reaper	2.263074866	0.992934744	1
Task6	CG9637 gene product from transcript CG9637-RC	2.262245866	0.999981541	1
CG8979	CG8979 gene product from transcript CG8979-RC	2.25238055	0.994400634	1
CG14341	CG14341 gene product from transcript CG14341-RA	2.251239845	0.999967447	1
CG2051	CG2051 gene product from transcript CG2051-RA	2.244527278	0.997495891	1
CG6023	CG6023 gene product from transcript CG6023-RA	2.241766689	0.96666987	1
CG4408	CG4408 gene product from transcript CG4408-RA	2.240448276	0.999952612	1
CG10738	CG10738 gene product from transcript CG10738-RD	2.239137041	0.993077931	1
eIF2B-delta	CG10315 gene product from transcript CG10315-RA	2.23509601	0.997920892	1
br	broad	2.234697279	0.972023894	1
mud	mushroom body defect	2.232210645	0.999582992	1
rumi	CG31152 gene product from transcript CG31152-RA	2.230037406	0.999976245	1
jbug	jitterbug	2.228186836	0.996656453	1
CG15745	CG15745 gene product from transcript CG15745-RB	2.227623952	0.999739725	1
Nc	Nedd2-like caspase	2.22178195	0.999494897	1
CG31549	CG31549 gene product from transcript CG31549-RA	2.215449916	0.999765545	1
CG42389	CG42389 gene product from transcript CG42389-RE	2.214210322	0.998735832	1
CG6428	CG6428 gene product from transcript CG6428-RA	2.213765316	0.993470416	1
Incenp	Inner centromere protein	2.213406593	0.996065085	1
CG14340	CG14340 gene product from transcript CG14340-RA	2.211638702	0.999390941	1
CG12868	CG12868 gene product from transcript CG12868-RB	2.211187478	0.998310694	1
CG17387	CG17387 gene product from transcript CG17387-RA	2.210030257	0.999945924	1
Fas2	Fasciclin 2	2.206758579	0.999185199	1
Gpo-1	Glycerophosphate oxidase-1	2.203641952	0.993436804	1
CG9302	CG9302 gene product from transcript CG9302-RA	2.203630907	0.99964841	1
bcd	bicoid	2.202949952	0.969365964	1
CG8188	CG8188 gene product from transcript CG8188-RB	2.202340572	0.999566548	1
CG5953	CG5953 gene product from transcript CG5953-RA	2.201633294	0.999777095	1
Ptp10D	Protein tyrosine phosphatase 10D	2.199797484	0.995355414	1
Wnt5	Wnt oncogene analog 5	2.199481896	0.995393864	1
CG1407	CG1407 gene product from transcript CG1407-RB	2.199160527	0.956645431	1
l(1)G0289	lethal (1) G0289	2.198310649	0.997578827	1
mthl8	methuselah-like 8	2.198030708	0.98132346	1
CG10947	CG10947 gene product from transcript CG10947-RC	2.193597882	0.991894828	1
ptc	patched	2.192396734	0.998178766	1
Fas2	Fasciclin 2	2.189324285	0.999885316	1
CG17327	CG17327 gene product from transcript CG17327-RB	2.186484072	0.999977141	1
fax	failed axon connections	2.185566893	0.966110831	1
Gap1	GTPase-activating protein 1	2.185522874	0.995063703	1
CG13361	CG13361 gene product from transcript CG13361-RA	2.182009666	0.975394124	1
CG32549	CG32549 gene product from transcript CG32549-RD	2.181426125	0.99996238	1
stil	stand still	2.180563116	0.999127424	1
CG2857	CG2857 gene product from transcript CG2857-RA	2.177439899	0.974661474	1
CG12264	CG12264 gene product from transcript CG12264-RA	2.174007149	0.999877947	1
pxb	CG33207 gene product from transcript CG33207-RB	2.172989021	0.994963481	1
CG42458	CG42458 gene product from transcript CG42458-RA	2.168397579	0.987828164	1
Orct2	Organic cation transporter 2	2.166984757	0.999517692	1
CG17352	CG17352 gene product from transcript CG17352-RA	2.166510248	0.971856929	1
Cht9	CG10531 gene product from transcript CG10531-RA	2.164974739	0.999966322	1
GstD10	Glutathione S transferase D10	2.155470403	0.995263246	1
CG11380	CG11380 gene product from transcript CG11380-RA	2.155338948	0.998370233	1
CG42254	CG42254 gene product from transcript CG42254-RB	2.154455788	0.996788551	1
c11.1	CG12132 gene product from transcript CG12132-RA	2.154183597	0.982699288	1
CG34396	CG34396 gene product from transcript CG34396-RC	2.152924625	0.980624973	1
CG34388	CG34388 gene product from transcript CG34388-RC	2.152446448	0.997937618	1
CG14624	CG14624 gene product from transcript CG14624-RA	2.140666329	0.991449557	1
CG11289	CG11289 gene product from transcript CG11289-RB	2.138510008	0.97668775	1
Sox14	Sox box protein 14	2.137399874	0.995759728	1
CG2765	CG2765 gene product from transcript CG2765-RE	2.135925284	0.99937863	1
GstD3	Glutathione S transferase D3	2.131949225	0.998798561	1

Annex 1. Differentially expressed genes in Apc Ras vs WT 4 weeks ACI comparison

symbol	genename	APC RAS vs WT 4week FC	APC RAS vs WT 4week PDE	APC RAS vs WT REJ
msd5	mitotic spindle density 5	2.130776604	0.994606877	1
CG5273	CG5273 gene product from transcript CG5273-RA	2.129653864	0.999226509	1
CG11170	CG11170 gene product from transcript CG11170-RB	2.127690194	0.996344539	1
cenB1A	centaurin beta 1A	2.126554566	0.969673109	1
CG32700	CG32700 gene product from transcript CG32700-RA	2.125838986	0.992926358	1
CG2658	CG2658 gene product from transcript CG2658-RB	2.124967746	0.998191787	1
CG8547	CG8547 gene product from transcript CG8547-RC	2.12379911	0.957468023	1
CG9917	CG9917 gene product from transcript CG9917-RA	2.121794525	0.999967909	1
Tsp42Eg	Tetraspanin 42Eg	2.120755889	0.988871569	1
CG8870	CG8870 gene product from transcript CG8870-RA	2.116951701	0.986703079	1
Traf4	TNF-receptor-associated factor 4	2.115970219	0.999104387	1
Dcp-1	Death caspase-1	2.115587598	0.999887215	1
Bin1	Bicoid interacting protein 1	2.11518772	0.999874978	1
rev7	CG2948 gene product from transcript CG2948-RA	2.108140442	0.995344685	1
O-fut1	O-fucosyltransferase 1	2.105683554	0.999699837	1
sni	sniffer	2.102710563	0.999972125	1
CG5205	CG5205 gene product from transcript CG5205-RA	2.096210836	0.999796234	1
CG15173	CG15173 gene product from transcript CG15173-RA	2.093452528	0.999707321	1
CG33136	CG33136 gene product from transcript CG33136-RA	2.089796755	0.999256173	1
CG31457	CG31457 gene product from transcript CG31457-RB	2.088916463	0.998987985	1
CG31025	CG31025 gene product from transcript CG31025-RA	2.085535745	0.97472947	1
l(2)k16918	lethal (2) k16918	2.083390504	0.950579846	1
CG12029	CG12029 gene product from transcript CG12029-RB	2.080801985	0.966422954	1
Ir100a	Ionotropic receptor 100a	2.078736108	0.997200766	1
Ero1L	Endoplasmic reticulum oxidoreductin-1-like	2.077962859	0.998012856	1
RfC4	Replication factor C subunit 4	2.076292317	0.998867528	1
18w	18 wheeler	2.07573386	0.984678347	1
GXIVsPLA2	CG17035 gene product from transcript CG17035-RC	2.075195654	0.975347996	1
Aats-trp	Tryptophanyl-tRNA synthetase	2.074933483	0.999879267	1
XRCC1	CG4208 gene product from transcript CG4208-RA	2.06929776	0.997397452	1
CG42565	CG42565 gene product from transcript CG42565-RA	2.066052173	0.987880325	1
CG7224	CG7224 gene product from transcript CG7224-RB	2.065139892	0.998056442	1
CG2865	CG2865 gene product from transcript CG2865-RA	2.061794022	0.999394099	1
Mocs1	CG33048 gene product from transcript CG33048-RA	2.06062557	0.99919217	1
CG13784	CG13784 gene product from transcript CG13784-RC	2.059181615	0.999796084	1
spas	spastin	2.05770177	0.988047545	1
PHGPx	CG12013 gene product from transcript CG12013-RC	2.054807718	0.999990819	1
CG13887	CG13887 gene product from transcript CG13887-RC	2.053563753	0.999965779	1
CG31115	CG31115 gene product from transcript CG31115-RB	2.051968422	0.999688892	1
ferrochelatase	CG2098 gene product from transcript CG2098-RC	2.043904276	0.995991102	1
CG6983	CG6983 gene product from transcript CG6983-RA	2.041119687	0.998522217	1
Ant2	Adenine nucleotide translocase 2	2.040361165	0.999757887	1
e(y)2b	enhancer of yellow 2b	2.026627129	0.972715848	1
CG5421	CG5421 gene product from transcript CG5421-RA	2.026130703	0.969650352	1
HBS1	CG1898 gene product from transcript CG1898-RA	2.016847292	0.999806483	1
ald	altered disjunction	2.008418768	0.99487316	1
CG10268	CG10268 gene product from transcript CG10268-RA	2.00812155	0.998759954	1
out	outsiders	2.004109002	0.996997511	1
Prp31	CG6876 gene product from transcript CG6876-RA	2.003558972	0.998560348	1
Aats-trp	Tryptophanyl-tRNA synthetase	2.000435142	0.999774191	1
Mical	Molecule interacting with CasL	-2.001827015	0.999934524	-1
Adk3	Adenylate kinase-3	-2.002252242	0.977199234	-1
CG32486	CG32486 gene product from transcript CG32486-RD	-2.019240715	0.999970288	-1
CG11163	CG11163 gene product from transcript CG11163-RD	-2.021569463	0.999908159	-1
mmy	mummy	-2.022160211	0.997385062	-1
CG33523	CG33523 gene product from transcript CG33523-RD	-2.02269488	0.978843897	-1
Cpr51A	Cuticular protein 51A	-2.025225161	0.968013503	-1
Klp98A	Kinesin-like protein at 98A	-2.025414354	0.998462572	-1
CG5707	CG5707 gene product from transcript CG5707-RA	-2.028492716	0.999990328	-1
Mctp	Multiple C2 domain and transmembrane protein	-2.034706161	0.992894393	-1
Myo95E	Myosin 95E	-2.037072789	0.998479022	-1
gukh	GUK-holder	-2.037342255	0.999997684	-1

Annex 1. Differentially expressed genes in Apc Ras vs WT 4 weeks ACI comparison

symbol	genename	APC RAS vs WT 4week FC	APC RAS vs WT 4week PDE	APC RAS vs WT REJ
CG2118	CG2118 gene product from transcript CG2118-RB	-2.037569166	0.996627267	-1
CG7458	CG7458 gene product from transcript CG7458-RA	-2.046302919	0.999876923	-1
CG12963	CG12963 gene product from transcript CG12963-RD	-2.049291525	0.984226283	-1
CG34394	CG34394 gene product from transcript CG34394-RD	-2.0511588	0.999988084	-1
CG5932	CG5932 gene product from transcript CG5932-RA	-2.05568619	0.955423037	-1
CG33232	CG33232 gene product from transcript CG33232-RD	-2.057074283	0.99972379	-1
CG5849	CG5849 gene product from transcript CG5849-RB	-2.057505601	0.999965596	-1
vnd	ventral nervous system defective	-2.065131664	0.99999593	-1
CG32813	CG32813 gene product from transcript CG32813-RE	-2.068465556	0.985690779	-1
CG32148	CG32148 gene product from transcript CG32148-RA	-2.069246016	0.994708141	-1
dpr7	CG33481 gene product from transcript CG33481-RC	-2.071974096	0.982447671	-1
cac	cacophony	-2.073870386	0.978726277	-1
Neu3	CG7649 gene product from transcript CG7649-RC	-2.078731279	0.971201306	-1
laza	lazaro	-2.085442629	0.992565226	-1
CG2678	CG2678 gene product from transcript CG2678-RA	-2.094529408	0.980995157	-1
CG18747	CG18747 gene product from transcript CG18747-RB	-2.095087596	0.980122347	-1
CG34376	CG34376 gene product from transcript CG34376-RB	-2.101376257	0.98787492	-1
CG12355	CG12355 gene product from transcript CG12355-RD	-2.10365988	0.965548384	-1
Tango13	Transport and Golgi organization 13	-2.103948207	0.999934685	-1
Ugt35a	UDP-glycosyltransferase 35a	-2.105457307	0.999521048	-1
luna	CG33473 gene product from transcript CG33473-RB	-2.10625848	0.980252606	-1
CG13607	CG13607 gene product from transcript CG13607-RC	-2.108045288	0.99999763	-1
dnc	dunce	-2.109089863	0.9988245	-1
Mgstl	Microsomal glutathione S-transferase-like	-2.116846253	0.999890861	-1
CG31004	CG31004 gene product from transcript CG31004-RC	-2.126320714	0.998851767	-1
Ugt86Dj	CG15902 gene product from transcript CG15902-RA	-2.13018981	0.971014417	-1
ZnT35C	CG3994 gene product from transcript CG3994-RA	-2.130560376	0.997928576	-1
Cyp4ac1	CG14032 gene product from transcript CG14032-RA	-2.135726643	0.999932742	-1
CG4893	CG4893 gene product from transcript CG4893-RA	-2.13926389	0.999926211	-1
CG5599	CG5599 gene product from transcript CG5599-RA	-2.139811788	0.999997796	-1
CG15044	CG15044 gene product from transcript CG15044-RA	-2.140037374	0.973910708	-1
Tsp29Fb	Tetraspanin 29Fb	-2.14038877	0.997051637	-1
CG3301	CG3301 gene product from transcript CG3301-RB	-2.143466517	0.99363042	-1
Mct1	Monocarboxylate transporter 1	-2.146772868	0.999867301	-1
HLHm7	E(spl) region transcript m7	-2.150092377	0.975497032	-1
dnd	dead end	-2.151274298	0.998522684	-1
Cyp6w1	CG8345 gene product from transcript CG8345-RA	-2.152735506	0.961500163	-1
Spn42Dc	Serpin 42Dc	-2.154259717	0.999892681	-1
Doa	Darkener of apricot	-2.156781712	0.957811291	-1
CG33514	CG33514 gene product from transcript CG33514-RA	-2.1651671	0.99722877	-1
CG10086	CG10086 gene product from transcript CG10086-RA	-2.165463584	0.998690311	-1
put	punt	-2.1700446	0.991895008	-1
CG10650	CG10650 gene product from transcript CG10650-RA	-2.170163889	0.999922592	-1
CG9672	CG9672 gene product from transcript CG9672-RA	-2.174735013	0.999581907	-1
CG13081	CG13081 gene product from transcript CG13081-RA	-2.174859761	0.957953662	-1
CG11967	CG11967 gene product from transcript CG11967-RA	-2.177200117	0.99999607	-1
CG30429	CG30429 gene product from transcript CG30429-RA	-2.182401388	0.953518982	-1
Trim9	CG31721 gene product from transcript CG31721-RB	-2.185090074	0.999010494	-1
CG8072	CG8072 gene product from transcript CG8072-RA	-2.189507719	0.991811397	-1
CG14253	CG14253 gene product from transcript CG14253-RB	-2.190823751	0.977059784	-1
CG13229	CG13229 gene product from transcript CG13229-RA	-2.191299599	0.99009697	-1
CG10562	CG10562 gene product from transcript CG10562-RA	-2.192618092	0.996381908	-1
Ugt86Dh	CG4772 gene product from transcript CG4772-RA	-2.192935612	0.987534095	-1
Fim	Fimbrin	-2.194416819	0.998595317	-1
CG10175	CG10175 gene product from transcript CG10175-RA	-2.204037083	0.995687803	-1
CG31454	CG31454 gene product from transcript CG31454-RA	-2.204336513	0.983345946	-1
Ptp99A	Protein tyrosine phosphatase 99A	-2.208753664	0.971791355	-1
CG3301	CG3301 gene product from transcript CG3301-RB	-2.224763307	0.957102796	-1
CG11739	CG11739 gene product from transcript CG11739-RC	-2.241772172	0.994132478	-1
CG5381	CG5381 gene product from transcript CG5381-RA	-2.242370764	0.999918499	-1
CG4783	CG4783 gene product from transcript CG4783-RA	-2.243173156	0.989026027	-1
CG6043	CG6043 gene product from transcript CG6043-RG	-2.245627908	0.98575387	-1

Annex 1. Differentially expressed genes in Apc Ras vs WT 4 weeks ACI comparison

symbol	genename	APC RAS vs WT 4week FC	APC RAS vs WT 4week PDE	APC RAS vs WT REJ
CG7777	CG7777 gene product from transcript CG7777-RB	-2.248174724	0.979954148	-1
CG6954	CG6954 gene product from transcript CG6954-RB	-2.250307462	0.999603442	-1
CG13323	CG13323 gene product from transcript CG13323-RA	-2.259209581	0.994283125	-1
Sema-5c	Semaphorin-5c	-2.260027113	0.999441116	-1
beat-IIIc	CG15138 gene product from transcript CG15138-RA	-2.273777412	0.994505211	-1
CG3987	CG3987 gene product from transcript CG3987-RA	-2.274291807	0.999651308	-1
Gpdh	Glycerol 3 phosphate dehydrogenase	-2.278056322	0.988461345	-1
mthl10	methuselah-like 10	-2.278604032	0.999890686	-1
Ca-alpha1D	Ca[2+]-channel protein alpha[[1]] subunit D	-2.281216843	0.980828122	-1
CG7997	CG7997 gene product from transcript CG7997-RB	-2.288249485	0.999987336	-1
Glycogenin	CG9480 gene product from transcript CG9480-RA	-2.289108111	0.993236525	-1
CG10283	CG10283 gene product from transcript CG10283-RB	-2.292127867	0.999004211	-1
Jon74E	Jonah 74E	-2.293954718	0.956225298	-1
CG30043	CG30043 gene product from transcript CG30043-RA	-2.301763683	0.989765843	-1
qtc	quick-to-court	-2.304934546	0.996773668	-1
RpS7	Ribosomal protein S7	-2.305343358	0.998172254	-1
dpr10	CG32057 gene product from transcript CG32057-RB	-2.306431687	0.999658352	-1
Pkg21D	cGMP-dependent protein kinase 21D	-2.307750752	0.964024721	-1
CG31345	CG31345 gene product from transcript CG31345-RA	-2.314018341	0.999592005	-1
Mitf	CG17469 gene product from transcript CG17469-RA	-2.326641693	0.986794952	-1
CG31102	CG31102 gene product from transcript CG31102-RA	-2.340156295	0.999973253	-1
Cyp12a4	CG6042 gene product from transcript CG6042-RA	-2.342141204	0.999270494	-1
CG30345	CG30345 gene product from transcript CG30345-RA	-2.347626243	0.982875524	-1
Pde6	Phosphodiesterase 6	-2.347858761	0.988037165	-1
CG30049	CG30049 gene product from transcript CG30049-RA	-2.350132996	0.970582959	-1
CG33013	CG33013 gene product from transcript CG33013-RC	-2.350743761	0.968438598	-1
CG40498	CG40498 gene product from transcript CG40498-RF	-2.351746042	0.958868048	-1
Syt1	Synaptotagmin 1	-2.353364872	0.986851582	-1
CG6126	CG6126 gene product from transcript CG6126-RA	-2.358422154	0.999962361	-1
CG15233	CG15233 gene product from transcript CG15233-RA	-2.365442331	0.999632259	-1
CG13704	CG13704 gene product from transcript CG13704-RA	-2.366665601	0.99996426	-1
CG6465	CG6465 gene product from transcript CG6465-RA	-2.367154309	0.985009452	-1
cic	capicua	-2.36970039	0.999942701	-1
CG5267	CG5267 gene product from transcript CG5267-RA	-2.373038299	0.998520901	-1
CG17834	CG17834 gene product from transcript CG17834-RA	-2.377793177	0.976399709	-1
unc-5	CG8166 gene product from transcript CG8166-RA	-2.378782169	0.983736033	-1
CG9339	CG9339 gene product from transcript CG9339-RG	-2.392158597	0.999943648	-1
CG4653	CG4653 gene product from transcript CG4653-RA	-2.392557236	0.962773455	-1
FucTA	CG6869 gene product from transcript CG6869-RA	-2.403282172	0.996927624	-1
RpS11	Ribosomal protein S11	-2.417350256	0.953056139	-1
Pka-R1	cAMP-dependent protein kinase R1	-2.425426914	0.993963528	-1
CG5568	CG5568 gene product from transcript CG5568-RA	-2.426517865	0.981950932	-1
Gpdh	Glycerol 3 phosphate dehydrogenase	-2.427036823	0.999750183	-1
glob1	globin 1	-2.43585161	0.999947719	-1
CG11961	CG11961 gene product from transcript CG11961-RB	-2.437926539	0.999779366	-1
Ect4	CG34373 gene product from transcript CG34373-RD	-2.441301756	0.990927369	-1
CG10663	CG10663 gene product from transcript CG10663-RB	-2.442714208	0.991793079	-1
MESK2	Misexpression suppressor of KSR 2	-2.444865615	0.986356035	-1
CG10877	CG10877 gene product from transcript CG10877-RA	-2.453247937	0.999022424	-1
CG10184	CG10184 gene product from transcript CG10184-RA	-2.470574067	0.965999859	-1
CG31763	CG31763 gene product from transcript CG31763-RA	-2.475844496	0.992215834	-1
oc	ocelliless	-2.48575648	0.997594814	-1
CG9380	CG9380 gene product from transcript CG9380-RC	-2.492414853	0.999999921	-1
CG7497	CG7497 gene product from transcript CG7497-RB	-2.493116099	0.989005339	-1
CG6967	CG6967 gene product from transcript CG6967-RD	-2.500760819	0.998117611	-1
lbk	lambik	-2.510242027	0.999122932	-1
CG10178	CG10178 gene product from transcript CG10178-RA	-2.51352796	0.997980902	-1
CG15117	CG15117 gene product from transcript CG15117-RA	-2.531764614	0.999999031	-1
klu	klumpfuss	-2.532581161	0.996910964	-1
CG10479	CG10479 gene product from transcript CG10479-RA	-2.53544554	0.999014441	-1
CG7470	CG7470 gene product from transcript CG7470-RA	-2.53709847	0.965640826	-1
CG10827	CG10827 gene product from transcript CG10827-RA	-2.537250323	0.977135253	-1

Annex 1. Differentially expressed genes in Apc Ras vs WT 4 weeks ACI comparison

symbol	genename	APC RAS vs WT 4week FC	APC RAS vs WT 4week PDE	APC RAS vs WT REJ
Rgk3	CG34397 gene product from transcript CG34397-RC	-2.537660988	0.999950003	-1
CG10077	CG10077 gene product from transcript CG10077-RA	-2.539365016	0.997736071	-1
tkv	thickveins	-2.547332924	0.99645384	-1
ptr	proximal to raf	-2.558335058	0.99914421	-1
sut2	sugar transporter 2	-2.562236347	0.982981998	-1
CG10943	CG10943 gene product from transcript CG10943-RA	-2.58729458	0.994217945	-1
CG1681	CG1681 gene product from transcript CG1681-RA	-2.588018233	0.975575005	-1
jing	CG9397 gene product from transcript CG9397-RI	-2.606883709	0.999819612	-1
decay	death executioner caspase related to Apopain/Yama	-2.60730962	0.999300013	-1
pcl	pepsinogen-like	-2.622172853	0.993810517	-1
beat-IIa	beaten path IIa	-2.630303945	0.961416168	-1
aay	astray	-2.631239119	0.999962824	-1
cindr	CIN85 and CD2AP orthologue	-2.641562179	0.969585512	-1
for	foraging	-2.645799403	0.997488401	-1
CG13917	CG13917 gene product from transcript CG13917-RB	-2.648693049	0.999241893	-1
CG3277	CG3277 gene product from transcript CG3277-RC	-2.651921309	0.99987741	-1
CG13300	CG13300 gene product from transcript CG13300-RA	-2.656943591	0.991582484	-1
Pdp1	PAR-domain protein 1	-2.666120185	0.985986608	-1
Stat92E	Signal-transducer and activator of transcription at 92E	-2.669190889	0.999394756	-1
luna	CG33473 gene product from transcript CG33473-RB	-2.671433222	0.999756397	-1
wit	wishful thinking	-2.674043366	0.997050746	-1
mthl10	methuselah-like 10	-2.678153674	0.999991957	-1
CG5697	CG5697 gene product from transcript CG5697-RA	-2.678625566	0.999999997	-1
CG9743	CG9743 gene product from transcript CG9743-RA	-2.684771976	0.999999729	-1
CG33099	CG33099 gene product from transcript CG33099-RA	-2.693253325	0.98604538	-1
CG31704	CG31704 gene product from transcript CG31704-RA	-2.693679891	0.977928387	-1
KCNQ	KCNQ potassium channel	-2.695233715	0.997462841	-1
CG8907	CG8907 gene product from transcript CG8907-RA	-2.696642715	0.983389307	-1
CG16986	CG16986 gene product from transcript CG16986-RA	-2.70071897	0.99951832	-1
CG6527	CG6527 gene product from transcript CG6527-RA	-2.719418621	0.973696796	-1
CG13086	CG13086 gene product from transcript CG13086-RA	-2.721476511	0.995108879	-1
CG34010	CG34010 gene product from transcript CG34010-RA	-2.722525075	0.999026017	-1
smp-30	Senescence marker protein-30	-2.723537827	0.971167803	-1
CG3308	CG3308 gene product from transcript CG3308-RA	-2.743612554	0.999822171	-1
CG17855	CG17855 gene product from transcript CG17855-RA	-2.748834591	0.999941889	-1
CG15309	CG15309 gene product from transcript CG15309-RA	-2.752327092	0.989313947	-1
CG11155	CG11155 gene product from transcript CG11155-RA	-2.75703257	0.985699106	-1
CG11068	CG11068 gene product from transcript CG11068-RA	-2.76203345	0.992685728	-1
CG3734	CG3734 gene product from transcript CG3734-RA	-2.775549281	0.985271882	-1
CG13827	CG13827 gene product from transcript CG13827-RA	-2.777469853	0.999832706	-1
Cg25C	Collagen type IV	-2.789407655	0.966011762	-1
Cyp9b2	Cytochrome P450-9b2	-2.801302227	0.999756668	-1
CG30463	CG30463 gene product from transcript CG30463-RB	-2.815674473	0.996179769	-1
nimC3	nimrod C3	-2.851937026	0.998354482	-1
Fer1	48 related 1	-2.864203007	0.975059714	-1
CG8301	CG8301 gene product from transcript CG8301-RA	-2.865796745	0.996974616	-1
CG15186	CG15186 gene product from transcript CG15186-RA	-2.869217418	0.999545029	-1
CG6234	CG6234 gene product from transcript CG6234-RA	-2.87576681	0.999861768	-1
CG5011	CG5011 gene product from transcript CG5011-RA	-2.87623745	0.990184003	-1
CG10170	CG10170 gene product from transcript CG10170-RA	-2.877989412	0.999797916	-1
pros	prospero	-2.883687123	0.951324734	-1
CG17278	CG17278 gene product from transcript CG17278-RA	-2.88766499	0.987725551	-1
CG32407	CG32407 gene product from transcript CG32407-RA	-2.903610575	0.99825584	-1
CG14741	CG14741 gene product from transcript CG14741-RB	-2.943349183	0.999995175	-1
tej	tejas	-2.953711173	0.999045763	-1
Dl	Delta	-2.962590479	0.99999999	-1
CG12560	CG12560 gene product from transcript CG12560-RB	-2.965889979	0.999348183	-1
CG7992	CG7992 gene product from transcript CG7992-RA	-2.967307619	0.960882954	-1
CG15422	CG15422 gene product from transcript CG15422-RA	-2.970738366	0.999956263	-1
sba	six-banded	-2.972768448	0.991466608	-1
fus	fusilli	-2.978834583	0.999956008	-1
Cbl	CG7037 gene product from transcript CG7037-RB	-2.994141522	0.999998785	-1

Annex 1. Differentially expressed genes in Apc Ras vs WT 4 weeks ACI comparison

symbol	genename	APC RAS vs WT 4week FC	APC RAS vs WT 4week PDE	APC RAS vs WT REJ
CG42336	CG42336 gene product from transcript CG42336-RB	-3.003063414	0.999997761	-1
CG10249	CG10249 gene product from transcript CG10249-RJ	-3.027469934	0.9986168	-1
a	arc	-3.054899059	0.9998288	-1
Tsp29Fa	Tetraspanin 29Fa	-3.062581848	0.99999977	-1
fok	fledgling of Klp38B	-3.078142166	0.999977877	-1
CG10168	CG10168 gene product from transcript CG10168-RA	-3.106933376	0.999991317	-1
CG13492	CG13492 gene product from transcript CG13492-RC	-3.110338984	0.997888834	-1
HLHmgamma	E(spl) region transcript mgamma	-3.123105635	0.999999512	-1
CG3902	CG3902 gene product from transcript CG3902-RA	-3.139904491	0.999997102	-1
sens-2	senseless-2	-3.19161265	0.96511273	-1
CG12910	CG12910 gene product from transcript CG12910-RA	-3.196298026	0.999971757	-1
m-cup	mann-cup	-3.215147373	0.999951982	-1
osp	outspread	-3.226102828	0.965274826	-1
CG18869	CG18869 gene product from transcript CG18869-RA	-3.240008704	0.999780544	-1
CG8690	CG8690 gene product from transcript CG8690-RA	-3.242949014	0.960379997	-1
tap	target of Poxn	-3.25469998	0.986969059	-1
CG7678	CG7678 gene product from transcript CG7678-RA	-3.262091648	0.989196367	-1
CG34376	CG34376 gene product from transcript CG34376-RB	-3.272784387	0.999380247	-1
Tie	Tie-like receptor tyrosine kinase	-3.273980517	0.9999321	-1
Damm	Death associated molecule related to Mch2	-3.282245253	0.999695673	-1
corto	CG2530 gene product from transcript CG2530-RA	-3.282609841	0.984324359	-1
CG4753	CG4753 gene product from transcript CG4753-RB	-3.283004127	0.997633384	-1
CG32687	CG32687 gene product from transcript CG32687-RA	-3.308817524	0.993417486	-1
Gpdh	Glycerol 3 phosphate dehydrogenase	-3.315672033	0.999994274	-1
CG11155	CG11155 gene product from transcript CG11155-RA	-3.316571609	0.997148574	-1
CG2177	CG2177 gene product from transcript CG2177-RA	-3.319959119	0.980958778	-1
Dat	Dopamine N acetyltransferase	-3.322323008	0.999808391	-1
ect	ectodermal	-3.332207956	0.992123896	-1
rap	retina aberrant in pattern	-3.348699489	0.975185056	-1
CG31431	CG31431 gene product from transcript CG31431-RA	-3.364939036	0.999980856	-1
dally	division abnormally delayed	-3.388524535	0.985576839	-1
Sytbeta	Synaptotagmin beta	-3.407684196	0.987452546	-1
Ih	I[[h]] channel	-3.408985655	0.999860314	-1
CG8008	CG8008 gene product from transcript CG8008-RB	-3.468984129	0.999954703	-1
CG32264	CG32264 gene product from transcript CG32264-RH	-3.490969546	0.9998165	-1
CG9380	CG9380 gene product from transcript CG9380-RC	-3.504297307	0.999344165	-1
CG15127	CG15127 gene product from transcript CG15127-RA	-3.507136981	0.995532468	-1
CG31248	CG31248 gene product from transcript CG31248-RA	-3.522077199	0.999997465	-1
CG10157	CG10157 gene product from transcript CG10157-RA	-3.52518586	0.999440056	-1
CG34401	CG34401 gene product from transcript CG34401-RA	-3.531026999	0.999949121	-1
amon	amontillado	-3.603141812	0.984680745	-1
CG42397	CG42397 gene product from transcript CG42397-RA	-3.607321252	0.956074929	-1
cry	cryptochrome	-3.613426722	0.999942942	-1
Pal	Peptidyl-alpha-hydroxyglycine-alpha-amidating lyase	-3.629871136	0.959707893	-1
CG11878	CG11878 gene product from transcript CG11878-RA	-3.631965544	0.999892274	-1
Nplp2	Neuropeptide-like precursor 2	-3.632695064	0.999993606	-1
CG2201	CG2201 gene product from transcript CG2201-RA	-3.645077139	0.999420209	-1
nrv3	nervana 3	-3.6893105	0.989238449	-1
Esyt2	CG6643 gene product from transcript CG6643-RA	-3.69279391	0.991785978	-1
CG34176	CG34176 gene product from transcript CG34176-RA	-3.711383258	0.999750654	-1
CG4752	CG4752 gene product from transcript CG4752-RA	-3.750048336	0.9999116	-1
7B2	CG1168 gene product from transcript CG1168-RB	-3.760773493	0.987719055	-1
Apc	APC-like	-3.787631406	0.998844837	-1
CG15611	CG15611 gene product from transcript CG15611-RB	-3.855655196	0.999999368	-1
CG30106	CG30106 gene product from transcript CG30106-RA	-3.856606983	0.999014858	-1
Ahcy89E	Adenosylhomocysteinase 89E	-3.95155604	0.993857621	-1
CG9568	CG9568 gene product from transcript CG9568-RA	-3.982812415	0.987439033	-1
CG7777	CG7777 gene product from transcript CG7777-RB	-4.033007502	0.999999578	-1
CG6006	CG6006 gene product from transcript CG6006-RC	-4.099715298	0.999974241	-1
CG6018	CG6018 gene product from transcript CG6018-RA	-4.103287972	0.9999646	-1
CG32633	CG32633 gene product from transcript CG32633-RA	-4.217555223	0.999861011	-1
Takl1	Tak1-like 1	-4.219471572	0.999843305	-1

Annex 1. Differentially expressed genes in Apc Ras vs WT 4 weeks ACI comparison

symbol	genename	APC RAS vs WT 4week FC	APC RAS vs WT 4week PDE	APC RAS vs WT REJ
CDase	Ceramidase	-4.269583093	0.999999228	-1
kar	karmoisin	-4.296537313	0.999972649	-1
LvpD	Larval visceral protein D	-4.350181126	0.997258162	-1
DAAM	Dishevelled Associated Activator of Morphogenesis	-4.352308236	0.989607703	-1
CG2556	CG2556 gene product from transcript CG2556-RA	-4.403568805	0.999999976	-1
CG42336	CG42336 gene product from transcript CG42336-RB	-4.426586305	0.999985513	-1
CG11241	CG11241 gene product from transcript CG11241-RB	-4.427835011	0.999979324	-1
CG16997	CG16997 gene product from transcript CG16997-RB	-4.433425998	0.999485757	-1
Dl	Delta	-4.434625682	0.999501744	-1
CG16732	CG16732 gene product from transcript CG16732-RB	-4.469786481	0.999980603	-1
CG4363	CG4363 gene product from transcript CG4363-RA	-4.486262166	0.97551224	-1
CG34198	CG34198 gene product from transcript CG34198-RA	-4.577718851	0.999996173	-1
tomboy20	CG14690 gene product from transcript CG14690-RA	-4.669825063	0.999978501	-1
Tsp42Er	Tetraspanin 42Er	-4.678483117	0.999989	-1
CG30283	CG30283 gene product from transcript CG30283-RB	-4.68037981	0.999999948	-1
CG31997	CG31997 gene product from transcript CG31997-RA	-4.791619088	0.999103013	-1
Rab9	CG9994 gene product from transcript CG9994-RA	-4.798086411	0.9999802	-1
LvpH	Larval visceral protein H	-4.83758972	0.982952282	-1
CG13278	CG13278 gene product from transcript CG13278-RA	-4.85770351	0.98860486	-1
MtnC	Metallothionein C	-4.87024236	0.974586428	-1
unc-104	CG8566 gene product from transcript CG8566-RB	-4.918028307	0.999571996	-1
CG31076	CG31076 gene product from transcript CG31076-RA	-4.931070393	0.999999621	-1
CG6129	CG6129 gene product from transcript CG6129-RD	-5.024686822	0.999999512	-1
CG6287	CG6287 gene product from transcript CG6287-RA	-5.039776596	0.999951654	-1
CG15629	CG15629 gene product from transcript CG15629-RA	-5.055061818	0.998029864	-1
CG33514	CG33514 gene product from transcript CG33514-RA	-5.11278435	0.999998422	-1
nub	nubbin	-5.128002517	0.99482515	-1
bib	big brain	-5.167053945	0.997187496	-1
Jon65Aiii	Jonah 65Aiii	-5.239088399	0.962185932	-1
m1	E(spl) region transcript m1	-5.324420613	0.999963753	-1
CG42249	CG42249 gene product from transcript CG42249-RC	-5.333046317	0.977421114	-1
Jheh3	Juvenile hormone epoxide hydrolase 3	-5.373722966	0.999540241	-1
CG9360	CG9360 gene product from transcript CG9360-RA	-5.471718231	0.986818805	-1
bru-2	bruno-2	-5.496655766	0.999905304	-1
Mad	Mothers against dpp	-5.504418476	0.999988174	-1
Fps85D	Fps oncogene analog	-5.557638875	0.999996161	-1
CG34236	CG34236 gene product from transcript CG34236-RB	-5.813071801	0.999873083	-1
mex1	midgut expression 1	-6.258454655	0.99999998	-1
NPFR1	neuropeptide F receptor	-6.325409673	0.99467701	-1
Jon99Ci	Jonah 99Ci	-6.635743813	0.951434617	-1
LvpL	Larval visceral protein L	-6.940923049	0.965713246	-1
CG2082	CG2082 gene product from transcript CG2082-RC	-6.995014187	0.999709866	-1
CG14989	CG14989 gene product from transcript CG14989-RB	-7.076250183	0.999913831	-1
Tsp42Eq	Tetraspanin 42Eq	-7.218457948	0.999999918	-1
unc-13-4A	CG32381 gene product from transcript CG32381-RB	-7.355670003	0.990957182	-1
CG13565	CG13565 gene product from transcript CG13565-RA	-7.632994882	0.999432437	-1
CG5506	CG5506 gene product from transcript CG5506-RA	-7.764718713	0.9563761	-1
Calx	Na/Ca-exchange protein	-7.947299757	0.999950113	-1
CG31198	CG31198 gene product from transcript CG31198-RA	-8.019597306	0.981528323	-1
mira	miranda	-8.042098705	0.999999778	-1
CG5246	CG5246 gene product from transcript CG5246-RA	-8.182254438	0.999980779	-1
Ptx1	CG1447 gene product from transcript CG1447-RC	-8.210966398	0.992814575	-1
Irc	Immune-regulated catalase	-8.348716516	0.999910694	-1
CG12026	CG12026 gene product from transcript CG12026-RB	-8.412203054	0.999772516	-1
CG6006	CG6006 gene product from transcript CG6006-RC	-8.427975444	0.999999982	-1
cad	caudal	-9.19965244	0.998780055	-1
Nep1	Neprilysin 1	-9.453822193	0.996824096	-1
CG33127	CG33127 gene product from transcript CG33127-RA	-11.2125099	0.999804393	-1
CG17778	CG17778 gene product from transcript CG17778-RA	-11.5290385	0.99999666	-1
CG2082	CG2082 gene product from transcript CG2082-RC	-12.31709238	0.999994965	-1
CG14358	CG14358 gene product from transcript CG14358-RB	-12.99800906	0.998344506	-1
Dad	Daughters against dpp	-14.32614306	0.999618266	-1

Annex 1. Differentially expressed genes in Apc Ras vs WT 4 weeks ACI comparison

symbol	genename	APC RAS vs WT 4week FC	APC RAS vs WT 4week PDE	APC RAS vs WT REJ
Ast	Allatostatin	-18.26999663	0.992360132	-1
CG30090	CG30090 gene product from transcript CG30090-RA	-23.18004438	0.999999998	-1
npf	neuropeptide F	-25.67037667	0.997179776	-1
CG5804	CG5804 gene product from transcript CG5804-RA	-35.22420183	1	-1
Ast-C	Allatostatin C	-154.909822	0.999999989	-1

Annex 2. Differentially expressed genes in Apc-Ras vs WT 1 week ACI comparison ordered by gene function

symbol	Function	Fold Change	Present in APC	Present in RAS
kirre	Cell adhesion and Polarity	7.933765753	No	Yes
Tsp	**Cell adhesion and Polarity**	**7.392953233**	**No**	**No**
blot	**Cell adhesion and Polarity**	**6.911772046**	**No**	**No**
Ama	Cell adhesion and Polarity	4.867243472	Yes	Yes
plx	**Cell adhesion and Polarity**	**4.606497368**	**No**	**No**
rst	**Cell adhesion and Polarity**	**3.233328966**	**No**	**No**
CG17304	**Cell adhesion and Polarity**	**2.598818566**	**No**	**No**
Gli	**Cell adhesion and Polarity**	**2.107874468**	**No**	**No**
scrib	Cell adhesion and Polarity	2.021504174	No	Yes
btsz	Cell adhesion and Polarity	-2.023985199	No	Yes
Ten-m	Cell adhesion and polarity	-2.052806785	Yes	No
Cad89D	**Cell adhesion and Polarity**	**-2.053378845**	**No**	**No**
CG1399	**Cell adhesion and Polarity**	**-2.058166174**	**No**	**No**
CG3259	**Cell adhesion and Polarity**	**-2.215404875**	**No**	**No**
Lectin-galC1	**Cell adhesion and Polarity**	**-2.224778934**	**No**	**No**
sinu	Cell adhesion and Polarity	-2.264987416	No	Yes
CG42256	**Cell adhesion and Polarity**	**-2.341181024**	**No**	**No**
CG34347	**Cell adhesion and Polarity**	**-2.503240867**	**No**	**No**
beat-IIIc	Cell adhesion and Polarity	-2.542367589	Yes	Yes
CG42330	**Cell adhesion and Polarity**	**-2.617465202**	**No**	**No**
beat-IIa	Cell adhesion and Polarity	-3.290682645	Yes	No
CG30359	**Metabolism**	**9.814621258**	**No**	**No**
CG7900	Metabolism	9.098810132	Yes	No
CG3348	Metabolism	8.074320504	Yes	Yes
GstD2	Metabolism	8.010877361	No	Yes
CG10140	Metabolism	6.957993051	Yes	No
CG17119	**Metabolism**	**6.607731764**	**No**	**No**
CG15829	**Metabolism**	**4.859232861**	**No**	**No**
CG3635	Metabolism	4.722666978	No	Yes
CG17930	Metabolism	4.697973533	Yes	No
CG34319	**Metabolism**	**4.372555591**	**No**	**No**
CG10725	**Metabolism**	**4.2737516**	**No**	**No**
GstD5	Metabolism	3.83222039	No	Yes
ImpL3	Metabolism	3.651276332	Yes	Yes
CG13248	Metabolism	3.565864763	No	Yes
Ugt86Di	Metabolism	3.504399966	Yes	No
CG30502	Metabolism	3.270830514	Yes	No
CG15828	**Metabolism**	**3.242386492**	**No**	**No**
ferrochelatase	Metabolism	2.998682927	No	Yes
CG10154	Metabolism	2.848509962	Yes	No
CG4860	Metabolism	2.793658752	Yes	No
CG10924	**Metabolism**	**2.734070075**	**No**	**No**
Ant2	Metabolism	2.724278065	No	Yes
CG9009	**Metabolism**	**2.70534458**	**No**	**No**
CG17929	**Metabolism**	**2.704713143**	**No**	**No**
CG3397	Metabolism	2.687287448	Yes	No
CG30022	Metabolism	2.619558901	No	Yes
CG7593	Metabolism	2.610557595	Yes	Yes
Pfk	Metabolism	2.559993154	No	Yes
CG3036	Metabolism	2.534410046	No	Yes
CG14297	Metabolism	2.49231601	No	Yes
alpha-Est3	Metabolism	2.463059931	Yes	No
GstS1	**Metabolism**	**2.379431332**	**No**	**No**
Ndae1	Metabolism	2.371483535	Yes	No
GstD9	Metabolism	2.360335473	No	Yes
CG7149	**Metabolism**	**2.318341776**	**No**	**No**
Pect	**Metabolism**	**2.242011874**	**No**	**No**
Gfat1	Metabolism	2.206479947	Yes	No
CG15739	**Metabolism**	**2.202358969**	**No**	**No**
CG4267	**Metabolism**	**2.186766023**	**No**	**No**
Cht4	**Metabolism**	**2.166477292**	**No**	**No**
PH4alphaEFB	Metabolism	2.121385363	No	Yes

Annex 2. Differentially expressed genes in Apc-Ras vs WT 1 week ACI comparison ordered by gene function

symbol	Function	Fold Change	Present in APC	Present in RAS
CG10638	**Metabolism**	**2.05155883**	**No**	**No**
CG31530	**Metabolism**	**2.000563562**	**No**	**No**
Cyp6g2	**Metabolism**	**-2.067304289**	**No**	**No**
CG33177	**Metabolism**	**-2.073234252**	**No**	**No**
CG10863	**Metabolism**	**-2.074372715**	**No**	**No**
CG3835	**Metabolism**	**-2.083954587**	**No**	**No**
CG15547	**Metabolism**	**-2.102497185**	**No**	**No**
Ucp4B	**Metabolism**	**-2.115077825**	**No**	**No**
CG4020	**Metabolism**	**-2.116765622**	**No**	**No**
Glycogenin	**Metabolism**	**-2.135322251**	**No**	**No**
CG15534	**Metabolism**	**-2.163700357**	**No**	**No**
Ugt35a	Metabolism	-2.188586014	No	Yes
CG5568	Metabolism	-2.200582638	Yes	No
CG33346	**Metabolism**	**-2.204433028**	**No**	**No**
Dat	Metabolism	-2.238840835	No	Yes
CG1315	**Metabolism**	**-2.277503597**	**No**	**No**
CG33281	**Metabolism**	**-2.298585735**	**No**	**No**
CG8834	Metabolism	-2.304220236	No	Yes
CG6283	Metabolism	-2.33547327	Yes	No
CG9914	**Metabolism**	**-2.33595425**	**No**	**No**
CS-2	**Metabolism**	**-2.371825938**	**No**	**No**
CG13325	**Metabolism**	**-2.374352724**	**No**	**No**
kar	Metabolism	-2.396544448	No	Yes
CG15117	**Metabolism**	**-2.442880307**	**No**	**No**
Atet	Metabolism	-2.444597209	Yes	No
CG10170	**Metabolism**	**-2.478726112**	**No**	**No**
cry	Metabolism	-2.482135595	No	Yes
Cyp6a19	Metabolism	-2.544158523	No	Yes
Cyp4ac2	**Metabolism**	**-2.578835085**	**No**	**No**
CG6018	**Metabolism**	**-2.582399354**	**No**	**No**
Npc2d	Metabolism	-2.586817541	Yes	Yes
CG14856	**Metabolism**	**-2.604534311**	**No**	**No**
Cyp6d5	Metabolism	-2.610715794	No	Yes
CG11342	Metabolism	-2.628652394	Yes	No
CG5932	**Metabolism**	**-2.629413365**	**No**	**No**
CG12766	Metabolism	-2.685396339	Yes	No
CG16965	**Metabolism**	**-2.709134031**	**No**	**No**
Jheh3	Metabolism	-2.742896709	No	Yes
CG9743	**Metabolism**	**-2.761961788**	**No**	**No**
CG3544	**Metabolism**	**-2.781845505**	**No**	**No**
Cyp6a23	**Metabolism**	**-2.78258961**	**No**	**No**
CDase	**Metabolism**	**-2.797743549**	**No**	**No**
CG16732	**Metabolism**	**-2.801898688**	**No**	**No**
Cyp9b1	Metabolism	-2.813243208	Yes	Yes
Cyp4ac1	**Metabolism**	**-2.868911137**	**No**	**No**
Cyp6a9	Metabolism	-2.937495298	Yes	Yes
CG18869	**Metabolism**	**-2.959257891**	**No**	**No**
CG1681	Metabolism	-3.001437878	No	Yes
CG32444	**Metabolism**	**-3.025152149**	**No**	**No**
CG14740	Metabolism	-3.070025244	Yes	Yes
CG8093	Metabolism	-3.115126886	Yes	Yes
CG7997	Metabolism	-3.139328652	Yes	Yes
CG33099	**Metabolism**	**-3.149725633**	**No**	**No**
CG6206	**Metabolism**	**-3.166850345**	**No**	**No**
CG10877	Metabolism	-3.177065344	Yes	Yes
CG10168	**Metabolism**	**-3.226647919**	**No**	**No**
CG8693	Metabolism	-3.254787857	No	Yes
Cyp9f2	Metabolism	-3.29883411	Yes	Yes
Ahcy89E	Metabolism	-3.355434708	No	Yes
CG9747	**Metabolism**	**-3.379545005**	**No**	**No**
CG7470	Metabolism	-3.391726207	No	Yes
CG11241	Metabolism	-3.404654379	No	Yes

Annex 2. Differentially expressed genes in Apc-Ras vs WT 1 week ACI comparison ordered by gene function

symbol	Function	Fold Change	Present in APC	Present in RAS
Cyp6w1	Metabolism	-3.413130977	No	Yes
CG7678	Metabolism	-3.60363882	Yes	Yes
CG11878	**Metabolism**	**-3.91299748**	**No**	**No**
Cyp12a4	**Metabolism**	**-3.963977134**	**No**	**No**
CG14741	Metabolism	-4.018694117	Yes	Yes
CG9463	**Metabolism**	**-4.023001066**	**No**	**No**
CG7298	**Metabolism**	**-4.162428845**	**No**	**No**
CG9468	Metabolism	-4.351305335	Yes	No
CG9466	**Metabolism**	**-5.00481916**	**No**	**No**
CG15531	**Metabolism**	**-5.866256622**	**No**	**No**
CG3301	Metabolism	-6.243975745	Yes	Yes
CG15629	Metabolism	-6.499139442	Yes	Yes
LvpH	**Metabolism**	**-6.697758039**	**No**	**No**
CG6295	**Metabolism**	**-7.763407728**	**No**	**No**
CG9360	**Metabolism**	**-9.374719419**	**No**	**No**
CG17145	Metabolism	-10.71263032	Yes	No
CG5804	Metabolism	-14.83971653	No	Yes
tw	Other	18.18928401	Yes	No
LysX	**Other**	**10.76853614**	**No**	**No**
l(2)01810	Other	9.829470564	No	Yes
sn	**Other**	**8.612470594**	**No**	**No**
tau	Other	7.476293273	Yes	No
mp	**Other**	**6.501395166**	**No**	**No**
CG4726	Other	6.367737	No	Yes
Hk	**Other**	**5.241850717**	**No**	**No**
CG6330	Other	4.850249158	No	Yes
exu	Other	4.362966047	Yes	Yes
CG5621	**Other**	**4.265499473**	**No**	**No**
CG10641	Other	4.183657533	Yes	Yes
rtet	Other	4.090438427	Yes	No
CG18594	**Other**	**3.742063234**	**No**	**No**
CG17124	Other	3.63578331	Yes	No
Gr94a	**Other**	**3.552231599**	**No**	**No**
Ir	**Other**	**3.539498744**	**No**	**No**
Mmp2	Other	3.394291755	No	Yes
Rh2	**Other**	**3.376268087**	**No**	**No**
Tret1-1	Other	3.243704003	No	Yes
fax	**Other**	**3.188996933**	**No**	**No**
Dgp-1	Other	3.050502608	No	Yes
Cpr66D	**Other**	**2.987363096**	**No**	**No**
spel1	Other	2.856575447	No	Yes
Rbp9	**Other**	**2.817991672**	**No**	**No**
scf	**Other**	**2.752054209**	**No**	**No**
CG42825	**Other**	**2.732374873**	**No**	**No**
CG6610	Other	2.702681511	Yes	No
WASp	**Other**	**2.699274891**	**No**	**No**
slow	Other	2.697280769	Yes	No
CG5958	Other	2.682086964	Yes	No
Tg	**Other**	**2.644502819**	**No**	**No**
wus	Other	2.618453286	No	Yes
Ir94a	Other	2.603069251	No	Yes
krimp	**Other**	**2.566298542**	**No**	**No**
rgn	Other	2.525461015	No	Yes
NtR	Other	2.50263254	No	Yes
Cad96Ca	Other	2.43795343	Yes	No
Ppn	**Other**	**2.412309036**	**No**	**No**
CG10527	**Other**	**2.390018901**	**No**	**No**
Duox	**Other**	**2.305974697**	**No**	**No**
Ir94c	Other	2.279314063	No	Yes
CG1529	**Other**	**2.25431711**	**No**	**No**
Pen	Other	2.231179513	No	Yes
CG14204	**Other**	**2.204009791**	**No**	**No**

Annex 2. Differentially expressed genes in Apc-Ras vs WT 1 week ACI comparison ordered by gene function

symbol	Function	Fold Change	Present in APC	Present in RAS
sprt	Other	2.202828094	No	Yes
shu	Other	2.197896694	No	Yes
CG31145	**Other**	**2.177765293**	**No**	**No**
Def	**Other**	**2.175456732**	**No**	**No**
wun2	Other	2.166593884	No	Yes
eys	**Other**	**2.139103847**	**No**	**No**
dbr	**Other**	**2.126811457**	**No**	**No**
CG2100	**Other**	**2.124941774**	**No**	**No**
CG13623	**Other**	**2.11227748**	**No**	**No**
rols	**Other**	**2.109965054**	**No**	**No**
fne	**Other**	**2.108084483**	**No**	**No**
bw	Other	2.0999507	No	Yes
cenB1A	**Other**	**2.097044764**	**No**	**No**
esc	Other	2.092992811	No	Yes
CG1792	**Other**	**2.081151589**	**No**	**No**
CHKov2	**Other**	**2.079900448**	**No**	**No**
Cad96Cb	**Other**	**2.07073311**	**No**	**No**
Spn5	**Other**	**2.05911142**	**No**	**No**
borr	Other	2.039979677	No	Yes
nec	**Other**	**2.037439291**	**No**	**No**
Klp61F	Other	2.032112134	No	Yes
CG42458	**Other**	**2.031228573**	**No**	**No**
bora	Other	2.02338917	No	Yes
pch2	Other	2.010822099	No	Yes
CG17272	**Other**	**2.004742053**	**No**	**No**
CG4973	Other	2.000726846	Yes	No
CG3225	**Other**	**-2.00357172**	**No**	**No**
CG33523	**Other**	**-2.004365083**	**No**	**No**
CG11155	Other	-2.010003758	Yes	Yes
CG30344	**Other**	**-2.03460507**	**No**	**No**
dnr1	Other	-2.03923664	No	Yes
CG6126	**Other**	**-2.040647345**	**No**	**No**
CG12071	**Other**	**-2.042366162**	**No**	**No**
ste24b	**Other**	**-2.044834425**	**No**	**No**
Spn4	Other	-2.060975081	No	Yes
Mct1	**Other**	**-2.063336636**	**No**	**No**
Or33a	**Other**	**-2.064454371**	**No**	**No**
Spn3	**Other**	**-2.067415287**	**No**	**No**
Zasp66	**Other**	**-2.075011004**	**No**	**No**
CG5599	**Other**	**-2.078545002**	**No**	**No**
CG3308	Other	-2.102623952	Yes	No
CG34360	**Other**	**-2.111794129**	**No**	**No**
sba	**Other**	**-2.117209109**	**No**	**No**
aay	Other	-2.117922301	No	Yes
CG6928	**Other**	**-2.124465796**	**No**	**No**
CG1724	**Other**	**-2.133003124**	**No**	**No**
CG1637	Other	-2.133993931	No	Yes
CG31087	**Other**	**-2.161324356**	**No**	**No**
Sry-alpha	**Other**	**-2.206184183**	**No**	**No**
Tango13	**Other**	**-2.209496167**	**No**	**No**
Muc68Ca	**Other**	**-2.212392548**	**No**	**No**
Acp62F	**Other**	**-2.214635026**	**No**	**No**
Ptr	**Other**	**-2.215307344**	**No**	**No**
gukh	**Other**	**-2.239591407**	**No**	**No**
CG4325	Other	-2.26061089	Yes	No
Gr89a	**Other**	**-2.268571892**	**No**	**No**
CG9664	**Other**	**-2.313580922**	**No**	**No**
CG9527	**Other**	**-2.31851877**	**No**	**No**
CG8837	**Other**	**-2.346330291**	**No**	**No**
Takr86C	**Other**	**-2.35154783**	**No**	**No**
CG16781	**Other**	**-2.356778642**	**No**	**No**
CG42321	**Other**	**-2.376632722**	**No**	**No**

Annex 2. Differentially expressed genes in Apc-Ras vs WT 1 week ACI comparison ordered by gene function

symbol	Function	Fold Change	Present in APC	Present in RAS
sut4	Other	-2.38689246	Yes	No
pain	**Other**	**-2.390160422**	**No**	**No**
hig	Other	-2.397925421	No	Yes
laza	**Other**	**-2.412094611**	**No**	**No**
Sln	**Other**	**-2.499929225**	**No**	**No**
CG32850	**Other**	**-2.50069085**	**No**	**No**
Prestin	**Other**	**-2.54675921**	**No**	**No**
RpS7	**Other**	**-2.552829938**	**No**	**No**
CG34401	Other	-2.577526486	Yes	Yes
CG31102	**Other**	**-2.616977714**	**No**	**No**
osp	Other	-2.65043888	Yes	Yes
IM10	**Other**	**-2.661106215**	**No**	**No**
a	**Other**	**-2.671543427**	**No**	**No**
unc-104	Other	-2.761432211	Yes	No
MtnC	**Other**	**-2.848916939**	**No**	**No**
sick	Other	-2.849936724	Yes	Yes
Cbl	Other	-2.852149278	Yes	No
PGRP-SC2	**Other**	**-2.853492986**	**No**	**No**
CG14120	Other	-2.875207341	No	Yes
CG8713	**Other**	**-2.930469358**	**No**	**No**
HdacX	**Other**	**-2.937903079**	**No**	**No**
CG42269	**Other**	**-2.9384821**	**No**	**No**
CG30345	**Other**	**-3.151585776**	**No**	**No**
CG9509	**Other**	**-3.16138462**	**No**	**No**
m-cup	**Other**	**-3.19191883**	**No**	**No**
CG10912	**Other**	**-3.199741512**	**No**	**No**
Grip	other	-3.22624334	Yes	Yes
Ih	**Other**	**-3.2751832**	**No**	**No**
CG2201	**Other**	**-3.278954786**	**No**	**No**
CG3277	Other	-3.317035265	No	Yes
CG6527	Other	-3.323653343	Yes	No
CG15309	Other	-3.354780829	No	Yes
CG9989	**Other**	**-3.513025983**	**No**	**No**
CG33514	**Other**	**-3.604639508**	**No**	**No**
vkg	Other	-3.861408427	Yes	No
smp-30	Other	-3.941107832	No	Yes
Pkg21D	Other	-4.012514468	No	Yes
Calx	**Other**	**-4.042082708**	**No**	**No**
stl	Other	-4.139248877	Yes	Yes
CG6484	Other	-4.374471091	Yes	Yes
CG10559	**Other**	**-4.39424869**	**No**	**No**
CG10621	**Other**	**-4.532151714**	**No**	**No**
Cg25C	Other	-4.825524704	Yes	Yes
tomboy20	Other	-6.627165039	Yes	No
CG12026	Other	-6.870935547	Yes	No
CG4462	Other	-6.940925176	Yes	Yes
be	Other	-7.168185459	No	Yes
CG6129	Other	-7.359329899	Yes	No
CG6006	**Other**	**-8.484896293**	**No**	**No**
Ast-C	**Other**	**-19.87087114**	**No**	**No**
DNaseII	**Other (Apoptosis)**	5.181418548	No	Yes
Naam	**Other (Apoptosis)**	**3.460544653**	**No**	**No**
ec	**Other (Apoptosis)**	**2.328651514**	**No**	**No**
Fhos	**Other (Apoptosis)**	**-2.331118548**	**No**	**No**
GlcT-1	**Other (Apoptosis)**	**-2.402347692**	**No**	**No**
CG5254	**Other (Apoptosis)**	-2.439286536	Yes	No
CG30116	**Other (Apoptosis)**	**-2.455071934**	**No**	**No**
CG14526	**Other (Proteolysis)**	**8.837821**	**No**	**No**
CG11192	**Other (Proteolysis)**	**5.199843835**	**No**	**No**
CG5390	**Other (Proteolysis)**	**2.759108961**	**No**	**No**
CG14869	**Other (Proteolysis)**	2.011257566	No	Yes
CG30088	**Other (Proteolysis)**	**-2.03069768**	**No**	**No**

Annex 2. Differentially expressed genes in Apc-Ras vs WT 1 week ACI comparison ordered by gene function

symbol	Function	Fold Change	Present in APC	Present in RAS
iotaTry	**Other (Proteolysis)**	-2.113758538	No	Yes
CG5255	**Other (Proteolysis)**	**-2.198953504**	**No**	**No**
CG4723	**Other (Proteolysis)**	**-2.254090187**	**No**	**No**
Jon44E	**Other (Proteolysis)**	**-2.402224838**	**No**	**No**
kappaTry	**Other (Proteolysis)**	**-2.426317807**	**No**	**No**
CG3344	**Other (Proteolysis)**	**-2.433593705**	**No**	**No**
CG4653	**Other (Proteolysis)**	-2.448980261	No	Yes
CG9673	**Other (Proteolysis)**	-2.5128631	No	Yes
CG8952	**Other (Proteolysis)**	-2.576598316	No	Yes
CG16749	**Other (Proteolysis)**	-2.724589999	No	Yes
CG31198	**Other (Proteolysis)**	-2.756859451	No	Yes
zetaTry	**Other (Proteolysis)**	**-2.759401633**	**No**	**No**
Jon65Aiii	**Other (Proteolysis)**	**-2.863450345**	**No**	**No**
CG15255	**Other (Proteolysis)**	-3.020475935	No	Yes
CG30283	**Other (Proteolysis)**	**-3.106240018**	**No**	**No**
CG33127	**Other (Proteolysis)**	**-3.156607083**	**No**	**No**
CG4678	**Other (Proteolysis)**	-3.215087806	Yes	Yes
CG30049	**Other (Proteolysis)**	-3.243634653	No	Yes
CG10051	**Other (Proteolysis)**	**-3.287618349**	**No**	**No**
alphaTry	**Other (Proteolysis)**	**-3.42079335**	**No**	**No**
etaTry	**Other (Proteolysis)**	-3.455923097	No	Yes
Jon99Fi	**Other (Proteolysis)**	-3.528032378	Yes	No
CG10477	**Other (Proteolysis)**	**-3.636889383**	**No**	**No**
epsilonTry	**Other (Proteolysis)**	**-3.702984504**	**No**	**No**
CG30043	**Other (Proteolysis)**	**-4.204832307**	**No**	**No**
CG16997	**Other (Proteolysis)**	-4.358698563	No	Yes
CG10663	**Other (Proteolysis)**	-4.358992203	Yes	No
CG10472	**Other (Proteolysis)**	-4.527965581	Yes	Yes
betaTry	**Other (Proteolysis)**	**-4.685639192**	**No**	**No**
CG30090	**Other (Proteolysis)**	**-4.863858215**	**No**	**No**
Jon25Biii	**Other (Proteolysis)**	-5.617442362	Yes	No
CG17633	**Other (Proteolysis)**	**-5.670415071**	**No**	**No**
CG18180	**Other (Proteolysis)**	**-5.70544714**	**No**	**No**
Jon65Aii	**Other (Proteolysis)**	-6.719187339	Yes	Yes
CG5246	**Other (Proteolysis)**	-6.941070661	No	Yes
Jon99Ci	**Other (Proteolysis)**	**-7.557904878**	**No**	**No**
Bace	**Other (Proteolysis)**	-8.013710552	Yes	No
Jon74E	**Other (Proteolysis)**	-8.073414687	Yes	No
CG12374	**Other (Proteolysis)**	-10.21732337	Yes	Yes
Jon65Ai	**Other (Proteolysis)**	-10.36357776	Yes	No
stg	Proliferation	6.340772953	No	Yes
Mkp3	Proliferation	5.245907111	No	Yes
msd1	**Proliferation**	**3.83081083**	**No**	**No**
CHKov1	Proliferation	2.941583189	Yes	No
CG7922	Proliferation	2.90429135	Yes	No
polo	Proliferation	2.622321497	No	Yes
cnn	Proliferation	2.56936913	No	Yes
cerv	**Proliferation**	**2.486307629**	**No**	**No**
lds	**Proliferation**	**2.405166306**	**No**	**No**
cmet	Proliferation	2.399092734	No	Yes
pav	Proliferation	2.379322786	No	Yes
mad2	Proliferation	2.3520829	No	Yes
pim	Proliferation	2.333740413	No	Yes
sti	Proliferation	2.321856494	No	Yes
CycB	Proliferation	2.276940483	No	Yes
mei-38	**Proliferation**	**2.272755766**	**No**	**No**
RPA2	Proliferation	2.192309994	No	Yes
Z600	**Proliferation**	**2.178097689**	**No**	**No**
rod	**Proliferation**	**2.15854999**	**No**	**No**
Cks30A	Proliferation	2.138000341	No	Yes
cdc2	Proliferation	2.122547482	No	Yes
dmt	**Proliferation**	**2.114997335**	**No**	**No**

Annex 2. Differentially expressed genes in Apc-Ras vs WT 1 week ACI comparison ordered by gene function

symbol	Function	Fold Change	Present in APC	Present in RAS
ial	Proliferation	2.112008551	No	Yes
mod(mdg4)	**Proliferation**	**2.085415586**	**No**	**No**
feo	Proliferation	2.050834794	No	Yes
fzy	Proliferation	2.041742535	No	Yes
Incenp	**Proliferation**	**2.025890343**	**No**	**No**
svp	**Signalling and regulation of transcription**	**19.06645304**	**No**	**No**
fz3	Signalling and regulation of transcription	15.00427013	Yes	No
Lim3	Signalling and regulation of transcription	9.793604962	Yes	No
drm	**Signalling and regulation of transcription**	**8.550712363**	**No**	**No**
hh	**Signalling and regulation of transcription**	**7.261660483**	**No**	**No**
os	**Signalling and regulation of transcription**	**7.09544671**	**No**	**No**
ImpL2	Signalling and regulation of transcription	6.673466435	Yes	Yes
slbo	**Signalling and regulation of transcription**	**6.24673069**	**No**	**No**
mirr	**Signalling and regulation of transcription**	**5.82772484**	**No**	**No**
CG7056	Signalling and regulation of transcription	4.756159642	Yes	No
kek1	**Signalling and regulation of transcription**	**4.215478997**	**No**	**No**
sob	**Signalling and regulation of transcription**	**3.927942945**	**No**	**No**
Pvf2	**Signalling and regulation of transcription**	**3.857345224**	**No**	**No**
dimm	Signalling and regulation of transcription	3.706700047	No	Yes
bnl	**Signalling and regulation of transcription**	**3.646069437**	**No**	**No**
rho	**Signalling and regulation of transcription**	**3.543405024**	**No**	**No**
upd3	Signalling and regulation of transcription	3.488887903	Yes	Yes
fred	**Signalling and regulation of transcription**	**3.385407448**	**No**	**No**
CG34372	**Signalling and regulation of transcription**	**3.341962608**	**No**	**No**
dmrt93B	Signalling and regulation of transcription	3.312553213	Yes	No
sna	Signalling and regulation of transcription	3.179396467	No	Yes
otk	**Signalling and regulation of transcription**	**3.073974455**	**No**	**No**
Ilp6	**Signalling and regulation of transcription**	**3.037988623**	**No**	**No**
CG33275	**Signalling and regulation of transcription**	**2.879445639**	**No**	**No**
sog	**Signalling and regulation of transcription**	**2.864924286**	**No**	**No**
CG3074	**Signalling and regulation of transcription**	**2.8469727**	**No**	**No**
l(2)k16918	**Signalling and regulation of transcription**	**2.839293311**	**No**	**No**
Wnt5	**Signalling and regulation of transcription**	**2.781043168**	**No**	**No**
spri	**Signalling and regulation of transcription**	**2.737624251**	**No**	**No**
p53	**Signalling and regulation of transcription**	**2.673639768**	**No**	**No**
lab	Signalling and regulation of transcription	2.609381973	No	Yes
piwi	**Signalling and regulation of transcription**	**2.583241331**	**No**	**No**
argos	**Signalling and regulation of transcription**	**2.581679289**	**No**	**No**
sty	**Signalling and regulation of transcription**	**2.581116299**	**No**	**No**
jumu	Signalling and regulation of transcription	2.395581577	No	Yes
CG32758	Signalling and regulation of transcription	2.374794982	No	Yes
mthl8	**Signalling and regulation of transcription**	**2.293712898**	**No**	**No**
pigs	**Signalling and regulation of transcription**	**2.255176598**	**No**	**No**
Gap1	**Signalling and regulation of transcription**	**2.251101188**	**No**	**No**
Ote	Signalling and regulation of transcription	2.240992696	No	Yes
edl	Signalling and regulation of transcription	2.189711948	Yes	No
Idgf4	**Signalling and regulation of transcription**	**2.115411506**	**No**	**No**
CG12370	**Signalling and regulation of transcription**	**2.10475769**	**No**	**No**
18w	Signalling and regulation of transcription	2.046012497	No	Yes
CG6854	Signalling and regulation of transcription	2.009540722	No	Yes
Epac	**Signalling and regulation of transcription**	**2.004145132**	**No**	**No**
Ras85D	Signalling and regulation of transcription	2.001436623	No	Yes
mthl10	**Signalling and regulation of transcription**	**-2.014991304**	**No**	**No**
Stat92E	**Signalling and regulation of transcription**	**-2.037937061**	**No**	**No**
sqz	**Signalling and regulation of transcription**	**-2.047744373**	**No**	**No**
CG14471	**Signalling and regulation of transcription**	**-2.093366953**	**No**	**No**
CG10737	Signalling and regulation of transcription	-2.123724165	No	Yes
cic	Signalling and regulation of transcription	-2.197556027	Yes	No
CG31431	**Signalling and regulation of transcription**	**-2.205590026**	**No**	**No**
bru-2	Signalling and regulation of transcription	-2.233909591	No	Yes
CG32055	**Signalling and regulation of transcription**	**-2.254162781**	**No**	**No**
Gyc-89Db	**Signalling and regulation of transcription**	**-2.25429736**	**No**	**No**

Annex 2. Differentially expressed genes in Apc-Ras vs WT 1 week ACI comparison ordered by gene function

symbol	Function	Fold Change	Present in APC	Present in RAS
srp	**Signalling and regulation of transcription**	**-2.257803191**	**No**	**No**
trk	**Signalling and regulation of transcription**	**-2.267846928**	**No**	**No**
MESK2	**Signalling and regulation of transcription**	**-2.315915882**	**No**	**No**
Clk	**Signalling and regulation of transcription**	**-2.330596469**	**No**	**No**
Egfr	**Signalling and regulation of transcription**	**-2.35975681**	**No**	**No**
CG11347	**Signalling and regulation of transcription**	**-2.434290806**	**No**	**No**
Pdp1	**Signalling and regulation of transcription**	**-2.453192158**	**No**	**No**
Mes2	**Signalling and regulation of transcription**	**-2.466317279**	**No**	**No**
dnt	Signalling and regulation of transcription	-2.502520883	Yes	No
exex	**Signalling and regulation of transcription**	**-2.620646717**	**No**	**No**
CG2678	**Signalling and regulation of transcription**	**-2.666296599**	**No**	**No**
Doa	Signalling and regulation of transcription	-2.721259336	No	Yes
fus	Signalling and regulation of transcription	-2.743539511	No	Yes
spz	Signalling and regulation of transcription	-2.752578319	No	Yes
wit	**Signalling and regulation of transcription**	**-2.782583759**	**No**	**No**
CG7431	**Signalling and regulation of transcription**	**-2.85669672**	**No**	**No**
CG15611	**Signalling and regulation of transcription**	**-2.953751801**	**No**	**No**
Fps85D	Signalling and regulation of transcription	-2.965787626	Yes	No
CG14375	**Signalling and regulation of transcription**	**-3.063236509**	**No**	**No**
CG17278	Signalling and regulation of transcription	-3.222888014	Yes	No
Gyc-89Da	Signalling and regulation of transcription	-4.610172769	Yes	No
luna	Signalling and regulation of transcription	-4.775750326	Yes	No
Mad	Signalling and regulation of transcription	-5.010461861	Yes	Yes
Mip	**Signalling and regulation of transcription**	**-6.307957863**	**No**	**No**
CG31763	Signalling and regulation of transcription	-7.577620188	Yes	Yes
CG5630	Unknown	7.199284824	Yes	Yes
CG13117	Unknown	6.433091869	No	Yes
CG14545	Unknown	6.309860002	No	Yes
CG13654	**Unknown**	**5.784203535**	**No**	**No**
CG12702	**Unknown**	**4.380168289**	**No**	**No**
CG16995	**Unknown**	**3.755180926**	**No**	**No**
CG12483	**Unknown**	**3.739267624**	**No**	**No**
CG42390	Unknown	3.342007872	No	Yes
CG11686	Unknown	3.30881611	Yes	No
CG17744	**Unknown**	**2.957372395**	**No**	**No**
CG15818	**Unknown**	**2.883597728**	**No**	**No**
CG13405	**Unknown**	**2.843839628**	**No**	**No**
CG13631	**Unknown**	**2.8386157**	**No**	**No**
CG14294	Unknown	2.791162484	No	Yes
CG10947	Unknown	2.763154621	No	Yes
CG7224	Unknown	2.732704064	No	Yes
CG31344	Unknown	2.656920871	Yes	No
CG34259	**Unknown**	**2.570899109**	**No**	**No**
CG42389	**Unknown**	**2.546753425**	**No**	**No**
Tsp96F	Unknown	2.53050689	No	Yes
CG32652	**Unknown**	**2.482695195**	**No**	**No**
CG15745	**Unknown**	**2.472677882**	**No**	**No**
CG5399	**Unknown**	**2.459397824**	**No**	**No**
CG7194	**Unknown**	**2.445135484**	**No**	**No**
CG10420	Unknown	2.351297813	No	Yes
CG10943	**Unknown**	**2.32502107**	**No**	**No**
CG9184	Unknown	2.31993173	Yes	No
CG30269	**Unknown**	**2.312528934**	**No**	**No**
CG10555	**Unknown**	**2.299144577**	**No**	**No**
CG31058	Unknown	2.295788616	Yes	No
CG12713	**Unknown**	**2.282353629**	**No**	**No**
CG13599	Unknown	2.273278774	No	Yes
CG9917	**Unknown**	**2.219727282**	**No**	**No**
CG17264	**Unknown**	**2.201446403**	**No**	**No**
Os-C	**Unknown**	**2.1975482**	**No**	**No**
CG4674	Unknown	2.187723401	No	Yes
CG34261	**Unknown**	**2.178286262**	**No**	**No**

Annex 2. Differentially expressed genes in Apc-Ras vs WT 1 week ACI comparison ordered by gene function

symbol	Function	Fold Change	Present in APC	Present in RAS
CG7730	Unknown	2.129276009	No	Yes
CG7800	**Unknown**	**2.119335484**	**No**	**No**
CG17715	**Unknown**	**2.107695037**	**No**	**No**
CG10098	**Unknown**	**2.106867938**	**No**	**No**
sip2	Unknown	2.082201048	No	Yes
Tsp42Ei	**Unknown**	**2.058986298**	**No**	**No**
CG13822	**Unknown**	**2.058637738**	**No**	**No**
CG42565	Unknown	2.058220787	Yes	No
Elongin-B	**Unknown**	**2.051961576**	**No**	**No**
Arc2	**Unknown**	**2.046268547**	**No**	**No**
CG33221	**Unknown**	**2.040737948**	**No**	**No**
CG17816	**Unknown**	**2.027754045**	**No**	**No**
CG6310	**Unknown**	**2.017812225**	**No**	**No**
CG42254	**Unknown**	**2.014545493**	**No**	**No**
CG3630	**Unknown**	**2.01060586**	**No**	**No**
m1	**Unknown**	**-2.004205546**	**No**	**No**
CG6490	Unknown	-2.017861307	Yes	No
ptr	Unknown	-2.020005486	No	Yes
CG8008	Unknown	-2.02964396	Yes	No
CG18622	**Unknown**	**-2.042283858**	**No**	**No**
CG3332	**Unknown**	**-2.045501402**	**No**	**No**
CG18747	Unknown	-2.060043829	No	Yes
CG15605	**Unknown**	**-2.075954811**	**No**	**No**
CG12910	Unknown	-2.092046819	No	Yes
CG10494	**Unknown**	**-2.092744821**	**No**	**No**
CG32450	Unknown	-2.093594246	Yes	No
CG8788	Unknown	-2.099354887	No	Yes
CG6108	Unknown	-2.10386484	Yes	Yes
CG7083	Unknown	-2.122727238	No	Yes
Ect4	**Unknown**	**-2.134784831**	**No**	**No**
CG31710	**Unknown**	**-2.15154711**	**No**	**No**
CG1722	**Unknown**	**-2.153475067**	**No**	**No**
CG32352	Unknown	-2.16143012	Yes	Yes
CG18404	**Unknown**	**-2.202597285**	**No**	**No**
CG12992	Unknown	-2.208776741	No	Yes
CG5770	**Unknown**	**-2.210237127**	**No**	**No**
CG30460	Unknown	-2.242505159	No	Yes
CG7970	Unknown	-2.248107408	No	Yes
CG2556	Unknown	-2.256440734	No	Yes
CG15465	**Unknown**	**-2.263342186**	**No**	**No**
CG10283	Unknown	-2.281457017	No	Yes
CG13607	**Unknown**	**-2.289327604**	**No**	**No**
CG17855	**Unknown**	**-2.304684135**	**No**	**No**
CG42367	Unknown	-2.337962909	No	Yes
CG30154	Unknown	-2.345184823	No	Yes
ect	Unknown	-2.36171969	Yes	Yes
olf186-M	Unknown	-2.40145315	No	Yes
CG4928	**Unknown**	**-2.411811174**	**No**	**No**
CG34406	Unknown	-2.473037413	No	Yes
CG3288	**Unknown**	**-2.474192517**	**No**	**No**
CG9498	**Unknown**	**-2.516392029**	**No**	**No**
CG8678	**Unknown**	**-2.55080352**	**No**	**No**
CG13829	Unknown	-2.69252043	No	Yes
CG17186	Unknown	-2.744798483	Yes	No
CG32264	Unknown	-2.800174403	Yes	Yes
CG32407	Unknown	-2.829378403	No	Yes
CG13917	**Unknown**	**-2.891449077**	**No**	**No**
CG13492	Unknown	-3.020803333	Yes	Yes
CG15186	Unknown	-3.042934606	Yes	No
CG14691	Unknown	-3.077367799	Yes	No
CG31076	Unknown	-3.149125857	No	Yes
Tsp42Eq	Unknown	-3.188240337	No	Yes

Annex 2. Differentially expressed genes in Apc-Ras vs WT 1 week ACI comparison ordered by gene function

symbol	Function	Fold Change	Present in APC	Present in RAS
CG13827	**Unknown**	**-3.28155843**	**No**	**No**
CG34198	Unknown	-3.289868552	No	Yes
CG9896	**Unknown**	**-3.296113522**	**No**	**No**
CG16782	**Unknown**	**-3.29651197**	**No**	**No**
fok	Unknown	-3.412995577	No	Yes
CG34376	**Unknown**	**-3.45958855**	**No**	**No**
CG31286	**Unknown**	**-3.464932666**	**No**	**No**
CG16986	**Unknown**	**-3.645739783**	**No**	**No**
CG14253	Unknown	-3.94318849	Yes	No
CG8997	**Unknown**	**-3.956923691**	**No**	**No**
CG7953	**Unknown**	**-4.09921527**	**No**	**No**
CG32521	Unknown	-4.165921934	No	Yes
CG12057	Unknown	-4.781875476	Yes	No
CG12464	Unknown	-4.889808491	No	Yes
Tsp42Er	Unknown	-5.060279778	No	Yes
CG8661	**Unknown**	**-5.157102728**	**No**	**No**
CG5506	**Unknown**	**-5.51032711**	**No**	**No**
CG11068	Unknown	-5.552573059	Yes	No
CG4377	Unknown	-6.021206876	Yes	Yes
CG6043	Unknown	-6.951726035	Yes	Yes
CG5107	Unknown	-8.363804478	Yes	No
CG34040	**Unknown**	**-9.63859957**	**No**	**No**
CG34386	**Unknown**	**-15.92995967**	**No**	**No**
CG4363	Unknown	-20.7767971	No	Yes
CG2082	Unknown	-21.16634434	Yes	Yes

Annex 3. Genes comprising glucose metabolism KEGG terms altered in GSEA
00010 Glycolisis

PROBE	RANK IN GENE LIST	RANK METRIC SCORE	RUNNING ES	CORE ENRICHMENT
CG9008	156	2.29527235	0.025061209	No
CG10467	765	1.48292625	3.29E-04	No
CG7024	1222	1.364699364	-0.014078926	No
CG7362	1885	1.273125768	-0.046609566	No
CG10924	2755	1.195680141	-0.09711213	No
CG11876	2870	1.187448621	-0.086833134	No
CG5261	3078	1.171411514	-0.08432082	No
Pglym87	3404	1.150265932	-0.09167608	No
CG7430	4477	1.089102745	-0.16030566	No
CG13334	5106	1.056189537	-0.1936513	No
l(1)G0334	5206	1.05126071	-0.18439586	No
CG9629	5289	1.047699451	-0.17382719	No
fbp	6161	1.003747821	-0.22763927	No
Fdh	6625	-1.000307441	-0.24858862	No
CG9010	6964	-1.015916348	-0.25919643	No
Hex-t1	7768	-1.059076309	-0.30661446	No
Aldh-III	8655	-1.109921455	-0.35989532	No
CG2767	8791	-1.117792964	-0.3524532	No
CG9961	9040	-1.135313034	-0.35384104	No
Ald	9108	-1.140433669	-0.34054106	No
CG11249	9390	-1.160766125	-0.34417397	No
Aldh	9588	-1.177222252	-0.34075952	No
CG2964	9962	-1.209159136	-0.35102162	No
CG10996	10503	-1.261266708	-0.3739033	Yes
Pglym78	10576	-1.27088213	-0.35886708	Yes
ImpL3	10663	-1.282731652	-0.34476605	Yes
PyK	10682	-1.285653591	-0.32513058	Yes
CG31075	10777	-1.297917366	-0.31142595	Yes
Gapdh2	11145	-1.357886672	-0.31876448	Yes
Hex-C	11246	-1.379393101	-0.30420756	Yes
CG4988	11483	-1.440810919	-0.29961628	Yes
Pgm	11520	-1.455288887	-0.2786507	Yes
Gapdh1	11613	-1.483796	-0.26173586	Yes
Eno	11651	-1.500034332	-0.24011703	Yes
Pgk	11697	-1.516487837	-0.2188738	Yes
CG15400	11878	-1.612656116	-0.20694555	Yes
CG7069	11946	-1.66657114	-0.18501565	Yes
Pgi	12083	-1.809397697	-0.16631027	Yes
Pfk	12112	-1.83675766	-0.13844222	Yes
AcCoAS	12181	-1.958597898	-0.111803055	Yes
Hex-A	12184	-1.962662816	-0.07977207	Yes
Pepck	12294	-2.250081539	-0.05165995	Yes
CG32444	12405	-3.843135357	0.002501382	Yes

Annex 3. Genes comprising glucose metabolsm KEGG terms altered in GSEA
00020 Citrate cycle

PROBE	RANK IN GENE LIST	RANK METRIC SCORE	RUNNING ES	CORE ENRICHMENT
CG6439	705	1.508094311	-0.025446218	Yes
CG5214	860	1.454268694	-0.007567699	Yes
CG7024	1222	1.364699364	-0.008253019	Yes
Irp-1B	1248	1.359815836	0.01806324	Yes
CG6255	1736	1.290991902	0.005678416	Yes
CG3483	1780	1.284672379	0.028977036	Yes
CG6140	2396	1.226280808	0.004918824	Yes
SdhC	2432	1.22308445	0.027579525	Yes
Idh	2485	1.219060063	0.04878508	Yes
CG10749	2556	1.211936235	0.068390235	Yes
CG10924	2755	1.195680141	0.0773316	Yes
CG11876	2870	1.187448621	0.09287729	Yes
l(1)G0255	3069	1.172072411	0.10132678	Yes
CG5261	3078	1.171411514	0.12508878	Yes
CG1516	3223	1.16206181	0.13768557	Yes
Acon	3224	1.162046671	0.16189776	Yes
CG7998	3907	1.120483398	0.13023065	Yes
l(1)G0156	4035	1.113487482	0.14318666	Yes
Scsalpha	4071	1.111523151	0.16352288	Yes
CG7430	4477	1.089102745	0.15354604	Yes
CG4706	4502	1.088132501	0.17428222	Yes
skap	4518	1.087475777	0.1957307	Yes
l(1)G0334	5206	1.05126071	0.16221794	No
ATPCL	5614	1.031335711	0.15087613	No
Irp-1A	5655	1.029569387	0.16910148	No
CG7349	6245	1.000289202	0.14243183	No
Sucb	6565	-0.32566902	0.12348537	No
CG5362	6897	-1.01203537	0.11787195	No
CG10748	7021	-1.018787265	0.12917745	No
Nc73EF	7052	-1.020227313	0.14801478	No
CG5028	7573	-1.048431039	0.12791407	No
CG5718	7739	-1.057665586	0.13664174	No
CG10219	7900	-1.065807104	0.14594235	No
SdhB	9889	-1.202712059	0.01064046	No
CG14740	10383	-1.249642968	-0.003089891	No
CG31874	10614	-1.276109219	0.004946014	No
CG32026	11004	-1.331124187	0.001302516	No
CG4095	11199	-1.368475556	0.014166877	No
CG6629	12126	-1.851222634	-0.021956878	No
Pepck	12294	-2.250081539	0.011454411	No

Annex 3. Genes comprising glucose metabolism terms altered in GSEA
00190 Oxidative phosphorilation

PROBE	RANK IN GENE LIST	RANK METRIC SCORE	RUNNING ES	CORE ENRICHMENT
CG1268	201	2.135895014	-0.001206367	Yes
Vha68-1	286	1.905317903	0.005451743	Yes
CG13167	353	1.775536656	0.012652788	Yes
CG40002	427	1.683242917	0.018633006	Yes
CG7580	606	1.560060978	0.015220687	Yes
CG7181	613	1.555649161	0.025735937	Yes
ox	624	1.548007011	0.035872515	Yes
CG12859	694	1.512964964	0.040973082	Yes
CG3621	776	1.478581548	0.044856604	Yes
ND23	788	1.474231124	0.054390255	Yes
CG7712	828	1.461552739	0.061561882	Yes
l(2)06225	889	1.445017457	0.06691229	Yes
Pdsw	924	1.433694839	0.07429268	Yes
CG3560	1026	1.404535532	0.076029405	Yes
CG3192	1053	1.398756385	0.08381193	Yes
CG5037	1075	1.393597245	0.09196375	Yes
Oscp	1305	1.350123167	0.082927726	Yes
CG5389	1308	1.349778533	0.0923116	Yes
CG11015	1366	1.34135282	0.09717232	Yes
ATPsyn-b	1437	1.329562068	0.10089463	Yes
CG5548	1464	1.326440215	0.10816571	Yes
CG3214	1488	1.323278308	0.115657896	Yes
Vha100-2	1571	1.311543584	0.1182789	Yes
CG8680	1728	1.291814327	0.114754856	Yes
CG9013	1896	1.272074223	0.11019849	Yes
CG31644	1979	1.264261007	0.112485096	Yes
CG31648	1988	1.26357162	0.12077234	Yes
CG3683	1995	1.263123989	0.12921874	Yes
CG3321	2000	1.262579918	0.1378236	Yes
CG1746	2086	1.252746701	0.13978529	Yes
CG2249	2101	1.251311898	0.1474989	Yes
CG14508	2140	1.24854207	0.1532452	Yes
cype	2218	1.240976453	0.1557729	Yes
sun	2241	1.238440514	0.16274622	Yes
CG9603	2291	1.234520197	0.16750063	Yes
Vha13	2294	1.234340668	0.17606808	Yes
CG12400	2418	1.224149585	0.17474362	Yes
SdhC	2432	1.22308445	0.18233874	Yes
CG8102	2448	1.222079396	0.18976445	Yes
Nurf-38	2464	1.220718145	0.19718054	Yes
Vha14	2583	1.209499121	0.19615825	Yes
CG2014	2633	1.20560801	0.20070817	Yes
CG32230	2713	1.198934078	0.20277622	Yes
CG9350	2845	1.189110637	0.2005547	Yes
CG9306	2936	1.182196379	0.20161167	Yes
l(3)neo18	2955	1.180715442	0.20850137	Yes
CG14482	2998	1.176377296	0.21341264	Yes
CG3446	3025	1.174339771	0.21960801	Yes
levy	3039	1.173452377	0.22685212	Yes
ATPsyn-gamma	3095	1.170181513	0.23066457	Yes
CoVa	3110	1.168970227	0.23779581	Yes
VhaM9.7-2	3207	1.163291216	0.23823214	Yes
l(1)G0230	3263	1.158788204	0.241964	Yes
CG8310	3427	1.148576617	0.23685883	Yes
CG18624	3447	1.147133589	0.24342987	Yes
ND42	3553	1.141133428	0.2429791	Yes
CG12079	3595	1.138517976	0.24770378	Yes
l(2)35Di	3668	1.134103894	0.2498814	Yes
CG14909	3715	1.131351709	0.25414962	Yes
RFeSP	3764	1.128182888	0.25823313	Yes
ATPsyn-beta	3812	1.125499725	0.2623788	Yes
CG10396	3885	1.121575952	0.26446784	Yes

Annex 3. Genes comprising glucose metabolism terms altered in GSEA
00190 Oxidative phosphorilation

CG31477	3897	1.121124268	0.27150416	Yes
NP15.6	4091	1.110662222	0.2636962	No
blw	4180	1.105988383	0.2643765	No
CG7211	4393	1.094522357	0.2549124	No
CG10664	4424	1.092578053	0.26020488	No
CG11043	4553	1.085475683	0.25749388	No
Vha16-2	4618	1.08217442	0.2599535	No
VhaPPA1-1	4697	1.077921629	0.26124686	No
CG1970	4856	1.069282532	0.25598666	No
CG15434	4888	1.067638159	0.2610216	No
Vha100-3	5061	1.058588266	0.25454962	No
CG4769	5093	1.056812286	0.25950798	No
CG11913	5214	1.050780773	0.25720087	No
CG9140	5276	1.048285484	0.25966427	No
VhaAC39	5455	1.038677096	0.25256452	No
Vha55	5651	1.029968858	0.24402352	No
CG9065	5725	1.026145816	0.24535649	No
CG5703	5728	1.025881052	0.2524496	No
CG10320	5760	1.024007559	0.25717598	No
CG6737	6233	1.000774026	0.2259484	No
CG7349	6245	1.000289202	0.23213014	No
mtacp1	6292	0.448419362	0.23156838	No
Vha44	6631	-1.000638008	0.21121469	No
VhaSFD	6742	-1.005839229	0.20940128	No
Vha16-3	6777	-1.007297873	0.21376601	No
Vha26	6780	-1.007432103	0.22072867	No
CG6020	7070	-1.021044374	0.20449592	No
CG7678	7093	-1.02211535	0.20993932	No
CG6485	7130	-1.024023533	0.21426001	No
CG6914	7210	-1.027842641	0.21511805	No
ND75	7515	-1.044671059	0.19783506	No
Vha16	7570	-1.048053145	0.20086491	No
CG5718	7739	-1.057665586	0.19471101	No
CG30093	7759	-1.058602095	0.20065592	No
CG10219	7900	-1.065807104	0.19683194	No
CG1076	7962	-1.069437027	0.19944495	No
CG5075	8587	-1.106226683	0.1566275	No
Vha36	8601	-1.106989026	0.16340156	No
Vha68-2	8734	-1.114622593	0.16057207	No
CG17856	8795	-1.117962122	0.16360942	No
CG12203	9041	-1.135421872	0.15175645	No
CG8029	9118	-1.140911102	0.1536576	No
CG3803	9470	-1.166995049	0.13342543	No
Vha100-1	9564	-1.174956203	0.13418773	No
SdhB	9889	-1.202712059	0.11639936	No
VhaM9.7-1	10119	-1.222587228	0.10646135	No
CG4169	10611	-1.275523663	0.07563495	No
CG12602	11393	-1.416680098	0.022271715	No
CG11423	11584	-1.474148273	0.017277917	No
CG30354	11860	-1.600589514	0.006280133	No
CG7026	12114	-1.84085238	-0.001232991	No
CG6629	12126	-1.851222634	0.010966899	No
CG18193	12203	-1.995125532	0.01890941	No

Annex 3. Genes comprising glucouse metabolism terms altered in GSEA
00620 Pyruvate metabolism

PROBE	RANK IN GENE LIST	RANK METRIC SCORE	RUNNING ES	CORE ENRICHMENT
CG31674	803	1.469804645	-0.039687682	No
CG7848	830	1.460729361	-0.016833704	No
CG14022	1157	1.37814045	-0.01959771	No
CG7024	1222	1.364699364	-0.001450346	No
CG1707	1746	1.290005803	-0.021615922	No
CG7362	1885	1.273125768	-0.011003916	No
Menl-2	2268	1.236512542	-0.020705866	No
Acyp2	2495	1.218268275	-0.018131709	No
CG10749	2556	1.211936235	-0.002271058	No
CG10924	2755	1.195680141	0.002176592	No
CG11876	2870	1.187448621	0.013261652	No
CG5261	3078	1.171411514	0.016568532	No
CG1516	3223	1.16206181	0.024799218	No
CG10932	3505	1.144080162	0.021668117	No
CG7998	3907	1.120483398	0.008451053	No
Acyp	4026	1.114248157	0.017962951	No
CG7430	4477	1.089102745	2.56E-04	No
CG4365	4495	1.088484883	0.01747758	No
CG13334	5106	1.056189537	-0.013702098	No
l(1)G0334	5206	1.05126071	-0.003733017	No
CG9629	5289	1.047699451	0.007546973	No
CG11198	6236	1.000633717	-0.051693782	No
CG6083	6645	-1.001320243	-0.0675112	No
CG5362	6897	-1.01203537	-0.07047715	No
CG10748	7021	-1.018787265	-0.06299935	No
CG11052	7054	-1.020362735	-0.04815179	No
CG9149	7140	-1.024332523	-0.037513025	No
Mdh	7161	-1.025304079	-0.021612763	No
CG9436	7282	-1.030914664	-0.013685736	No
CG18371	8461	-1.099149108	-0.08996391	No
CG11249	9390	-1.160766125	-0.14501688	No
Aldh	9588	-1.177222252	-0.14080383	No
CG2964	9962	-1.209159136	-0.15024681	No
CG10863	10343	-1.245261192	-0.15963794	No
ImpL3	10663	-1.282731652	-0.16346686	No
PyK	10682	-1.285653591	-0.14295797	No
CG31075	10777	-1.297917366	-0.12837209	No
CG7069	11946	-1.66657114	-0.19415075	Yes
Men	12110	-1.835114598	-0.1759562	Yes
CG6084	12116	-1.842330337	-0.14488928	Yes
AcCoAS	12181	-1.958597898	-0.11659704	Yes
Pepck	12294	-2.250081539	-0.08719888	Yes
CG12766	12355	-2.755319834	-0.044974405	Yes
CG10970	12363	-3.010788202	0.005890545	Yes

Annex 4. RNAi screen gene list in Apc Ras background

number	Gene symbol	Viena RNAi	Selected by	Effect	Result
1	Aats-trp	107049	Up in Apc Ras	Yes	Small clones along the gut
2	AcCoAS	100281	Up in Apc Ras	No	=
3	alph	105483	Up in Apc Ras	Yes	Variable
4	Alr	108383	Up in Apc Ras	No	=
5	Ank	25946	Others	No	=
6	Ank2	107238	Others	No	=
7	Anxb11	101313	Up in Apc Ras	No	=
8	Aph-4	110043	Up in Apc Ras	No	=
9	ase	108511	Others	No	=
10	Asph	101484	Others	No	=
11	atl	6719	Others	No	=
12	atpalpha	12330	Others	Yes	Reduction anterior clone
13	bai	100612	Others	Yes	Invasion of the proventricle
14	beat IIIc	109015	Others	No	=
15	bitesize	102608	Others	No	=
16	blot	101083	Up in Apc Ras	No	=
17	blow	102163	Up in Apc Ras	No	=
18	bnl	101377	Up in Apc Ras	No	=
19	br	104648	Up in Apc Ras	No	=
20	Brwd3	110808	Others	Yes	Reduction anterior clone
21	btl	110277	Others	No	=
22	b-tub at 56D	24138	Others	Yes	Small clones along the gut
23	bw	101584	Up in Apc Ras	Yes	Reduction anterior clone
24	bwa	101366	Up in Apc Ras	No	=
25	c11.1	110241	Up in Apc Ras	No	=
26	cactin	106979	Up in Apc Ras	Yes	Small clones along the gut
27	Cad96Ca	1091	Up in Apc Ras	No	=
28	CG10006	44538	Others	No	=
29	CG10163	15295	Up in Apc Ras	No	=
30	CG1021	37336	Up in Apc Ras	Yes	Reduction anterior clone
31	CG10420	108354	Up in Apc Ras	No	=
32	CG10638	102914	Up in Apc Ras	No	=
33	CG10641	31308	Others	Yes	Small clones along the gut
34	CG10700	107394	Up in Apc Ras	No	=
35	CG10802	31353	Up in Apc Ras	No	=
36	CG10916	107518	Up in Apc Ras	Yes	Reduction anterior clone
37	CG10924	13929	Others	No	=
38	CG11188	106977	Up in Apc Ras	Yes	Small clones along the gut
39	CG11710	109760	Up in Apc Ras	No	=
40	CG11778	106218	Others	Yes	ND
41	CG11897	105174	Up in Apc Ras	No	=
42	CG13398	103418	Others	No	=
43	CG13623	110643	Up in Apc Ras	Yes	clones similar to wt
44	CG13887	23208	Up in Apc Ras	No	=
45	CG14339	101072	Up in Apc Ras	No	=
46	CG14709	101221	Up in Apc Ras	No	=
47	CG14743	105880	Up in Apc Ras	No	=
48	CG42666	103667	Up in Apc Ras	Yes	Small clones along the gut
49	CG15097	109428	Up in Apc Ras	No	=

Annex 4. RNAi screen gene list in Apc Ras background

number	Gene symbol	Viena RNAi	Selected by	Effect	Result
50	CG15173	105382	Up in Apc Ras	No	=
51	CG1673	110229	Up in Apc Ras	No	=
52	CG17119	107195	Up in Apc Ras	No	ND
53	CG1718	105608	Others	No	ND
54	CG17187	40051	Up in Apc Ras	Yes	Small clones along the gut
55	CG17387	32901	Up in Apc Ras	No	ND
56	CG17739	106131	Others	No	=
57	CG18193	102812	Up in Apc Ras	No	=
58	CG2004	25389	Up in Apc Ras	No	=
59	CG2017	107015	Up in Apc Ras	No	=
60	CG2219	107995	Others	No	ND
61	CG3008	103828	Up in Apc Ras	No	ND
62	CG31055	106359	Up in Apc Ras	Yes	ND
63	CG31075	101809	Others	No	=
64	CG31216	102796	Up in Apc Ras	No	=
65	CG3125	110612	Others	No	=
66	CG31534	21366	Others	No	=
67	CG32138	34412	Others	Yes	Reduction anterior clone
68	CG32280	108754	Up in Apc Ras	No	=
69	CG32369	103923	Up in Apc Ras	Yes	Reduction anterior clone
70	CG32549	42258	Up in Apc Ras	No	=
71	CG33275	15927	Up in Apc Ras	No	=
72	CG34372	107979	Up in Apc Ras	Yes	Small clones along the gut
73	CG3523	108339	Up in Apc Ras	No	=
74	CG3635	37135	Up in Apc Ras	No	=
75	CG3788	100076	Up in Apc Ras	No	=
76	CG4096	109025	Up in Apc Ras	No	=
77	CG42251	109557	Up in Apc Ras	No	=
78	CG42321	107000	Others	Yes	Small clones along the gut
79	CG42389	105154	Up in Apc Ras	No	=
80	CG5036	104796	Others	No	=
81	CG5273	107408	Up in Apc Ras	Yes	Small clones along the gut
82	CG5644	102841	Up in Apc Ras	No	=
83	CG6330	104776	Up in Apc Ras	No	=
84	CG6428	110692	Up in Apc Ras	No	=
85	CG6744	103374	Others	No	=
86	CG6854	12762	Up in Apc Ras	Yes	Small clones along the gut
87	CG7044	27811	Up in Apc Ras	Yes	Reduction anterior clone
88	CG7130	110526	Up in Apc Ras	No	=
89	CG7145	108797	Up in Apc Ras	No	ND
90	CG7188	110358	Up in Apc Ras	Yes	Small clones along the gut
91	CG7526	104254	Others	No	=
92	CG7860	108281	Others	Yes	Small clones along the gut
93	CG8486 (piezo)	105132	Up in Apc Ras	No	=
94	CG8642	101888	Up in Apc Ras	No	=
95	CG8918	28995	Up in Apc Ras	No	=
96	CG9098	105144	Up in Apc Ras	Yes	Invasion of the proventricle
97	ci	105620	Others	No	=
98	cip4	108625	Others	No	=

Annex 4. RNAi screen gene list in Apc Ras background

number	Gene symbol	Viena RNAi	Selected by	Effect	Result
99	contactin	28294	Others	Yes	ND
100	corin	39535	Others	No	=
101	Corp	102751	Up in Apc Ras	No	=
102	CrebA	110650	Others	Yes	ND
103	csk	102313	Up in Apc Ras	Yes	Small clones along the gut
104	cv-2	109915	Up in Apc Ras	No	=
105	Cyp6a2	108766	Up in Apc Ras	No	=
106	da	105258	Others	Yes	ND
107	Dac	106040	Others	No	=
108	daw	105309	Up in Apc Ras	No	=
109	Dcp-1	107560	Others	No	=
110	Def	102437	Up in Apc Ras	No	=
111	Dgp-1	109410	Up in Apc Ras	No	=
112	Dl	109491	Others	No	=
113	DNAseII	100014	Up in Apc Ras	No	=
114	drk	105498	Others	No	=
115	dSmurf b	107395	Others	No	=
116	Duox	2593	Up in Apc Ras	No	ND
117	edl	51819	Up in Apc Ras	No	=
118	eIF2B-delta	104403	Up in Apc Ras	Yes	Small clones along the gut
119	eIF4E	107595	Others	No	=
120	emp	12232	Up in Apc Ras	No	=
121	Eph	110448	Others	No	=
122	Ets21C	106153	Up in Apc Ras	No	=
123	Ets98B	107292	Others	No	=
124	Fas1	101779	Up in Apc Ras	No	=
125	Fas3	26850	Up in Apc Ras	No	=
126	fat-spondin	105844	Others	No	=
127	form3	45594	Others	No	=
128	Gadd45	100413	Up in Apc Ras	No	=
129	Gap1	105383	Up in Apc Ras	No	=
130	GB13F	100011	Others	Yes	Reduction anterior clone
131	gw	103581	Others	Yes	Small clones along the gut
132	GXIVsPLA2	100558	Up in Apc Ras	Yes	Variable
133	Herc2	45302	Others	No	=
134	hh	109454	Up in Apc Ras	Yes	Small clones along the gut
135	hMCC	103335	Others	No	=
136	HNF4	12692	Others	No	=
137	how	100775	Up in Apc Ras	No	=
138	Hsc70-4	101734	Others	Yes	Small clones along the gut
139	Iap2	2973	Others	Yes	Small clones along the gut
140	Ice	28065	Others	No	=
141	ImpL2	106543	Up in Apc Ras	Yes	Reduction anterior clone
142	ImpL3	110190	Up in Apc Ras	No	=
143	Irbp	110409	Up in Apc Ras	No	=
144	jdp	100788	Others	No	=
145	jhamt	103958	Others	Yes	Small clones along the gut
146	Jupiter	110140	Up in Apc Ras	No	=
147	kcnq	106655	Others	No	=

Annex 4. RNAi screen gene list in Apc Ras background

number	Gene symbol	Viena RNAi	Selected by	Effect	Result
148	kek1	101166	Up in Apc Ras	No	=
149	kek2	42450	Up in Apc Ras	No	=
150	kirre	109585	Up in Apc Ras	No	=
151	kis	109414	Others	No	=
152	kon	37283	Up in Apc Ras	Yes	Variable
153	Krn	104299	Up in Apc Ras	No	=
154	KrT95D	105151	Up in Apc Ras	No	=
155	Lac	107450	Up in Apc Ras	No	=
156	Lag1	109418	Others	No	=
157	LKB1	108356	Others	No	=
158	loco	9248	Up in Apc Ras	Yes	Reduction anterior clone
159	lvph	106220	Others	No	=
160	Magu	106494	Others	Yes	Small clones along the gut
161	mct1	106773	Others	Yes	Small clones along the gut
162	Mmp1	101505	Up in Apc Ras	Yes	Reduction anterior clone
163	Mmp2	107888	Up in Apc Ras	No	=
164	mthl5	101593	Up in Apc Ras	No	=
165	Myc	106066	Others	Yes	Small clones along the gut
166	Nc	100424	Others	No	=
167	nec	108366	Up in Apc Ras	No	ND
168	nonA	26441	Others	Yes	Reduction anterior clone
169	norpA	105676	Others	No	=
170	oatp30B	22983	Others	Yes	Small clones along the gut
171	p120ctn	103063	Others	No	=
172	para	104775	Others	No	=
173	Pendulin (pen)	102627	Others	No	=
174	Pepck	20529	Up in Apc Ras	Yes	Reduction anterior clone
175	Pfk	105666	Up in Apc Ras	No	=
176	Pgi	24257	Up in Apc Ras	No	=
177	PhKgamma	110638	Up in Apc Ras	No	=
178	pk	101480	Others	No	=
179	Pka-C1	101524	Others	No	=
180	prc	100357	Up in Apc Ras	No	=
181	prominin	106533	Others	No	=
182	pros54	110659	Others	Yes	Reduction anterior clone
183	Prosbeta2R2	103323	Up in Apc Ras	No	=
184	Pten	(cr.II)	Others	No	=
185	Pvf2	7628	Up in Apc Ras	No	=
186	Pvf3	105008	Up in Apc Ras	No	=
187	Pvr	105353	Up in Apc Ras	Yes	Small clones along the gut
188	pxn	107180	Others	No	=
189	RanGap	108264	Others	Yes	Small clones along the gut
190	rhoGAP5a	102000	Others	No	=
191	Rim	39384	Others	No	=
192	rk	105360	Others	No	=
193	Rock	104675	Others	No	=
194	RPA2	102306	Up in Apc Ras	Yes	Small clones along the gut
195	rpr	101234	Up in Apc Ras	No	=
196	rumi	14480	Others	No	=

Annex 4. RNAi screen gene list in Apc Ras background

number	Gene symbol	Viena RNAi	Selected by	Effect	Result
197	salm	101052	Up in Apc Ras	No	=
198	scf	105422	Up in Apc Ras	No	ND
199	scyl	25506	Up in Apc Ras	No	=
200	sens	106028	Others	Yes	Small clones along the gut
201	Sickie	104551	Others	No	=
202	slik	43783	Others	Yes	Reduction anterior clone
203	slmb	34273	Others	Yes	Reduction anterior clone
204	slo (slowpoke)	104421	Others	Yes	Small clones along the gut
205	smo	108351	Others	Yes	Small clones along the gut
206	sns	109442	Others	No	=
207	Sox14	107146	Others	No	=
208	spinophilin	105888	Others	No	ND
209	Spn5	28340	Up in Apc Ras	Yes	Reduction anterior clone
210	spri	101164	Up in Apc Ras	No	=
211	sprt	107873	Up in Apc Ras	No	=
212	Src42	100708	Others	No	=
213	stc	47973	Others	Yes	Reduction anterior clone
214	Su(Dx) b	103814	Others	No	=
215	tacc	101439	Others	No	=
216	Thor	100739	Up in Apc Ras	No	=
217	Tollo (dTLR8)	27099	Others	No	=
218	Tribbles	106774	Others	No	=
219	Tsp	100721	Up in Apc Ras	No	=
220	Ugt36Ba	102613	Up in Apc Ras	No	=
221	upd2	14664	Up in Apc Ras	No	ND
222	upd3	106869	Up in Apc Ras	No	=
223	vari	104548	Up in Apc Ras	No	=
224	wus	110270	Up in Apc Ras	No	=
225	mtSSB	107322	Others	Yes	Small clones along the gut
226	tam	106955	Others	No	=
227	mt DNA helicase	108644	Others	Yes	Reduction anterior clone
228	sod	108307	Others	No	=
229	sesB	48581	Others	Yes	Reduction anterior clone
230	Sod2	110547	Others	Yes	Reduction anterior clone
231	mt TFB2	107086	Others	Yes	Small clones along the gut
232	boi	3060	Others	Yes	Small clones along the gut
233	iHog	1001	Others	No	=
234	scribble	41845	Others	No	=
235	lic/MPK3	20166	Others	No	=
236	Dp110	107390	Others	Yes	clones similar to wt
237	Cdc42	100794	Others	No	=
238	fkh	106644	Others	No	=
239	E-cad	2781	Others	Yes	Reduction anterior clone
240	Ipk2	43825	Others	Yes	ND
241	p53	103001	Others	No	=
242	UAS-p53R155H	n/a	Others	No	ND
243	lok30	n/a	Others	No	ND
244	mnkP6	n/a	Others	No	=
245	Mlh1	105425	Others	Yes	Reduction anterior clone

Annex 4. RNAi screen gene list in Apc Ras background

number	Gene symbol	Viena RNAi	Selected by	Effect	Result
246	Msh6	108076	Others	Yes	Reduction anterior clone

Annex 5. List of binding sites present in the promoters of Dpp pathway components and the related TF

TF name	Dad_12879729	Dad_12880619	Mad_3159630	Med_27436787	put_10451421	tkv_5237358	tkv_5242606	tkv_5244250	tkv_5271353	n° genes
achi	0	0	0	0	1	0	0	1	0	2
ap	0	0	0	0	0	1	0	0	0	1
ara	0	2	1	0	1	1	0	1	1	4
bap	0	0	0	0	0	0	0	1	0	1
B-H1	0	0	0	0	0	0	0	2	0	1
B-H2	0	0	0	0	0	0	0	2	0	1
brk	1	1	0	0	2	0	0	0	0	2
br_Z1	0	0	0	0	0	0	0	1	0	1
br_Z2	0	0	0	0	0	0	0	0	1	1
br_Z3	0	0	0	0	0	0	0	1	0	1
br_Z4	0	0	0	0	0	1	0	1	0	1
bsh	0	0	0	0	0	0	0	2	0	1
cad	0	0	0	0	0	0	0	0	1	1
caup	0	2	1	0	1	1	0	1	1	4
CG11085	0	0	0	0	0	0	0	2	0	1
CG13424	0	0	0	0	0	0	0	2	0	1
CG15696	0	0	0	0	0	0	0	2	0	1
CG18599	0	0	0	0	0	1	0	0	0	1
CG34031	0	0	0	0	0	0	0	2	0	1
CG42234	0	0	0	0	0	1	0	0	0	1
CG4328	0	0	0	0	0	1	0	0	1	1
CG9876	0	0	0	0	0	1	0	0	0	1
ct	0	0	0	0	1	0	0	0	0	1
Deaf1	0	0	0	0	0	0	1	1	1	1
Dfd	0	0	0	0	0	0	0	1	0	1
dl_1	0	0	1	0	0	0	0	1	0	2
dl_2	0	0	0	0	0	0	0	1	0	1
Dr	0	0	0	0	0	1	1	1	0	1
Eip74EF	0	1	1	0	0	0	0	0	0	2
eve	0	0	0	0	0	0	0	1	0	1
fkh	0	0	0	0	0	0	0	1	0	1

Annex 5. List of binding sites present in the promoters of Dpp pathway components and the related TF

TF name	Dad_12879729	Dad_12880619	Mad_3159630	Med_27436787	put_10451421	tkv_5237358	tkv_5242606	tkv_5244250	tkv_5271353	n° genes
gt	0	0	0	0	0	0	2	0	0	1
h	0	0	0	0	0	0	0	0	2	1
Hmx	0	0	0	0	0	0	0	2	0	1
hth	0	0	0	0	1	0	0	1	0	2
ind	0	0	0	0	0	1	0	0	0	1
kni	0	0	0	0	0	0	1	0	0	1
Lag1	0	0	1	0	0	0	0	0	0	1
lbe	0	0	0	1	0	0	0	0	0	1
lbl	0	0	0	0	0	2	0	0	0	1
mirr	3	5	4	8	0	0	0	2	1	4
NK7.1	0	0	0	0	0	0	0	2	0	1
odd	0	0	0	0	0	0	0	0	1	1
OdsH	0	0	0	0	0	1	0	0	0	1
onecut	0	2	0	0	1	0	0	1	2	3
Optix	1	1	0	1	2	1	1	0	2	4
ovo	0	0	0	0	0	0	1	0	0	1
pan	0	0	0	1	0	0	0	1	1	2
Pph13	0	0	0	0	0	1	0	0	0	1
prd	0	0	0	0	0	0	1	0	0	1
ro	0	0	0	0	0	1	0	0	0	1
run::Bgb	0	0	0	0	1	0	0	1	0	2
Rx	0	0	0	0	0	1	0	0	0	1
Scr	0	0	0	0	0	0	0	1	0	1
sd	1	1	0	0	0	1	0	0	1	2
Six4	0	0	0	1	1	0	0	0	0	2
slou	0	0	0	0	0	0	0	2	0	1
slp1	0	0	0	0	0	0	0	1	0	1
sna	0	0	0	0	0	0	0	1	0	1
so	1	1	0	1	1	0	0	0	0	3
Su(H)	0	0	0	1	0	0	0	0	0	1
tin	0	0	0	0	0	1	0	0	1	1

Annex 5. List of binding sites present in the promoters of Dpp pathway components and the related TF

TF name	Dad_12879729	Dad_12880619	Mad_3159630	Med_27436787	put_10451421	tkv_5237358	tkv_5242606	tkv_5244250	tkv_5271353	n° genes
tup	0	0	0	0	0	0	0	2	0	1
unc-4	0	0	0	0	0	0	0	2	0	1
usp	0	0	1	0	1	0	0	0	0	2
vis	0	0	0	0	1	0	0	1	0	2
vnd	0	0	0	0	0	1	0	0	0	1
vvl	0	1	0	0	0	0	2	0	0	2
z	0	0	0	0	0	0	1	0	0	1
zen	0	0	0	0	0	0	0	1	0	1

El següent manuscrit ha estat acceptat el dia 7 de gener de 2014
a la revista *Plos One*

Conserved mechanisms of tumorigenesis in the *Drosophila* adult midgut

Òscar Martorell[1,2], Anna Merlos-Suárez[3], Kyra Campbell[1,2], Francisco M. Barriga[3], Christo P. Christov[4], Irene Miguel-Aliaga[5], Eduard Batlle[3,6], Jordi Casanova[1,2] and Andreu Casali[1,2,7]

1. Cell and Developmental Biology Program. Institute for Research in Biomedicine (IRB), Baldiri Reixach 10, 08028 Barcelona, Spain.

2. Institut de Biologia Molecular de Barcelona (IBMB-CSIC), Baldiri Reixach 10, 08028 Barcelona, Spain.

3. Oncology Program. Institute for Research in Biomedicine (IRB), Baldiri Reixach 10, 08028 Barcelona, Spain.

4. Department of Zoology, University of Cambridge, Downing Street, Cambridge CB2 3EJ, UK

5. MRC Clinical Sciences Centre, Imperial College London, Du Cane Road, London W12 0NN, UK.

6. Institució Catalana de Recerca i Estudis Avançats (ICREA)

7. Correspondence: andreu.casali@irbbarcelona.org, phone: +34 934 034 966.

Abstract

Whereas the series of genetic events leading to colorectal cancer (CRC) have been well established, the precise functions that these alterations play in tumor progression and how they disrupt intestinal homeostasis remain poorly characterized. Activation of the Wnt/Wg signaling pathway by a mutation in the gene APC is the most common trigger for CRC, inducing benign lesions that progress to carcinomas due to the accumulation of other genetic alterations. Among those, Ras mutations drive tumour progression in CRC, as well as in most epithelial cancers. As mammalian and *Drosophila*'s intestines share many similarities, we decided to explore the alterations induced in the *Drosophila* midgut by the combined activation of the Wnt signaling pathway with gain of function of Ras signaling in the intestinal stem cells. Here we show that compound Apc-Ras clones, but not clones bearing the individual mutations, expand as aggressive intestinal tumor-like outgrowths. These lesions reproduce many of the human CRC hallmarks such as increased proliferation, blockade of cell differentiation and cell polarity and disrupted organ architecture. This process is followed by expression of tumoral markers present in human lesions. Finally, a metabolic behavioral assay shows that these flies suffer a progressive deterioration in intestinal homeostasis, providing a simple readout that could be used in screens for tumor modifiers or therapeutic compounds. Taken together, our results illustrate the conservation of the mechanisms of CRC tumorigenesis in *Drosophila*, providing an excellent model system to unravel the events that, upon mutation in Apc and Ras, lead to CRC initiation and progression.

Introduction

Activating mutations in the Wnt and Ras signaling pathways are common in many epithelial cancers. Colorectal cancer (CRC), for example, usually starts with mutations in APC, a negative regulator of the Wnt signaling pathway[1-3] followed, in ~50% of CRC patients, by the oncogenic activation of K-Ras, an event that correlates with the onset of malignancy[4]. This process can be reproduced in mouse models for CRC, where the conditional deletion of APC in the intestinal epithelium imposes a stem/progenitor-like phenotype, leading to massive crypt hyperproliferation and formation of benign tumors known as adenomas[3,5-7]. In turn, expression of K-Ras gain of function alleles in Apc mutant tumor cells induces the development of large, aggressive adenocarcinomas[7,8]. However, whereas this genetic events leading to CRC have been well established, the precise genetic programs that these alterations impose, which role play in tumor progression and how they disrupt intestinal homeostasis remain poorly characterized.

It has been shown that the removal of APC specifically in the intestinal stem cells (ISCs), but not in their progeny, leads to the formation of lesions that progress to adenomas in less than three weeks, suggesting that ISCs may represent the cell of origin of CRC[9]. Mammalian ISCs are located at the base of the intestinal crypts, where they self-renew and generate a transient amplifying population. These progenitor cells undergo several rounds of division while moving upwards along the crypt axis and finally arrest and differentiate towards enterocytes, enteroendocrine cells or goblet cells[10]. Interestingly, there are many relevant similarities between mammalian and *Drosophila* intestines[11,12]. The adult *Drosophila* midgut epithelium is also maintained by a population of ISCs that regenerate the stem cell pool or become quiescent progenitor cells (known as enteroblasts, or EB), which ultimately differentiate towards enterocytes (ECs) or enteroendocrine cells (EEs)[13,14]. The Wg/Wnt signaling pathway is required for both mammalian and fly intestinal stem cell homeostasis[15-18], and its constitutive activation in *Drosophila* through mutations in the APC homologues, Apc and Apc2, results in ISC hyperproliferation and midgut hyperplasia[17]. Moreover, EGFR/Ras signaling pathway activity also promotes ISC division and is therefore required for ISC proliferation[19-25].

Drosophila has been widely used to recapitulate key aspects of human cancer[26].

Here, we generated clones that combined the loss of Apc with the expression of the oncogenic form of Ras, Ras^{V12}. We show that these compound Apc-Ras clones, but not clones bearing the individual mutations, expand as aggressive intestinal tumor-like over-growths that reproduce many hallmarks of human CRC. Of note, similar conclusions about the ability to form tumors upon loss of Apc and oncogenic Ras expression have been reached in an recent study[27]. Moreover, we show that flies bearing Apc-Ras clones suffer a progressive deterioration in intestinal homeostasis, providing a simple readout that could be used in screens for tumor modifiers or therapeutic compounds. Our results show that the mechanisms leading to tumorigenesis in the human colon upon mutation of Apc and Ras are conserved in the *Drosophila* adult midgut, providing an excellent model system to analyze the genetic events involved in tumor initiation and progression.

Results

Combination of Apc mutations and oncogenic Ras expression induces the outgrowth of clones in the adult *Drosophila* midgut

The similarities between mammalian and *Drosophila* intestines prompted us to investigate whether the generation of compound Apc-Ras clones in the adult midgut epithelia, mutant for both forms of the *Drosophila* APC gene, *Apc* and *Apc2*, and over-expressing the oncogenic form of Ras, UAS-Ras^{V12} (refs [28,29]), would reproduce the first steps of CRC. In order to test this hypothesis we induced, by means of the MARCM technique[30], GFP-marked Apc-Ras clones in the ISCs, the only dividing cells in the adult midgut[13,14]. As controls, we generated *i*) wild type clones, *ii*) clones mutant for *Apc* and *Apc2* (Apc clones) and *iii*) clones over-expressing UAS-Ras^{V12} (Ras clones).

We first noticed that flies bearing Apc-Ras clones had a shorter life span compared to flies bearing control clones, displaying a ~50% survival rate four weeks after clone induction (Fig. 1a). We also observed that, one week after clone induction, Apc-Ras and control clones showed relatively small differences in clone size, number and distribution along the anterior and posterior midgut (Fig. 1b,c,e,g,i,k and Table 1). Four weeks after clone induction, wild-type clones did not change noticeably (Fig. 1d,k

and Table 1) and Apc clones slightly increased in size but remained similar in number and distribution (Fig. 1f,k,l,m and Table 1). However, most Apc-Ras clones disappeared, but the few remaining were dramatically enlarged and usually localized in the anterior-most part of the anterior midgut (Fig. 1j,k,l,m and Table 1). In contrast, Ras clones also disappeared but the few remaining were small and localized mostly in the central region of the gut (M) (Fig. 1b,h,l,m and Table 1), suggesting the existence of a mechanism able to induce the disappearance of Ras^{V12}-expressing cells. This mechanism of clone decline does not rely on apoptosis, as the over-expression of the anti-apoptotic viral protein P35 or the apoptosis inhibitor Diap1 did not noticeably increase the number of Apc-Ras clones (Fig. 2a,b).

We also observed that Apc-Ras clones, but not control clones, occupied almost all the luminal space (Fig. 2c), colonized the surrounding wild type intestinal epithelium (Fig. 2d, arrow) and, in 17% of the cases (n=117), grew below the wild type epithelia, suggesting invasive abilities (Fig. 2e), although we were not able to detect any disruption of the basal membrane (Fig. 3a). We conclude that loss of Apc combined with activated Ras expression has a synergistic effect able to induce "tumor-like" over-growths to an extent never achieved by clones generated individually, reproducing the initial events in the adenoma to carcinoma transition of CRC.

Apc-Ras clones show many tumoral hallmarks.

Further characterization of Apc-Ras clones showed that they display many tumoral characteristics. We first found that they had an enhanced proliferation rate, with a remarkable increase in the number of cells positive for the mitotic marker phospho-histone 3 (PH3) compared to the surrounding wild type epithelium (Fig. 3b). As expected, Armadillo (Arm), the *Drosophila* homolog of β-catenin, was homogeneously enriched in all Apc-Ras cells (Fig. 3c), reflecting the constitutive activation of the Wg signaling pathway. Moreover, Arm staining around the membrane in Apc-Ras cells (Fig. 3c, arrow), which differs from the apicolateral staining in adjacent normal ISCs (Fig. 3c, arrowhead), indicated loss of cell polarity. This loss of polarity was confirmed by the delocalization of the septate junction marker and neoplastic tumor suppressor Discs large (Dlg)[31] (Fig. 3d). We also observed an aberrant tissue organization, as small fragments

of the actin-rich microvilli present on the apical, luminal domain of the ECs were not correctly oriented with respect to the apico-basal axis of the midgut (Fig. 3e, arrow). Electron microscope analysis of a wild type midgut showed that is lined by a simple epithelium where each cell, including the ISCs, stands on the basal lamina (Fig. 3g), as previously described[32]. In contrast, Apc-Ras clones showed an aberrant, dysplastic, highly disorganized tissue with multiple lumens and several layers of non-polarized cells that did not stand on the basal lamina (Fig. 2h,i). Finally, Apc-Ras clones, but not control clones, expressed the tumoral marker Singed (Sn) (Fig. 2f and Supplementary Fig. 1a). Sn is the *Drosophila* homolog of the actin-bundling protein Fascin1 (ref [33]), a key component of filopodia that has been identified as a target of the β-catenin-TCF signaling in CRC cells and is over-expressed in the invasive front during tumor progression[34]. Interestingly, Sn expression was also localized at the edge of the clones (Supplementary Fig. 1b). In summary, our results show that, four weeks after induction, Apc-Ras clones display tumor-like characteristics. Thus, the synergistic action of loss of Apc and activated Ras is enough to transform normal intestinal epithelia to "tumor-like" over-growths.

Apc-Ras clones display cell heterogeneity

We next analyzed the cellular composition of Apc-Ras clones. Similar to human CRC, which recapitulates the cell hierarchy of the normal intestinal mucosa[35,36], we detected in Apc-Ras clones cells with phenotypes reminiscent to ISCs, marked by Delta (Dl) (Fig. 4a,c), EEs, marked by Prospero (Pros) (Fig. 4a,d, arrow), ECs, marked by the POU domain protein 1 (Pdm1) (Fig. 4a,d, arrowhead) and EBs, marked by the expression of Su(H)mCherry (Fig. 4e). We noticed, however, that most cells within Apc-Ras clones were negative for ISC, EB and differentiation markers (Fig. 4c,d,e). In order to further characterize this phenotype, we sorted cells by flow cytometry from wild type, Apc and Apc-Ras clones four weeks after clone induction (Fig. 4f). Analysis of expression levels by qRT-PCR showed that the Wg/Wnt target gene Frizzled3 (Fz3), the Ras target gene Rhomboid (Rho) and Sn were expressed as expected (Fig. 4g), validating our sorting strategy. qRT-PCR analysis also showed a decrease in the RNA levels of Dl, Pros and the EC marker Myosin31DF (Myo31DF) in Apc-Ras clones (Fig. 4h), confirming that many cells within these clones must belong to a new cell type that do not express any of the

known cell markers. As the qRT-PCR analysis also showed that the JAK/STAT pathway transcription factor stat92e, required for EB differentiation[37-39], was down-regulated in Apc-Ras clones (Fig. 4h), we considered the possibility that this new cell type could be formed by EBs that fail to differentiate and named them "EB-like" cells (Fig. 4b).

In normal tissue, ISCs fuel growth through accelerated division rates and/or predominance of symmetric division [40]. As there were few ISCs in Apc-Ras clones (Fig. 4c,h), we considered the non-mutually exclusive possibility that the proliferation of this new "EB-like" cell population could also account for the growth of Apc-Ras clones. In order to address this issue, we stained Apc-Ras clones with the mitotic marker phospho-histone 3 (PH3). We observed that most $PH3^{+}$ cells within the clones showed a very low or non detectable Dl staining (Fig. 4i, arrowheads), characteristic of EBs[41], in contrast to the surrounding wild type epithelia where PH3 staining colocalized with the high Dl staining characteristic of ISCs (Fig. 4h, arrow). Therefore, our results suggests that the "EB-like" population in Apc-Ras clones could be formed by EBs that failed to differentiate and acquired the capacity to proliferate, possibly accounting for the massive growth of Apc-Ras clones.

Gut physiology is altered in flies bearing Apc-Ras clones

Since Apc-Ras clones occupy most of the intestinal lumen, we wondered whether gut physiology would be affected. Using a recently developed quantitative assay[42], we observed a severe decrease in the fecal output of flies bearing Apc-Ras clones (Fig. 5a, b). A time-course analysis revealed that this reduction was progressive and associated with tumor development, given that four weeks after induction flies were much more severely affected than younger flies (Fig. a). The reduction in fecal output was preceded by an increase in intestinal transit time, as two days after feeding control flies with blue food their guts appeared "clean" (Fig. 5c,d), in contrast to flies bearing Apc-Ras clones, whose guts remained blue for up to a week (Fig. 5c,e). We also observed that while flies with Apc clones only displayed an obvious phenotype four weeks after induction, flies with Apc-Ras clones showed reduced intestinal transit just two weeks after induction, and a severe reduction in fecal output three weeks after induction (Fig. 5c). These results show that the tumor burden affects the intestinal physiology of the flies and provides a

simple strategy for drug screening in CRC treatment as the correlation between this phenotype and tumor severity provides a simple readout for tumor modifiers and/or potential therapeutic compounds.

Discussion

The development of human CRC is a multistep process, characterized by the accumulation of mutations in different oncogenes and tumor suppressor genes, which lead to the progression from normal mucosa to carcinoma. In this paper we demonstrate that activation of the Wg/Wnt and Ras signaling pathways, the two main players in the onset of human CRC, generate tumors in the *Drosophila* adult midgut. Remarkably, these tumors reproduce many of the hallmarks of human CRC, such as increased proliferation, loss of cell differentiation and polarity, cell heterogeneity, aberrant cell organization and expression of tumoral markers. Taken together, our results show that *Drosophila*, an organism widely recognized by the amenability of its genetics, which has already been used to model human diseases[12,26,43], is an excellent system to understand basic genetic questions about human CRC progression.

Surprisingly, we have also found out that the *Drosophila* CRC model shows characteristics that go beyond genetic interactions. For example, the majority of human gastrointestinal tumors are localized in the colon and rectum, yet most of the genetically engineered mouse models of CRC manifest almost exclusively lesions in the small intestine[44]. These results suggest the existence of intrinsic genetic differences along the gastrointestinal tract that render cells refractory to tumor formation and/or to tumor suppression mechanisms in specific regions. Remarkably, we have identified regional differences in *Drosophila*, where Apc-Ras clones tend to develop in the most anterior part of the anterior region. As it has been recently described the existence of a regional organization with distinct morphological and genetic properties along the anteroposterior axis of the adult *Drosophila* midgut[45,46], its likely that factors regulating the survival of Apc-Ras clones in the anterior midgut will be identified in the near future.

Moreover, Ras clones are eliminated from the anterior and posterior midgut four weeks after clone induction through an apoptosis-independent process, suggesting the existence of a Ras^{V12}-driven tumor suppression mechanism. Expression of Ras^{V12} in a

single epithelial cell within a monolayer of wild type cells has been shown to induce its apical extrusion or basal protrusion[47], while Ras^{V12} expression in ECs is sufficient to promote their delamination from the epithelia[21], suggesting that similar events may take place in ISCs upon Ras^{V12} expression. Alternatively, Ras^{V12} may induce tumor suppression by promoting cellular senescence, as described in yeast and mammals[48]. Due to the similarities in the signaling pathways controlling intestinal development both in mammals and *Drosophila*, we envisage that elucidation of the mechanism allowing Ras^{V12} clones to bypass tumor suppression will be of importance to understand the regional differences in tumor development along the gastrointestinal tract.

Materials & Methods

Clone generation. MARCM clones were generated by a 1hr heat shock at 37ºC of 2-5 days old females and were marked by the progenitor cell marker escargot (esg) Gal4 line driving the expression of UAS GFP. Although esg is expressed only in the progenitor cells (ISCs and EBs), the amount of GFP produced in our experimental conditions was enough to be detected also in EEs and ECs.

Genotypes. *yw UAS flp ; esg Gal4 UAS-GFP/CyO; FRT82B Gal80/TM6b* flies were crossed with *yw hsp70-flp;UAS-Ras^{V12}/CyO; FRT82B/TM6b* flies to generate control and Ras clones, and were crossed to *yw hsp70-flp;UAS-Ras^{V12}/CyO; FRT82B Apc2^{N175K}Apc^{Q8} /TM6b* flies to generate Apc and Apc-Ras clones. *yw hsp70-flp; esg Gal4 UAS-GFP UAS-Ras^{V12}/CyO; FRT82B Gal80/TM6b* were crossed with *yw hsp70-flp; Sp/CyO; FRT82B Apc2^{N175K}Apc^{Q8}/TM6b* or *yw hsp70-flp; Sp/CyO; Su(H)mCherry FRT82B Apc2^{N175K}Apc^{Q8}/TM6b* to generate the Apc-Ras clones described in Figure 4. $Apc2^{N175K}$ is a loss-of-function allele, Apc^{Q8} is a null allele, and UAS-Ras^{V12} is a gain-of-function transgene. Stocks were obtained form Bloomington Stock Center and VDRC. The Su(H)mCherry stock was a gift from Sarah Bray.

Staining and antibodies. Adult female flies were dissected in PBS. All the digestive tract was removed and fixed in PBS and 4% electron microscopy grade paraformaldehyde (Polysciences, USA) for 35 minutes. Samples were rinsed 3 times with PBS, 4% BSA, 0.1% Triton X-100 (PBT-BSA), incubated with the primary antibody

overnight at 4°C and with the secondary antibody for 2 hours at room temperature. Finally, the samples were rinsed 3 times with PBT-BSA and mounted in DAPI-containing media (Vectashield, USA). All the steps were performed without mechanical agitation. Primary antibodies mouse α-Pros (1:100), α-Dl (1:10), α-Arm (1:10), α-Dlg (1:250) and α-Sn (1:50) were obtained from the Developmental Studies Hybridoma Bank (DSHB), rabbit α-PH3 (1:100) from Cell Signalling (USA), rabbit α-Pdm1 (1:1000) was a gift of Dr.Yang Xiaohang (Institute of Molecular and Cell Biology, Singapore), rabbit α-laminin (1:1000) was from Sigma (USA) and goat α-GFP (1:500) was form Abcam (UK). Secondary antibodies were from Invitrogen (USA). TRICT-conjugated Phalloidin (Sigma, USA) was used at 5μg/ml. Images were obtained on a Leica SPE or Leica SP5 confocal microscopy and processed in Photoshop CS5 (Adobe, USA).

Quantifications. GFP area was calculated using ImageJ 1.34s (Rasband, W.S., http://rsb.info.nih.gov/ij/). Statistical analysis was performed applying the Wilcoxon Signed-Ranks Test. Differences were considered significative when $p<0.05$.

Clone gene expression analysis. *Drosophila* midguts were dissected from control, Apc or Apc-Ras flies four weeks after induction. In order to obtain single cell suspensions, samples were incubated in PBS containing 0,4mg/ml dispase (Gibco) for 15 min at 37ºC, syringed using a 27G needle and washed twice with PBS. After selecting for the viable population (propidium iodide negative), GFP^+ cells were isolated by fluorescence activated cell sorting (FACS) using a FACSAria 2.0 (BD Biosciences) and RNA was extracted and amplified as recently described[49]. Gene expression levels were assessed using Power Sybr Green quantitative PCR (Applied Biosystems) following the manufacturer's instructions. Actin 5C was used as an endogenous control for normalization and differences in target gene expression were determined using the StepOne 2.0 software (Applied Biosystems). All measurements were performed in triplicate from three independent sorting experiments. Primer pairs for each gene were the following:

Dl forward) GAGCAAGTCGAGTGTCCAAA

Dl reverse) GCACCAACAAGCTCCTCAT

Fz3 forward) TGCTCTGCTCGTCTCTGTTT

Fz3 reverse) ATGCACAACTCGTGCTTCTC

Myo31DF forward) GATCCAGGTGAAGAGACGGT

Myo31DF reverse) TTCCAAACCATTGAGGATGA

Pro forward) CCGATGATCTGTTGATTGCT

Pro reverse) GGTACCTCAATGTGGTTATTGC

Rho forward) CTCCATCATTGAGATTGCCA

Rho reverse) GACGATATTGAAGCCCAGGT

Sn forward) AGGATCTGCATAAGATCGCA

Sn reverse) CAGCTGCGTGGATCAATAAT

Stat92e forward) GTTGCGACTGGATCTCTGAC

Stat92e reverse) ATCTGCTTGAACAGGTGCAG

Intestinal physiology assays. Defecation assays were performed and quantified as previously described[42]. At least 20 flies of each genotype were monitored over the course of four weeks in fly vials with standard food at 25^{o}C. Once a week, they were individually transferred to clear plastic cuvettes containing the same food supplemented with 0.5% bromophenol blue for 72 hours. Digital images of the cuvette walls were obtained using an Epson Perfection 4990 Photo scanner. After each defecation assay, flies were transferred to food without the dye in order to monitor the dye's intestinal transit by visually monitoring the dye's clearance time.

Acknowledgments

We are thankful to the IRB Cell separation Unit and the Electron cryo-microscopy laboratory from the Scientific & Technological Centre (University of Barcelona), to Dr. Iglesias and Dr. Lloreta for help with the interpretation of EM data, and to Bloomington stock center for fly stocks. We also thank G. Darras, P. Okenve, and members of Casanova and Llimargas labs for discussions, Y. Rivera for technical help, and M. Furriols, M. Rahman, D. Shaye and T. Stracker for comments on the manuscript. O.M. is a recipient of a FPU fellowship from the MEC.

References

1. Fearon ER, Vogelstein B (1990) A genetic model for colorectal tumorigenesis. Cell 61: 759–767.

2. Korinek V, Barker N, Morin PJ, van Wichen D, de Weger R, et al. (1997) Constitutive transcriptional activation by a beta-catenin-Tcf complex in APC-/- colon carcinoma. Science 275: 1784–1787.

3. Morin PJ, Morin PJ, Sparks AB, Sparks AB, Korinek V, et al. (1997) Activation of beta-catenin-Tcf signaling in colon cancer by mutations in beta-catenin or APC. Science 275: 1787–1790.

4. Ohnishi T, Tomita N, Monden T, Ohue M, Yana I, et al. (1997) A detailed analysis of the role of K-ras gene mutation in the progression of colorectal adenoma. British journal of cancer 75: 341–347. Available: http://eutils.ncbi.nlm.nih.gov/entrez/eutils/elink.fcgi?dbfrom=pubmed&id=9020477&retmode=ref&cmd=prlinks.

5. van de Wetering M, Sancho E, Verweij C, de Lau W, Oving I, et al. (2002) The beta-catenin/TCF-4 complex imposes a crypt progenitor phenotype on colorectal cancer cells. Cell 111: 241–250. Available: http://eutils.ncbi.nlm.nih.gov/entrez/eutils/elink.fcgi?dbfrom=pubmed&id=12408868&retmode=ref&cmd=prlinks.

6. Batlle E, Henderson JT, Beghtel H, van den Born MMW, Sancho E, et al. (2002) Beta-catenin and TCF mediate cell positioning in the intestinal epithelium by controlling the expression of EphB/ephrinB. Cell 111: 251–263. Available: http://eutils.ncbi.nlm.nih.gov/entrez/eutils/elink.fcgi?dbfrom=pubmed&id=12408869&retmode=ref&cmd=prlinks.

7. Sansom OJ, Reed KR, Hayes AJ, Ireland H, Brinkmann H, et al. (2004) Loss of Apc in vivo immediately perturbs Wnt signaling, differentiation, and migration. Genes & development 18: 1385–1390. Available: http://eutils.ncbi.nlm.nih.gov/entrez/eutils/elink.fcgi?dbfrom=pubmed&id=15198980&retmode=ref&cmd=prlinks.

8. Janssen K-P, Alberici P, Fsihi H, Gaspar C, Breukel C, et al. (2006) APC and oncogenic KRAS are synergistic in enhancing Wnt signaling in intestinal tumor formation and progression. Gastroenterology 131: 1096–1109. Available: http://eutils.ncbi.nlm.nih.gov/entrez/eutils/elink.fcgi?dbfrom=pubmed&id=17030180&retmode=ref&cmd=prlinks.

9. Barker N, Ridgway RA, van Es JH, van de Wetering M, Begthel H, et al. (2009) Crypt stem cells as the cells-of-origin of intestinal cancer. Nature 457: 608–611. Available: http://eutils.ncbi.nlm.nih.gov/entrez/eutils/elink.fcgi?dbfrom=pubmed&id=19092804&retmode=ref&cmd=prlinks.

10. van der Flier LG, Clevers H (2009) Stem cells, self-renewal, and differentiation in the intestinal epithelium. Annual review of physiology 71: 241–260. Available: http://eutils.ncbi.nlm.nih.gov/entrez/eutils/elink.fcgi?dbfrom=pubmed&id=18808327&retmode=ref&cmd=prlinks.

11. Casali A, Batlle E (2009) Intestinal stem cells in mammals and Drosophila. Cell Stem Cell 4: 124–127. doi:10.1016/j.stem.2009.01.009.

12. Apidianakis Y, Rahme LG (2011) Drosophila melanogaster as a model for human intestinal infection and pathology. Disease models & mechanisms 4: 21–30. Available: http://eutils.ncbi.nlm.nih.gov/entrez/eutils/elink.fcgi?dbfrom=pubmed&id=21183483&retmode=ref&cmd=prlinks.

13. Micchelli CA, Perrimon N (2006) Evidence that stem cells reside in the adult Drosophila midgut epithelium. Nature 439: 475–479. Available: http://eutils.ncbi.nlm.nih.gov/entrez/eutils/elink.fcgi?dbfrom=pubmed&id=16340959&retmode=ref&cmd=prlinks.

14. Ohlstein B, Spradling A (2006) The adult Drosophila posterior midgut is maintained by pluripotent stem cells. Nature 439: 470–474. Available: http://eutils.ncbi.nlm.nih.gov/entrez/eutils/elink.fcgi?dbfrom=pubmed&id=16340960&retmode=ref&cmd=prlinks.

15. Pinto D, Gregorieff A, Begthel H, Clevers H (2003) Canonical Wnt signals are essential for homeostasis of the intestinal epithelium. Genes & development 17: 1709–1713. Available: http://eutils.ncbi.nlm.nih.gov/entrez/eutils/elink.fcgi?dbfrom=pubmed&id=12865297&retmode=ref&cmd=prlinks.

16. Lin G, Xu N, Xi R (2008) Paracrine Wingless signalling controls self-renewal of Drosophila intestinal stem cells. Nature 455: 1119–1123. Available: http://eutils.ncbi.nlm.nih.gov/entrez/eutils/elink.fcgi?dbfrom=pubmed&id=18806781&retmode=ref&cmd=prlinks.

17. Lee W-C, Beebe K, Sudmeier L, Micchelli CA (2009) Adenomatous polyposis coli regulates Drosophila intestinal stem cell proliferation. Development 136: 2255–2264. Available: http://eutils.ncbi.nlm.nih.gov/entrez/eutils/elink.fcgi?dbfrom=pubmed&id=19502486&retmode=ref&cmd=prlinks.

18. Cordero JB, Stefanatos RK, Myant K, Vidal M, Sansom OJ (2012) Non-autonomous crosstalk between the Jak/Stat and Egfr pathways mediates Apc1-driven intestinal stem cell hyperplasia in the Drosophila adult midgut. Development 139: 4524–4535. Available: http://eutils.ncbi.nlm.nih.gov/entrez/eutils/elink.fcgi?dbfrom=pubmed&id=23172913&retmode=ref&cmd=prlinks.

19. Xu N, Wang SQ, Tan D, Gao Y, Lin G, et al. (2011) EGFR, Wingless and JAK/STAT signaling cooperatively maintain Drosophila intestinal stem cells. Developmental biology 354: 31–43. Available: http://eutils.ncbi.nlm.nih.gov/entrez/eutils/elink.fcgi?dbfrom=pubmed&id=21440535&retmode=ref&cmd=prlinks.

20. Jiang H, Grenley MO, Bravo M-J, Blumhagen RZ, Edgar BA (2011) EGFR/Ras/MAPK signaling mediates adult midgut epithelial homeostasis and regeneration in Drosophila. Cell Stem Cell 8: 84–95. Available: http://eutils.ncbi.nlm.nih.gov/entrez/eutils/elink.fcgi?dbfrom=pubmed&id=21167805&retmode=ref&cmd=prlinks.

21. Buchon N, Broderick NA, Kuraishi T, Lemaitre B (2010) Drosophila EGFR pathway coordinates stem cell proliferation and gut remodeling following infection. BMC biology 8: 152. Available: http://eutils.ncbi.nlm.nih.gov/entrez/eutils/elink.fcgi?dbfrom=pubmed&id=21176204&retmode=ref&cmd=prlinks.

22. Biteau B, Jasper H (2011) EGF signaling regulates the proliferation of intestinal stem cells in Drosophila. Development 138: 1045–1055. Available: http://eutils.ncbi.nlm.nih.gov/entrez/eutils/elink.fcgi?dbfrom=pubmed&id=21307097&retmode=ref&cmd=prlinks.

23. Apidianakis Y, Pitsouli C, Perrimon N, Rahme L (2009) Synergy between bacterial infection and genetic predisposition in intestinal dysplasia. Proceedings of the National Academy of Sciences of the United States of America 106: 20883–20888. Available: http://eutils.ncbi.nlm.nih.gov/entrez/eutils/elink.fcgi?dbfrom=pubmed&id=19934041&retmode=ref&cmd=prlinks.

24. Ragab A, Buechling T, Gesellchen V, Spirohn K, Boettcher A-L, et al. (2011) Drosophila Ras/MAPK signalling regulates innate immune responses in immune and intestinal stem cells. The EMBO journal 30: 1123–1136. Available: http://eutils.ncbi.nlm.nih.gov/entrez/eutils/elink.fcgi?dbfrom=pubmed&id=21297578&retmode=ref&cmd=prlinks.

25. Jiang H, Edgar BA (2011) Intestinal stem cells in the adult Drosophila midgut. Experimental cell research 317: 2780–2788. Available: http://eutils.ncbi.nlm.nih.gov/entrez/eutils/elink.fcgi?dbfrom=pubmed&id=21856297&retmode=ref&cmd=prlinks.

26. Gonzalez C (2013) Drosophila melanogaster: a model and a tool to investigate malignancy and identify new therapeutics. Nat Rev Cancer. Available: http://eutils.ncbi.nlm.nih.gov/entrez/eutils/elink.fcgi?dbfrom=pubmed&id=23388617&retmode=ref&cmd=prlinks.

27. Wang C, Zhao R, Huang P, Yang F, Quan Z, et al. (2013) APC loss-induced intestinal tumorigenesis in Drosophila: Roles of Ras in Wnt signaling activation

and tumor progression. Developmental biology 378: 122–140. Available: http://eutils.ncbi.nlm.nih.gov/entrez/eutils/elink.fcgi?dbfrom=pubmed&id=23570874&retmode=ref&cmd=prlinks.

28. Karim FD, Rubin GM (1998) Ectopic expression of activated Ras1 induces hyperplastic growth and increased cell death in Drosophila imaginal tissues. Development 125: 1–9. Available: http://eutils.ncbi.nlm.nih.gov/entrez/eutils/elink.fcgi?dbfrom=pubmed&id=9389658&retmode=ref&cmd=prlinks.

29. Brand AH, Perrimon N (1993) Targeted gene expression as a means of altering cell fates and generating dominant phenotypes. Development 118: 401–415. Available: http://eutils.ncbi.nlm.nih.gov/entrez/eutils/elink.fcgi?dbfrom=pubmed&id=8223268&retmode=ref&cmd=prlinks.

30. Lee T, Luo L (1999) Mosaic analysis with a repressible cell marker for studies of gene function in neuronal morphogenesis. Neuron 22: 451–461. Available: http://eutils.ncbi.nlm.nih.gov/entrez/eutils/elink.fcgi?dbfrom=pubmed&id=10197526&retmode=ref&cmd=prlinks.

31. Goulas S, Conder R, Knoblich JA (2012) The par complex and integrins direct asymmetric cell division in adult intestinal stem cells. Cell Stem Cell 11: 529–540. Available: http://eutils.ncbi.nlm.nih.gov/entrez/eutils/elink.fcgi?dbfrom=pubmed&id=23040479&retmode=ref&cmd=prlinks.

32. Shanbhag S, Tripathi S (2009) Epithelial ultrastructure and cellular mechanisms of acid and base transport in the Drosophila midgut. The Journal of experimental biology 212: 1731–1744. Available: http://eutils.ncbi.nlm.nih.gov/entrez/eutils/elink.fcgi?dbfrom=pubmed&id=19448082&retmode=ref&cmd=prlinks.

33. Bryan J, Edwards R, Matsudaira P, Otto J, Wulfkuhle J (1993) Fascin, an echinoid actin-bundling protein, is a homolog of the Drosophila singed gene product. Proceedings of the National Academy of Sciences of the United States of America 90: 9115–9119. Available: http://eutils.ncbi.nlm.nih.gov/entrez/eutils/elink.fcgi?dbfrom=pubmed&id=8415664&retmode=ref&cmd=prlinks.

34. Vignjevic D, Schoumacher M, Gavert N, Janssen K-P, Jih G, et al. (2007) Fascin, a novel target of beta-catenin-TCF signaling, is expressed at the invasive front of human colon cancer. Cancer research 67: 6844–6853. Available: http://eutils.ncbi.nlm.nih.gov/entrez/eutils/elink.fcgi?dbfrom=pubmed&id=17638895&retmode=ref&cmd=prlinks.

35. Merlos-Suárez A, Barriga FM, Jung P, Iglesias M, Céspedes MV, et al. (2011) The intestinal stem cell signature identifies colorectal cancer stem cells and predicts

disease relapse. Cell Stem Cell 8: 511–524. Available: http://eutils.ncbi.nlm.nih.gov/entrez/eutils/elink.fcgi?dbfrom=pubmed&id=21419747&retmode=ref&cmd=prlinks.

36. Schepers AG, Snippert HJ, Stange DE, van den Born M, van Es JH, et al. (2012) Lineage tracing reveals Lgr5+ stem cell activity in mouse intestinal adenomas. Science 337: 730–735. Available: http://eutils.ncbi.nlm.nih.gov/entrez/eutils/elink.fcgi?dbfrom=pubmed&id=22855427&retmode=ref&cmd=prlinks.

37. Jiang H, Patel PH, Kohlmaier A, Grenley MO, McEwen DG, et al. (2009) Cytokine/Jak/Stat signaling mediates regeneration and homeostasis in the Drosophila midgut. Cell 137: 1343–1355. Available: http://eutils.ncbi.nlm.nih.gov/entrez/eutils/elink.fcgi?dbfrom=pubmed&id=19563763&retmode=ref&cmd=prlinks.

38. Lin G, Xu N, Xi R (2010) Paracrine unpaired signaling through the JAK/STAT pathway controls self-renewal and lineage differentiation of drosophila intestinal stem cells. Journal of molecular cell biology 2: 37–49. Available: http://eutils.ncbi.nlm.nih.gov/entrez/eutils/elink.fcgi?dbfrom=pubmed&id=19797317&retmode=ref&cmd=prlinks.

39. Beebe K, Lee W-C, Micchelli CA (2010) JAK/STAT signaling coordinates stem cell proliferation and multilineage differentiation in the Drosophila intestinal stem cell lineage. Developmental biology 338: 28–37. Available: http://eutils.ncbi.nlm.nih.gov/entrez/eutils/elink.fcgi?dbfrom=pubmed&id=19896937&retmode=ref&cmd=prlinks.

40. O'Brien LE, Soliman SS, Li X, Bilder D (2011) Altered modes of stem cell division drive adaptive intestinal growth. Cell 147: 603–614. Available: http://eutils.ncbi.nlm.nih.gov/entrez/eutils/elink.fcgi?dbfrom=pubmed&id=22036568&retmode=ref&cmd=prlinks.

41. Ohlstein B, Spradling A (2007) Multipotent Drosophila intestinal stem cells specify daughter cell fates by differential notch signaling. Science 315: 988–992. Available: http://eutils.ncbi.nlm.nih.gov/entrez/eutils/elink.fcgi?dbfrom=pubmed&id=17303754&retmode=ref&cmd=prlinks.

42. Cognigni P, Bailey AP, Miguel-Aliaga I (2011) Enteric neurons and systemic signals couple nutritional and reproductive status with intestinal homeostasis. Cell metabolism 13: 92–104. Available: http://eutils.ncbi.nlm.nih.gov/entrez/eutils/elink.fcgi?dbfrom=pubmed&id=21195352&retmode=ref&cmd=prlinks.

43. Brumby AM, Richardson HE (2005) Using Drosophila melanogaster to map human cancer pathways. Nat Rev Cancer 5: 626–639. Available: http://eutils.ncbi.nlm.nih.gov/entrez/eutils/elink.fcgi?dbfrom=pubmed&id=16034

67&retmode=ref&cmd=prlinks.

44. Boivin GP, Washington K, Yang K, Ward JM, Pretlow TP, et al. (2003) Pathology of mouse models of intestinal cancer: consensus report and recommendations. Vol. 124. pp. 762–777. Available: http://eutils.ncbi.nlm.nih.gov/entrez/eutils/elink.fcgi?dbfrom=pubmed&id=12612914&retmode=ref&cmd=prlinks.

45. Buchon N, Osman D, David FPA, Fang HY, Boquete J-P, et al. (2013) Morphological and molecular characterization of adult midgut compartmentalization in Drosophila. Cell Rep 3: 1725–1738. doi:10.1016/j.celrep.2013.04.001.

46. Marianes A, Spradling AC (2013) Physiological and stem cell compartmentalization within the Drosophila midgut. Elife 2: e00886. doi:10.7554/eLife.00886.

47. Hogan C, Dupré-Crochet S, Norman M, Kajita M, Zimmermann C, et al. (2009) Characterization of the interface between normal and transformed epithelial cells. Nature cell biology 11: 460–467. Available: http://eutils.ncbi.nlm.nih.gov/entrez/eutils/elink.fcgi?dbfrom=pubmed&id=19287376&retmode=ref&cmd=prlinks.

48. Longo VD (2004) Ras: the other pro-aging pathway. Science of aging knowledge environment : SAGE KE 2004: pe36. Available: http://eutils.ncbi.nlm.nih.gov/entrez/eutils/elink.fcgi?dbfrom=pubmed&id=15456908&retmode=ref&cmd=prlinks.

49. Gonzalez-Roca E, Garcia-Albéniz X, Rodriguez-Mulero S, Gomis RR, Kornacker K, et al. (2010) Accurate expression profiling of very small cell populations. PloS one 5: e14418. Available: http://eutils.ncbi.nlm.nih.gov/entrez/eutils/elink.fcgi?dbfrom=pubmed&id=21203435&retmode=ref&cmd=prlinks.

Figure Legends

Figure 1. Loss of Apc combined with activated Ras expression has a synergistic activity inducing over-growths in the adult *Drosophila* gut. **a**, life span of flies bearing wild type, Apc, Ras and Apc-Ras clones. **b**, diagram of an adult *Drosophila* midgut. A, M, and P mark the areas used to analyze clone distribution along the anteroposterior axis (**m**). **c-j**, adult midguts showing wild type, Apc, Ras and Apc-Ras clones marked by GFP (green) one and four weeks after induction. **k**, box-plot graph of clone area (GFP^+) per anterior gut area one and four weeks after clone induction. **l**, box-plot graph of the total number of clones in the anterior gut four weeks after clone induction. **m**, histogram of the clone area (GFP^+) distribution along the anteroposterior axis four weeks after induction.

Figure 2. The Ras^{V12}-driven tumor suppressor mechanism does not depend on apoptosis. **a-b**, adult midguts bearing Apc-Ras clones over-expressing the anti-apoptotic transgenes **a**, UAS-P35 (Apc-Ras-UAS P35) or **b**, UAS Diap1 (Apc-Ras-UAS Diap1) four weeks after clone induction. **c-e**, Apc-Ras clones four weeks after induction detected by DAPI (**c**, blue) or GFP (**d-e**, green). Apc-Ras clones invade most of the luminal space (**c**), invade the surrounding wild type epithelium (arrow), marked on its apical side by phalloidin (red) (**d**) and, in some cases, grow towards the muscular layer (**e**).

Figure 3. Apc-Ras clones (green) show tumor-like characteristics. **a**, Apc-Ras clones do not break the basal lamina, marked by laminin B (blue). **b,** Apc-Ras clones show a high number of mitotic cells marked by PH3 staining (blue). **c**, Arm (red) is expressed at high levels in Apc-Ras clones (arrow). In neighbouring wild type ISCs Arm does not localize in the domain that contacts the basal lamina (arrowhead). **d**, The basolateral marker Dlg (red) is delocalized from the membrane in Apc-Ras clones. **e**, The actin binding protein Phalloidin, normally accumulated in the apical side of the enterocytes, shows heterogeneous and delocalized expression in Apc-Ras clones. **f,** Expression of the tumoral marker Singed (red) in Apc-Ras clones. **g,** Electron micrograph of an wild type midgut epithelium. **h**, Electron micrograph of an Apc-Ras clone showing non-polarized cells located far from the basal lamina (arrowhead) and aberrant tissue organization, bar 10 μm. **i**, Electron micrograph of an Apc-Ras clone showing multiple lumens (arrowheads), bar 5 μm. L, lumen. M, muscle.

Figure 4. Apc-Ras clones (green) show cell heterogeneity. **a,** Diagram of the normal adult midgut division-differentiation process. **b**, Diagram of Apc-Ras clones, mainly composed by an "EB-like" population that fails to differentiate. **c-e**, Apc-Ras clones contain few ISCs, marked by Dl (red) (**c**), EE cells, marked by Pros (blue, arrow) and ECs, marked by Pdm1 (red, arrowhead) (**d**) and EBs, marked by Su(H)mCherry (red) (**e**). **f**, Graphs of the clone (GFP^+) population four weeks after clone induction sorted by FACS and used for qRT-PCR analysis. **g**, Validation of the sorting strategy. qRT-PCR analysis shows the increase of the Wg target gene Frizzled3 (Fz3) expression in Apc and Apc-Ras clones, and the increase of the EGFR/Ras pathway target gene Rhomboid (Rho) and the tumoral marker Sn only in Apc-Ras clones. **h**, qRT-PCR analysis showing the decrease in Apc-Ras clones of the ISC marker Dl, the EE cell marker Pros, the EC marker Myo31DF and the JAK/STAT transcription factor stat92e. Note that, as expected, Dl expression is up-regulated in Apc clones due to the increase in the ISC number upon Wg pathway activation..**i**, Staining of Apc-Ras clones with the ISC marker Dl (red) and the mitotic marker PH3 (blue). Note that most dividing cells do not show Dl staining (arrowhead). In contrast, dividing cells outside the clone show high levels of Dl staining (arrow).

Figure 5. Apc-Ras clones affect gut physiology. **a,** Flies bearing Apc-Ras clones show a decline in the number of fecal depositions. **b**, box-plot showing the reduction in the number of fecal deposits four weeks after clone induction. **c**, Graph showing the number of flies that retain bromophenol blue in their intestines after 72h of being exposed to a bromophenol blue-free diet. **d-e**, Abdomen of a wild type fly (**d**) or a fly bearing Apc-Ras clones four weeks after induction (**e**) after 72h of being exposed to a bromophenol blue-free diet.

Supplementary Figure 1. Expression of the tumoral marker Singed (Sn). **a**, Wild type, Apc and Ras clones (green) four weeks after clone induction do not express Sn (red). Sn is only expressed in the tracheal cells that surrounds the intestinal epithelia. **b**, In Apc-Ras clones (green) four weeks after clone induction, Sn (red) is expressed on the clone edge.

Table 1. Clone characterization. Quantification of the number, size and distribution of the clones of the different genotypes analyzed. (A) anterior midgut, (M) Fe/Cu domain, (P) posterior midgut, (W) weeks after clone induction, (n) number of guts analyzed.

Genotype	W	n	Number of clones *(num clones ± SD)*			Clone size *(GFP^+ area/domain area ± SD)*			Clone distribution *(GFP^+ area/total area ± SD)*		
			A	**M**	**P**	**A**	**M**	**P**	**A**	**M**	**P**
Wild Type	1	8	37±10	2±2	58±13	3±2	0,1±0,1	3±2	49±10	0,3±0,3	51±10
Apc	1	10	30±7	6±4	40±14	8±7	2±1	11±5	32±12	2±1	66±12
Ras	1	9	15±5	5±2	16±10	3±2	16±15	3±3	39±19	31±19	31±23
Apc-Ras	1	10	23±8	5±3	23±6	7±4	8±9	4±2	52±15	10±9	38±18
Wild Type	4	10	25±7	8±4	24±4	3±1	4±3	4±2	38±12	9±7	53±13
Apc	4	10	33±10	7±5	37±6	11±8	2±2	15±7	36±19	0,7±0,8	63±18
Ras	4	12	2±1	2±1	2±2	0,2±0,2	12±7	0,4±0,5	10±10	76±12	14±14
Apc-Ras	4	19	3±2	2±2	3±3	26±16	19±25	3±5	82±22	11±15	7±14

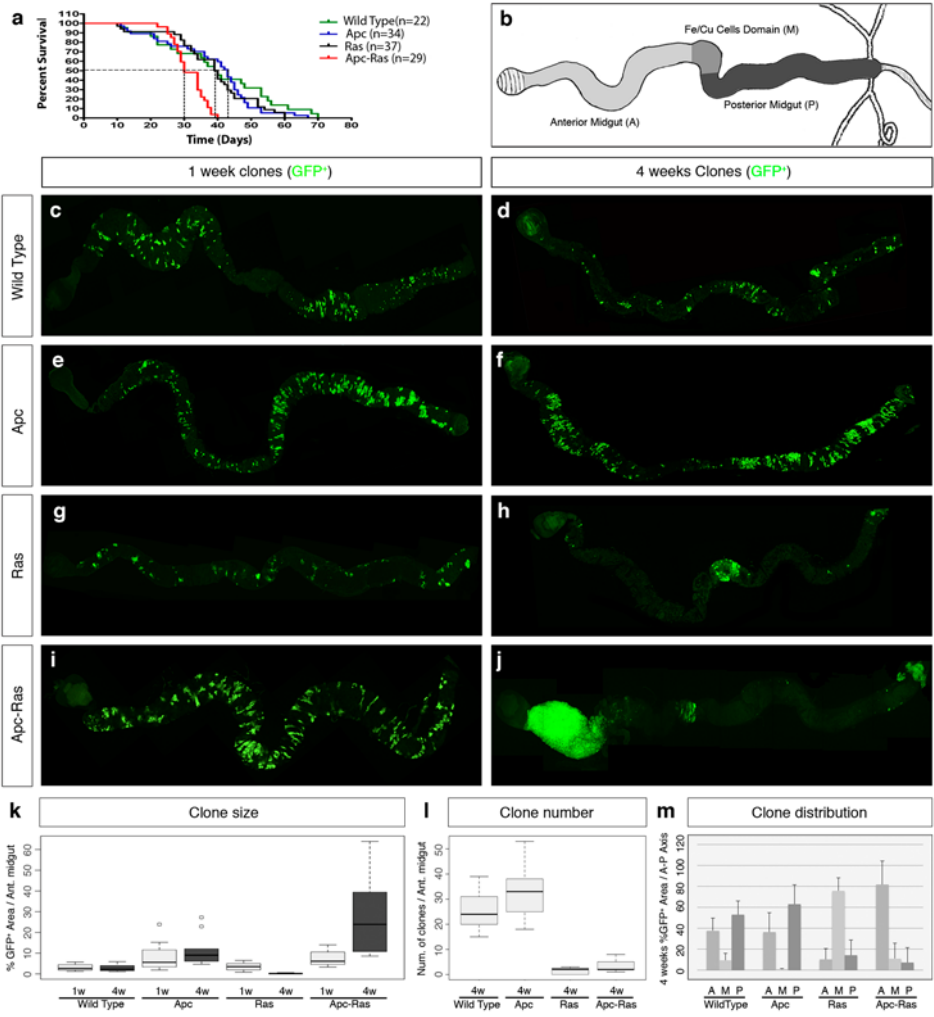

Figure 1 Martorell *et al*

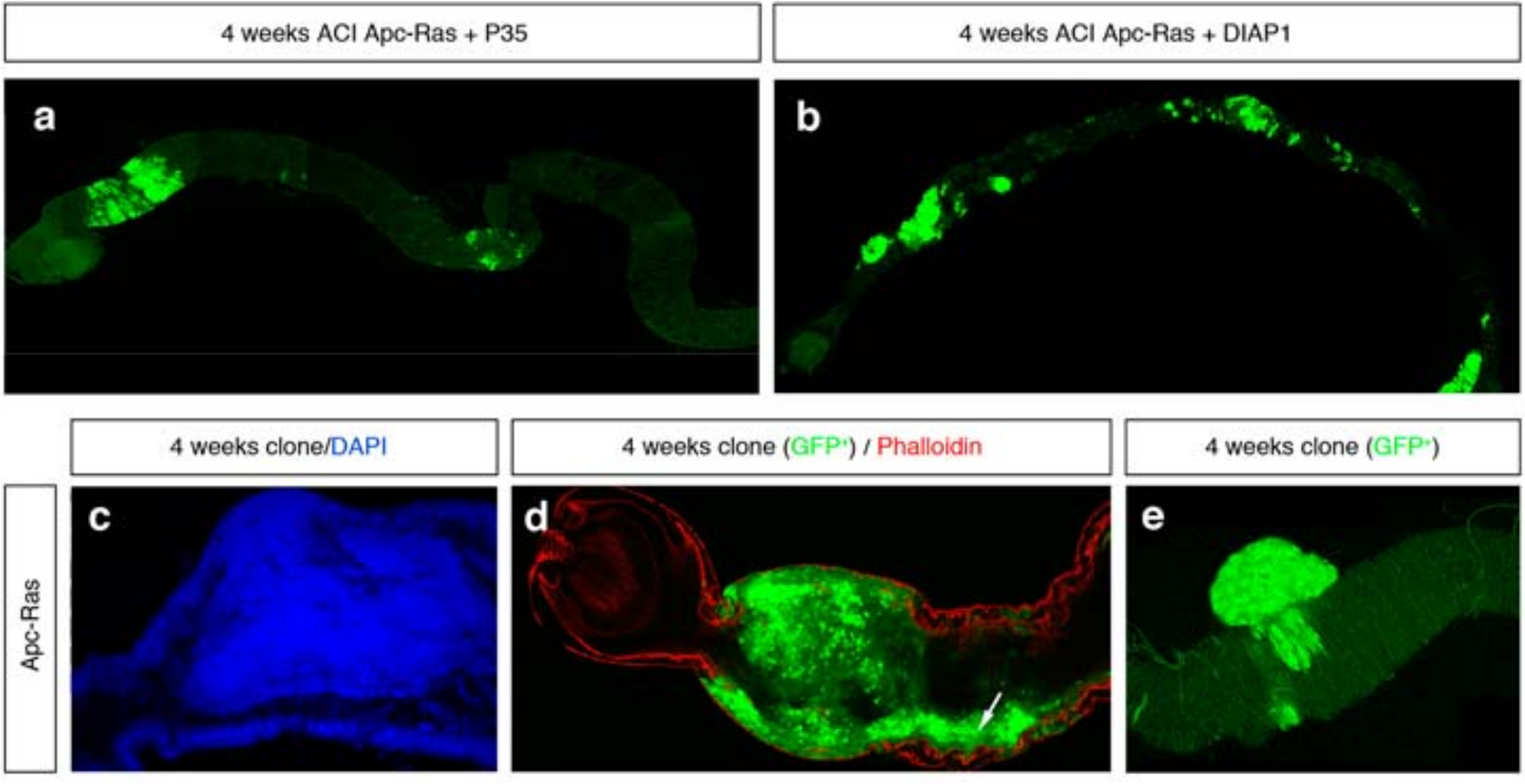

Figure 2 Martorell et al

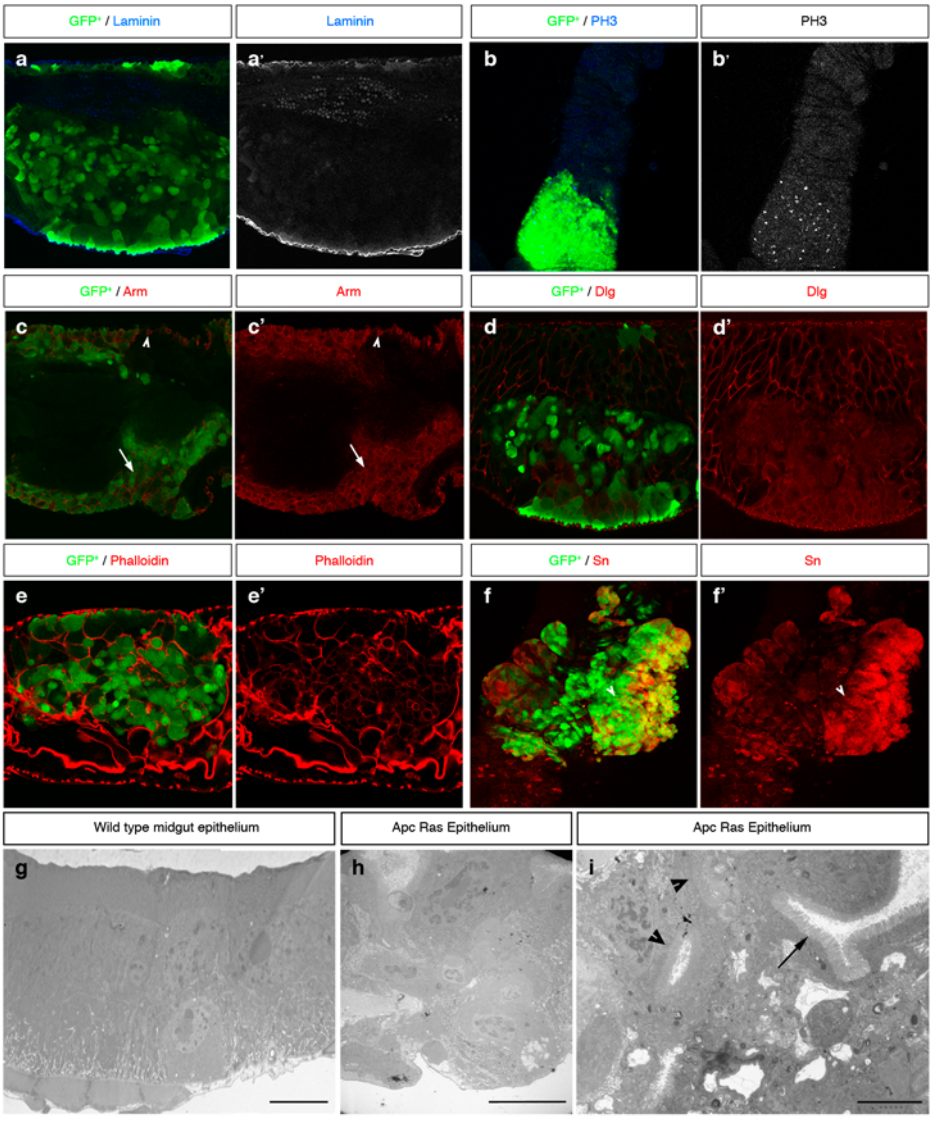

Figure 3 Martorell et al

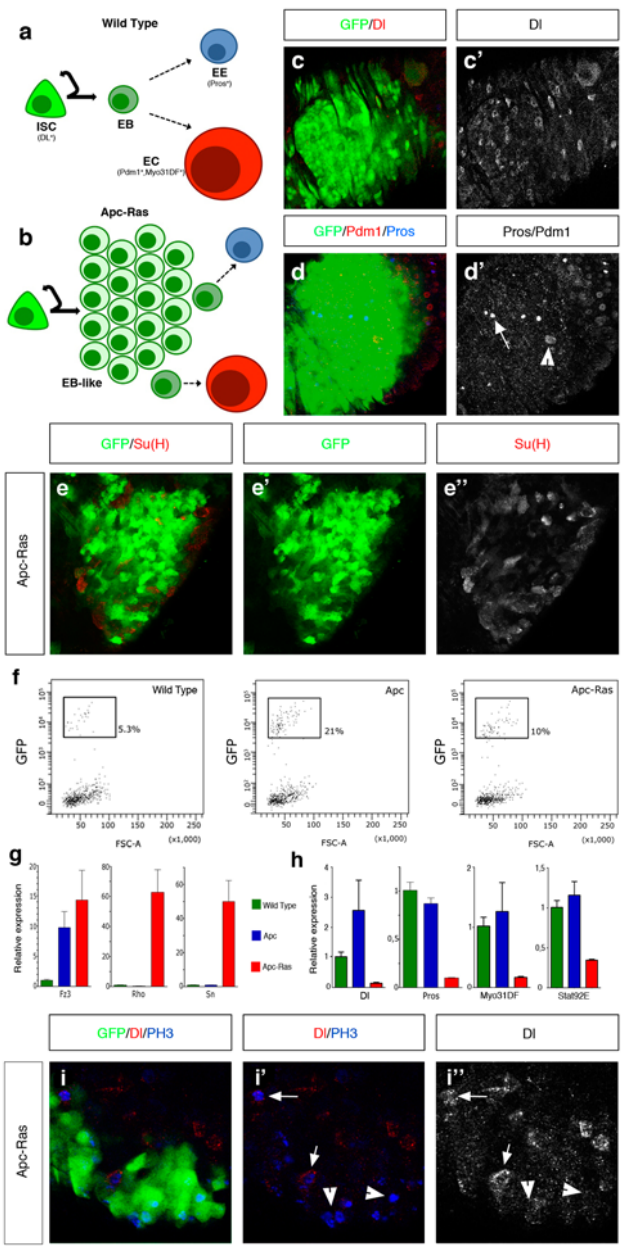

Figure 4 Martorell et al

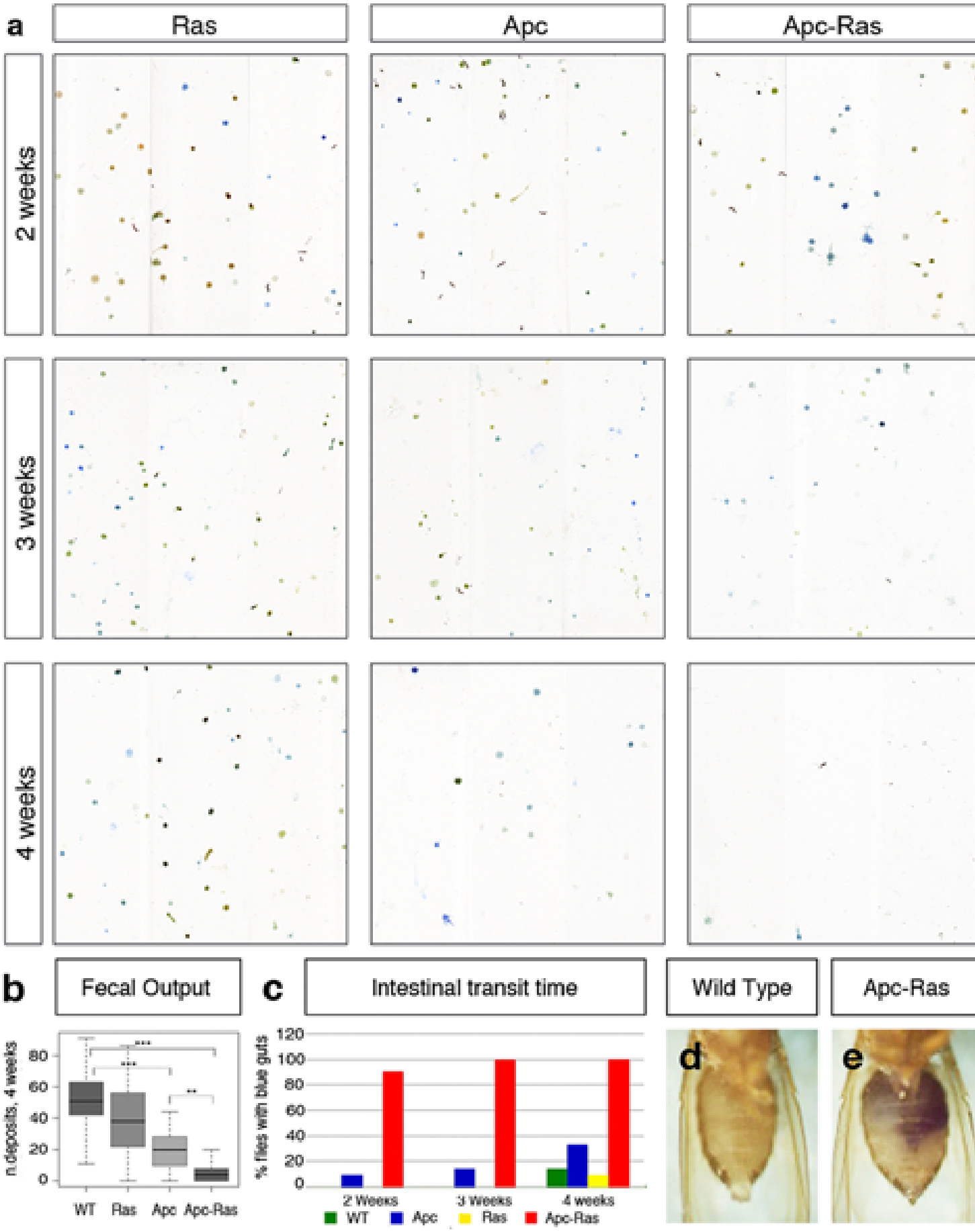

Figure 5 Martorell et al

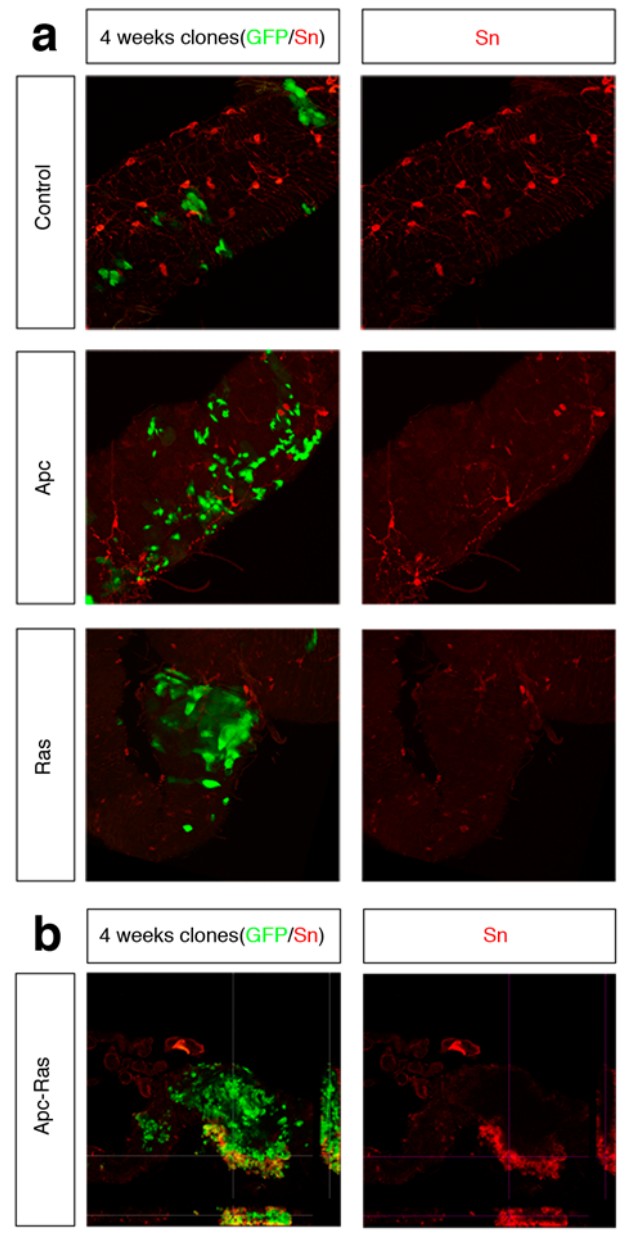

Supplementary 1 Martorell et al

Resum

iNTRODUCCIÓ

El càncer colorectal

Durant dècades, molts investigadors han intentat esbrinar quines són les causes de l'origen i el desenvolupament dels processos tumorals. Cada càncer és un món i aconsegueix les capacitats tumorigèniques per diferents vies. De sempre, l'objectiu dels investigadors ha estat descobrir quins són els mecanismes moleculars que dirigeixen el creixement tumoral en cada tipus de tumor i trobar les vies comuns per trobar una cura universal. Però aquests mecanismes lluny de ser simples vies han resultat ser una extensa xarxa de processos interconnectats de la qual encara queden molts serrells per entendre. Un cop descoberta I entesa, aquesta xarxa de processos podrà ser utilitzada per generar medicaments que bloquegin el creixement tumoral i eventualment destrueixin el tumor.

Un dels càncers més comuns als països desenvolupats és el càncer colorectal (CRC). El terme CRC inclou totes aquelles lesions tumorals que ocorren a l'intestí gros, el recte i l'apèndix. El 85% dels casos són càncers esporàdics i no heretats i creixen normalment en forma de un tumor benigne anomenat pòlip adenomatós. Aquests càncers ocorren per l'acumulació de mutacions al llarg de la vida del pacient (E. R. Fearon, 2011). De CRC esporàdic hi ha dos grans grups, els que tenen alterat el sistema de reparació de errors d'aparellament de bases deguts a la replicació, que augmenta de forma dràstica el número d'acumulacions acumulades i els que tenen problemes en la segregació cromosòmica que acaba creant situacions de pèrdua o guany de regions cromosòmiques (Network, 2012). Ambdós casos acaben convergint en l'alteració de 4 vies de senyalització que controlen la proliferació i els processos de diferenciació a l'intestí adult. Aquestes vies de senyalització són: la via de Wnt, la via de EGFR, la via de TGF-β i la via de la PI3K. L'alteració d'aquestes 4 vies conjuntament amb la pèrdua de la proteïna TP53 produeix suficients alteracions en les cèl·lules del colon com per induir un procés tumorogènic maligne.

Més d'un 90% de CRC tenen alteracions a la via de Wnt i la seva activació és considerada un dels primers esdeveniments en la progressió del CRC. Majoritàriament aquestes alteracions es troben al gen APC, *Adenomatous Polyposis Coli*, un regulador negatiu de la via de Wnt que al ser alterat produeix l'activació constitutiva de la via de Wnt. L'alteració de la via de Wnt provoca un augment de les cèl·lules progenitores de

l'intestí i també de la seva taxa de divisió a l'intestí creant així un teixit amb sobreproliferació.

La segona via de senyalització més alterada durant la progressió del CRC és la via de RTK-RAS amb alteracions activadores de la via presents en un 60% dels casos de CRC. Les mutacions de la via de Ras són majoritàriament posterior a les alteracions a la via de Wnt com s'ha pogut comprovar reiteradament. L'activació d'aquestes dues vies, Wnt I RAS estan considerats els dos principals efectors de la progressió primerenca del càncer colorectal. Alteracions a les vies de TP53 (64%), PI3K (50%) or TGF-β (27%) són considerats també esdeveniments crítics pel desenvolupament de tumors malignes al colon.

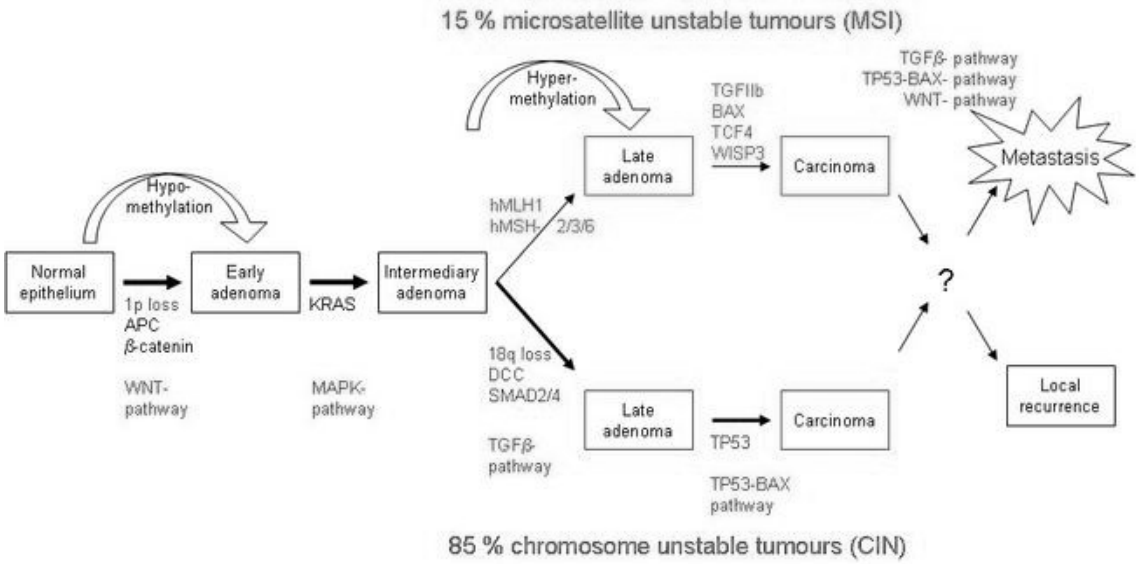

Figura 1. Seqüència Adenoma-Carcinoma. La progressió des d'un teixit normal a un carcinoma requereix la acumulació de diverses mutacions.

Mutacions de pèrdua de funció en la via de senyalització TGF-β es troben en un 30% dels casos de CRC. Aquestes mutacions eviten la funció de TGF-β com a citostàtic i factor anti-tumorogènic. La majoria de mutacions ocorren el receptor TGF-β II i en el transductor SMAD 4. També és important remarcar que alguns tumors tot i no tenir mutacions identificables en la via de TGF-β, no responen a TGF-β suggerint que poden haver-hi altres mecanismes d'evasió de la via.

L'Intestí mig de la Drosòfila adulta com a model per l'estudi del CRC.

L'intestí de Drosòfila es subdivideix en 3 parts: esòfag, intestí mitja i intestí posterior. Aquest estudi s'ha dut a terme amb l'intestí mitja de la mosca Drosòfila adulta. L'intestí mitjà es pot subdividir fins en 14 subregions amb diferent morfologia, expressió gènica i tipus cel·lulars. De totes les subregions hi ha una, la secció gàstrica que és la més diferent i és on resideixen les cèl·lules secretores d'àcid i on hi ha el pH més àcid. L'intestí esta recobert per dues capes de músculs, visceral i longitudinal, i per tràquees que aporten els requeriments d'oxigen que l'òrgan necessita.

L'intestí esta sotmès a un gran estres mecànic i per això necessita una renovació de les seves cèl·lules constant. Aquest rol de renovació es dut a terme per les cèl·lules mare de l'intestí que es divideixen cada cert temps i aporten noves cèl·lules a l'intestí. Quan una cèl·lula mare intestinal es divideix, la divisió que ocorre és asimètrica. Això vol dir que les dues cèl·lules resultants de la divisió no són idèntiques. De la divisió d'una cèl·lula mare en resulten una nova cèl·lula mare i un Enteroblast. L'enteroblast és una cèl·lula indiferenciada que es diferenciarà sense divisió cap a un dels dos tipus madurs de l'intestí: els enteròcits, amb funcions absortives i les cèl·lules enteroendocrines amb funcions endocrinològiques.

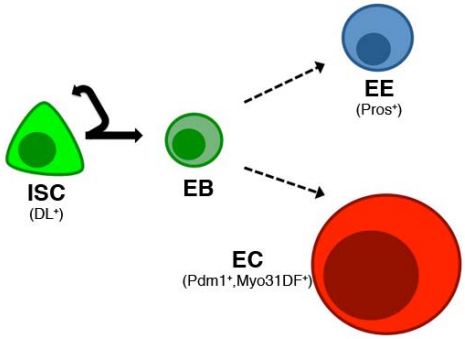

Figura 2. Diagrama de la jerarquia cel·lular de l'intestí mig

Aquest procés esta altament controlat per múltiples vies de senyalització que controlen que la cèl·lula mare només es divideixi quan és necessari. Si aquestes vies de senyalització es veuen alterades, la cèl·lula mare pot veure's afectada i començar a dividir-se sense control, començant així un tumor. Les vies de senyalització que indueixen la divisió de la cèl·lula mare són la via de Wingless/Wnt, la via de EGFR i la via de Jak-Stat. Pel contrari la via de Notch bloqueja la divisió i indueix la diferenciació de l'enteroblast.

OBJECTIUS

L'objectiu principal d'aquesta tesi és establir i caracteritzar un model de CRC *a Drosòfila* per comprendre millor els processos tumorals i alhora identificar nous gens implicats en la progressió del CRC . En conseqüència , els objectius específics són :

- A causa de la rellevància de la inactivació del gen APC i l'activació del gen K - RAS en la progressió del CRC , l'objectiu principal d'aquest treball és l'establiment i la caracterització dels clons que porten alteracions genètiques en els gens APC i Ras al Drosòfila intestí mig d'adults com un model de CRC .

- Realitzar un perfil transcripcional de cèl·lules Apc-Ras per identificar nous gens i funcions que intervenen en la progressió dels tumors.

- A causa del paper de la via de senyalització TGF-β com una barrera de creixement durant la progressió del CRC, vàrem decidir investigar el paper de la via de Dpp en la progressió dels clons Apc-Ras .

RESULTATS

Establiment i caracterització d'un model de càncer colorectal a Drosòfila.

Per a generar el model de càncer colorectal a l'intestí mig adult vam utilitzar la tècnica MARCM per induir clons a l'intestí. Vam crear quatre tipus de clones diferents: clons amb cèl·lules normals (Clons control), clons amb cèl·lules mutants pel gen Apc (clons Apc), clons amb cèl·lules sobreexpresant una forma activada del gen ras (clons Ras) i clons mutants per Apc i sobreexpresant la forma activada de Ras. (clons Apc-Ras). Els clons es van analitzar una setmana després de la inducció i quatre setmanes després de la inducció. Els clons Apc-Ras creixien molt més que la resta i de forma interessant només es desenvolupaven a la part més anterior del intestí mig tot i que es generaven al llarg de tot l'intestí. Aquest efecte de desaparició dels clons també el vam observar en els clons Ras que només sobrevivien a la regió central de l'intestí tot i que no creixien com els clons Apc-Ras. Posteriorment vam comprovar que aquesta desaparició de clons era degut a la delaminació dels clons per mitjà de la proteïna Cdc42 i no per cap mecanisme de mort per apoptosi.

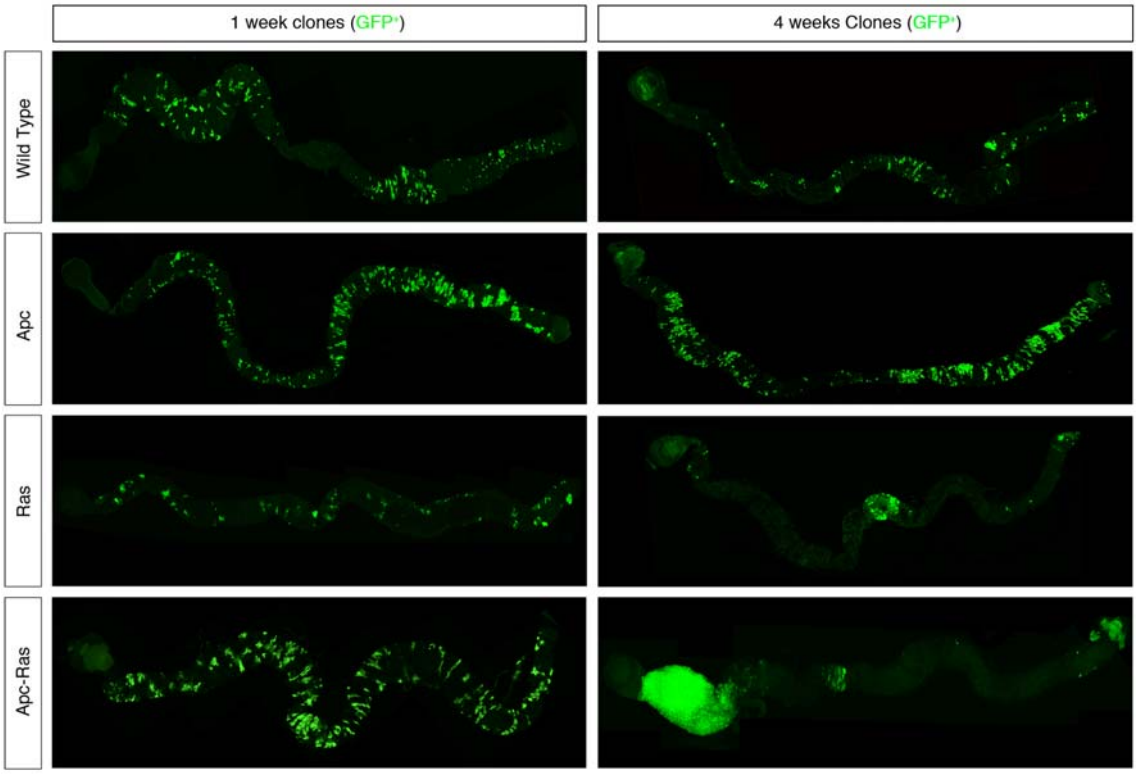

Figura 3. Visió general dels intestins amb clons MARMC. Les diferències durant la progressió clonal són notables especialment els clons Apc-Ras que es desenvolupen de forma important en la part anterior de l'intestí.

Posteriorment, vam procedir a la caracterització dels clons. Els clons Apc-Ras mostraven una alta capacitat de proliferació, ja que presentaven un elevat nombre de cèl·lules positives pel marcador de divisió PH3. Am és a més els clons Apc-Ras presentaven baixos nivells de diferenciació cel·lular una característica típica dels tumors avançats. Els clons Apc-Ras mostraven baixos nombres de cèl·lules enteroendocrines i d'enteròcits marcades. Alhora, els tumors també mostraven baixos nivells de cèl·lules mare. Aquests resultats es van comprovar tant per immunotinció com per PCR quantitativa pels marcador de cèl·lula diferenciada. Els clons Apc-Ras també mostraven severs signes de pèrdua de polaritat cel·lular i pèrdua d'organització tissular com molts dels càncers que provenen de teixits epitelials. Finalment també es va comprovar que mostraven expressió per un marcador de tumors intestinals avançat, Fascin (Singed a Drosòfila) i que no generaven metàstasis.

Un cop el model es va caracteritzar i efectivament es va confirmar que tenia característiques tumorals es va procedir a fer un assaig fisiològic i es va veure que els clons Apc-ras afectaven severament la fisiologia de l'intestí reduint el nombre de deposicions i allargant el temps de trànsit intestinal. Aquest assaig pot ser utilitzat en el futur com un assaig ràpid per a comprovar l'efectivitat de medicaments anti-tumorals.

Perfil transcripcional de cèl·lules de l'intestí mig de Drosòfila

Un dels objectius d'aquests treball era la identificació de nous gens implicats en la progressió tumoral. Per aquest motiu es va decidir fer un perfil transcripcional de les cèl·lules dels clons control, Apc, Ras i Apc-Ras per a poder-los comparar entre si. Vam observar que el perfil de Apc-Ras presentava moltes diferencies significatives amb la mostra control i de forma interessant molts dels gens que mostraven diferencies significatives entre els clons control i els clons Apc-Ras no mostraven diferencies en els clons Apc o Ras. Aquest resultat ens mostra que la co-activació de les vies de senyalització de Wingless i EGFR produeix un efecte sinèrgic que comporta l'expressió diferencial de gens específics en els clons Apc-Ras. Es possible que part d'aquests gens Apc-Ras específics siguin essencials per a la progressió dels clons Apc-Ras.

El perfil transcripcional de les cèl·lules Apc-Ras mostrà que les cèl·lules tenen alts nivells de gens de proliferació com per exemple *String*. A més a més mostrà que hi ha molts gens de metabolisme afectats i possiblement reflecteixi la falta de enteròcits, els gens que realitzen el metabolisme absortiu de l'intestí. També mostrà que molts dels principals factors de senyalització estan alterats en les cèl·lules Apc-Ras com per exemple molts dels components de la via de Dpp/TGF o de la via Hedgehog. A més a més molts factors de transcripció també mostraven alteració en els seus nivells d'expressió com el factor repressor Mirror, o els inductors de migració Serpent i Snail.

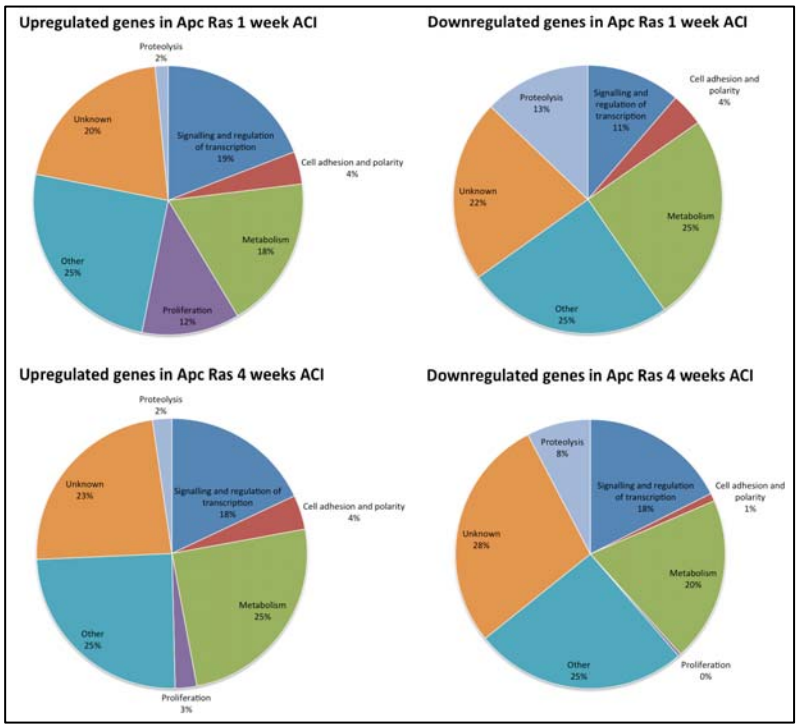

Figura 4. Perfil transcripcional dels clons Apc-Ras 1 i 4 setmanes després de la inducció

El perfil transcripcional de les cèl·lules Apc-Ras també mostrava que els perfils del mateix genotip però en dos moments diferents d'anàlisi (una setmana després de la inducció o 4 setmanes després de la inducció) també mostraven força diferències. En particular, la quantitat de gens que mostraven alteració en els seus nivells compartits per les cèl·lules a una i quatre setmanes després de la inducció era al voltant del 50%. Això suggereix que és possible que hi hagi gens que són importants per a la iniciació del tumor però no per a la seva progressió i viceversa. Alhora la comparació d'aquests dos perfils transcripcionals va mostrar que les cèl·lules Apc-ras sofreixen un canvi metabòlic que es sol produir en les cèl·lules tumorals, l'efecte Warburg. L'efecte Warburg és el desacoblament de la glucòlisi del cicle de Krebs i la cadena de transport d'electrons. Per aquesta via les cèl·lules obtenen menys energia per molècula de glucosa emprada però per altre banda poden utilitzar els metabòlits intermitjos per a la producció de noves biomolècules necessàries per a la creació de noves membranes i orgànuls.

Finalment, es va fer un cribratge funcional de RNAi en les cèl·lules Apc-ras per observar la absència de quins gens produïa efecte sobre el creixement dels clons Apc-ras. Es van identificar 62 gens essencials per a la progressió correcte dels clons Apc-Ras. Com a exemple, la absència de Hedgehog o el seu receptor produeix una reducció important en la mida dels clons Apc-Ras indicant que la via de senyalització Hedgehog és necessària pel creixement dels clons Apc-Ras en el intestí mig de Drosòfila.

La via de senyalització Dpp actua com a supressor de tumor durant la progressió dels clons Apc-ras en el intestí mig de Drosòfila.

L'anàlisi del perfil transcripcional de les cèl·lules Apc-Ras van mostrar que hi havia un silenciament transcripcional de tots els components de la via de Dpp. Per veure si aquest silenciament tenia alguna funció vam activar de manera forçada la via mitjançant la addicció d'un al·lel activat del receptor de la via de Dpp a les cèl·lules Apc-Ras. Sorprenentment, la activació de la via de Dpp en els clons Apc-Ras bloquejava el seu creixement notablement. A més a més la activació de la via de senyalització Dpp induïa la diferenciació cel·lular tant dels clones Apc-Ras com de cèl·lules mare control. Aquests resultats indiquen que el silenciament transcripcional de la via de senyalització Dpp és essencial per al progres dels clons Apc-Ras a l'intestí mig de Drosòfila.

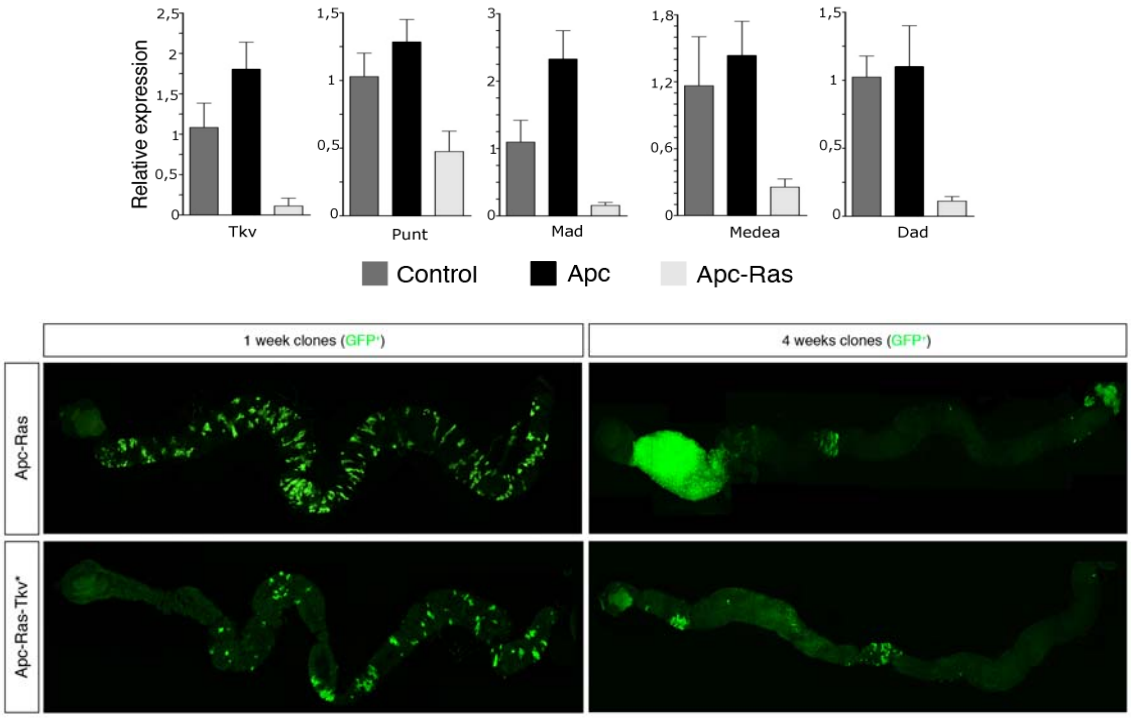

Figura 5. El silenciament de la via Dpp és essencial pel creixement dels clons Apc-Ras. A dalt: Nivells transcripcionals des components de la via de senyalització Dpp. A sota: Visió general dels clons Apc-Ras amb la via de Dpp activada

Vam suggerir la possibilitat de que aquest silenciament transcripcional estigues sent dut a terme per un sol factor de transcripció i efectivament vam trobar un factor de transcripció que tenia llocs d'unió per tots els components de la via de senyalització Dpp i que a més a mes estava sobreexpressat a les cèl·lules Apc-Ras, el factor de transcripció Mirror. Mirror, un repressor transcripcional, efectivament era essencial pel creixement dels clones Apc-Ras ja que la seva absència per RNAi produïa una notable reducció de la mida dels clons Apc-Ras. A més a més l'absència de Mirror era suficient per tornar a la normalitat els nivells d'alguns components de la via de senyalització així com també dels marcador de diferenciació i del factor de transcripció Jak-Stat, silenciat en les cèl·lules Apc-Ras. A més a més vam demostrar amb un experiment epistàtic que l'efecte observat per l'absència de Mirror en els clons Apc-Ras és bàsicament pel silenciament dels components de la via de Dpp.

Finalment, vam observar que els les dues proteïnes homòlogues a Mirror en humans, IRX3 i IRX5 tenien nivells elevats en mostres d'adenoma i que la seva absència correlacionava inversament amb els nivells de Smad3, el transductor de la via de Dpp/TGF-β. A més a més la seva expressió en cèl·lules de CRC que responen al tractament amb TGF-β era suficient per baixar la seva resposta a la meitat.

Discussió

Aquest treball demostra la idoneïtat de l'ús de Drosòfila com a organisme model per estudiar la formació de tumors en un sistema in vivo i alhora, obre diverses noves preguntes que cal abordar amb cura durant els propers anys.

En les nostres condicions els clons que expressen l'al·lel Ras^{V12} (clons Apc-Ras i Ras) tendeixen a desaparèixer de l'epiteli durant la progressió del clon. A més a més, aquesta desaparició induïda per l'expressió de l'al·lel Ras^{V12} no és a l'atzar i els clons progressen I sobreviuen en posicions específiques. D'aquest resultat en sorgeixen tres preguntes : Per què Ras^{V12} porten clons desapareixen al llarg del temps? Per Ras i Apc-Ras clons sobreviure en regions específiques de l'intestí? Pot establir-se cap paral·lelisme entre Drosòfila i mamífers en el comportament de les cèl·lules Ras^{V12}?

Com hem comentat prèviament, els clons desapareixen per extrusió de les cèl·lules Ras^{V12} mitjançant l'acció de la GTPasa Cdc42. Un mecanisme similar s'ha descrit a cultius humans on cèl·lules humanes expressant Ras^{V12} són extruïdes d'una monocapa de cultiu cel·lular només quan es troben envoltades de cèl·lules control. Aquest mecanisme podria ser una explicació de perquè les mutacions Ras^{V12} no apareixen en estadis primerencs de càncer colorectal, ja que possiblement necessitin mutacions prèvies per poder romandre al epiteli intestinal.

La supervivència en regions específiques podria ser deguda a diferències regionals (anatòmiques o genètiques) al llarg de l'intestí. Recentment s'ha descrit que la regió més anterior del intestí mig, on els clons Apc-Ras es desenvolupen, mostra unes característiques especials molt concretes tant en organització i morfologia cel·lular com en expressió específica de molts gens. En models de ratolí, també s'ha demostrat que hi ha diferències regionals ja que el model de ratolí més emprat com a model de càncer colorectal, el ratolí Apc^{min} només genera pòlips en el intestí prim i mai afecta l'intestí gros. Mentre que si fem que aquest ratolí expressi ara més a més l'al·lel oncogènic de Ras ara els clons es desenvolupen ara també en l'intestí gros. Tot això demostra que al llarg de l'intestí hi ha diferències que afecten a l'aparició o la progressió de tumors i podria explicar en part el perquè és tan infreqüent el càncer de intestí prim i tan freqüent el de còlon o intestí gros.

Aquest treball també ha servit per a identificar múltiples gens que podrien estar implicats en tumorogènesi. Molècules de senyalització, factors de transcripció, molècules d'adhesió i enzims metabòlics. A més a més el cribratge de RNAi ha servit per confirmar la necessitat d'alguns d'aquests gens durant la progressió dels clons Apc-Ras.

Finalment s'ha pogut identificar el rol essencial del silenciament transcripcional la via de senyalització de Dpp durant la progressió dels clons Apc-Ras. Aquest silenciament té un rol similar al que exerceixen les mutacions de la via de TGF-β en el càncer colorectal. En ambdós organismes el rol de la via de Dpp/ TGF-β exerceix un rol de supressió tumoral que les cèl·lules cancerígenes han d'evadir. Aquest treball ha demostrat que el factor de transcripció Mirror pot reprimir negativament els nivells transcripcionals dels components d'aquesta via i així aconseguir evitar el rol citostàtic que aquesta exerceix. Aquests resultats han estat confirmats en cèl·lules en cultiu humà i evidencien que no són sempre necessàries mutacions per a que el càncer pugui progressar i que la regulació transcripcional pot ser un esdeveniment crític per a la activació o repressió de vies de senyalització durant el creixement del tumor.

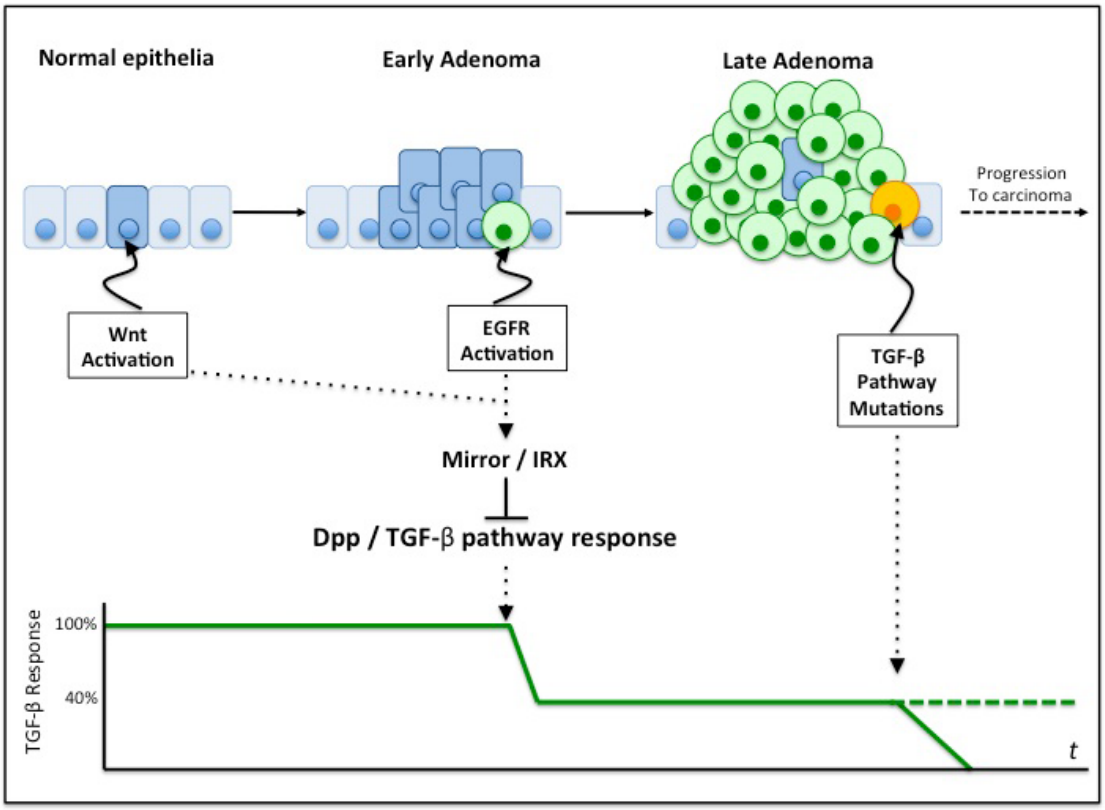

Figura 6. El factor de transcripció de Mirror reprimeix la via de Dpp per evadir el seu efecte citostàtic durant la progressió tumoral

CONCLUSIONS

Segons els resultats , les conclusions són les següents:

1 . La co-activació clonal de les vies de senyalització Wg i EGFR indueix l'aparició de sobrecreixements de tipus tumoral a l'intestí mig adult de Drosòfila.

2 . L'expressió de RAS^{V12} indueix l'extrusió de la majoria dels clons per l'activació de la proteïna Cdc42.

3 . Clons Apc-Ras presenten hiperproliferació i el pèrdua de diferenciació cel·lular, pèrdua de polaritat cel·lular i desorganització general del teixit.

4 . Apc - Ras no mostren metàstasi.

5 . Els Clons Apc-Ras alteren la fisiologia normal de l'intestí mitjà adult reduint el nombre de deposicions fecals i fent més lent el trànsit intestinal.

6 . El perfil transcripcional de les cèl·lules Apc-Ras revela una activitat sinèrgica de l'activació del Wg i EGFR vies amb gens alterats específicament en els clons Apc-Ras però no alterats en els clons amb una sola alteració.

7 . el perfil dels clons Apc-Ras és ric en gens de proliferació i molècules de senyalització, i presenta alteracions metabòliques similars a les que ocorren durant la progressió del CRC humà.

8 . Les cèl·lules Apc-Ras presenten un silenciament transcripcional dels components de la via de senyalització Dpp.

9 . El silenciament transcripcional de la via Dpp en les cèl·lules Apc-Ras és essencial per a la correcta progressió dels clons Apc-Ras.

10 . L'activació de la via de senyalització Dpp en cèl·lules Apc-Ras indueix un bloqueig en el creixement clonal i un augment de cèl·lules diferenciades.

11 . Els nivells del factor de transcripció Mirror estan elevats en les cèl·lules Apc-Ras i són responsables del silenciament transcripcional de la via Dpp.

12 . L'expressió de Mirror és essencial per a la progressió del clon Apc – Ras.

13 . L'absència de Mirror a les cèl·lules Apc-Ras produeix una disminució de l'àrea del clon i restaura la diferenciació normal del clon.

14 . Mirror regula negativament els nivells de Stat92E en cèl·lules Apc-Ras.

15 . Irx3 i IRX5 tenen nivells elevats en els adenomes de còlon i la seva expressió es correlaciona inversament amb la capacitat de resposta de les cèl·lules SW837 al tractament amb TGF-β.